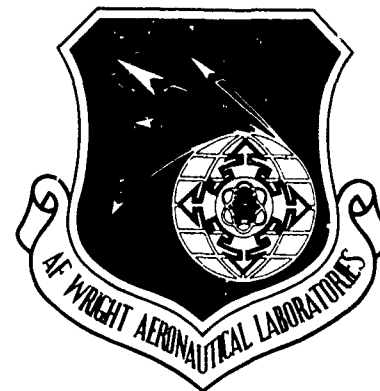


12

AFWAL-TR-85-3096

VOLUME I

# DESIGN METHODOLOGY AND LIFE ANALYSIS OF POSTBUCKLED METAL AND COMPOSITE PANELS



AD-A171 253

R. B. DEO

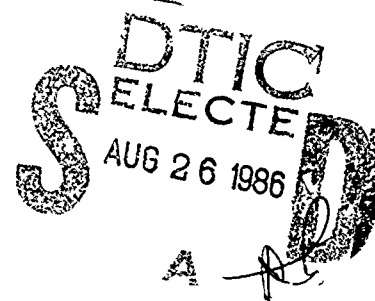
B. L. AGARWAL

E. MADENCI

Northrop Corporation  
Aircraft Division  
One Northrop Avenue  
Hawthorne, California 90250

DECEMBER 1985

Final Report for Period September 1981 - August 1985



Approved for public release; distribution unlimited

DTIC FILE COPY

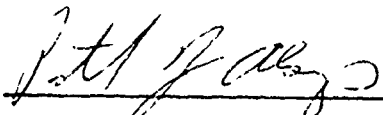
FLIGHT DYNAMICS LABORATORY  
AIR FORCE WRIGHT AERONAUTICAL LABORATORIES  
AIR FORCE SYSTEMS COMMAND  
WRIGHT-PATTERSON AIR FORCE BASE, OHIO 45433

NOTICE

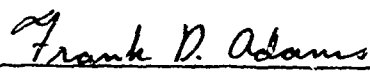
When Government drawings, specifications, or other data are used for any purpose other than in connection with a definitely related Government procurement operation, the United States Government thereby incurs no responsibility nor any obligation whatsoever; and the fact that the government may have formulated, furnished, or in any way supplied the said drawings, specifications, or other data, is not to be regarded by implication or otherwise as in any manner licensing the holder or any other person or corporation, or conveying any rights or permission to manufacture use, or sell any patented invention that may in any way be related thereto.

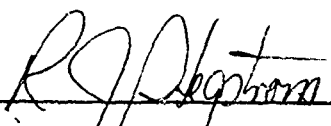
This report has been reviewed by the Office of Public Affairs (ASD/PA) and is releasable to the National Technical Information Service (NTIS). At NTIS, it will be available to the general public, including foreign nations.

This technical report has been reviewed and is approved for publication.

  
PATRICK J. ALSUP, 2Lt, USAF  
Fatigue, Fracture & Reliability Group  
Structural Integrity Branch  
Structures and Dynamics Division  
Flight Dynamics Laboratory

FOR THE COMMANDER

  
FRANK D. ADAMS, Chief  
Structural Integrity Branch  
Structures and Dynamics Division  
Flight Dynamics Laboratory

  
ROGER J. HEGSTROM, Colonel, USAF  
Chief, Structures and Dynamics Division  
Flight Dynamics Laboratory

If your address has changed, if you wish to be removed from our mailing list, or if the addressee is no longer employed by your organization please notify AFWAL/FIBEC W-PAFB, OH 45433 to help us maintain a current mailing list.

Copies of this report should not be returned unless return is required by security considerations, contractual obligations, or notice on a specific document.

## **DISCLAIMER NOTICE**

**THIS DOCUMENT IS BEST QUALITY  
PRACTICABLE. THE COPY FURNISHED  
TO DTIC CONTAINED A SIGNIFICANT  
NUMBER OF PAGES WHICH DO NOT  
REPRODUCE LEGIBLY.**

Unclassified

SECURITY CLASSIFICATION OF THIS PAGE

AD-A171253

## REPORT DOCUMENTATION PAGE

1a REPORT SECURITY CLASSIFICATION Unclassified		1b RESTRICTIVE MARKINGS										
2a SECURITY CLASSIFICATION AUTHORITY		3 DISTRIBUTION/AVAILABILITY OF REPORT Approved for public release; distribution unlimited										
2b DECLASSIFICATION/DOWNGRADING SCHEDULE												
4 PERFORMING ORGANIZATION REPORT NUMBER(S) NOR 86-39		5 MONITORING ORGANIZATION REPORT NUMBER(S) AFWAL-TR-85-3096, Vol. I										
6a NAME OF PERFORMING ORGANIZATION Northrop Corporation	6b OFFICE SYMBOL (If applicable)	7a NAME OF MONITORING ORGANIZATION Air Force Wright Aeronautical Laboratories Flight Dynamics Laboratory (AFWAL/FIBEC)										
6c ADDRESS (City, State and ZIP Code) Hawthorne, CA 90250		7b ADDRESS (City, State and ZIP Code) Wright-Patterson Air Force Base Ohio 45433										
8a NAME OF FUNDING/SPONSORING ORGANIZATION Flight Dynamics Laboratory	8b OFFICE SYMBOL (If applicable) AFWAL/FIBEC	9 PROCUREMENT INSTRUMENT IDENTIFICATION NUMBER F33615-81-C-3208										
8c ADDRESS (City, State and ZIP Code) Wright-Patterson Air Force Base Ohio 45433		10 SOURCE OF FUNDING NOS <table border="1"><thead><tr><th>PROGRAM ELEMENT NO</th><th>PROJECT NO</th><th>TASK NO</th><th>WORK UNIT NO</th></tr></thead><tbody><tr><td>62201F</td><td>2401</td><td>01</td><td>54</td></tr></tbody></table>		PROGRAM ELEMENT NO	PROJECT NO	TASK NO	WORK UNIT NO	62201F	2401	01	54	
PROGRAM ELEMENT NO	PROJECT NO	TASK NO	WORK UNIT NO									
62201F	2401	01	54									
11 TITLE (Include Security Classification) Design Methodology and Life Analysis of Post-buckled Metal and Composite Panels - Volume I												
12 PERSONAL AUTHOR(S) R. B. Deo, B. L. Agarwal, E. Madenci												
13a TYPE OF REPORT Final	13b TIME COVERED FROM 9/81 TO 8/85	14 DATE OF REPORT (Yr, Mo, Day) 1985 December 22	15 PAGE COUNT 306									
16 SUPPLEMENTARY NOTATION												
17 COSATI CODES <table border="1"><thead><tr><th>FIELD</th><th>GROUP</th><th>SUB GR</th></tr></thead><tbody><tr><td></td><td>13</td><td>13</td></tr><tr><td></td><td>11</td><td>04</td></tr></tbody></table>		FIELD	GROUP	SUB GR		13	13		11	04	18 SUBJECT TERMS (Continue on reverse if necessary and identify by block number) BUCKLING, COMPOSITE PANELS, COMPRESSION LOAD, CURVED PANELS, DESIGN, DURABILITY, FATIGUE, LIFE PREDICTION, METAL PANELS, POSTBUCKLING, RAYLEIGH-RITZ METHOD, SHEAR, TOTAL POTENTIAL.	
FIELD	GROUP	SUB GR										
	13	13										
	11	04										
19 ABSTRACT (Continue on reverse if necessary and identify by block number) The objectives of this program were to develop an experimentally validated analysis capability and simple to use design procedures for curved metal and composite postbuckled panels loaded in compression or shear. The program plan was to first review the available analysis methods for postbuckled panels and then extend or modify these to develop a design methodology for curved postbuckled panels. This methodology was used in designing curved panels for a test program to generate design validation and fatigue life data.  The program was performed in four tasks. Task I consisted of selecting analysis methods and design procedures for postbuckled metal and composite panels. The design methodology selected was semiempirical in nature and based on classical methods for metal panels with some modifications made for application to composite materials. The analysis procedures were coded in computer programs that can be used as efficient design tools. A series of tests on curved metal and composite panels were conducted in Task II to assess the accuracy												
20 DISTRIBUTION/AVAILABILITY OF ABSTRACT UNCLASSIFIED/UNLIMITED <input type="checkbox"/> SAME AS RPT <input checked="" type="checkbox"/> DTIC USERS <input type="checkbox"/>		21 ABSTRACT SECURITY CLASSIFICATION Unclassified										
22a NAME OF RESPONSIBLE INDIVIDUAL Patrick J. Alsup	22b TELEPHONE NUMBER (Include Area Code) (513) 255-6104	22c OFFICE SYMBOL AFWAL/FIBEC										

DD FORM 1473, 83 APR

EDITION OF 1 JAN 73 IS OBSOLETE.

Unclassified  
SECURITY CLASSIFICATION OF THIS PAGE

A



Unclassified

SECURITY CLASSIFICATION OF THIS PAGE

of the design procedures. The results from Task II showed that the semiempirical strength predictions were conservative for composite panels by approximately 30 percent. In Task III nonempirical analysis methods based on the principle of minimum potential energy were developed to predict the displacement and strain fields in curved metal and composite panels. These predictions were compared against the test data generated in Task II. The predictions showed the same trends as the measured data. However, the numerical values could not be accurately matched. Additional work necessary to enhance the predictive capability was identified. Under Task IV, the semiempirical design methodology was documented in a Preliminary Design Guide for postbuckled metal and composite panels.

The significant conclusions of the program and details pertaining to activities performed under the various tasks are documented in this final report designated as Volume I. The computer programs are documented in Volume II - Software Documentation. The preliminary Design Guide forms Volume III of the documentation for this contract.

Unclassified

SECURITY CLASSIFICATION OF THIS PAGE

### PREFACE

The work documented in this report was performed by Northrop Corporation, Aircraft Division, Hawthorne, California under Contract F33615-81-C-3708 sponsored by the Air Force Wright Aeronautical Laboratories, Flight Dynamics Laboratory, AFWL/FIBL. The work was performed in the period from September 1981 through August 1985. The Air Force Program Monitors were Capt. M. L. Becker (September 1981 to June 1983), Capt. M. Sobota (June 1983 to February 1985), and Lt. P. Alsup (February 1985 onwards) who reviewed and suggested improvements to the report.

Dr. B. L. Agarwal was the Northrop Program Manager and Principal Investigator until June 1983. From June 1983 onwards Dr. R. B. Deo was the Principal Investigator. The following Northrop personnel also contributed to the performance of the contract in their respective areas of responsibility:

E. Madenci/Dr. N. J. Kudva	Analysis
F. Uldrich	Specimen Fabrication
M. Kerbow	Testing
R. Cordero	Data Analysis/Graphics
K. H. Gonzalez/B. Tuzzolino	Documentation

The results of the program were used to develop a preliminary design guide for postbuckled structures. The Design Guide (Initial Release) is published separately as Volume III.



Accession For	
NTIS GRA&I	<input checked="checked" type="checkbox"/>
DTIC TAB	<input type="checkbox"/>
Unannounced	<input type="checkbox"/>
Justification	
By	
Distribution/	
Availability Codes	
Dist	Avail and/or Special
A-1	23
	Wend

## TABLE OF CONTENTS

<u>SECTION</u>	<u>PAGE</u>
PREFACE. . . . .	iii
LIST OF ILLUSTRATIONS. . . . .	vii
LIST OF TABLES . . . . .	xi
1 INTRODUCTION . . . . .	1
1.1 Background. . . . .	1
1.2 Program Objectives. . . . .	2
1.3 Program Summary . . . . .	2
1.4 Report Outline. . . . .	3
2 SELECTION OF ANALYTICAL METHODS. . . . .	5
2.1 Background. . . . .	5
2.2 Technology Assessment . . . . .	6
2.2.1 Semiempirical Static Analysis Methods. . . . .	6
2.2.2 Non-Empirical Static Analysis Methods. . . . .	20
2.2.3 Fatigue Analysis Methods . . . . .	27
2.3 Selection of Analytical Methods . . . . .	36
2.3.1 Compression Panels . . . . .	38
2.3.2 Shear Panels . . . . .	59
3 EXPERIMENTAL PROGRAM . . . . .	69
3.1 Introduction. . . . .	69
3.2 Design of Curved Test Panels. . . . .	70
3.2.1 Design Criteria. . . . .	72
3.2.2 Curved Shear Panel Design. . . . .	74
3.2.3 Curved Compression Panel Design. . . . .	84
3.3 Test Plan . . . . .	93
3.3.1 Test Matrix. . . . .	95
3.3.2 Instrumentation. . . . .	97
3.3.3 Test Fixture . . . . .	100
3.4 Fabrication of Composite Test Panels. . . . .	105
3.5 Test Results. . . . .	108
3.5.1 Compression Panel Static Tests . . . . .	108
3.5.2 Compression Panel Fatigue Tests. . . . .	116

## TABLE OF CONTENTS (Continued)

<u>SECTION</u>		<u>PAGE</u>
	3.5.3 Shear Panel Static Tests . . . . .	124
	3.5.4 Shear Panel Fatigue Tests. . . . .	131
4	DEVELOPMENT OF ANALYSIS METHODS. . . . .	137
	4.1 Introduction. . . . .	137
	4.2 Compression Panel Analysis. . . . .	137
	4.2.1 Geometry and Boundary Conditions . . . . .	138
	4.2.2 Strain Energy Expressions. . . . .	138
	4.2.3 Governing Equations. . . . .	142
	4.2.4 Numerical Solution Procedure . . . . .	154
	4.2.5 Displacement Predictions . . . . .	157
	4.3 Shear Panel Analysis. . . . .	157
	4.3.1 Panel Geometry and Assumptions . . . . .	160
	4.3.2 Strain Energy Expressions. . . . .	165
	4.3.3 Governing Equations and Solution Procedure . . . . .	170
	4.3.4 Displacement Predictions . . . . .	171
	4.4 Fatigue Analysis Approach . . . . .	172
	4.4.1 Metal Panels . . . . .	177
	4.4.2 Composite Panels . . . . .	179
5	DISCUSSION OF RESULTS. . . . .	181
	5.1 Introduction. . . . .	181
	5.2 Curved Panels Under Static Compression Load . . . . .	181
	5.3 Curved Panels Under Compression Fatigue Loading . . . . .	194
	5.4 Curved Panels Under Shear Loading . . . . .	194
	5.5 Curved Shear Panels Under Fatigue Loading . . . . .	211
	5.6 Discussion of Analysis and Test Data Correlation. . . . .	211
6	CONCLUSIONS. . . . .	215
	6.1 Design and Analysis Methodology for Curved Composite Post- buckled Panels. . . . .	215
	6.2 Design and Analysis Methodology for Curved Metal Post- buckled Panels. . . . .	216
	6.3 Recommendations for Future Work. . . . .	217
	REFERENCES . . . . .	218

TABLE OF CONTENTS (Continued)

<u>SECTION</u>	<u>PAGE</u>
APPENDIX A - COMPRESSION AND SHEAR PANEL STRAIN DATA . . . . .	226
APPENDIX B - ANALYSIS DETAILS. . . . .	284

# LIST OF ILLUSTRATIONS

<u>FIGURE</u>		<u>PAGE</u>
2.1	Metal Shear Panel Fatigue Data (Reference 3) . . . . .	28
2.2	Fatigue Crack Propagation in Metal Compression Panels (Reference 82). . . . .	30
2.3	Composite Shear Panel Fatigue Response . . . . .	31
2.4	Composite Compression Panel Fatigue Response . . . . .	33
2.5	Fatigue Response of Flat Panels Under Combined Loading (Reference 25) . . . . .	34
2.6	Axial Compressive Buckling (Reference 34) Coefficients for Long Curved Plates. . . . .	40
2.7	Skin Width $b_w$ for Composite Panel Initial Buckling Strain Calculations. . . . .	42
2.8	Crippling Stress $F_{cs}$ for Two Corner Sections Z, J and Channel Sections (Reference 34). . . . .	44
2.9	Plate Element Models of Hat- and J-Section Stiffeners. . . . .	46
2.10	Ply Drop-Offs in Hat-Section Stiffener . . . . .	49
2.11	Comparison of Analytical and Experimental Data for Stiffener Crippling. . . . .	56
2.12	Comparison of Analytical and Experimental Data for Composite Compression Panels . . . . .	58
2.13	Application of Tension Field Theory to Shear Panels. . . . .	60
3.1	Shear Panel Design Procedure . . . . .	75
3.2	Buckling Load of a Curved Graphite-Epoxy Plate Under Shear Loading ( $\underline{45}$ $\underline{2}$ /90/ $\underline{45}$ $\underline{2}$ ) Layup . . . . .	77
3.3	Buckling Load of a Curved Graphite/Epoxy Plate Under Shear Loading ( $\underline{45}$ /90/0/90/ $\underline{45}$ ) Layup. . . . .	78
3.4	Composite Shear Panel Design . . . . .	80
3.5	Shear Buckling Coefficient for Long Simply Supported Curved Plates (Reference 34). . . . .	82

# LIST OF ILLUSTRATIONS (Continued)

<u>FIGURE</u>		<u>PAGE</u>
3.6	Metal Shear Panel Configuration Stringers are AND10138-1206 and Frames are AND10138-1306 Aluminum Z-Sections . . . . .	83
3.7	Compression Panel Design Procedure . . . . .	85
3.8	Compression Load Structural Efficiency Comparison For Hat-, J-, and Blade-Configurations . . . . .	86
3.9	Composite Compression Panel Configuration. . . . .	89
3.10	Z-Section 7075-T6 Aluminum Stringer AND10138-1004 Configuration. . . . .	92
3.11	Metal Compression Panel Configuration. . . . .	94
3.12	Compression Panel Instrumentation. . . . .	98
3.13	Shear Panel Instrumentation. . . . .	99
3.14	Test Set-Up for Compression Panels . . . . .	101
3.15	Composite Compression Panel Instrumentation and Test Set-Up. . . . .	102
3.16	Shear Panel Test Fixture Schematic . . . . .	103
3.17	View of Test Fixture Showing Loading Arrangement and Test Panel. . . . .	104
3.18	Intermediate Step in Composite Shear Panel Fabrication Illustrating Frame and Stringer Mandrels Located on Skin Template . . . . .	106
3.19	Detail View of Frame Mandrels. . . . .	107
3.20	Shear Panel Assembly Prior to Cure . . . . .	109
3.21	Cured Composite Shear Panel. . . . .	110
3.22	Graphite/Epoxy Compression Panel Ready for Potting of the Ends . . . . .	111
3.23	Progression of Buckle Pattern With Load for Metal Compression Panel MC1. . . . .	113
3.24	Failed Metal Compression Panel MC1 . . . . .	117
3.25	Progression of Buckle Pattern with Load for Composite Compression Panel CC1 . . . . .	119
3.26	Composite Compression Panel CC1 Failure Mode . . . . .	122

# LIST OF ILLUSTRATIONS (Continued)

<u>FIGURE</u>		<u>PAGE</u>
3.27	Fatigue Cracks in Metal Panel MC4. . . . .	126
3.28	Diagonal Buckle Pattern in Metal Shear Panels. . . . .	127
3.29	Static Failure Mode of Curved Composite Shear Panel CS1. . . . .	128
3.30	Close-Up of Composite Shear Panel Failure by Stiffener/Web Separation . . . . .	129
3.31	Applied Torque to Panel Shear Flow Conversion Calibration. . . . .	130
3.32	Fatigue Failure Mode of Aluminum Shear Panel MS5 . . . . .	134
4.1	Comparison of Metal Compression Panel Test Data with Predictions	139
4.2	Metal Compression Panel Web Static Strain Response . . . . .	156
4.3	End-Shortening for Metal Compression Panels. . . . .	158
4.4	End-Shortening for Composite Compression Panels. . . . .	159
4.5	Curved Shear Panel Geometry and Coordinate System. . . . .	161
4.6	Assumed Out-of-Plane Displacement Parameters $\alpha$ , $\lambda$ , and $f$ . . . . .	163
4.7	In-Plane Deformation Parameters. . . . .	164
4.8	Out-of-Plane Displacement at Panel Center as a Function of Applied Shear Load for Metal Panel. SHRPAN1 Predictions. . . . .	173
4.9	Out-of-Plane Displacement at Panel Center as a Function of Applied Shear Load for Composite Panel. SHRPAN1 Predictions. . . . .	174
4.10	Out-of-Plane Displacement Contours for Metal Shear Panel. SHRPAN1 Predictions. . . . .	175
4.11	Out-of-Plane Displacement Contours for Composite Shear Panel. SHRPAN1 Predictions. . . . .	176
4.12	Life Prediction Methodology for Postbuckled Metal Panels . . . . .	178
4.13	Life Prediction Methodology for Postbuckled Composite Panels . . . . .	180
5.1	Comparison of Metal Compression Panel Test Data with Predictions. . . . .	183



# LIST OF ILLUSTRATIONS (Continued)

<u>FIGURE</u>		<u>PAGE</u>
5.2	Metal Compression Panel Web Static Strain Response . . . . .	185
5.3	Out-of-Plane Displacements of Metal Compression Panels . . . . .	186
5.4	Stiffener Axial Strains for Metal Compression Panels . . . . .	187
5.5	Comparison of Composite Compression Panel Test Data with Pre- dictions . . . . .	190
5.6	Composite Compression Panel CCl Web Strain Response. . . . .	191
5.7	Out-of-Plane Displacements for Composite Compression Panel CCl .	192
5.8	Stiffener Axial Strains for Composite Panel CCl. . . . .	193
5.9	Comparison of S-N Data for Metal and Composite Compression Panels . . . . .	195
5.10	Normalized Fatigue Response of Compression Panels. . . . .	196
5.11	Comparison of Metal Shear Panel Static Test Data with Predic- tions. . . . .	198
5.12	Metal Panel Web Maximum Shear Strains as a Function of Applied Load . . . . .	200
5.13	Stringer Strains for Metal Shear Panels. . . . .	201
5.14	Ring Strains for Metal Shear Panels. . . . .	202
5.15	Diagonal Tension Angle as a Function of Applied Load for Metal Shear Panels . . . . .	203
5.16	Comparison of Composite Shear Panel Static Test Data with Pre- dictions . . . . .	206
5.17	Composite Panel Web Maximum Shear Strains as a Function of Applied Load . . . . .	207
5.18	Stringer Strains for Composite Shear Panels. . . . .	208
5.19	Ring Strains for Composite Shear Panels. . . . .	209
5.20	Diagonal Tension Angle as a Function of Applied Load for Composite Shear Panels . . . . .	210
5.21	Normalized Fatigue Response Metal and Composite of Shear Panels.	212

# LIST OF TABLES

<u>TABLE</u>		<u>PAGE</u>
2.1	Summary of Experimental Data for Postbuckled Panels. . . . .	7
2.2	Summary of Life Prediction Models for Composites . . . . .	37
2.3	Correlation of Semiempirical Stiffener Crippling Predictions With Test Data . . . . .	54
2.4	Comparison of Analytical Predictions and Test Data for Stiffened Compression Panels . . . . .	57
2.5	Summary of Shear Panel Analysis Comparison with Test Data. . . .	67
3.1	Data Gaps in the Current Technology for Design and Life Analysis of Curved Postbuckled Panels . . . . .	71
3.2	Design Loads for Metal and Composite Test Panels . . . . .	73
3.3	Graphite/Epoxy Material Properties . . . . .	73
3.4	Composite and Metal Shear Panel Design Summary . . . . .	81
3.5	Composite and Metal Compression Panel Design Summary . . . . .	90
3.6	Compression and Shear Panel Test Matrix. . . . .	96
3.7	Composite and Metal Compression Panel Static Test Results. . . .	112
3.8	Composite and Metal Compression Panel Fatigue Test Results . . .	118
3.9	Composite and Metal Shear Panel Static Test Results. . . . .	125
3.10	Composite and Metal Shear Panel Fatigue Test Results . . . . .	132
5.1	Curved Metal Compression Panel Static Data . . . . .	182
5.2	Composite Compression Panel Static Test Data Correlation with Predictions. . . . .	189
5.3	Metal Shear Panel Static Test Data Correlation with Predictions.	197
5.4	Composite Shear Panel Static Test Data Correlation with Pre- dictions . . . . .	205

## SECTION 1

### INTRODUCTION

#### 1.1 BACKGROUND

Several recent studies have demonstrated that the structural efficiency of future USAF aircraft can be improved by taking advantage of the postbuckled strength of stiffened panels. A majority of these studies, performed under the auspices of the USAF, the U.S. Navy and NASA, have provided a sizeable data base on the static and fatigue behavior of postbuckled stiffened panels. The test data from the experimental studies have been used to verify the predominantly empirical design methodology for postbuckled panels and to establish static and fatigue failure characteristics of metal and composite panels. The results of the correlation between the semiempirical design methodology and the experimental data indicate several shortcomings in the analysis capabilities as well as lack of essential test data.

The application of existing postbuckling methodology to the design of advanced composite panels has resulted in unconservative designs due to the presence of additional failure modes, such as delamination in the skin, stiffener/web separation and compression failure of the skin. Such failure modes are not accounted for in the existing methodology. These deficiencies in the analysis and design methodology have to be corrected to realize the full weight savings potential of postbuckled designs.

Aircraft panels operating in the postbuckling range are usually curved. These panels are subjected to shear, compression (or tension), and a combination of compression (or tension) and shear loads. Extensive test data are available for flat metal and composite panels subjected to shear or compression loading. However, the test data for curved shear or compression panels are minimal and insufficient to develop and verify improved analysis methods. These gaps in the available test data need to be filled.

Damage tolerance and durability requirements for the design of U.S. military aircraft call for the economic life of an aircraft to be greater than the design service life when subjected to the design service loads. A fatigue design methodology for metal or composite postbuckled panels is not available and test data are sketchy or incomplete. Additional experimental data must be generated to identify and meet the fatigue requirements of postbuckled designs.

#### 1.2 PROGRAM OBJECTIVES

In view of the above postbuckling technology needs, a combined analytical and experimental program was undertaken to develop a unified design methodology, design validation data and fatigue life data for composite and metal panels operating in the postbuckled regime. The specific objectives of the program were to develop an experimentally validated analysis capability and simple to use, yet accurate, design procedures for curved metal and composite postbuckled panels loaded in compression or shear. Inherent in this program objective was the need to develop techniques to predict the initial buckling load, ultimate failure load and failure mode, and fatigue life of postbuckled panels.

The results of the design methodology development program are documented in this report.

#### 1.3 PROGRAM SUMMARY

The program plan was to first review the available analysis and design techniques for metal and composite panels and establish a design methodology for curved postbuckled panels loaded in compression or shear. This methodology was then used in designing curved panels for a test program to generate design validation and fatigue life data.

All panels were cylindrically curved and had a radius of 45 inches. The composite panels were stiffened with hat section stringers and in the case of the composite shear panels J-section frames were used as circumferential stiffeners. The composite compression panels were not circumferentially stiffened in the test section since they simulated the region between two adjacent bulkheads. The metal panels were stiffened with Z-section stringers

and in the case of shear panels circumferential Z-section frames. Fabrication of the composite panels was accomplished using specially designed tooling with careful attention paid to details at the stringer/frame intersection.

The test plan called for static and fatigue tests on the curved metal and composite panels loaded either in compression or in shear. The static test data were used to verify the semiempirical design methodology, whereas the fatigue test data were utilized to determine the fatigue failure modes and obtain load versus life data to formulate fatigue analyses approaches.

Comparison of the static test data with the semiempirical design methodology demonstrated a need to develop a more rigorous analysis procedure for postbuckled panels. In addition, the fatigue analysis method proposed requires that the local skin displacements be known. Therefore, rigorous analysis methods using the principle of minimum potential energy were developed for the compression and the shear panels. The predictions from the rigorous analysis are compared with the test data.

Finally, the semiempirical design methodology for curved composite and metal panels subjected to compression or shear loads in the postbuckled regime was documented in a Preliminary Design Guide.

#### 1.4 REPORT OUTLINE

The program was performed in four tasks. Task I consisted of selecting analysis methods and design procedures for postbuckled metal and composite panels. These methods were selected from the available technology on postbuckled structures design. The selected design methodology and an assessment of the technology available prior to the start of this program are documented in Section 2. Design of postbuckled composite and metal panels, panel fabrication and testing were accomplished in Task II entitled "Experimental Test Program." A description of Task II and the test data obtained are documented in Section 3. Task III consisted of comparing the test results with the predictions based on the design methodology selected in Task I, and of developing the more rigorous strain energy based analyses for the compression and shear panels. Under Task III, a fatigue analysis approach for postbuckled panels was also developed on the basis of the test data generated in

Task II. Development of the compression and shear panel analyses based on the principle of minimum potential energy is detailed in Section 4 along with the proposed fatigue analysis approaches. Correlation of test data with results of the analysis is discussed in Section 5. The Preliminary Design Guide developed in Task IV is published separately as Volume III of the Final Report. The program conclusions and recommendations for future work are summarized in Section 6.

## SECTION 2

### SELECTION OF ANALYTICAL METHODS

#### 2.1 BACKGROUND

The large deflections associated with postbuckled structures make the elementary theories of structural analysis inapplicable to determining the detailed stress field in such structures, and in general, closed-form or analytical solutions cannot be obtained. In current design practice, semi-empirical analysis methods are most widely used in sizing stiffened panels operating in the postbuckled range. The semiempirical analysis methods are attractive for use in actual design situations due to their simplicity, ease of application and the built-in conservatism in the static analysis results. The main drawback of these methods, besides the weight penalty associated with the conservatism in the analysis, is that they do not provide a detailed stress or displacement field in the postbuckled stiffened panels. Determination of the stress field is essential in formulating a viable fatigue analysis approach. A few numerical solutions have been attempted, and although these techniques provide the local displacements and stresses, they are cumbersome to use, and too expensive in terms of computer costs to be considered viable design tools.

The design and analysis approach adopted in this program was to review the available technology base on postbuckled metal and composite panels and then select a semiempirical methodology for modification and subsequent use in the test program. The purpose of the modifications was to extend the applicability of the analysis techniques, developed for metal panels, to composite panels. The semiempirical methodology was used to design the program test panels which in turn provided verification test data. Recognizing the previously mentioned drawbacks in the semiempirical techniques, development of a new non-empirical analysis methodology with the objective of predicting the total postbuckling behavior of compression or shear loaded panels was also undertaken. It was envisioned that the results of this rigorous analysis would find immediate application in formulating approaches to fatigue analysis

of postbuckled stiffened panels.

In this section, an assessment of the current technology related to design, analysis and fatigue life prediction of postbuckled structures is presented and the analytical methods selected for use in the program are detailed. The objectives of this technology assessment were: (a) to enable selection of promising analytical methods for further verification, and for test panel design; and (b) to compile test data that could be used in characterizing the fatigue behavior of postbuckled panels. The technology assessment was also used to select an approach to developing a non-empirical analysis methodology for postbuckled compression and shear panels.

## 2.2 TECHNOLOGY ASSESSMENT

An exhaustive review of several preliminary design studies and test programs was conducted towards selecting design methods for postbuckled metal and composite panels loaded in compression or shear. The currently available design and analysis methodologies were assessed for simplicity, accuracy and generality. The following paragraphs describe in a summary form the state-of-the-art methodology for design, analysis, and durability validation of postbuckled metal and composite panels.

### 2.2.1 Semi-Empirical Static Analysis Methods

The semi-empirical analysis methods evolved from an extensive data base for metal panels and their final form is a result of several modifications. The numerous sources of postbuckled panel test data surveyed and their contributions to the development of the semi-empirical analysis techniques are summarized in Table 2.1. A detailed discussion of the significant contributions is presented in the following paragraphs.

Shear Panels - The semi-empirical analysis and design method currently used for stringer stiffened panels loaded in shear or a combination of shear and compression loading has evolved over the years from the "tension field theory." This theory was originally conceived by Wagner (Reference 1) for thin flat metallic shear webs. Based on the results of several hundred tests, some empirical constants were introduced in this theory to broaden its applicability by Kuhn (Reference 2). The theory was extended to the analysis



TABLE 2.1. SUMMARY OF EXPERIMENTAL DATA FOR POSTBUCKLED PANELS (SHEET 1 OF 4)

REFERENCE	MATERIAL	PANEL GEOMETRY	LOAD CONDITION	STIFFENER/WEB ATTACHMENT METHOD	TEST ENVIRONMENT	TEST CONDITION	TEST FIXTURE	MERIT FOR ANALYSIS DEVELOPMENT (1)	REMARKS
KUHN (2)	ALUMINUM	FLAT	SHEAR	RIVETED	RTD (2)	STATIC	CANTILEVER AND SIMPLE SUPPORTED BEAM	3	LARGE NUMBER OF PANEL TESTS WITH VARIOUS GEOMETRIES FORM A SOLID BASE FOR ANALYSIS DEVELOPMENT
TSONGAS (3)	ALUMINUM	FLAT	SHEAR	RIVETED	RTD	STATIC AND FATIGUE	ECCENTRICALLY LOADED CANTILEVER BEAM	3	FOURTEEN BEAM TESTS WITH DIFFERENT WEB THICKNESSES FORM A USEFUL BODY OF EXPERIMENTAL DATA
BAREVICS (4)	ALUMINUM AND TITANIUM	FLAT	SHEAR	RIVETED	RTD	STATIC	ECCENTRICALLY LOADED CANTILEVER BEAM	3	TESTS ON TWO DIFFERENT MATERIAL SYSTEMS POINTED OUT SHORTCOMINGS OF TEN. JON FIELD THEORY
KUHN (2)	ALUMINUM	CURVED	SHEAR	RIVETED	RTD	STATIC	COMPLETE CYLINDER UNDER TORSION	3	A TOTAL OF 12 CYLINDERS WITH DIFFERENT WEB THICKNESSES AND STIFFENER THICKNESSES WERE EXAMINED
CURRENT PROGRAM	ALUMINUM	CURVED	SHEAR COMPRESSION	RIVETED	RTD	STATIC AND FATIGUE	TRIANGULAR BOX UNDER TORSION	3	TEST DATA DEMONSTRATED FATIGUE PROBLEMS OF METAL PANELS
PETERSON (5)	ALUMINUM	CURVED	COMBINED COMPRESSION AND SHEAR	RIVETED	RTD	STATIC	COMPLETE CYLINDER UNDER TENSION AND COMPRESSION	3	A TOTAL OF 5 TESTS EXAMINED THE EFFECT OF VARYING THE RATIO OF AXIAL COMPRESSION AND SHEAR LOADING ON PANEL BEHAVIOR
KAMINSKI (6)	BORON-EPOXY	FLAT	SHEAR	-	RTD	STATIC AND FATIGUE	PICTURE FRAME	1	TESTS DEMONSTRATED POST-BUCKLING STRENGTH OF COMPOSITE PANELS
FANT (7)	GRAPHITE-EPOXY	FLAT	SHEAR	-	RTD	STATIC	PICTURE FRAME	2	SEVERAL DIFFERENT LAMINATE CONFIGURATIONS AND THICKNESSES EXAMINED
PHIM (8)	GRAPHITE-EPOXY	FLAT	SHEAR	-	RTD	STATIC AND FATIGUE	PICTURE FRAME	2	SEVERAL DIFFERENT LAMINATE CONFIGURATIONS AND MATERIAL SYSTEMS EXAMINED
BHATIA (9)	GRAPHITE-EPOXY	FLAT	SHEAR	-	RTD	STATIC AND FATIGUE	PICTURE FRAME	2	SEVERAL DIFFERENT LAMINATE CONFIGURATIONS AND ASPECT RATIOS EXAMINED
FOREMAN (10)	GRAPHITE-EPOXY AND KEVLAR EPOXY	FLAT	SHEAR	-	RTD	STATIC AND FATIGUE	PICTURE FRAME	1	DATA PRIOR TO FAILURE MAY BE USEFUL
NOTES (1) MERIT OF TEST DATA 1-FAIR 2 GOOD, 3-EXCELLENT (2) RTD - ROOM TEMPERATURE DRY									

TABLE 2.1. SUMMARY OF EXPERIMENTAL DATA FOR POSTBUCKLED PANELS (SHEET 2 OF 4)

REFERENCE	MATERIAL	PANEL GEOMETRY	LOAD CONDITION	STIFFENER GEOMETRY	STIFFENER/WEB ATTACHMENT METHOD	TEST ENVIRONMENT	TEST CONDITION	TEST FIXTURE	MERIT FOR ANALYSIS DEVELOPMENT (1)	REMARKS
RICH (11)	GRAPHITE- EPOXY AND KEVLAR EPOXY	FLAT	SHEAR	-	-	RTD (2)	STATIC AND FATIGUE	ECCENTRICALLY LOADED CANTILEVER BEAM	3	STRENGTH DATA BELIEVED TO BE MORE RELIABLE THAN PICTURE FRAME TEST DATA
FAHRT (7)	GRAPHITE- EPOXY AND BORON- EPOXY	FLAT	SHEAR	HAT AND ANGLE	BONDED	RTD	STATIC	PICTURE FRAME	2	SEVERAL DIFFERENT PANEL WEB CONFIGURATIONS EXAMINED
LEHMAN (12)	GRAPHITE- EPOXY	FLAT	SHEAR	HAT	COCURED	RTD	FATIGUE	PICTURE FRAME	1	SINGLE PANEL TEST TO ESTABLISH POSTBUCKLING STRENGTH
AGARWAL (13)	GRAPHITE- EPOXY	FLAT	SHEAR	HAT AND I-SECTION	COCURED	RTD	STATIC AND FATIGUE	ECCENTRICALLY LOADED CANTILEVER BEAM	3	VARIATIONS IN STIFFENER SPACING AND SHAPE PROVIDE VALUABLE EXPERIMENTAL DATA
AGARWAL (14)	GRAPHITE- EPOXY	FLAT	SHEAR	HAT	COCURED	KTD	STATIC AND FATIGUE	ECCENTRICALLY LOADED CANTILEVER BEAM	3	REPLICATED TESTS PROVIDE STATISTICALLY RELIABLE DATA
OCTROM (15)	GRAPHITE- EPOXY	FLAT	SHEAR	J-SECTION	COCURED	RTD	STATIC AND FATIGUE	PICTURE FRAME	2	PANEL FAILURE AFFECTED BY STRESS CONCENTRATION IN THE DIAGONAL CORNERS
REIERI (16)	GRAPHITE- EPOXY	FLAT	SHEAR	HAT	COCURED	RTD	STATIC AND FATIGUE	MODIFIED PICTURE FRAME	2	TEST DATA MAY HAVE BEEN AFFECTED BY TEST FIXTURE DESIGN
DASTIN (17)	GRAPHITE- EPOXY	FLAT	SHEAR	HAT	COCURED AND STITCHED	RTD, ETD (3) ETW (4)	STATIC AND FATIGUE	PICTURE FRAME	2	UNREPLICATED UNINSTRUMENTED TESTS TO ESTABLISH THE EFFECT OF DIFFERENT DESIGN VARIABLES
SURDENAS (18)	GRAPHITE- EPOXY	FLAT	SHEAR	HAT AND BEAD	COCURED	RTD, RTW (5) ETW	STATIC AND FATIGUE	ECCENTRICALLY LOADED CANTILEVER BEAM	3	SIX UNREPLICATED TESTS TO ESTABLISH THE EFFECT OF FATIGUE LOADING AND ENVIRONMENTAL EXPOSURE
FOREMAN (19)	KEVLAR- WEB AND GRAPHITE STIFFENERS	FLAT	SHEAR	HONEYCOMB FILLED HAT	COCURED	RTD (2)	STATIC AND FATIGUE	CANTILEVER BEAM	1	TEST DATA AFFECTED BY POOR PANEL QUALITY
NOTES (1) MERIT OF TEST DATA 1 FAIR, 2 GOOD, 3-EXCELLENT (2) RTD - ROOM TEMPERATURE DRY (3) ETD - ELEVATED TEMPERATURE DRY (4) ETW - ELEVATED TEMPERATURE WET (5) RTW - ROOM TEMPERATURE WET										

TABLE 2.1. SUMMARY OF EXPERIMENTAL DATA FOR POSTBUCKLED PANELS (SHEET 3 OF 4)

REFERENCE	MATERIAL	PANEL GEOMETRY	LOAD CONDITION	STIFFENER GEOMETRY	STIFFENER/WEB ATTACHMENT METHOD	TEST ENVIRONMENT	TEST CONDITION	TEST FIXTURE	MERIT FOR ANALYSIS DEVELOPMENT (1)	REMARKS
AGARWAL (20)	GRAPHITE-EPOXY	FLAT	SHEAR	HAT	COCURED	RTD	FATIGUE	ECCENTRICALLY LOADED CANTILEVER BEAM	3	TESTS DEMONSTRATED CONCEPTS FOR IMPROVING STIFFENER/WEB INTERFACE STRENGTH
BHATIA (21)	GRAPHITE-EPOXY	FLAT	COMBINED SHEAR, COMPRESSION AND BENDING	HAT	COCURED	RTD	STATIC AND FATIGUE	ECCENTRICALLY LOADED CANTILEVER BEAM	3	ONLY TEST DATA CURRENTLY AVAILABLE FOR COMPOSITE PANELS SUBJECTED TO COMBINED LOAD
GRIMES (22)	GRAPHITE-POLYIMIDE	FLAT	SHEAR	HAT	COCURED	RTD (3) RTW (4)	STATIC AND FATIGUE	ECCENTRICALLY LOADED CANTILEVER BEAM	3	SEVERAL PANELS ARE TO BE TESTED TO EVALUATE THE NEW MATERIAL SYSTEM
AGARWAL (23)	GRAPHITE-EPOXY	FLAT	SHEAR	HAT	COCURED	RTD	STATIC AND FATIGUE	ECCENTRICALLY LOADED CANTILEVER BEAM	3	A PROGRAM CURRENTLY UNDERWAY AT NORTHROP PANELS TO BE SUBJECTED TO SPECTRUM FATIGUE LOADING. REPLICATED TESTS WILL PROVIDE RELIABLE DATA
GARRETT (24)	GRAPHITE-EPOXY	FLAT	SHEAR	HAT	DIFFERENT IMPROVEMENT CONCEPT TO BE EXAMINED	RTD	STATIC AND FATIGUE	MODIFIED PICTURE FRAME	3	SEVERAL DIFFERENT STIFFENER/WEB INTERFACE IMPROVEMENT CONCEPTS TO BE EXAMINED
E'ES (25)	GRAPHITE-EPOXY	FLAT	COMBINED SHEAR AND COMPRESSION	HAT	COCURED	RTD ETW	STATIC AND FATIGUE	BOX BEAM	3	EXPERIMENTAL DATA TO BE GENERATED FOR PANELS SUBJECTED TO COMBINED LOADING. REPLICATED TESTS TO PROVIDE RELIABLE DATA
STARNES (26)	GRAPHITE-EPOXY	FLAT	COMPRESSION	I-SECTION	COCURED	RTD	STATIC	FLAT END TESTING	3	VARIOUS DESIGN CONFIGURATIONS PROVIDE USEFUL TEST DATA
GARRETT (27)	GRAPHITE-EPOXY	FLAT	COMBINED COMPRESSION AND SHEAR	HAT	COCURED	RTD ETW	STATIC AND FATIGUE	TRIANGULAR BOX	3	REPLICATED TESTS PROVIDE USEFUL DATA BASE
FANT (7)	GRAPHITE-EPOXY AND BORON-EPOXY	CURVED	SHEAR	-	-	RTD	STATIC	COMPLETE CYLINDER IN TORSION	2	ONE GRAPHITE AND ONE BORON PANEL TESTED TO DEMONSTRATE THE POST-BUCKLING STRENGTH OF CURVED PANELS

NOTES (1) MERIT OF TEST DATA 1-FAIR, 2-GOOD, 3-EXCELLENT  
(2) RTD - ROOM TEMPERATURE DRY (3) RTW - ROOM TEMPERATURE WET  
(4) ETW - ELEVATED TEMPERATURE WET

TABLE 2.1. SUMMARY OF EXPERIMENTAL DATA FOR POSTBUCKLED PANELS (SHEET 4 OF 4)

REFERENCE	MATERIAL	PANEL GEOMETRY	LOAD CONDITION	STIFFENER GEOMETRY	STIFFENER/WEB ATTACHMENT METHOD	TEST ENVIRONMENT	TEST CONDITION	TEST FIXTURE	MERIT FOR ANALYSIS DEVELOPMENT (1)	REMARKS
H0 (28)	KEVLAR-EPOXY	CURVED	SHEAR	-	-	RTD (2)	STATIC	COMPLETE CYLINDER IN TORSION	2	VERY THIN KEVLAR-EPOXY PANELS DEMONSTRATED POST-BUCKLING STRENGTH
AGARWAL (29)	GRAPHITE-EPOXY	CURVED	COMPRESSION	HAT	COCURED	RTD	STATIC AND FATIGUE	FLAT END TESTING	2	POSTBUCKLING STRENGTH UNDER COMPRESSION LOADING DEMONSTRATED
AGARWAL (30)	GRAPHITE-EPOXY	CURVED AND FLAT	COMPRESSION	HAT	COCURED	RTD	STATIC AND FATIGUE	FLAT END TESTING	3	REPLICATED TESTS DEMONSTRATED THE USEFULNESS OF CURRENT DESIGN METHODS AND PROVIDED EXTENSIVE STRAIN DATA
HINKLE (31)	GRAPHITE-EPOXY	CURVED	COMPRESSION	HAT	COCURED	RTD	STATIC AND FATIGUE	FLAT END TESTING	3	REPLICATED TESTS PROVIDED USEFUL EXPERIMENTAL DATA
CURRENT PROGRAM	GRAPHITE-EPOXY AND ALUMINUM	CURVED R = 45 IN	COMPRESSION AND SHEAR	HAT	COCURED	RTD	STATIC AND FATIGUE	FLAT END TESTING AND TRIANGULAR BOX	3	REPLICATED TESTS PROVIDED USEFUL EXPERIMENTAL DATA
GARRETT (32)	GRAPHITE-EPOXY	CURVED R = 42 IN R = 21 IN	COMBINED COMPRESSION AND SHEAR	HAT	COCURED	RTD ETW	STATIC AND FATIGUE	TRIANGULAR BOX	3	REPLICATED TESTS PROVIDED USEFUL EXPERIMENTAL DATA
NOTES (1) MERIT OF TEST DATA 1-FAIR, 2-GOOD, 3-EXCELLENT (2) RTD - ROOM TEMPERATURE DRY										

of curved panels as well. The empirical constants were chosen such that the theory yields conservative results over the entire range of its applicability.

The tests conducted by Kuhn (Reference 2) at NACA generated elaborate experimental data which were used to formulate the theory, while tests conducted throughout the industry verified the strength predictions. The flat beams tested by NACA may be divided into three groups: small but heavily loaded beams (12 inches deep); medium-sized beam (25 or 40 inches deep), which formed the largest group; and large beams (75 inches deep).

Small but heavily loaded beams were tested using a simply supported beam loaded at the beam center. The lateral movement of the compression chords was restricted to prevent lateral buckling. The medium sized and large beams were tested as eccentrically loaded cantilever beams. Uprights or stiffeners on these panels consisted of single or double angles or Z-sections. A number of variations in upright and web geometry were tested. The experimental data generated from these tests are well documented in Reference 2 and are quite useful for a design methodology development over a large spectrum of panel configurations.

In the late 1960's, the results of 14 full-scale shear beams were reported in Reference 3. The beams had thin, chem-milled aluminum webs with lands to which lipped and unlipped Z-stiffeners and T-flanges of the same material were riveted. The web and stiffener thicknesses were varied to verify the tension field theory. The panels were tested at Room Temperature Dry (RTD) conditions through the use of an eccentrically loaded cantilever beam. The load was incremented in small steps. Between increments the load was dropped to zero to observe permanent buckling in the web. Based upon the results of static tests some modifications to the tension field theory were recommended.

As part of an SST technology program a number of aluminum and titanium shear panel tests were conducted as discussed in Reference 4. Results of 18 aluminum and titanium shear panel tests were reported. Panels were tested through the use of eccentrically loaded cantilever beams. The

test panels consisted of angle, J- and Z-section stiffeners which were riveted to the panel web. The aluminum and titanium panels had identical configurations to evaluate the usefulness of tension field theory to accommodate different material systems. The tests conducted on aluminum and titanium panels under this program pointed out deficiencies of tension field theory and provided very useful data for future analysis development.

Almost all of the information available on curved web systems in diagonal tension has been obtained on circular cylinders tested in torsion. Because cylinders are more expensive to manufacture and test than plane web beams, the total number of cylinder tests is rather small. The tension field theory for curved panels has thus seen a limited verification. A total of 12 tests were reported in Reference 2. In these tests an unconventional arrangement of double stringers was used to eliminate bending stresses in the stringer. The rings were made relatively large to preclude ring failure. All the cylinders tested were 15 inches in radius, a dimension which is not quite representative of real aircraft panel configuration. However, variety of ring spacings and web thicknesses were tested. All cylinders were tested statically under RTD conditions. The results of these cylinder tests are well documented in Reference 2 and have been used to modify the tension field theory for application to curved web systems.

The only results available for metal panels subjected to combined loading are reported in Reference 5. Five cylinders were tested under combined compression and shear loading. All cylinders were identical in construction and geometry. The cylinders were 15 inches in radius and contained Z-section stringers and rings which were bolted to the cylinder web. The ratio of torsional and compression load was varied for each cylinder. All the cylinders were tested statically under RTD conditions. The results of these tests are uniquely suited to verification of analyses for metal curved panels under combined loading.

Data from the tests described in the preceding paragraphs (References 2 through 5) were used to examine the validity of the tension field theory. The results showed that the internal loads predicted by the tension field theory were conservative by as much as 50 percent for aluminum beams and by as much as 90 percent for the titanium beams. In some

cases, failure load predictions based on local crippling of stiffeners were found to be unconservative. The primary reason for this unconservatism in predicting stiffener failure was the inability of tension field theory to accurately compute stresses in the eccentric stiffeners, especially for panel loads several times the initial skin buckling load.

The introduction of advanced composite materials as viable candidates in airframe usage has stimulated a large number of studies in recent years to determine their postbuckling behavior. One of the earliest demonstrations of the postbuckling strength of composite materials was presented in Reference 6. Several boron/epoxy unstiffened shear panels were tested statically and under fatigue loading at load magnitudes several times their initial buckling load. In similar studies in References 7, 8 and 10 the postbuckling strength of graphite/epoxy and Kevlar/epoxy materials was demonstrated. The test data for composite flat shear panels were obtained in these studies through the use of picture frame test setups. This test setup results in the introduction of severe stress concentrations in the diagonal corners, which influence the panel failure load as well as the mode of failure. Thus, the test data generated in the above studies are of limited use for the purpose of failure analysis development and strength verification. However, the test data are useful in determining the panel response before failure. Some of the unstiffened composite shear panel data were obtained from tests in an eccentrically loaded cantilever beam setup. Although the strain data generated in these tests are not extensive, the data are more reliable and suited to failure analysis verification.

Several composite stiffened flat panels have been tested under shear loading over the past decade through the use of various test methods. In Reference 7, several panels containing bonded hat and angle section stiffeners were examined. The panel web thickness was varied to study its effect on postbuckling behavior. The panels were tested in a picture frame. Although severe stress concentrations affected most of the panel failure modes, some panels failed away from the region of stress concentrations. An examination of these results indicates that variations in panel thickness are most influential in determining the magnitude of postbuckling deformations which a panel can sustain. Panels containing thin webs can sustain loads much higher than their initial buckling load without failure, as compared to

panels containing thicker webs. For example, a panel containing a 4-ply web failed at a load of 10 times its initial buckling load, whereas a similar panel containing an 8-ply web failed at a load 5 times its initial buckling load. The failures in most cases were due to stiffener/web separation. The stiffener shape, as would be expected in practical structural designs, does not seem to affect the failure load or mode of failure in any significant way.

In Reference 13, the influence of various design parameters on the behavior of composite tension field panels was investigated. The stiffener spacing was varied to change the onset of initial buckling load. The stiffener shape was varied to study the differences between the behavior of a panel containing a closed section ("hat") and an open section ("I") stiffener. The graphite-epoxy stiffened panels in this study were designed using the metal panel tension field theory with modifications that account for the directional dependence of the composite web moduli. The panels were tested under static and constant-amplitude fatigue loading. The test results were used to verify the design methodology. Two failure modes somewhat different from metal panel failure modes were discovered. One mode of failure, stiffener/web separation, was due to separation of stiffeners from the panel web. The second mode, compression failure, was due to deep buckles resulting in large compressive stresses in the web corners. The test fixture used in this study was an eccentrically loaded cantilever beam which in Reference 2 has been demonstrated to apply a uniform shear to the panel. The stiffener shape (Hat or I-section) did not seem to affect panel postbuckling behavior. Additional static tests on similar panels were performed in Reference 14. Heavily instrumented and carefully replicated tests established the static behavior of the panels. In a similar manner, the fatigue behavior of identical panels was studied for panels subjected to fully reversed fatigue loading. The panels consisted of cocured hat stiffeners. The panel failure was due to stiffener/web separation. These test data proved valuable for analysis verification and modifications.

In Reference 15, J-stiffened composite shear webs were examined. The test specimen contained three integrally cocured J-stiffeners. The panels were tested statically as well as under constant-amplitude fatigue loading (with no load reversal). The test setup used for testing these panels was



a "picture frame." The statically tested panels failed prematurely due to separation of the stiffeners from the panel skin in the diagonal corners of the test fixture. The results of these tests may be useful in predicting the lower bound of panel strength.

In Reference 16, the test specimens contained two hat stiffeners (simulating a fuselage panel), and two blade stiffeners (simulating the fuselage frames or bulkheads). The panels were tested through the use of a modified picture frame in which the load is applied along one edge, as opposed to along the panel diagonal in a conventional picture frame test setup. The panels tested statically under this program failed due to separation of the blade stiffeners from the skin. The hat stiffeners were unaffected. From phenomenological considerations it would seem logical for stiffener/web separation to occur between hat stiffeners and the panel skin where maximum peel and interlaminar shear stresses are introduced due to the buckles. The relative magnitude of peel and interlaminar stresses should be small near the blade stiffeners. Thus, the blade stiffener/skin separation mode of failure was not anticipated.

In a recently completed Advanced Composite Center Fuselage Program (References 17 and 18), a few graphite/epoxy stiffened and unstiffened shear panels were tested. The tests were conducted on panels subjected to different environmental conditions as well as on panels containing impact damage. None of the test conditions was replicated. Because the panels were tested as part of a design verification program, no attempt was made to obtain extensive strain distributions or to replicate test conditions. Although the test results have limited value in analysis verification, they do provide valuable design data. Evaluation of a variety of design concepts and stiffener/web interface improvements to increase the strength of post-buckled composite panels was conducted in References 19 through 25.

In Reference 19, a Kevlar panel with embedded graphite plies in the stiffener flanges was examined for postbuckling strength. However, uncertainty in the panel quality casts some doubt on the reliability of the test results.

The shear panels tested in Reference 20 incorporated a design improvement at the stiffener/web interface. The improvement consisted of

applying a single layer of FM-300 film adhesive between the interface before the panel was cured. Another panel was fabricated with an extra layer of 3501-6 resin at the interface. Both panels when tested showed significant improvement in the stiffener/web interface strengths.

The postbuckling behavior of flat stiffened multibay composite panels was examined in Reference 21. The panels were subjected to a combination of inplane shear, compression, and bending loads. Because test results for panels under combined load are rare in the literature, the results of this study are valuable for preliminary analysis verification. The panels tested under this program consisted of a 10-ply graphite/epoxy web with cocured hat section stringers and bead section frames. The panels were designed to buckle at 30 percent of the design limit load. Extensive instrumentation was provided to measure the stress distribution as well as the postbuckling behavior. A significant loss in the panel initial buckling load was reported due to fatigue loading.

The postbuckling behavior of graphite/epoxy polyimide panels was examined under a Navy contract (Reference 22). The panels in this program were identical to the panels tested earlier in Reference 14 except for the materials. The results of this program showed that the strength of polyimide materials under out-of-plane loads was rather poor. This poor strength was manifested as skin/stiffener separation which was a severe problem in these panels.

As part of the Wing/Fuselage program (Reference 25), several composite stiffened flat panels were designed, fabricated and tested. These panels consisted of two cocured hat stiffeners. The overall panel dimensions were 22 by 26 inches. A total of 12 panels were tested to determine the postbuckling behavior under combined compression and shear loading. Replicated tests were used to examine the static as well as fatigue behavior under RTD conditions as well as under Elevated Temperature Wet (ETW) conditions. A flight by flight spectrum loading typical of a Mach 2 fighter aircraft was used to study durability of these panels for two lifetimes of fatigue loading. The results of this study are potentially useful in developing a design methodology for postbuckled panels subjected to combined loading.

Another design improvement for the stiffener/web interface was examined in Reference 24. The results of this study show that tailoring the skin/stiffener interface results in improved fatigue life. The tailoring consisted of tapering the flanges of the stiffeners at the interface with the skin. This tapering was accomplished by selectively dropping off the flange plies. The influence of environment and combined loads on flat composite stiffened panels is examined in Reference 27. This study is currently in progress and will provide much needed data for analysis development and verification.

The analysis methodology for curved composite panels under shear loading is still in its infancy. This is primarily due to a lack of reliable, detailed test data. The postbuckling strength of curved composite shear panels was demonstrated in Reference 7 where a graphite/epoxy and a boron/epoxy panel were tested through the use of a cylinder torque test. These data in conjunction with data from Reference 27 and those being generated in Reference 32 will prove valuable in verifying the applicability of the modified tension field theory to curved composite shear panels.

Compression Panels - The semiempirical postbuckling analysis of flat and curved stiffened panels loaded in compression is generally done in steps because it involves several complexities which are difficult to account for simultaneously. The method normally used to analyze metal panels is in four parts:

1. Determine the panel initial buckling load.
2. Determine the compressive strength of the stiffener alone.
3. Determine the effective width of the skin for a load equal to the compressive strength of the stiffener alone.
4. Determine the total load carried by the panel by taking into account the load on the stiffener plus the effective width of the skin, plus the critical buckling load of the skin.

The above method requires calculation of the panel buckling load, the behavior of the skin after buckling and the failure strength of a column of any arbitrary shape. For design purposes, the above process is generally repeated several times to obtain positive margins on all structural elements.

Analytical and semiempirical methods for predicting the initial buckling load of the skin are well developed for metal and composite panels and are extensively documented in References 34 through 39, for example. These methods vary widely in rigor and accuracy. The analysis methods developed for metals up to the early 1950's and documented in References 34 and 35, are semiempirical in nature and are based on the results of an extensive test data base.

Several more rigorous analytical methods were made possible by the evolution of high-speed digital computers. Some of the most recent and advanced analysis methods for linear bifurcation buckling analysis are described in References 40, 41 and 42 (Computer codes SX8, BUCLASP2, and VIPASA). Computer code SX8 is based upon the Rayleigh-Ritz energy principle for analysis of flat composite and metal stiffened panels. The stiffeners are assumed to be axial members and their effect on panel behavior is included by taking into consideration the bending and torsional stiffnesses of the discrete stiffeners in the energy expression for the panel. In doing so, the effects of stiffener shape are neglected. The main advantage of this method is that arbitrary boundary conditions along the panel edges can be analyzed.

The computer codes BUCLASP-2 and VIPASA (References 41 and 42) are quite similar to each other except in their ability to solve cases with different loading and boundary conditions. These methods are based on solving exact force-displacement relations for a plate-strip element with the assumption of simple support boundary conditions along the edges normal to the longitudinal direction and arbitrary boundary conditions along the longitudinal edges. An assembly method, similar to the one used in finite element analysis, is used to generate any desired panel configuration. The advantage of this method of analysis is that both general and local instability modes can be simultaneously predicted. Additionally, any combination of

local and general instability modes, which results in lower buckling loads, can also be predicted. This method of analysis was used very successfully to correlate experimental data for hat-stiffened and J-stiffened graphite-epoxy compression panels in References 43 and 44.

The analytical methods for determining the onset of buckling for curved-stiffened panels are limited in number and have developed along lines similar to the corresponding methods for flat panels. The methods described in References 41, 42 and 45 (Computer codes BUCLASP-2, VIPASA, and SS8) have been used more recently throughout the aircraft industry for metal and composite panels. These methods can also be used for flat-stiffened panels.

In order to predict stiffened panel behavior after initial buckling and the ultimate compressive strength of stiffeners, semiempirical techniques have to be utilized. The semiempirical methodology for predicting local buckling and crippling strength of metal stiffeners has been derived from a large data base and is documented in References 34 and 39 for various stiffener configurations. Test data on the crippling strength of composite stiffeners are sparse and as a result no definitive analysis techniques exist. One approach suggested in Reference 46 is based on tests performed on several composite stiffener elements. These tests included plates with both sides simply supported as well as plates with one edge free and the other edge simply supported. In Reference 46, the following empirical equation was suggested for use in predicting the crippling strength of composite plates:

$$F_{cc}/F_{cr} = \alpha(F_{cu}/F_{cr})^\beta$$

In the above equation,  $F_{cc}$  is the crippling stress,  $F_{cr}$  is the theoretical initial buckling stress, and  $F_{cu}$  is the plate compressive strength. The values of  $\alpha$  and  $\beta$  are material-dependent constants. The values of these constants for AS/3501-6 and T300/5208 graphite/epoxy systems were obtained in Reference 46 by fitting a curve to the test data. Validity of the empirical equation in predicting the crippling strength of built-up sections was demonstrated in Reference 46 by tests on square composite tubes.

Generally, metal compression panels sized using the above approach are conservatively designed. In recent studies (References 29 and 30), composite compression panels were designed using the above approach. The panels consisted of cocured hat-stiffeners and were designed to buckle at loads significantly below the panel ultimate strength. The methods used for determining initial buckling load and stiffener crippling strength were those mentioned above. The replicated tests indicated that the analysis methods were sufficiently accurate, although on the conservative side. However, additional verification of the semiempirical methodology for composite panels was necessary and, therefore, carried out in this program. Test data obtained in References 26, 29 through 31, 47 and 48 were used for verification. This process of correlating the data base with the semiempirical predictions, resulted in some modifications to the crippling strength prediction equation given above. These results and modifications are discussed in Section 2.3.

#### 2.2.2 Non-empirical Static Analysis Methods

Analysis of stringer stiffened panels loaded beyond skin buckling requires solution of nonlinear equations and no closed-form expressions describing the response can be obtained. Thus, numerical methods must be resorted to. The numerical methods of solution are generally iterative in nature, and their efficiency and utility are limited by the number of unknown variables in the solution process. Two of the most commonly used nonempirical solution methods for postbuckling analysis are Finite-Difference/Finite Element Methods (FD/FEM) and Rayleigh-Ritz type methods. Several applications of these techniques to postbuckled structures are discussed in the following paragraphs.

Finite Difference/Finite Element Methods - The main advantage of using FD/FEM is that several large computer codes exist (e.g., NASTRAN, STAGS, ANSYS) and are easy to access in the aerospace industry. However, a few basic problems in using these techniques make them undesirable for design purposes. The problems are related to questions of accuracy, efficiency, and convergence.

The accuracy of the finite element solution method depends upon the type and number of finite elements used to model structural behavior. Since the structural behavior is not known in advance, a general practice is to start with a reasonably fine mesh size and refine it subsequently to establish the accuracy of the solution. Thus, the solution process can be expensive if several such iterations are needed. The analytical solutions of problems involving large deflections are iterative in nature by themselves and this added iteration can make the solution economically unfeasible.

The efficiency of the finite element solution depends upon the nature of the problem and also upon the mesh size used to model structural response. For example, in order to model the stiffener/web separation, three-dimensional finite elements must be used in the interface area. Since the thickness of the interface is quite small, a large number of elements will be required in this region to avoid numerical difficulties as well as to model the behavior accurately. Recent experience at Northrop and results in the literature indicate that the interface stresses are sensitive to element size in structures involving small displacements. It can be anticipated that similar or even worse difficulties will be encountered in panels subjected to postbuckling deformations. Again due to the iterative nature of the solution process, a large number of elements can make the solution economically unfeasible.

The governing nonlinear equations for postbuckled structures are solved incrementally. A general practice is to increase the applied load or displacement in small increments with the size of these increments determining the progress of the solution towards the maximum applied load. Since the increment size is not known in advance, several trials are generally needed to obtain a convergent solution. Convergence difficulties are also encountered due to the size of the mesh used in making a geometric representation of the problem. Several such convergence difficulties have been reported in References 49 through 57 and are discussed below. Another simplifying assumption made in the application of FD/FEM to postbuckled structures is to model the skin separately without regard to the interaction effects of the skin and the stringers. Similar drawbacks also apply to finite difference solution methods.

Due to the difficulties encountered in the use of FD/FEM methods, most of the studies reported in the literature on postbuckled structures have been conducted making several simplifying assumptions. One of the most common assumptions made is to model the skin of the skin-stringer panel separately, without regard to the interacting effect of skin and stringers.

Sharifi (Reference 49) modeled the behavior of an unstiffened shear panel subjected to postbuckling loads, using finite elements, and showed that the postbuckling deflections could be predicted quite accurately. In a similar study by Bhatia (Reference 9) the STAGS program was used to predict the postbuckling behavior of composite shear webs. In these studies no attempt to predict failure was made. Turney and Wittrick (Reference 50) and Rushton (Reference 51) used a finite difference iterative method known as "dynamic relaxation" for the postbuckling analysis of square plates subjected to uniaxial compression and shear. Rectangular finite elements with bi-cubic Hermitian interpolation functions were used in Reference 52 to study the postbuckling behavior of uniaxially compressed sandwich panels.

Postbuckling behavior of stiffened shear webs was also studied by Stein and Starnes (Reference 53) through the use of the STAGS computer code. They conducted parametric comparisons on the efficiencies of metal and composite shear webs loaded up to about twice the buckling load. Several convergence difficulties were pointed out. This study demonstrated the usefulness of STAGS in performing postbuckling stress analysis, but failed to establish the accuracy of the solution process.

Vestergren and Knutsson (Reference 54) also used STAGS to study the postbuckling behavior of unstiffened compression and shear panels. The initial buckling loads were predicted quite accurately for compression as well as shear panels using the bifurcation analysis. However, the failure load predicted for compression panels was twice the experimentally obtained value. No data were presented for the failure load predictions of shear panels. Again, several difficulties in the use of computer code STAGS for analysis purposes were acknowledged.



The change in stiffness of a plate loaded under combined loading was discussed by Rothwell and Allahyari (Reference 55). The finite element analysis used in this reference provided guidelines for minimizing the loss of the beam flexural stiffness as a result of web buckling.

The postbuckling behavior of a composite panel shear web (excluding the stiffeners) was modeled in Reference 13 using the computer code NASTRAN. In this study, the web was assumed to be simply supported on all four edges. The analytically obtained displacements and strains in the postbuckling regime were shown to compare favorably with experimental values. Web rupture due to compressive stresses resulting from deep buckles was shown to be predictable. The analytical results in this study indicated a concentration of out-of-plane constraint forces in the diagonal corners where failure due to stiffener/web separation was observed. Since the stiffener/web interface was not modeled in the NASTRAN analysis, no accurate prediction of failure due to stiffener/web separation was made. Further attempts to enlarge the model to include the total panel behavior had to be aborted due to convergence difficulties. A NASTRAN finite element analysis of postbuckled shear panels was also attempted in Reference 16. The initial buckling load was shown to agree quite well with the experimental data. However, the analysis attempt was again aborted above 150 percent of the initial buckling load due to convergence difficulties.

In Reference 29, the postbuckling behavior of a composite stiffened compression panel was modeled through the use of the large deflection theory of NASTRAN. A convergence difficulty resulting from using a relatively coarse mesh size was encountered after the load exceeded twice the initial buckling load, and the solution attempt was aborted. However, a fairly good correlation with experimental data was observed for the results obtained.

Several recent attempts have been made at improving the efficiency and reducing the convergence difficulties of finite difference/finite element methods (References 56 and 57), but their implementation as a design tool in the near future is unlikely.

Rayleigh-Ritz Type Methods - These methods are widely used to model the behavior of complex structures, since they are conceptually simple

to use. The displacement field is approximated by assumed functions with unknown coefficients. The number of equations to be solved is reduced significantly when compared to the finite element methods, thus, reducing the computation time and cost. Furthermore, once the problem is formulated, parametric studies can be conducted with little additional cost. However, there are some difficulties in using this approach also. The main difficulty arises from selecting the deformed structural shape. This is usually resolved by selecting a shape which is a combination of several possible shapes. The experimentally observed behavior greatly enhances this selection process. The difficulty, which is common to all numerical methods (finite element methods as well), is that the computed deflections may be quite accurate, but the computed strains tend to be in error. This difficulty can be rectified by increasing the number of terms in the assumed displacement function. This increases the computation time required, but the relative magnitude of the increase is quite small for the Rayleigh-Ritz type of analysis as compared to the finite element analyses. However, since the advantages overshadow the disadvantages in a Rayleigh-Ritz solution, several such solution methods have been attempted over the years. As discussed below, these studies have addressed different aspects of the postbuckling problem.

The Rayleigh-Ritz technique was used to analyze an incomplete tension field stiffened beam by Denke (Reference 58). The wave form of the buckled surface was approximated by a function that contained the wave length, wave angle, and wave depth as parameters. Four additional parameters - namely, stiffener compressive strain, chord compressive strain, the chord bending deflection and the panel shearing strain - were introduced to account for the effect of inplane membrane forces. The resultant governing equations were solved to predict the principal midplane stresses, maximum web bending stresses, stiffener and chord compressive stress. A comparison with limited experimental data showed reasonably good correlation. This analysis was limited in scope, as it failed to include rotation and out-of-plane bending in the chords and stiffeners. In addition, the limited number of unknown terms (seven) restricted the accuracy of the solution process.

Levy, et al (References 59 and 60) used the Von Karman large deflection plate equations to study the postbuckling behavior of unstiffened metal plates loaded in shear. The Von Karman equations were solved approximately by assuming a truncated Fourier double sine series. The maximum number of terms in the solution was relatively small, which limited the accuracy of the results obtained.

The analyses in the above studies (References 58 through 60) were limited to a few terms in the assumed functions primarily due to the absence of high speed computers. Modern computers have increased the feasibility of introducing a significantly larger number of terms in the analysis at a reasonable cost.

Several later studies used considerably larger numbers of terms to obtain more accurate solutions. Mayers and Budiansky (Reference 61) used a combination of algebraic and trigonometric functions to represent the in-plane and out-of-plane deflections of a flat plate loaded in compression beyond initial buckling. The analytical results were shown to agree reasonably well with the test results. Since material plasticity was not included in these analyses, a small difference in the experimental and analytical results was to be expected which did, in fact, occur.

Chia and Prabhakara (Reference 62) presented an analysis based on the Von Karman type of large deflection equations. These equations were solved by expressing the force function and transverse deflection as a double Fourier series in terms of approximate beam Eigen functions for unsymmetrically laminated rectangular plates. These plates were subjected to uniaxial and biaxial compression. Both simply supported and clamped-boundary conditions were considered. Harris (References 63 and 64) presented approximate analytical expressions for the inplane stiffness immediately after buckling for rectangular composite plates subjected to biaxial compression.

Chan (Reference 65) presented a slightly different form of Rayleigh-Ritz analysis to obtain the postbuckling behavior of compression loaded composite flat plates. The solution was carried out with only the transverse displacement mode assumed. The inplane displacements were obtained exactly from the two membrane displacement equations. Although this method of solution reduces the number of simultaneous nonlinear equations to be solved, it introduces a few additional restrictions. The inplane

displacements become dependent on the assumed shape of transverse deflection and the resulting displacements are not in general capable of accommodating the imposed inplane boundary conditions. In addition, this analysis method cannot be extended to the analysis of stringer stiffened panels under general loading conditions. Further, the advantage offered by this method for postbuckling analysis is not as significant because in conventional applications of the Rayleigh-Ritz method, most of the resulting equations involving inplane displacements are linear in terms of transverse displacement coefficients and, thus, can easily be solved in terms of these transverse deflection coefficients.

The effect of inplane flexural and axial rigidity of stiffeners on the postbuckling behavior of square metal panels was examined in Reference 66. The panels were loaded in shear and compression. The Von-Karman equations were solved by assuming the shape of the normal displacement and the stress function. The analysis failed to include the torsion and out-of-plane flexibility of the stiffeners.

In an attempt to improve the empirical analysis of Kuhn, a rather rigorous analysis of flat tension field beams was formulated during the development of SST technology (Reference 67). The problem was formulated for a cantilever beam consisting of internal stiffeners. The beam displacement functions were selected to satisfy the boundary conditions imposed during the tests. This resulted in the inclusion of the shear and bending deformations of the beam; inplane bending, out-of-plane bending, axial deformation, rotation, and warping of internal stiffeners; inplane bending, axial deformation, rotation, and warping of the chords; and axial deformation, rotation, and warping of the two edge vertical stiffeners. The analysis was the first attempt to duplicate the exact mechanism of load introduction for the tension field shear beam specimen. The analysis was formulated and some results were presented for a single-bay panel. The cancellation of the SST program and some convergence difficulties in the solution process halted further development and verification of the analysis for multibay panels.

Khot (References 68 and 69) demonstrated the usefulness of this approach by studying the postbuckling behavior and imperfection sensitivity

of composite cylindrical shells loaded under axial compression. Dickson, et al, References 70 through 72, formulated the problem of composite stiffened panels in the postbuckling range using the Rayleigh-Ritz approach. In Reference 72, the Rayleigh-Ritz solution procedure has been used in conjunction with an optimization routine to design a curved composite stiffened panel. The analysis has also been extended to predicting the local stress state at the skin/stiffener interface in stiffened composite panels (Reference 73). Experimental evaluation of this predictive methodology, however, has not been carried out.

In References 74 and 75 the analysis suggested in Reference 58 for metal panels was modified for use with composite panels loaded in shear. The results of this analysis were compared with several existing composite panel tests. A fairly good correlation between measured and predicted maximum out-of-plane deflections and inplane strains in the panel center was demonstrated. This analysis, once again, demonstrated the usefulness of the Rayleigh-Ritz type of solutions to predict the postbuckling behavior of composite panels. Because of the limited number of terms used in the assumed functions, the predicted and measured values were not in as good agreement near the panel edges as at the center. This shortcoming can be improved by taking additional terms in the solution. Rapid convergence coupled with nominal computer run times makes the approach attractive for design purposes. The increasing popularity of the Rayleigh-Ritz approach is manifested in several recent studies (References 76 through 78) where attempts have been made to develop the technique into a design tool.

### 2.2.3 Fatigue Analysis Methods

The phenomenon of fatigue crack initiation and propagation in metallic structures has been studied by many investigators. As a result, several useful and practical damage propagation models have been established on the basis of classical linear elastic fracture mechanics. One such example is the Forman equation (Reference 79) which is useful in predicting the fatigue crack growth life of metallic structures. Before applying these techniques to postbuckled metal panels, however, test data are required to determine the fatigue failure modes of these panels. In addition, analytical techniques are needed to predict the local stress intensity factors.

The only fatigue test data available in the literature for postbuckled metal shear panels are shown in Figure 2.1. These data were obtained in Reference 3 from constant amplitude fatigue tests on multibay shear panels. The four panels tested in Reference 3 exhibited very short fatigue lives (500 to 4000 cycles) due to cracks initiating at the corners of the chem-milled stiffener attachment pads on the skin. These data show that fatigue is a serious concern in the design of postbuckled metal panels. Additional test data are required, however, to establish the fatigue failure modes and S-N curves for curved metal shear panels.

Compression fatigue test data for flat stiffened panels loaded in the postbuckling range have been obtained in References 80, 81 and 82. In these panels fatigue cracks occurred in the stiffeners at stiffener attachment fastener holes and propagated along the loading direction as illustrated in Figure 2.2. The fatigue failure mode for flat stiffened panels loaded in compression, however, is unique to this design. Crack initiation in the skins at these fastener holes is also possible depending on the local stresses in the skin and in the stiffener. Thus, to interrogate all possible modes of fatigue failure in postbuckled metal panels, additional tests on different designs, including curved panels, need to be conducted.

In order to develop a generally applicable fatigue life prediction methodology for postbuckled metal shear and compression panels, analytical techniques that can predict the local stress intensity factors are required. This in turn requires a knowledge of the detailed stress field in the skins and the stiffeners. As mentioned before, the local stress field can only be obtained from nonempirical analyses. Thus, a Rayleigh-Ritz type analysis in conjunction with a fatigue crack growth law such as that given by the Forman equation can be readily used to predict the fatigue life of postbuckled metal panels.

In contrast to the state-of-the-art in fatigue analysis of metals, fatigue analysis of composites is still in its infancy. However, a sizeable fatigue test data base for postbuckled composite panels is available and indicates that composite panels, in general, are extremely durable.

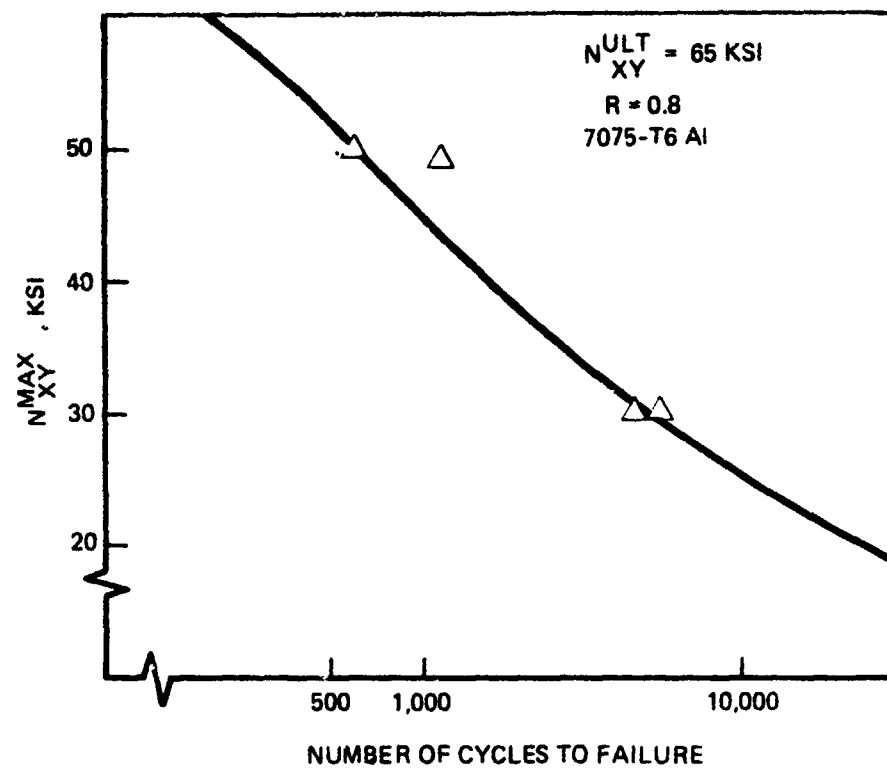


Figure 2.1. Metal Shear Panel Fatigue Data (Reference 3)

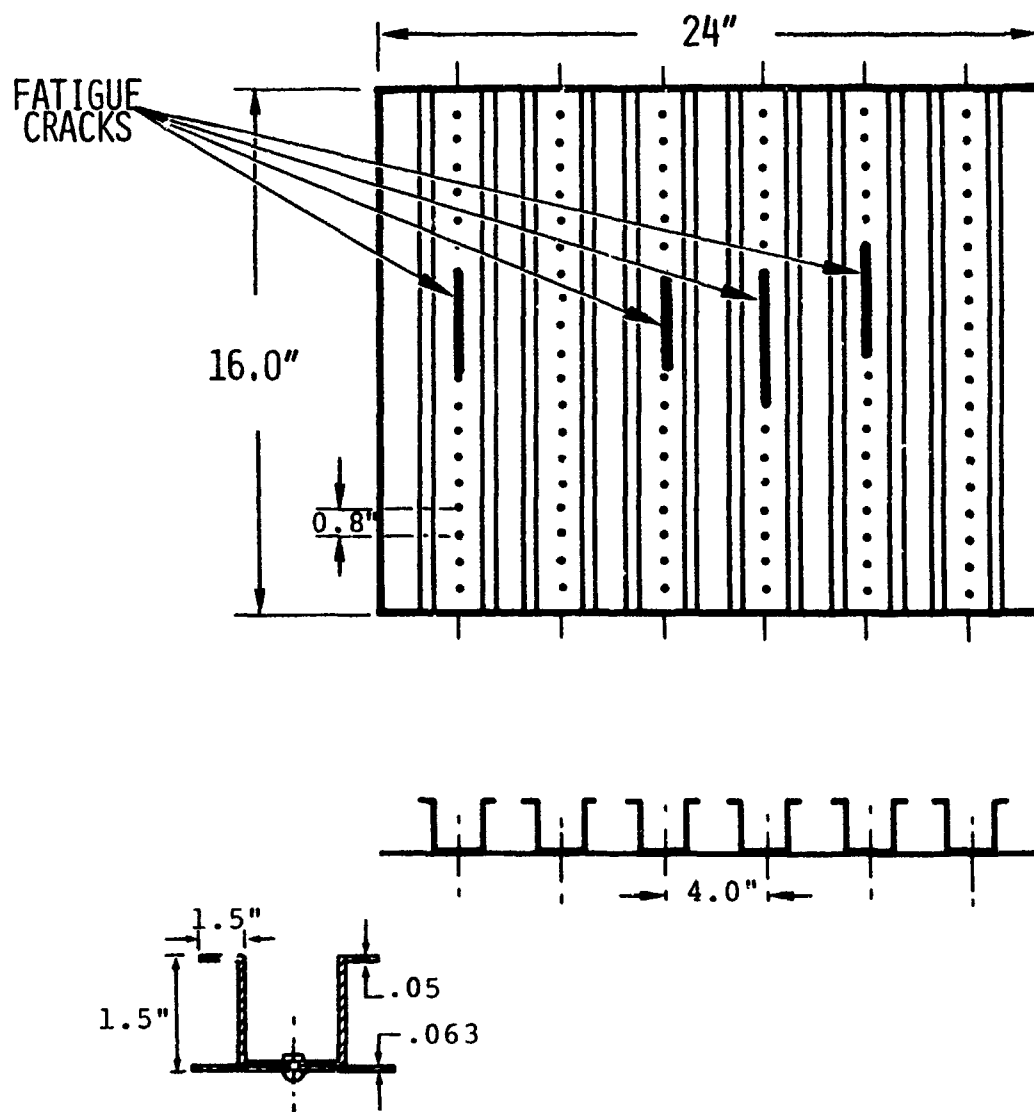


Figure 2.2. Fatigue Crack Propagation in Metal Compression Panels  
(Reference 82)



The fatigue test data generated in some of the investigations cited in Table 2.1 provide a good insight into the durability characteristics of postbuckled composite designs.

Test data for shear panels subjected to constant amplitude and spectrum fatigue loading are shown in Figure 2.3. These data were obtained from several test specimens in various government-funded programs. From Figure 2.3 it can be seen that the spectrum fatigue lives are considerably longer than constant amplitude fatigue lives; this illustrates the relatively high severity of constant amplitude loading. The test data from Reference 16 appear to be the lower bound for the fatigue data. The relatively steep S-N curve for these data is due to a design flaw at the stiffener skin junction where no ply drop-offs were included for a smooth transition. This design drawback when corrected for (Reference 83) yields a fatigue life comparable with the test data from References 14 and 23. The lack of tapered stiffener flanges in Reference 16 is also responsible for making the  $R = 0.1$  fatigue data appear more severe than the  $R = -1$  data of Reference 14. In all cases, however, it should be noted that the fatigue endurance limit is at least the design limit load. Thus, the data indicate extremely long fatigue lives at panel design limit load. In these designs, the panels were prevented from buckling during the level flight condition of a typical V/STOL aircraft. The minimum gage\* requirements resulted in panel failure load being much greater than the required ultimate load, a condition which is typical in most aircraft applications.

The fatigue response of composite compression panels is summarized in Figure 2.4. The data indicate that extremely long fatigue life can be expected for design limit strain levels of 2,500  $\mu$ inches/inch. Most postbuckled panels are buckling-critical and not strength-critical. The current design practice does not allow the average compressive limit strain to be higher than 3,000  $\mu$ inches/inch. Thus, fatigue for composite panels may not be a design driver.

---

\* Minimum gage defines the minimum laminate thickness. In current industry practice minimum laminate thickness ranges between 0.02 inch and 0.04 inch.

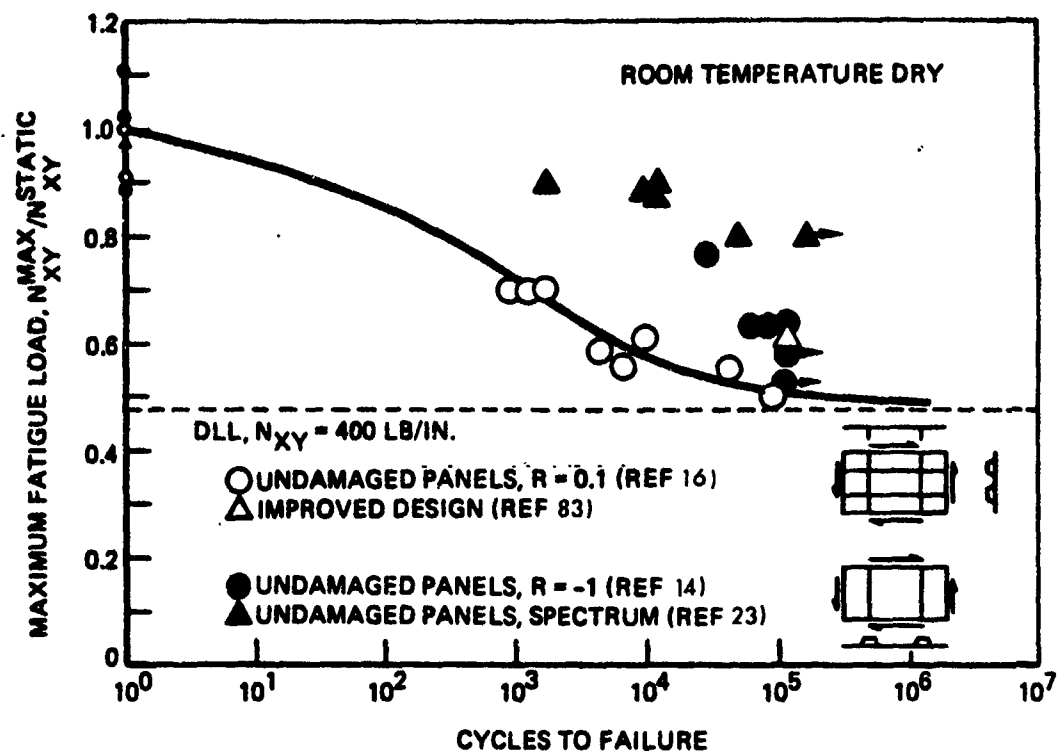


Figure 2.3. Composite Shear Panel Fatigue Response

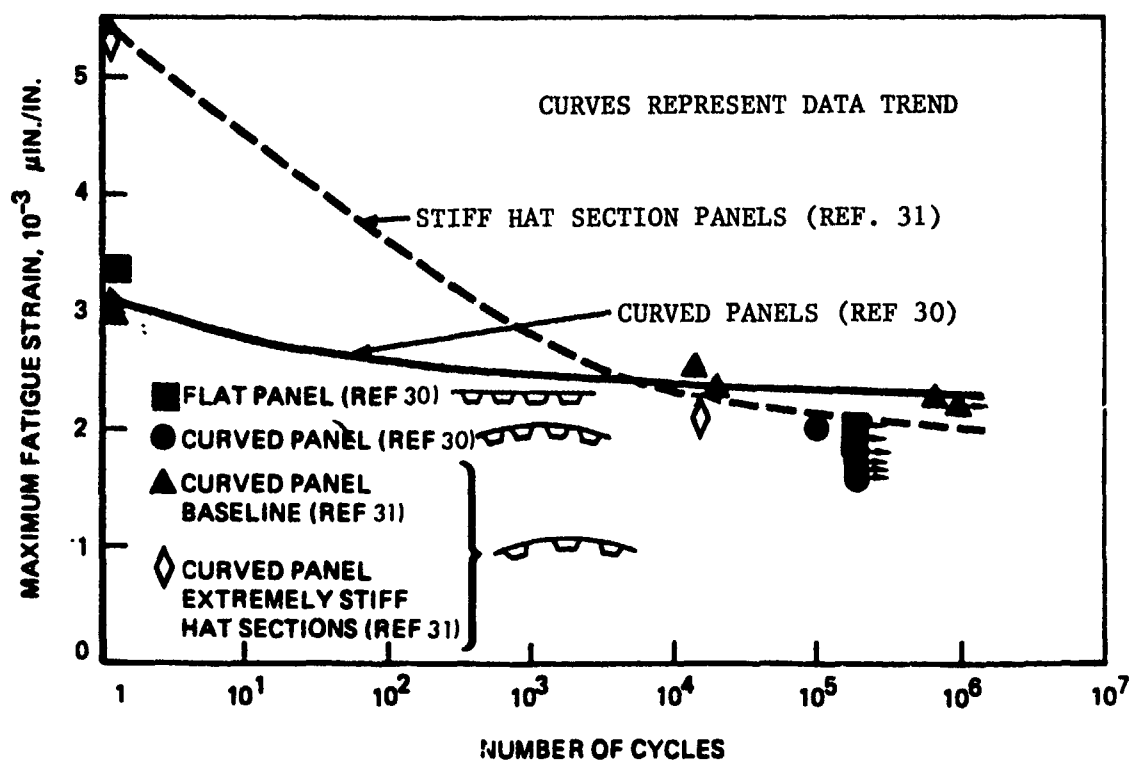


Figure 2.4. Composite Compression Panel Fatigue Response

The available test data for composite panels loaded under combined compression and shear also demonstrate the same trend. The test data (Reference 25) presented in Figure 2.5 indicate almost no loss in panel strength after two lifetimes of spectrum fatigue with the maximum load set at 71.6 percent of the failure load. Preliminary test data from ongoing Navy programs (References 28, 32) also indicate similar trends. The dominant failure mode in all these fatigue tests was stiffener/skin separation which is a direct consequence of initiation and propagation of delaminations in the skin/stiffener interface. Analytical prediction of fatigue life of postbuckled composite panels, therefore, requires a knowledge of the interfacial stresses and a fatigue analysis methodology that can predict damage propagation in composites.

Several analysis methods to predict skin/stiffener interfacial stresses and subsequent interface failure have been proposed (References 20, 73, 83 and 84). However, experimental validation of these methods has not been very successful. In Reference 20, Agarwal has proposed a stiffener/web interface stress analysis using a two-dimensional nonlinear model of a diagonal strip from a shear panel. The model utilizes a Rayleigh-Ritz type procedure to obtain the shear and normal stresses at the skin-stiffener interface. Experimental validation of the model was attempted by testing metal coupon specimens and comparing the measured failure loads with predictions. The coupon tests showed good agreement with the predictions which were based on a quadratic failure criterion. However, correlations with data from tests on stiffened composite panels have not been successful due to uncertainties in the interface properties and the validity of the quadratic failure criterion. The model proposed in Reference 84 by Tsai is similar to the beam model in Reference 20, except that Tsai uses experimentally measured out-of-plane displacements to obtain the stiffener web interfacial peel stresses.

In Reference 83 a detailed 3-D NASTRAN stress analysis of the stiffener/web interface has been performed. These results although useful for comparison with other simplified analyses, have not been experimentally validated and the method itself cannot be used as a cost-effective design tool. A more rigorous approach of first predicting the nonlinear post-buckled response of a stiffened composite panel and then using the local

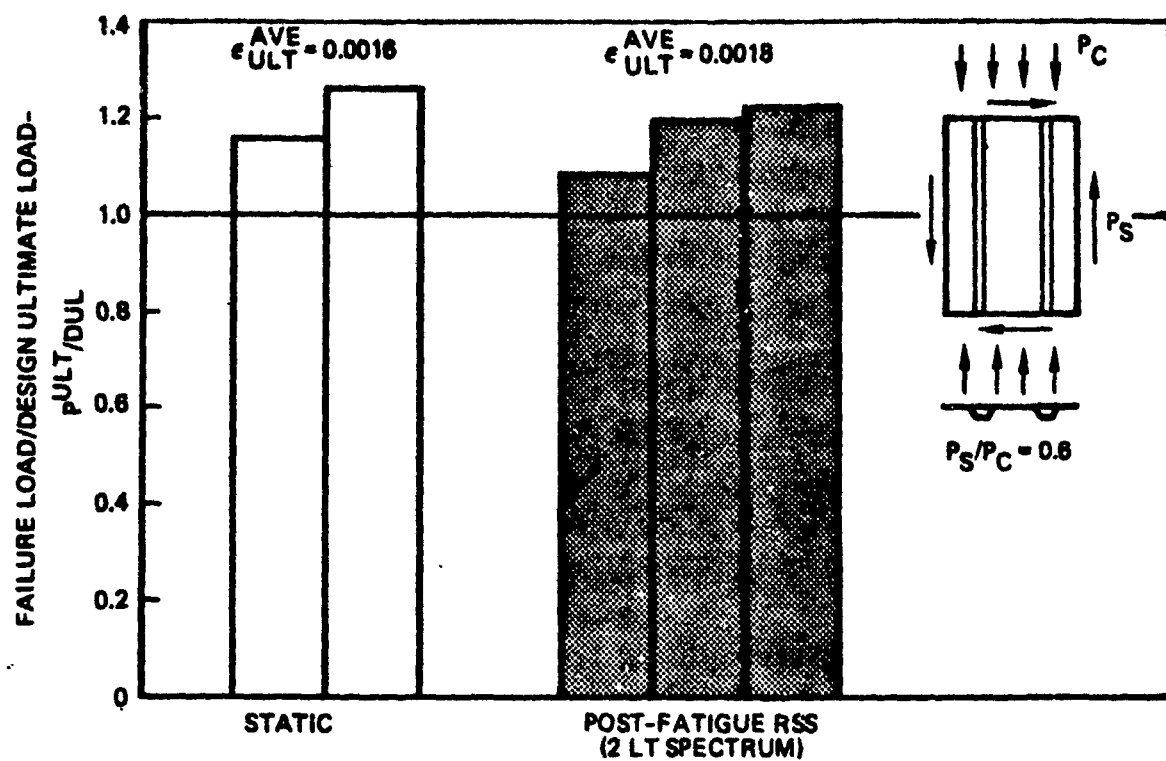


Figure 2.5. Fatigue Response of Flat Panels Under Combined Loading (Reference 25)

stress field in the skin to predict the stiffener/web interface stresses by a linear analysis has been developed in Reference 73. The global nonlinear analysis (Reference 72) and the local (stiffener/web interface) linear analysis (Reference 73) are both carried out using the Rayleigh-Ritz method. The analysis takes into consideration several skin/stiffener interface variables that are not accounted for in the simple beam models, and at the same time is less cumbersome to use than a finite element analysis. However, the results have not been experimentally validated. Thus, at present a fully developed stiffener/skin interface stress analysis methodology is not available for use in fatigue analysis of composite stiffened panels. The approach proposed in Reference 73, however, seems to be the most promising.

An extensive survey (Reference 85) of the available methods for fatigue life prediction of composites showed that these can be broadly classified as empirical techniques, degradation models, and damage propagation models. A summary comparison of the advantages and disadvantages of these methods is shown in Table 2.2 taken from Reference 85. Among these methods, the damage propagation models appear to be well suited to the fatigue analysis of postbuckled composite panels. In particular, the strain-energy-release-rate based delamination propagation model (Reference 86) appears most promising. It is necessary, however, to extend this model for application to postbuckled composite panels.

In summary, therefore, the observation of different failure modes in metal and composite postbuckled structures and the significantly different response of composite structures makes it essential that separate methodologies be developed to predict the fatigue life of metal and composite panels. A key prerequisite in both cases is that the local displacement or stress field in the postbuckled regime be known. In addition, for composite panels a validated methodology to predict the skin/stiffener interface stresses is required. Finally, development of a fatigue analysis methodology by coupling the local analyses with a crack growth or delamination growth law needs to be carried out.

### 2.3 SELECTION OF ANALYTICAL METHODS

A complete static analysis of postbuckled structures consists of predicting the initial buckling load of the skin, failure load of the

**TABLE 2.2. SUMMARY OF LIFE PREDICTION MODELS FOR COMPOSITES**

	Technique or model	Method	Advantages	Disadvantages
1	Empirical	<ul style="list-style-type: none"> <li>Experimental</li> </ul>	<ul style="list-style-type: none"> <li>Simple analysis</li> </ul>	<ul style="list-style-type: none"> <li>Extensive testing</li> <li>No general conclusions</li> <li>Conservative design</li> </ul>
2	Miner's rule	<ul style="list-style-type: none"> <li>Linear cumulative damage</li> </ul>	<ul style="list-style-type: none"> <li>Simple analysis</li> </ul>	<ul style="list-style-type: none"> <li>Loading sequence not accounted for</li> <li>Poor correlation</li> </ul>
3	Linear strength degradation	<ul style="list-style-type: none"> <li>Nonlinear damage accumulation based on linear strength degradation</li> </ul>	<ul style="list-style-type: none"> <li>Simple analysis</li> <li>Load sequence accounted for</li> </ul>	<ul style="list-style-type: none"> <li>Assumed strength degradation model does not agree with actual degradation generally observed in composites</li> </ul>
4	Wear-out model	<ul style="list-style-type: none"> <li>Strength degradation based on fracture mechanics of metals</li> <li>Statistical</li> </ul>	<ul style="list-style-type: none"> <li>Fatigue life and residual strength directly related to static strength</li> </ul>	<ul style="list-style-type: none"> <li>Extensive testing parameters depend on laminate and load spectrum</li> <li>Cannot be used for life prediction from S-N curves</li> </ul>
5	Strength degradation model and other statistical models	<ul style="list-style-type: none"> <li>Assumed strength degradation laws</li> <li>Statistical</li> </ul>	<ul style="list-style-type: none"> <li>Similar to wear-out model</li> </ul>	<ul style="list-style-type: none"> <li>Similar to wear-out model</li> </ul>
6	Delamination propagation model	<ul style="list-style-type: none"> <li>Delamination propagates under interlaminar stresses</li> <li>Growth-rate equation similar to crack growth equation in metals</li> </ul>	<ul style="list-style-type: none"> <li>Actual damage propagation modeled</li> <li>Constants depend on resin system only</li> <li>Correlates data well</li> </ul>	<ul style="list-style-type: none"> <li>Not applicable to nondelamination-prone laminates</li> <li>Interlaminar stress computation time-consuming</li> </ul>
7	Fracture mechanics delamination model	<ul style="list-style-type: none"> <li>Relating delamination growth rate to strain energy release rate</li> <li>Both modes I and II considered</li> </ul>	<ul style="list-style-type: none"> <li>Similar to delamination propagation model</li> <li>Strain energy release rate easier to obtain</li> <li>Delamination size determined more accurately</li> </ul>	<ul style="list-style-type: none"> <li>Not applicable to nondelamination-prone laminates</li> <li>Actual application to life prediction not investigated</li> </ul>
8	Intralaminar cracking model	<ul style="list-style-type: none"> <li>Strain energy density matrix cracking</li> </ul>	<ul style="list-style-type: none"> <li>Process of matrix cracking can be modeled by a single-strain energy density parameter</li> </ul>	<ul style="list-style-type: none"> <li>Not applicable to delamination-prone laminates</li> <li>Prediction not verified by data</li> </ul>

structure after skin buckling. The scope of this program encompassed cylindrically curved stiffened panels loaded in compression or shear only.

As discussed in subsection 2.2, several analysis methods, ranging from closed form semiempirical methods to extremely sophisticated large computer codes, are available to predict the initial buckling loads of curved panels. The main difficulty in accurately predicting the initial buckling load arises from a lack of definition of the exact boundary conditions and due to the presence of structural imperfections. In view of these uncertainties, semiempirical methods based on test data are best suited for preliminary analyses. Furthermore, due to the lack of a well-established, rigorous failure analysis methodology for postbuckled panels, semiempirical analysis methods have to be utilized for predicting the strength of curved metal or composite panels. Thus, to meet the objectives of the present program semiempirical analytical methods that are well documented for metal panels (e.g., References 2 and 34) were selected. Based on available test data for composite panels loaded in shear or compression, the semiempirical analyses were modified for generic application to composites.

The semiempirical analysis techniques selected are detailed in the following paragraphs. The modifications that extend the applicability of the analyses to composites along with supporting data are also discussed.

#### 2.3.1 COMPRESSION PANELS

Analysis of postbuckled curved compression panels is performed in the steps outlined below. The critical parameters in the analysis are evaluated in terms of strain, since strain is more convenient to use for composite panels whereas for metal panels it can be used interchangeably with stress. The analysis proceeds as follows:

- (a) Determine the buckling strains for all possible modes of instability. These include: skin buckling between stiffeners, Euler buckling of the stiffened panel, and stiffener crippling.
- (b) Determine the failure load due to Euler buckling, stiffener crippling and other modes of failure



peculiar to composite or metal panels. For composite panels the load for stiffener/web separation mode of failure needs to be calculated whereas for metal panels loads causing permanent set in the skin or the stiffener must be calculated.

- (c) The load carrying capacity of the panel is then determined as the lowest of the loads calculated in (b) above.

Calculation of Skin Buckling Strain/Load - The buckling stress for curved metal sheet panels can be calculated from:

$$F_{CR} = \frac{K_c \pi^2 E}{12(1-\nu^2)} \left( \frac{t_w}{b_s} \right)^2 \quad (1)$$

where,

$F_{CR}$	buckling stress, psi
$t_w$	thickness of the skin, in
$b_s$	stiffener spacing measured between the fastener lines, in
$E, \nu$	modulus and Poisson's ratio for the sheet material
$K_c$	buckling coefficient determined from Figure 2.6 (Reference 34 and 35)

The theoretical value of  $K_c$  is obtained from the buckling equations for thin cylindrical shells and is a function of the nondimensional curvature  $z$  of the panel expressed as

$$z = \frac{b_s^2 (1-\nu^2)^{1/2}}{rt_w}$$

where  $r$  is the radius of the cylindrical panel. Experimental data (Reference 35) have shown that  $K_c$  is also a function of the  $r/t$  ratio for the panel. The design curves of Figure 2.6, obtained from test data, show this dependence of  $K_c$  on  $r/t$ .

Compression buckling strains for curved composite panels can be accurately determined through the use of computer codes SS8 (Reference 45)

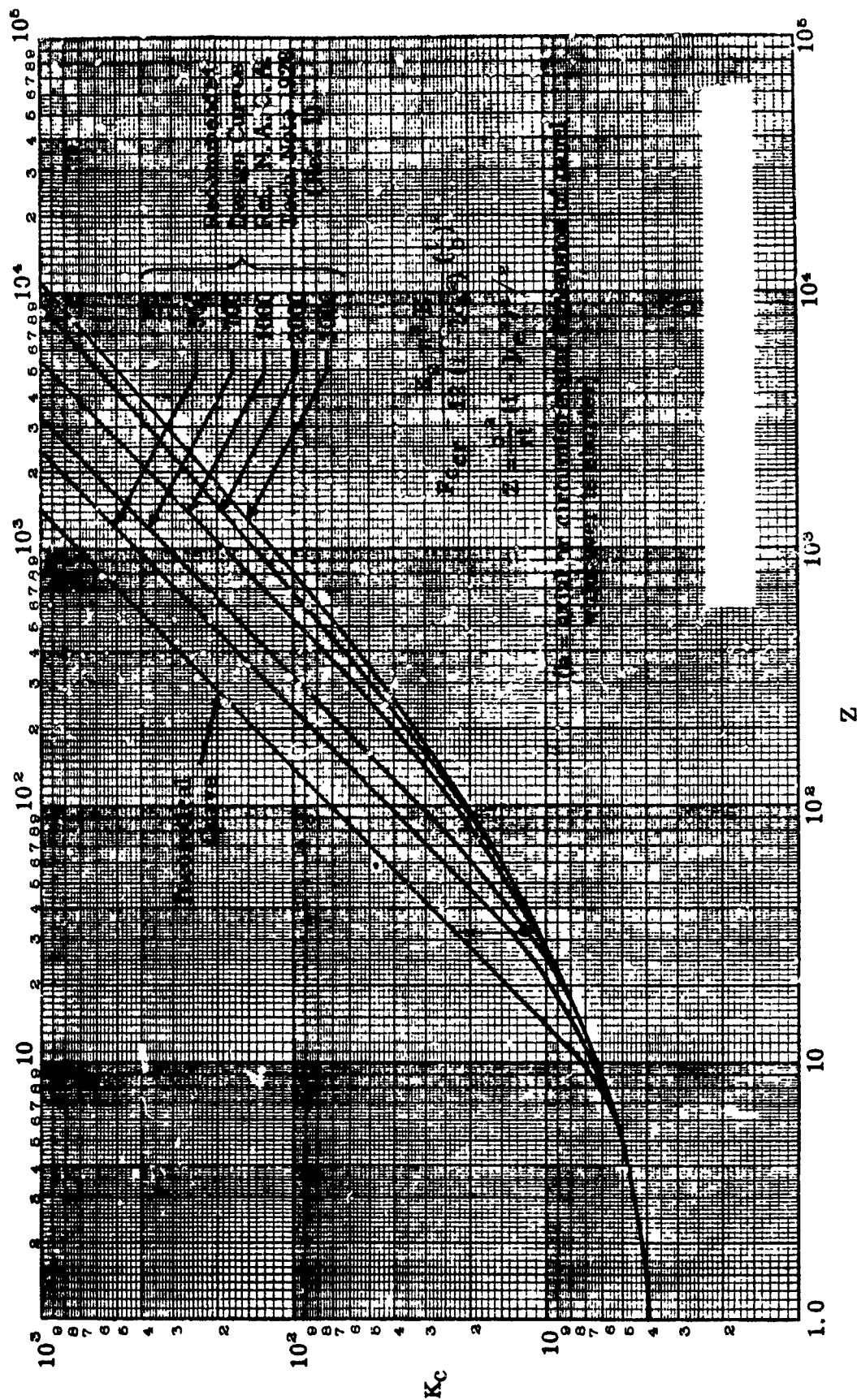


Figure 2.6. Axial Compressive Buckling Coefficients for Long Curved Plates (Reference 34)

and BUCLASP-2 (Reference 41), for example. However, for an approximate calculation of the skin buckling strain in cases where the stiffener spacing is realistic, the simplified equation given below can be used.

$$\epsilon_{cr}^w = \left(\frac{m\pi}{L}\right)^2 \frac{1}{E_{xw} t_w} \left[ D_{11} + 2(D_{12} + 2D_{66}) \left(\frac{nL}{mb_w}\right)^2 + D_{22} \left(\frac{nL}{mb_w}\right)^4 \right] + \frac{E_{yw}}{\left(\frac{m\pi}{L}\right)^2 R^2 \left[ E_{xw} - \left( 2\nu_{xyw} E_{yw} - \frac{E_{xw} E_{yw}}{G_{xyw}} \right) \left(\frac{nL}{mb_w}\right)^2 + E_{yw} \left(\frac{nL}{mb_w}\right)^4 \right]} \quad (2)$$

where  $D_{ij}$  are the terms of the bending stiffness matrix of the composite skin,  $E_{xw}$ ,  $E_{yw}$ ,  $G_{xyw}$ ,  $\nu_{xyw}$  and  $t_w$  are the web elastic constants and thickness, respectively,  $L$  is the panel length,  $b_w$  is the width of the skin,  $R$  is the radius of curvature of the panel and  $n$  and  $m$  are integer coefficients representing the number of half buckle waves in the width and length direction, respectively. The lowest value of strain for various values of  $n$  and  $m$  represents the buckling strain of the specimen.

The effective width of the skin,  $b_w$ , was assumed to be equal to the distance between the two adjacent stiffeners measured from one stiffener flange edge to the next stiffener flange edge as shown in Figure 2.7.\* Note that  $b_w$  is less than the stringer spacing  $b_s$ .

Equation (2) was derived in Reference 87 from the equations developed for the buckling of orthotropic complete cylinders by making simplifying assumptions.

Euler Buckling Strain Calculations - The Euler buckling strain for a stiffened panel is calculated by treating the panel as a wide column with the width set equal to the stiffener spacing. The critical strain is calculated using the standard column equation:

\*Note that this definition of  $b_w$  was used initially. The test data in Section 3 indicate that  $b_w$  should be measured between stiffener flange centerlines. See Section 5 for details.

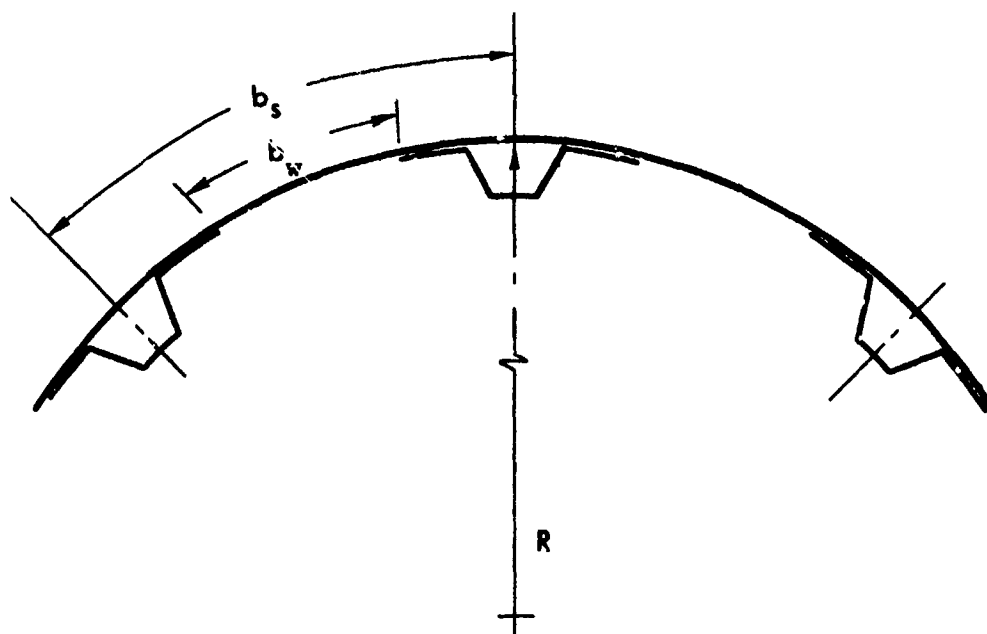


Figure 2.7 Skin Width  $b_w$  for Composite Panel Initial Buckling Strain Calculations,  $b_s$  = Stringer Spacing.

$$\epsilon_{CR}^E = \frac{C \pi^2 EI}{EA L^2} \quad (3)$$

where, EI is the equivalent bending stiffness of the panel, EA is the equivalent axial stiffness, L is the panel length, and C is the end fixity coefficient. The fixity coefficient depends upon the support conditions at the panel ends. Most compression panels are tested by flat end testing and the results obtained by using C = 4 are quite unconservative; therefore, a value of C = 3 is recommended. The values of C for other end conditions can be obtained from Reference 34 (Section A18.23).

Stiffener Crippling Strain/Stress Calculation - The crippling strength of metal stiffeners is calculated using the well established Needham and Gerard methods documented in Reference 34. In the present program, the Gerard method was used since it is a generalization of the Needham method and was derived from a broader data base. The empirical Gerard equation for calculating the crippling stress for 2 corner sections, such as the Z, J and channel sections, is:

$$\frac{F_{CS}}{F_{cy}} = 3.2 \left[ \left( \frac{t^2}{A} \right) \left( \frac{E}{F_{cy}} \right)^{1/3} \right]^{0.75} \quad (4)$$

where,

$F_{CS}$  = crippling stress for the section, psi

$F_{cy}$  = compressive yield stress of the material, psi

t = element thickness, in

A = section area, in<sup>2</sup>

A design curve based on Equation (3) is shown in Figure 2.8 taken from Reference 34. Additional crippling equations that apply to sections other than 2 corner sections are also given in Reference 34.

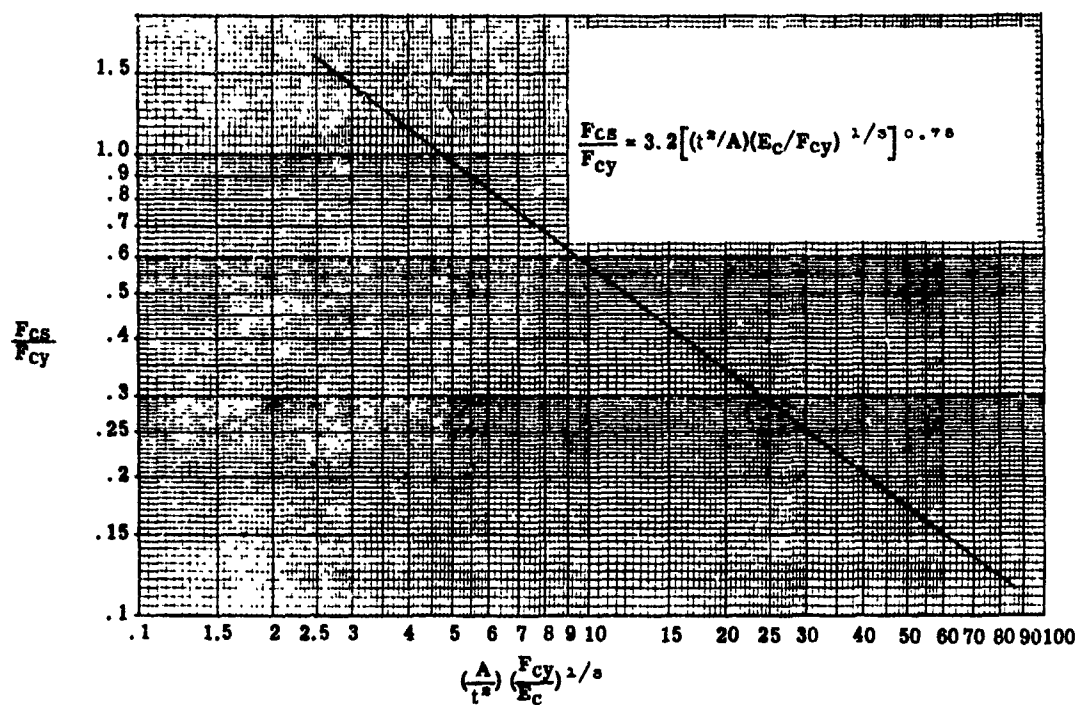


Figure 2.8. Crippling Stress  $F_{cs}$  for Two Corner Sections e.g., Z, J and Channel Sections (Reference 34, Figure C7-9)

In order to calculate the crippling strains for stiffeners made of composite materials, a semiempirical methodology was developed in the program. The methodology consists of modelling the stiffener in terms of interconnected flat plate elements, calculating the initial buckling and crippling strains for each element, and determining the crippling strain for the stiffener as the lowest strain that causes crippling of the most critical element in the stiffener section. It should be noted here that the absolute minimum of the crippling strains for the various plate elements is not necessarily the stiffener crippling strain; element criticality with respect to stiffener stability has to be considered as well. The procedural details of this methodology given in the following paragraphs provide additional clarifications relating to the determination of the most critical plate element.

The first step in calculating the stiffener crippling strain is to model the stiffener as an interconnected assembly of plate elements. As examples, plate element models of a hat-section and a J-section stiffener are shown in Figure 2.9. The hat-section stiffener is made up of six elements, whereas, the J-section stiffener consists of five elements.

The crippling strains for the plate elements are calculated from empirical equations of the form

$$\frac{\epsilon_{cs}}{\epsilon_{cr}} = \alpha \left( \frac{\epsilon_{cu}}{\epsilon_{cr}} \right)^{\beta} \quad (5)$$

where,

- $\epsilon_{cs}$  = crippling strain of the plate element
- $\epsilon_{cr}$  = initial buckling strain of the plate element
- $\epsilon_{cu}$  = compression ultimate strain for the plate element laminate
- $\alpha, \beta$  = material dependent coefficients obtained from test data

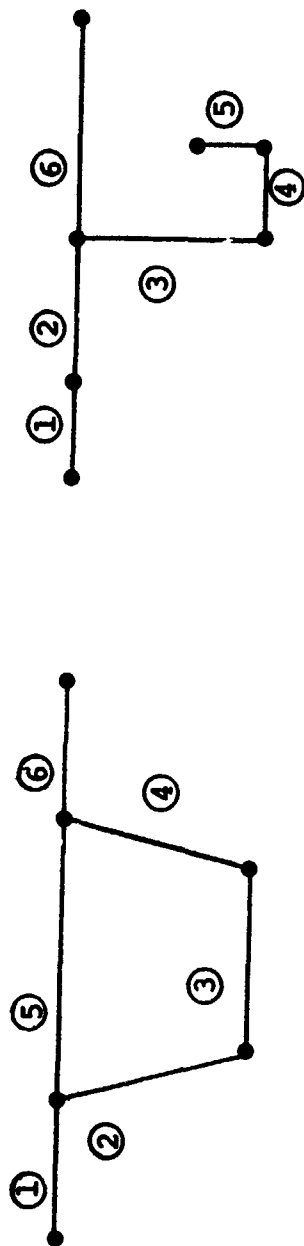


Figure 2.9 Plate Element Models of Hat- and J-Section Stiffeners.



Equation (5) has the same functional form as that used by Gerard (Reference 35) for metal stiffeners. The coefficients  $\alpha$  and  $\beta$  depend on the plate edge conditions and have been obtained in References 46 and 47 from a large data base for plate elements that are connected on both sides (e.g., elements 2, 3, 4 and 5 of the hat-section stiffener shown in Figures 2.9). The crippling strain for stiffener plate elements connected on both sides is given by (Reference 47):

$$\epsilon_{cs} = 0.56867 \epsilon_{cr} \left( \frac{\epsilon_{cu}}{\epsilon_{cr}} \right)^{0.47567} \quad (6)$$

where  $\epsilon_{cr}$ , the buckling strain for the plate element is given by (Reference 89):

$$\epsilon_{cr} = \frac{2\pi^2}{b^2 t E_x} \left( \sqrt{D_{11} D_{22}} + D_{12} + 2D_{66} \right) \quad (7)$$

In Equation (7)

$b$  = plate element width

$t$  = plate element thickness

$E_x$  = compression modulus of the plate laminate along the longitudinal direction

$D_{ij}$  = terms from the laminate bending stiffness matrix, ( $i, j = 1, 2, 6$ )

Equation (7) applies to plate elements for which the length to width ratio ( $L/b$ , where  $L$  = stiffener length) is at least 4.

The crippling strain for plate elements that are connected on one side only is calculated using the following equation:

$$\epsilon_{cc} = 0.4498 \epsilon_{cr} \left( \frac{\epsilon_{cu}}{\epsilon_{cr}} \right)^{0.72715} \quad (8)$$

where,

$$\epsilon_{cr} = \frac{12 D_{66}}{b^2 t E_x} + \frac{4\pi^2 D_{11}}{L^2 t E_x} \quad (9)$$

L = length of the stiffener

with the other nomenclature remaining the same as for Equations (6) and (7).

The coefficients in Equation (8) were obtained by fitting Equation (5) to the crippling data generated from tests on one-edge free plates in References 46 and 47. Data for two material systems, T300/5208 and AS/3501 graphite/epoxy, were pooled to obtain Equation (8).

In Equations (6) through (8), the thickness of plate elements attached to the skin is taken as the sum of the plate element and the co-cured skin thicknesses. In the case of the hat-section stiffener, crippling strains for plate elements representing the skin only, such as element 5 in Figure 2.9 are also calculated. Another consideration in calculating the crippling strain for stiffener flange elements attached to the skin is the choice of an appropriate element width. For example, in most practical designs the stiffener flanges attached to the skin are tapered by dropping-off plies as shown in Figure 2.10 for a hat-section stiffener. The flange plate element width in this case is defined as the width to the end of the taper with the weighted average of the element thickness added on to the attached skin thickness to obtain the total thickness for use in Equations (6) through (8).

Equations (6) through (8) are quite general in nature and take into account ply composition, stacking sequence, and material characteristics. The ply composition, i.e., the percentages of  $0^\circ$ ,  $45^\circ$  and  $90^\circ$  plies, is reflected in the compression ultimate strain  $\epsilon_{cu}$ . Stacking sequence effects are accounted for in the expression for  $\epsilon_{cr}$  where the bending stiffnesses  $D_{ij}$  are used. The  $D_{ij}$ 's and  $\epsilon_{cu}$  also account for mechanical property changes from one material system to another. Use of strain rather than stress for crippling calculations provides another significant advantage in that laminate non-linearity (e.g., stress-strain response

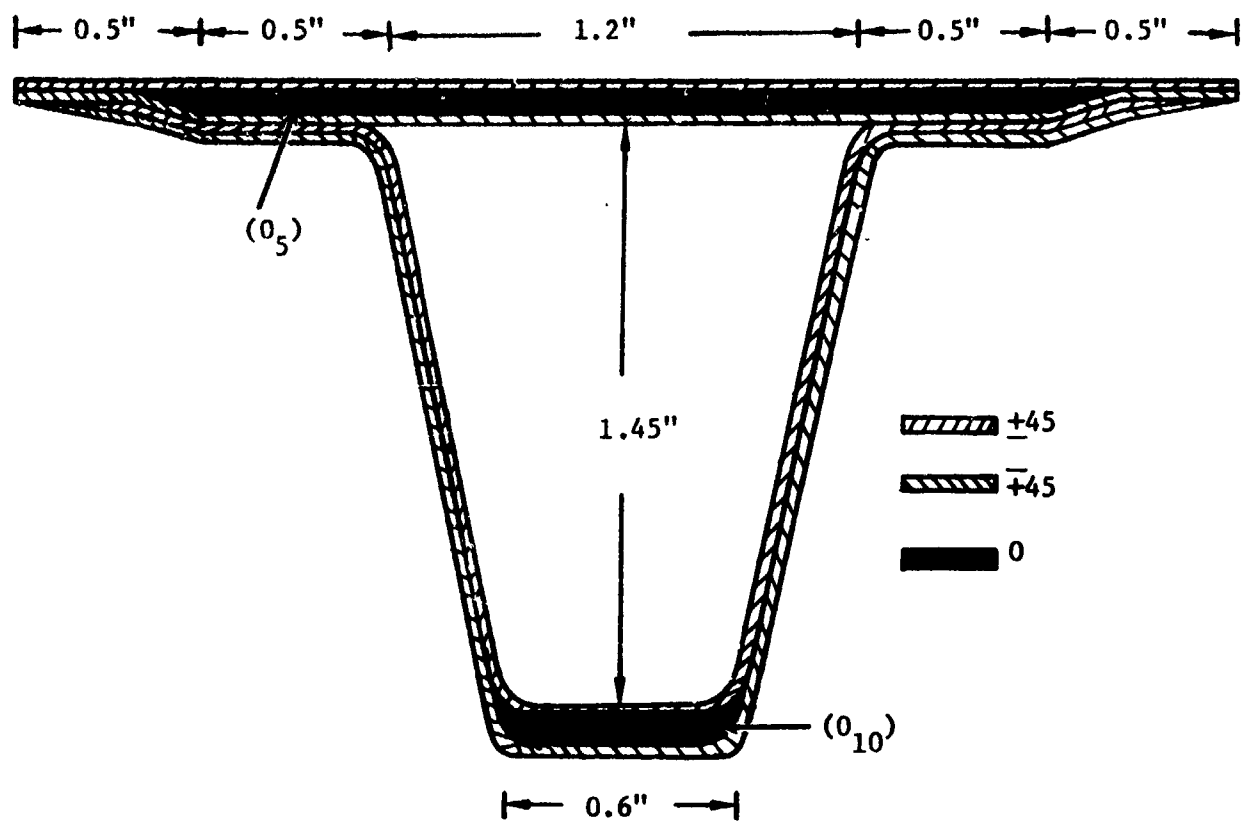


Figure 2.10 Ply Drop-Offs in Hat-Section Stiffener.

of  $\pm 45^\circ$  laminates) is accounted for by way of the compression ultimate strain  $\epsilon_{cu}$ .

Failure Load Calculation - The failure load for the panel is determined as the lowest of the loads calculated for the various instability modes mentioned above, for stiffener-web separation in composite panels, and for skin or stiffener yielding in metal panels. The methods for failure load calculation are given in the following paragraphs.

Failure Load Due to Euler Buckling - The failure load due to Euler buckling is calculated using the following equation:

$$P_E = \epsilon_{cr}^E (E_{xs} A_s + E_{xw} b_w t_w) \quad (10)$$

where,

$\epsilon_{cr}^E$  = Euler buckling strain determined using Equation (3)

$E_{xs}$  = Compression modulus of the stiffener in the loading direction

$A_s$  = Cross-sectional area of the stiffener

$E_{xw}$  = Compression modulus of the web (skin) in the loading direction

$b_w$  = Stiffener spacing

$t_w$  = Skin thickness

Failure Load Due to Stiffener Crippling - In order to determine the failure load due to stiffener crippling, it is necessary to determine the load carried by the stiffener and the panel web individually. The load carried by the stiffener ( $P_s$ ) is determined as follows:

1. Determine the two lowest crippling strains ( $\epsilon_{cc1}$ ) and ( $\epsilon_{cc2}$ ) of all the elements making up the cross-section using Equations (6) through (8).
2. If the element with the lowest crippling strain ( $\epsilon_{cc1}$ ) is normal to the axis of least bending stiffness of the cross-section, the stiffener

will fail at a strain equal to  $\epsilon_{cc1}$ , and the corresponding failure of the stiffener is given by:

$$P_S = E_{xs} A_x \epsilon_{cc1} \quad (11)$$

3. If the element with the lowest crippling strain is parallel to the axis of least bending stiffness of the cross-section, the stiffener will carry additional load until the second member in the cross-section becomes critical due to crippling. In this case the load carried by the stiffener is given by:

$$P_S = (EA)_1 (\epsilon_{cc1} - \epsilon_{cc2}) + \epsilon_{cc2} E_{xs} A_s \quad (12)$$

where  $(EA)_1$  is the extensional stiffness of the member becoming critical first, and the stiffener failure strain  $\epsilon_{cc}^S = \epsilon_{cc2}$ .

The total load carried by the panel is the sum of the load carried by the stiffener up to crippling and the load carried by the buckled skin. In order to calculate the load carried by the skin, the effective width concept is utilized. The effective width for metal panels is calculated using the semiempirical equation given below (Reference 34):

$$w = 1.9 t_w \sqrt{\frac{E}{F_{st}}} \quad (13)$$

where,

- $w$  = effective width of the skin after initial buckling
- $t_w$  = skin thickness
- $F_{st}$  = stress in the stringer

For composite panels, in the absence of any other guidelines, Equation (13) expressed in terms of strain is used to compute the effective skin width. Thus,

$$w = 1.9 t_w (\epsilon^s)^{-0.5} \quad (13A)$$

for composite skins where,  $\epsilon^S$  = strain in the stiffener.

Thus, the total load carried by the panel for a stiffener crippling mode of failure is given by:

$$P_{cc} = P_s + P_w \quad (14)$$

where,

$P_{cc}$  = load carried by the panel at stiffener crippling

$P_s$  = stiffener load given by Equation (12)

$P_w$  = load carried by the skin

The load  $P_w$  is calculated as:

$$P_w = F_{cs} w t_w = 1.9 t_w^2 \sqrt{E F_{cs}} \quad (15)$$

for metal panels, and for composite panels as:

$$P_w = 1.9 t_w^2 E_{xw} (\epsilon_{cc}^S)^{0.5} \quad (16)$$

Failure Load Due to Stiffener/Web Separation - Failure of composite stiffened panels due to stiffener/web separation is a common mode of failure in the postbuckling range. It is extremely difficult to predict this failure, even by using rather sophisticated analysis methods. The attempts to date on making such predictions have been inconclusive. A simple empirical equation to predict such failure was developed in this program. The correlation of experimental data with the predicted failure loads based upon this equation is surprisingly good. The empirical equation was derived by analogy with the crippling data for plates with one edge simply supported and one edge free. It is hypothesized that when the panel web strain reaches the crippling strain the interfacial stresses become high enough to cause failure. The equation should represent the lower bound on predicted failure loads. Any attempts to improve the interface (for example, by stitching, riveting, etc.) can result in higher failure loads.

$$P_{SS} = \epsilon_{SS} (E_{xs} A_s + E_{xw} b_w t_w) \quad (17)$$

where,

$$\epsilon_{SS} = 0.4498 \epsilon_{cr} \left( \frac{\epsilon_{cu}}{\epsilon_{cr}} \right)^{.72715} \quad (18)$$

$\epsilon_{SS}$  = Failure strain for stiffener/web separation

$P_{SS}$  = Failure load for the stiffener/web separation mode

The metal compression panel analysis methodology outlined in the preceding paragraphs has been experimentally validated (e.g., Reference 35) and is representative of current usage. In the case of composite panels, experimental validation was necessary before the methodology could be used in designing the program test panels. Composite compression panel test data available from some of the studies cited in Table 2.1 were utilized to validate the semiempirical analysis. Results of the correlation between the predictions and the test data are given in the following subsection.

#### Experimental Validation of Composite Compression Panel Analysis -

Experimental verification of the semiempirical equations was accomplished in two parts: (i) test data on stiffeners of various shapes (e.g., hat, channel, Z, cruciform) were compared with predictions made using Equations (6) through (8); and (ii) test data for flat and curved stiffened composite compression panels were compared with the initial buckling and failure strain predictions.

Stiffener local buckling and crippling test data for channel, Z, hat cruciform and I graphite/epoxy sections were obtained from References 46, 47 and 48. A summary comparison of the predictions with the test results is shown in Table 2.3. A comparison of the predicted and measured failure loads for the stiffeners as a function of the strain ratio  $\epsilon_F/\epsilon_{cu}$ , where,  $\epsilon_F$  is the strain at failure, is illustrated in Figure 2.11. As seen in the figure, a majority of the test data fall on or above the  $P_{exp}/P_{anl} = 1$  line, indicating conservatism in the analysis which is at most 25 percent. A few data points in Figure 2.11 fall below the  $P_{exp}/P_{anl} = 1$  line. However, these data correspond to stiffeners for which the failure strain was very close to the compression ultimate strain of the laminates and the failure mode was column buckling rather than crippling. Thus, the semiempirical












TABLE 2.3. CORRELATION OF SEMI-EMPIRICAL STIFFENER CRIPPLING PREDICTIONS  
WITH TEST DATA (Continued)

SPECIMEN NUMBER (REFERENCE)	PANEL TYPE	$\frac{\epsilon_{cr}}{\epsilon_{cu}}$	$\frac{\epsilon_F}{\epsilon_{cu}}$	EXPERIMENTAL VALUE		REMARKS
				BUCKLING	FAILURE	
CR1A MCAIR (48)		1.00	1.00	0.79	0.79	FAILURE DUE TO COLUMN BUCKLING
CR1B MCAIR (48)		0.222	0.298	0.85	1.10	FAILURE DUE TO FLANGE CRIPPLING
CR2A MCAIR (48)		0.820	0.820	0.77	0.77	FAILURE DUE TO FLANGE CRIPPLING
CR2B MCAIR (48)		0.169	0.277	1.02	1.15	FAILURE DUE TO FLANGE CRIPPLING
CR3A MCAIR (48)		1.00	1.00	0.91	0.91	NO BUCKLING UP TO FAILURE
CR3B MCAIR (48)		0.203	0.292	0.87	1.20	FAILURE DUE TO FLANGE CRIPPLING
CR3C MCAIR (48)		0.054	0.204	1.20	0.98	FAILURE DUE TO FLANGE CRIPPLING
C1A MCAIR (48)		0.53	0.53	0.95	0.95	FAILURE DUE TO COLUMN BUCKLING
C1B MCAIR (48)		0.039	0.164	1.49	1.06	FAILURE DUE TO WEB CRIPPLING
C2A MCAIR (48)		0.69	0.69	0.76	0.76	FAILURE DUE TO COLUMN BUCKLING
C2B MCAIR (48)		0.028	0.154	0.85	0.884	FAILURE DUE TO WEB CRIPPLING
C3A MCAIR (48)		1.00	1.00	0.85	0.85	NO BUCKLING UP TO FAILURE
C3B MCAIR (48)		0.048	0.218	1.09	0.94	FAILURE DUE TO WEB CRIPPLING
C3C MCAIR (48)		0.045	0.108	1.17	1.12	FAILURE DUE TO WEB CRIPPLING
H1 MCAIR (48)		0.688	0.688	1.04	1.04	FAILURE DUE TO FLANGE CRIPPLING

$\epsilon_{cr}$  - ANALYTICAL BUCKLING STRAIN,  $\epsilon_F$  - ANALYTICAL FAILURE STRAIN,  $\epsilon_{cu}$  - LAMINATE ULTIMATE STRAIN



TABLE 2.3. CORRELATION OF SEMI-EMPIRICAL STIFFENER CRIPPLING PREDICTIONS  
WITH TEST DATA (Concluded)

SPECIMEN NUMBER (REFERENCE)	PANEL TYPE	$\frac{\epsilon_{cr}}{\epsilon_{cu}}$	$\frac{\epsilon_F}{\epsilon_{cu}}$	EXPERIMENTAL VALUE ANALYTICAL VALUE		REMARKS
				BUCKLING	FAILURE	
9 GD (89)		0.108	0.245	1.35	1.11	FAILURE DUE TO FLANGE CRIPPLING
10 GD (89)		0.180	0.180	0.57	0.70	FAILURE DUE TO EULER BUCKLING
11 GD (89)		0.055	0.165	1.02	1.14	FAILURE DUE TO WEB CRIPPLING
12 GD (89)		0.126	0.287	1.15	1.28	FAILURE DUE TO WEB AND FLANGE CRIPPLING
13 GD (89)		0.126	0.287	0.87	0.78	FAILURE DUE TO COMBINED COLUMN BUCKLING AND CRIPPLING. PREDICTION BASED UPON CRIPPLING
14 GD (89)		0.126	0.288	1.12	1.24	FAILURE DUE TO WEB AND FLANGE CRIPPLING
15 GD (89)		0.126	0.256	1.12	1.27	FAILURE DUE TO FLANGE CRIPPLING
16 GD (89)		0.213	0.253	0.88	1.10	FAILURE DUE TO VERTICAL WEB CRIPPLING
17 GD (89)		0.213	0.253	-	0.43	PREMATURE FAILURE DUE TO COMBINED CRIPPLING AND COLUMN BUCKLING
18 GD (89)		0.083	0.154	1.21	1.18	FAILURE DUE TO VERTICAL WEB CRIPPLING
19 GD (89)		0.045	0.288	2.29	1.52	FAILURE DUE TO FLANGE AND WEB CRIPPLING

$\epsilon_{cu}$  - LAMINATE ULTIMATE ALLOWABLE STRAIN,  $\epsilon_{cr}$  - ANALYTICAL BUCKLING STRAIN,  $\epsilon_F$  - ANALYTICAL FAILURE STRAIN

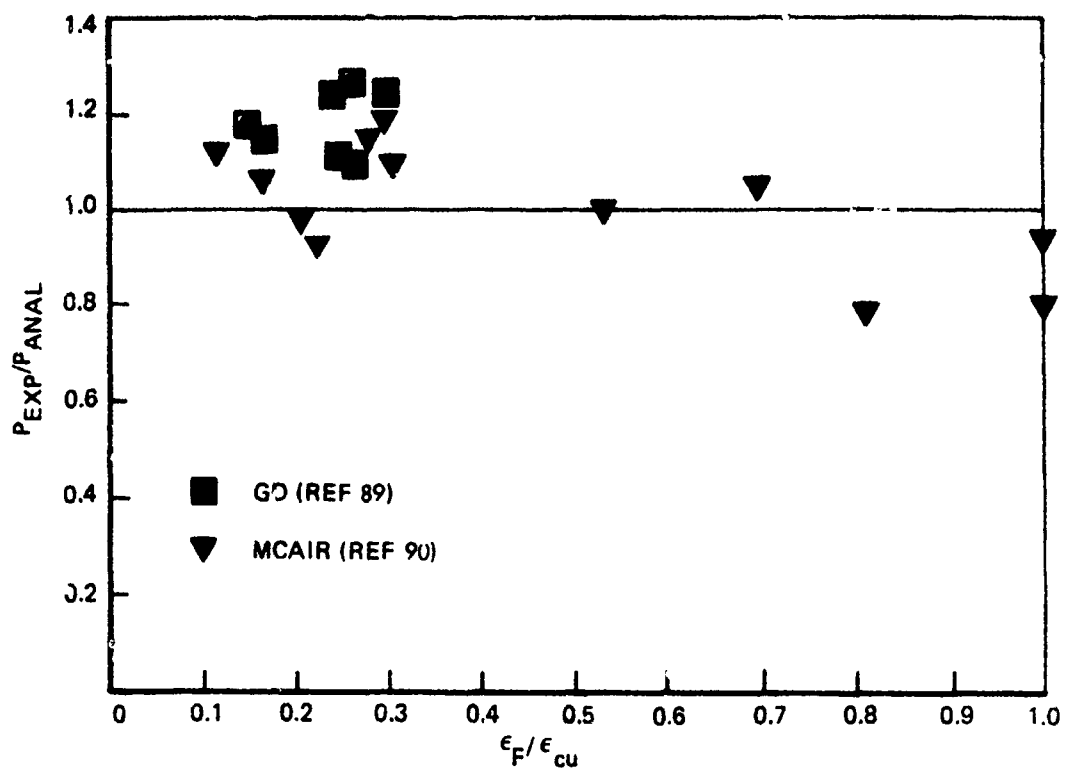








Figure 2.11. Comparison of Analytical and Experimental Data for Stiffener Crippling

stiffener crippling predictive methodology is substantiated by test data over a wide range of stiffener geometries and laminate lay-ups. The analysis can be used as a design tool with a high degree of confidence due to the built-in conservatism.

A similar comparison of analysis and test data was performed for stiffened compression panels. A majority of the data available in the literature pertained to flat panels. Table 2.4 summarizes the results of analytical failure predictions and measured data for a series of flat stiffened panels. To evaluate the accuracy of the predictions the failure load data were plotted as shown in Figure 2.12, where the ratio of the measured failure load to the analytically determined failure load ( $P_{exp}/P_{anl}$ ) is plotted against the failure strain to ultimate allowable strain ratio ( $\epsilon_F/\epsilon_{cu}$ ). The data trend is similar to that observed for stiffener crippling predictions in that a majority of the data fall on or above the  $P_{exp}/P_{anl} = 1.0$  line, indicating conservatism in the analysis of approximately 25 percent. A data point corresponding to NASA flat panels (Reference 26) falls approximately 20 percent below the analytically predicted failure value. However, this panel was designed such that failure occurred simultaneously with initial buckling of the skin and as such the panel was not loaded into the postbuckling range. Secondly, the initial buckling and failure strain of 6700  $\mu\text{in/in}$  is substantially greater than the current design allowable strain levels for strength critical parts which in turn are higher than the operating strain levels for postbuckled designs. Thus, the semiempirical analysis methodology for composite compression panels is well suited to the design of postbuckled panels where the operating strain levels are of the order of 2500-3500  $\mu\text{in/in}$ . As a design tool, the semiempirical methodology is somewhat on the conservative side and can be used with a high degree of confidence.

Automation of Stiffened Composite Panel Design Methodology - The semiempirical compression panel analysis documented in the preceding paragraphs has been used to develop a computer program named CRIP to provide an effective design tool. This program is fully documented in Reference 91 where its use is also demonstrated by a design example.

TABLE 2.4. COMPARISON OF ANALYTICAL PREDICTIONS AND TEST DATA FOR STIFFENED COMPRESSION PANELS

SPECIMEN NUMBER (REFERENCE)	PANEL TYPE	$\frac{\epsilon_{cr}}{\epsilon_{cu}}$	$\frac{\epsilon_F}{\epsilon_{cu}}$	EXPERIMENTAL VALUE ANALYTICAL VALUE		REMARKS
				BUCKLING	FAILURE	
NORTHROP/ NAVY (30)		0.0134	0.192	1.13	1.25	FAILURE DUE TO STIFFENER/WEB SEPARATION ( $\epsilon_{cu} = 0.015$ )
NORTHROP/ NAVY (30)		0.077	0.280	0.91	1.25	FAILURE DUE TO STIFFENER/WEB SEPARATION ( $\epsilon_{cu} = 0.015$ )
MCRAIR/NAVY (BASELINE) PANEL (90)		0.056	0.262	1.18	1.09	FAILURE DUE TO STIFFENER/WEB SEPARATION
AIR FORCE*		0.115	0.239	1.08	0.933	FAILURE DUE TO VERTICAL WEB CRIPPLING
U1 NASA (26)		0.561	0.561	0.78	0.81	ALL PANELS FAILED DUE TO STIFFENER/WEB SEPARATION ( $\epsilon_{cu} = 0.012$ )
U2 NASA (26)		0.258	0.379	0.87	1.04	
U3 NASA (26)		0.148	0.300	1.00	0.97	
U4 NASA (26)		0.253	0.376	0.83	1.18	
U5 NASA (26)		0.117	0.272	1.01	1.18	
U6 (NASA ) (26)		0.067	0.215	1.11	1.15	
U7 NASA (26)		0.067	0.215	1.14	1.13	
U8 NASA (26)		0.067	0.215	1.20	0.91	
20, 21 GD (89)		0.208	0.235	NOT AVAILABLE	1.24	FAILURE DUE TO STIFFENER/WEB SEPARATION ( $\epsilon_{cu} = 0.12$ )

$\epsilon_{cu}$  - LAMINATE ULTIMATE ALLOWABLE STRAIN,  $\epsilon_{cr}$  - ANALYTICAL BUCKLING STRAIN,  $\epsilon_F$  - ANALYTICAL FAILURE STRAIN

\* - TEST DATA SUPPLIED BY CAPT BECKER

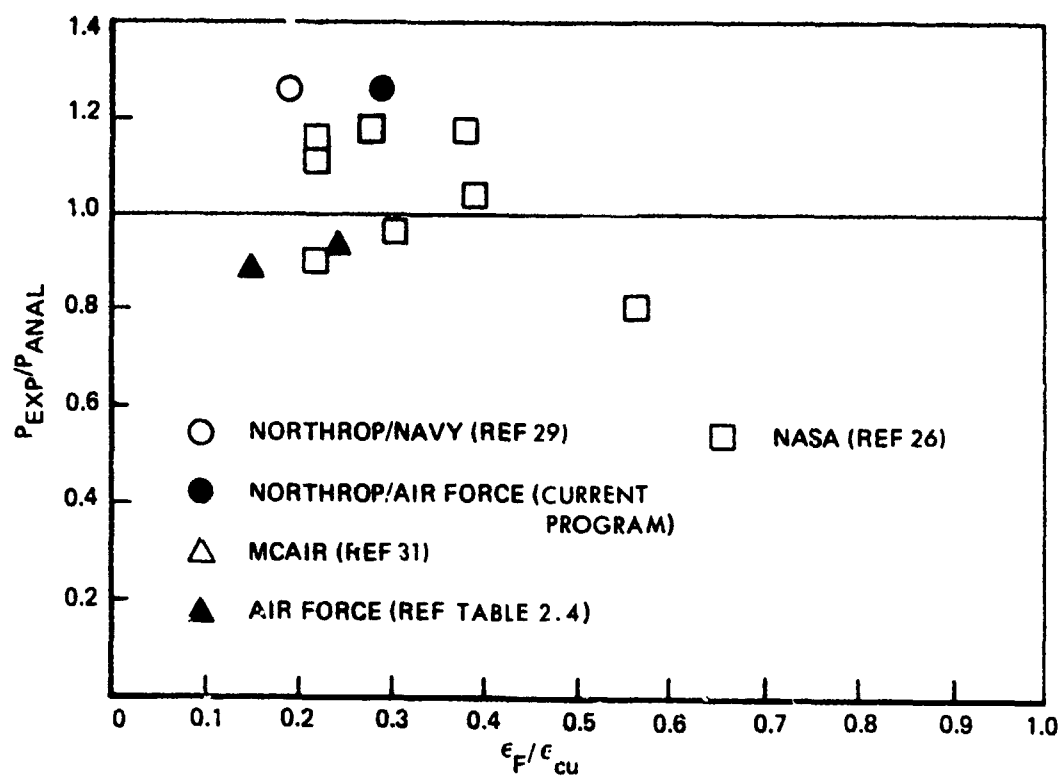


Figure 2.12. Comparison of Analytical and Experimental Data for Composite Compression Panels

The program has been written for interactive use and has several built-in stiffener shapes for application to a wide variety of designs.

### 2.3.2 Shear Panels

Flat or curved shear panel analysis is accomplished by means of the semiempirical tension field theory developed by Kuhn (Reference 2) for metal panels. In this program the tension field theory was modified for application to composite shear panels by taking into account material anisotropy.

The essential elements of the generalized (for application to metals as well as composites) tension field theory and its application are summarized in Figure 2.13. Details of the semiempirical analyses required to perform the various steps in Figure 2.13 are given in the following paragraphs. The equations as presented below pertain to cylindrically curved composite panels and to flat composite panels if terms incorporating the radius of curvature  $R$  are set equal to zero. Use of the appropriate values for elastic constants in the equations permits their direct application to metal panels. The analysis procedure is based entirely on the theory presented in Reference 2 unless specifically noted.

Computation of the Diagonal Tension Factor - The diagonal tension factor  $k$  characterizes the degree to which diagonal tension is developed in the skin of stiffened panels loaded in shear. A value of  $k = 0$  characterizes an unbuckled skin with no diagonal tension; a value of  $k = 1.0$  characterizes a web in pure diagonal tension. The diagonal tension factor is computed using the following expression:

$$k = \tanh \left[ \left( 0.5 + 300 \frac{t_w h_r}{R h_s} \right) \log \frac{\tau}{\tau_{cr}} \right] \quad (19)$$

where,

$t_w$  = web thickness

$h_r$  = ring spacing

$h_s$  = stringer spacing

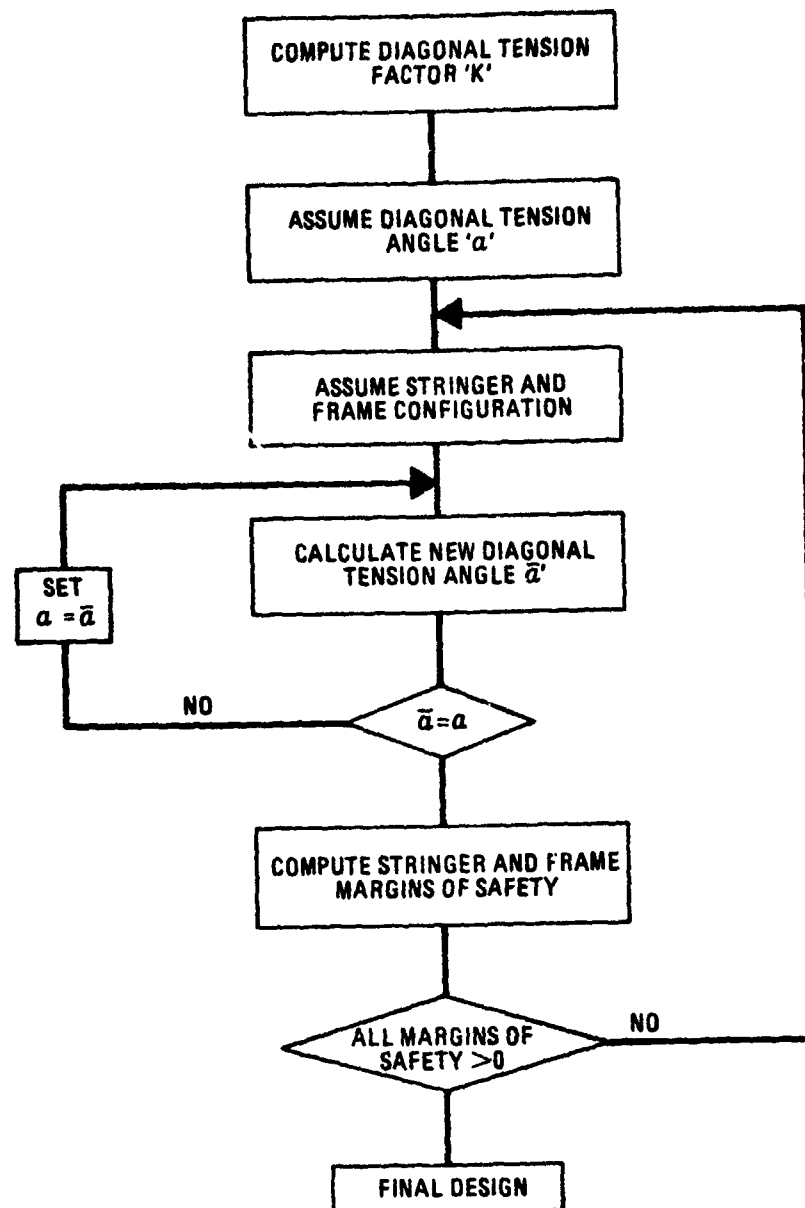


Figure 2.13 Application of Tension Field Theory to Shear Panels.

$R$  = panel radius  
 $\tau$  = applied shear stress  
 $\tau_{cr}$  = buckling shear stress of web

The shear buckling stress or strain for composite webs can be calculated using program SS8 (Reference 45). The buckling stress for curved metal webs can be calculated using:

$$\begin{aligned}
 \tau_{cr,elastic} &= \frac{K_{s1} \pi^2 E h_s^2}{12 R^2 Z^2} & \text{if } h_r \geq h_s \\
 &= \frac{K_{s2} \pi^2 E h_s^2}{12 R^2 Z^2} & \text{if } h_s \geq h_r
 \end{aligned} \tag{20}$$

where,

$K_{s1}, K_{s2}$  = critical shear stress coefficients for simply supported curved plates, given in Reference 2

$R$  = panel radius, in

$E$  = Young's modulus for the material, psi

$$\begin{aligned}
 Z &= \frac{h_s^2}{R t_w} \sqrt{(1 - \nu^2)} & \text{if } h_r \geq h_s \\
 &= \frac{h_r^2}{R t_w} \sqrt{(1 - \nu^2)} & \text{if } h_s \geq h_r
 \end{aligned}$$

$\nu$  = Poisson's ratio for the material

Computation of Diagonal Tension Angle ' $\alpha$ ' - An initial value is assigned to the diagonal tension angle ' $\alpha$ ' that defines the angle of the 'folds' in the buckled skin. For curved web systems  $\alpha = 30^\circ$  was found to be a convenient starting point. The actual value of  $\alpha$  is determined by the iterative procedure outlined below.

Using the assumed initial value of  $\alpha$ , a 'new' value for  $\alpha$  is calculated by the equation:



$$\alpha_1 = \tan^{-1} \left[ \frac{\epsilon - \epsilon_s}{\epsilon - \epsilon_r + R_f} \right]^{0.5} \quad (21)$$

$$\text{where, } \epsilon = \frac{\tau}{E_{w\alpha}} \left[ \frac{2k}{\sin 2\alpha} + \frac{E_{w\alpha}}{2G_{rs}} (1-k) \sin 2\alpha \right] \quad (21a)$$

$$\epsilon_s = \frac{-k\tau \cot \alpha}{\left[ \frac{\overline{EA}_s}{h_{sw} t} + 0.5 (1-k) E_{ws} \right]} \quad (21b)$$

$$\epsilon_r = \frac{-k\tau \tan \alpha}{\left[ \frac{\overline{EA}_r}{h_{rw} t} + 0.5 (1-k) E_{wr} \right]} \quad (21c)$$

$$R_f = \frac{1}{24} \left( \frac{h_s}{R} \right)^2 \quad \text{if } h_r > h_s \quad (21d)$$

$$= \frac{1}{8} \left( \frac{h_r}{R} \right)^2 \tan^2 \alpha \quad \text{if } h_s > h_r$$

For eccentric stringers and rings

$$\overline{EA}_s = EA_s \frac{EI_s}{EI_s} \quad (21e)$$

$$\overline{EA}_r = EA_r \frac{EI_r}{EI_r}$$

In Equations (21),  $\epsilon$  is the skin strain in the diagonal tension direction, and  $\epsilon_s$  and  $\epsilon_r$  are the strains in the stringer and the ring leg attached to the web averaged over their lengths, respectively.  $E_{w\alpha}$ ,  $E_{ws}$  and  $E_{wr}$  are the web moduli in the direction of the tension field, stringers and rings, respectively.  $G_{rs}$  is the web shear modulus.  $\overline{EA}_s$  and  $\overline{EA}_r$  are the effective

axial stiffnesses of the stringers and the rings, respectively.  $EI$  is the bending stiffness about the stiffener neutral axis and  $\overline{EI}$  the bending stiffness about the web midsurface.

In general,  $\alpha_1$ , the new diagonal tension angle will not equal the initially assumed value of  $30^\circ$ . Therefore,  $\alpha_1$  is used as the next guess and the computations of Equations (21) are repeated until the process converges, i.e.,  $\alpha_{\text{new}} \approx \alpha_{\text{old}}$ .

Once the diagonal tension angle has been determined with sufficient accuracy, the next step is to compute the margins of safety.

Computation of Stringer and Frame Margins of Safety - The diagonal tension angle value computed above is now substituted in Equations (21) to obtain the diagonal tension strain in the skin, the stringer strain, and the ring strain. Next, the stringer and ring strains averaged over the cross section and the length ( $\epsilon_{\text{ave}}$ ) and the maximum strains in the legs attached to the web ( $\epsilon_{\text{max}}$ ) are computed using the following equations:

$$\epsilon_{s_{\text{ave}}} = \epsilon_s \frac{\overline{EA}_s}{EA_s} \quad (22)$$

$$\epsilon_{s_{\text{max}}} = \epsilon_s \left[ 1 + 0.775 (1-k) (1-0.8 \frac{h_r}{h_s}) \right] \quad \text{if } h_s > h_r \quad (23)$$

$$\epsilon_{s_{\text{max}}} = \epsilon_s \left[ 1 + 0.775 (1-k) (1-0.8 \frac{h_s}{h_r}) \right] \quad \text{if } h_s < h_r$$

$$\epsilon_{r_{\text{ave}}} = \epsilon_r \frac{\overline{EA}_r}{EA_r} \quad (24)$$

$$\begin{aligned} \epsilon_{r_{\text{max}}} &= \epsilon_r \left[ 1 + 0.775 (1-k) (1-0.8 \frac{h_r}{h_s}) \right] \quad \text{if } h_s > h_r \\ &= \epsilon_r \left[ 1 + 0.775 (1-k) (1-0.8 \frac{h_s}{h_r}) \right] \quad \text{if } h_s < h_r \end{aligned} \quad (25)$$

The stringer and ring crippling mode of failure is then analyzed for by computing the stringer and ring forced crippling strains ( $\epsilon_{os}$  and  $\epsilon_{or}$ , respectively) using the following equations:

$$\epsilon_{os} = 0.00058 \left[ \left( \frac{\epsilon_{all} E_{cs}}{1000} \right)^{0.4} k^{2/3} \left( \frac{t_{us}}{t_w} \right)^{1/3} \right] \quad (26)$$

$$\epsilon_{or} = 0.00058 \left[ \left( \frac{\epsilon_{all} E_{cr}}{1000} \right)^{0.4} k^{2/3} \left( \frac{t_{ur}}{t_w} \right)^{1/3} \right] \quad (27)$$

where  $\epsilon_{all}$  is the laminate allowable strain,  $E_{cs}$  and  $E_{cr}$ , are the modulus of the stringer and ring leg attached to the web, respectively, and  $t_{us}$  and  $t_{ur}$  are the thickness of the stringer and the ring leg attached to the web.

The critical stiffener strains corresponding to the bending stiffness required for stiffener stability are calculated using Equations (28) and (29).

$$\epsilon_{sB} = \frac{4\pi^2 EI_s}{E_{xs} A_s h^2} \quad (28)$$

$$\epsilon_{rB} = \frac{4\pi^2 EI_r}{E_{xr} A_r h^2} \quad (29)$$

where,  $\epsilon_{sB}$  and  $\epsilon_{rB}$  are the Euler buckling strains for the stiffener and the ring, respectively.

The margins of safety can now be computed for each of the possible failure modes by comparing the calculated strain values with the allowables. Thus, to ensure positive margins, the following failure modes are examined and the corresponding inequalities verified.

- (i) For stringer and ring stability,  
i.e., no column failure
- $$\epsilon_{sB} > \epsilon_{s\text{ave}}$$
- $$\epsilon_{rB} > \epsilon_{s\text{ave}}$$
- (ii) For stability of the entire panel, i.e., to prevent buckling of the web as a whole, before formation of the tension field
- $$EI_s > E_s t_w^3 \left( \frac{3h_s}{h_r} - 2 \right) h_s$$
- $$EI_r > E_r t_w^3 \left( \frac{3h_r}{h_s} - 2 \right) h_r \quad (30)$$
- (iii) For prevention of forced crippling of stiffeners
- $$\epsilon_{os} > \epsilon_{s\text{max}}$$
- $$\epsilon_{or} > \epsilon_{r\text{max}}$$

An additional check needs to be performed for metal panels where yielding or permanent set in the web is likely due to excessive skin deformation. The only available criterion for permanent set check has been empirically obtained from tests on flat aluminum metal panels. Its applicability to other materials or curved panels has not been verified. Thus, in the absence of any other guidelines, the flat panel requirement that the maximum allowable value of the diagonal tension factor  $k_{all}$  be limited to

$$k_{all} = 0.78 - (t - 0.012)^{0.50} \quad (31)$$

at design ultimate load to prevent permanent buckling of the web at limit load, is used in the present analysis.

Experimental Validation of Shear Panel Analysis - The semiempirical analysis outlined above has been experimentally verified for metal panels in References 2 and 5. In order to validate the modifications introduced in the methodology for anisotropic materials, the analysis results were compared with available test data for composite shear panels. The analysis methodology was exercised on composite shear panels designed, fabricated and tested in References 13 through 17. In these studies a total of 7 panel configurations with different stiffener shapes, web thicknesses, web laminate orientations, and stiffener spacings were tested through the

use of various test setups. Table 2.5 summarizes some of the key parameters of the panels, and the ratio of the analytically predicted failure loads to the experimentally observed failure loads. The analytical predictions were based on stringer forced crippling mode of failure. The failure mode for all panels tested was separation of the stringers from the panel skin. The good agreement between the measured and predicted failure strains inspite of the difference in failure modes indicates that the two failure modes are closely related and it is hypothesized that forced crippling of the stringers in shear panels precipitates skin/stiffener separation. Thus, the stiffener forced crippling criteria can be used to predict stiffener/skin separation in composite shear panels.

**TABLE 2.5. CORRELATION OF SEMI-EMPIRICAL ANALYSIS WITH TEST DATA FOR SHEAR PANELS**

INVESTIGATOR (REFERENCE)	$h_s$ (INCH)	$h_r/h_s$	STIFFENER SHAPE	$EA_s$ (KSI)	$EI_s$ LB/IN <sup>2</sup> X 10	$\frac{\tau_{ULT}}{\tau_{cr}}$	$P_{ANL}/P_{EXP}$
NORTHROP/NAVY (14)	10	1.5	HAT	2.5	0.40	5	0.93
MCDONNELL/NAVY (16,94)	6	2.67	HAT	1.8	0.37	9.2	0.91 (1.03)*
LOCKHEED NAVY (15)	6	3.75	I	1.5	0.90	6	1.08
GRUMMAN/NAVY (17)	7	3.43	HAT	2.9	1.0	6	1.025
NORTHROP/IR&D (13)	13	1.15	HAT	2.9	0.73	10	1.05
NORTHROP/IR&D (13)	13	1.15	I	2.9	0.313	10	0.91
NORTHROP/IR&D (13)	9	1.66	HAT	2.9	0.30	7	0.80

\* = Failure due to ring crippling  
 $h_s$  = Stringer spacing  
 $h_r$  = Ring spacing  
 $EA_s$  = Stringer axial stiffness  
 $EI_s$  = Stringer bending

$\tau_{ULT}$  = Ultimate failure stress  
 $\tau_{cr}$  = Buckling stress  
 $P_{ANL}$  = Analytical failure load  
 $P_{EXP}$  = Experimental failure load

It should be noted that the forced crippling equations used in the analysis, Equations (26) and (27), do not specifically include the interface material properties. Additional verification using data generated for a variety of material systems is essential before the application of these equations to stiffener/web separation prediction can be generalized. Failure of the stiffener/web interface does not necessarily have to occur if the interfacial strength can sustain the applied stresses due to forced crippling. Thus, the forced crippling criterion seems to present a lower bound for the failure load of cocured composite stringers by stiffener/web separation. This information is of significance to designers.

All panels examined above consisted of composite stringers and metal frames (rings) with the exception of the panels in Reference 16. The ring crippling failure load and the stringer crippling failure load for the panels in Reference 16 were nearly equal in magnitude with analytically predicted failure due to stringer separation. Although the experimental data showed failures due to frame (ring) separation, subsequent efforts to improve the strength of these panels by improving the ring/web interface (Reference 83) resulted in failure due to stringer/web separation without much increase in the panel failure load, indicating both modes of failure to be quite close to each other as predicted.

The analytical and experimental correlations presented above, thus, mark a milestone in the analysis of postbuckled composite shear panels since they validate the modifications to the tension field theory.

Automation of Shear Panel Analysis Methodology - The modified tension field theory outlined above has been incorporated in a computer program called TENWEB that can be used as an efficient design tool. Detailed documentation for this shear panel analysis program is given in Reference 91. The program is interactive and has several built-in stiffener profiles for design flexibility.

Program TENWEB was used to design the shear panels tested in this study. Details of program operation are given in Reference 91.

## SECTION 3

### EXPERIMENTAL PROGRAM

#### 3.1 INTRODUCTION

The technology assessment documented in Section 2 showed that the current design methodology for postbuckled panels is predominantly empirical and was originally developed on the basis of flat metal panel test data. Although the methodology was later extended to curved metal panels, the data base to verify this extension was extremely limited. Since the near term application of postbuckled metal or composite panel designs is expected to be in curved fuselage structures, it is essential that the differences in the static and fatigue response of flat and curved panels be understood and the available data base on curved metal and composite panels be expanded for verification of the analysis methodology.

There are two main differences in the postbuckling behavior of curved and flat panels. First, evidence exists to show that the initial buckling load of curved metal panels, while higher than flat panels of the same size, is reduced significantly after repeated loading. Test data do not show the same phenomenon for flat metal panels. Test data show that the buckling load of composite flat panels is reduced due to fatigue loading.

Second, the buckling of curved shear panels produces significant inward normal forces on the stringers and frames. These forces may prove beneficial for cocured composite panels, since they tend to delay the separation of stringers and frames from the skin, which was found to be a primary mode of failure in flat composite tension field panels. These differences in the behavior of curved and flat panels may have a significant effect on their ultimate strength and fatigue life. Therefore, in this experimental program, curved metal and composite panels were tested to establish a reliable data base on their static and fatigue response. As a first step in developing a design methodology for curved postbuckled panels, it was also decided that the panels would be loaded either in compression or shear only, so that once panel behavior under these simpler

loading conditions was understood, the more complex case of combined loading could be addressed next.

Thus, the specific objective of the test program was to conduct static and fatigue tests on curved metal and composite panels, loaded well into the postbuckling range under compression or shear so that data could be obtained to fill the gaps in the current technology related to postbuckled aircraft structures. In order to define a cost-effective test matrix for the program, the most crucial data requirements were identified from the technology assessment of Section 2. These data gaps are summarized in Table 3.1 and were used in selecting the test matrix. Selection of the test specimen configuration, and the design criteria was based on the geometric and loading conditions encountered in actual aircraft fuselage construction. Design of the test specimens is detailed in Section 3.2.

A detailed rationale for the selected test matrix and the scope of the tests is given in Section 3.3. The other significant aspects of the experimental program such as fabrication of the test specimens, the test fixture and instrumentation used, and the test procedure are described in Section 3.4 through 3.6. The test data obtained are summarized in Section 3.7.

### 3.2 DESIGN OF CURVED TEST PANELS

Aircraft fuselage structural panels are rarely, if ever, of constant curvature. Typical military aircraft fuselage structures range approximately between 6 and 20 feet in diameter. Stiffened panels used in constructing large diameter fuselage have relatively mild curvatures, and flat panels can generally be used to simulate their behavior. Fuselage panels in fighter aircraft have considerably smaller radii of curvature. In order to duplicate the behavior of such panels and to evaluate the effect of curvature on postbuckling behavior, panels with relatively small radii of curvature must be tested. The panels selected for the present test program fall in this latter category and have a radius of 45 inches. This radius of curvature was selected since it is representative of small diameter fuselage panels and to enable demonstration of the most significant differences between the behavior of flat and curved postbuckled panels. The results obtained



TABLE 3.1. DATA GAPS IN THE CURRENT TECHNOLOGY FOR DESIGN AND LIFE ANALYSIS OF CURVED POSTBUCKLED PANELS

MATERIAL AND LOADING	DATA GAPS			REMARKS
	STATIC ANALYSIS VALIDATION	FATIGUE FAILURE MODE AND S-N RESPONSE		
METAL COMPRESSION PANELS	<ul style="list-style-type: none"> <li>R/t<sub>w</sub> ratio dependence of skin buckling load</li> <li>Skin buckle pattern progression with load</li> <li>Skin and stringer strain distribution</li> <li>Load to out-of-plane displacement relation</li> </ul>	<ul style="list-style-type: none"> <li>Failure mode</li> <li>Load vs. fatigue life curves</li> <li>Skin and stringer strain pattern correlation with S-N data</li> <li>Stiffness change with repeated loading</li> </ul>		<ul style="list-style-type: none"> <li>No fatigue data available for curved metal compression panels.</li> <li>Static strain distribution data useful in verifying non-empirical analysis</li> </ul>
COMPOSITE COMPRESSION PANELS	<ul style="list-style-type: none"> <li>Stiffener crippling strain</li> <li>Stiffener/web separation strain</li> <li>Skin buckle pattern progression with load</li> <li>Boundary conditions and skin dimensions for <math>\epsilon_{sk}</math> calculation</li> </ul>	<ul style="list-style-type: none"> <li>Fatigue failure modes</li> <li>Additional strain-life data to establish endurance limit</li> </ul>		<ul style="list-style-type: none"> <li>Semi-empirical static failure prediction methodology needs to be verified</li> <li>Force fatigue failures to uncover any possible modes other than stiffener/web separation</li> </ul>
METAL SHEAR PANELS	<ul style="list-style-type: none"> <li>Skin and stringer strain distribution in post-buckled regime</li> <li>Forced crippling load for stiffeners</li> <li>Failure mode identification</li> <li>Permanent set criterion</li> </ul>	<ul style="list-style-type: none"> <li>Failure mode</li> <li>Load vs. fatigue life curves</li> <li>Skin and stiffener strain pattern correlation with S-N data</li> <li>Stiffness change with repeated loading</li> </ul>		<ul style="list-style-type: none"> <li>Fatigue data not available</li> <li>Static strain distribution useful for non-empirical analysis verification</li> <li>Tension field theory applicability needs verification</li> </ul>
COMPOSITE SHEAR PANELS	<ul style="list-style-type: none"> <li>Skin dimensions and boundary conditions for <math>\epsilon_{sk}</math> calculations</li> <li>Failure mode identification</li> <li>Forced crippling strains for stiffeners</li> <li>Skin and stringer strain distribution</li> </ul>	<ul style="list-style-type: none"> <li>Failure mode</li> <li>Load vs. fatigue life curves</li> <li>Skin and stiffener strain distribution; correlation with S-N data</li> </ul>		<ul style="list-style-type: none"> <li>Fatigue data not available</li> <li>Applicability of modified tension field theory to curved composite panels needs verification</li> </ul>

will be directly applicable to a large number of future aircraft. In addition, the metal and composite panels are designed to satisfy the same design criteria so that their relative efficiencies can be compared.

The design of metal and composite shear and compression panels, and the design criteria are described in this section. The analysis methodology used for this purpose has been detailed in Section 2. The resulting panel configurations were used in the test program.

### 3.2.1 Design Criteria

The typical compression and shear loads acting on an aircraft fuselage panel can have a relatively wide range of values depending upon the panel location and the type of aircraft. However, panels allowed to buckle are generally lightly loaded and thus the loading range is significantly narrowed. A limit load intensity range of 300 to 800 pounds per inch for shear and compression panels can accommodate a large number of fighter as well as larger aircraft. Recent studies conducted under Navy sponsorship have concentrated on a limit load intensity of 400 pounds per inch. In order to extend the range of currently available experimental data, the panel configurations selected for this program were designed for a limit load intensity of 600 pounds per inch. The panels are designed to buckle at approximately 30 percent of the limit load and to withstand ultimate load (1.5 times design limit load) without rupture or collapse. The design loads for the metal and composite panels are summarized in Table 3.2.

### Material Selection

The composite shear and compression panels were fabricated using a combination of woven and unidirectional graphite/epoxy materials. The woven graphite/epoxy material selected was Hercules A370-5H/3501-6, whereas Hercules AS/3501-6 graphite/epoxy tape was used for the unidirectional material. These material systems are representative of the composite materials currently being used in fighter aircraft structures. The mechanical properties of these materials are summarized in Table 3.3.

The metal panels were fabricated using rolled aluminum sheet and extruded stringers. The alloy used was 7075 with a T6 heat treatment. The

**TABLE 3.2. DESIGN LOADS FOR METAL AND COMPOSITE TEST PANELS**

DESIGN LOADS	COMPRESSION PANELS $N_x$ , lbs/in	SHEAR PANELS $N_{xy}$ , lbs/in
SKIN BUCKLING LOAD, $N_{cr}$	200	200
DESIGN LIMIT LOAD, DLL	600	600
DESIGN ULTIMATE LOAD, DUL	900	900

**TABLE 3.3. GRAPHITE/EPOXY MATERIAL PROPERTIES**

PROPERTY	AS/3501-6	A370-5H/3501-6 (FABRIC)
$E_1^C$ , psi	$18.7 \times 10^6$	$10.0 \times 10^6$
$E_2^C$ , psi	$1.87 \times 10^6$	$9.2 \times 10^6$
$G_{12}$ , psi	$0.85 \times 10^6$	$0.9 \times 10^6$
$\nu_{12}$	0.3	0.055

properties for this material were obtained from MIL-HDBK-5.

### 3.2.2 Curved Shear Panel Design

A flow chart summarizing the design procedure for curved composite and metal shear panels is shown in Figure 3.1. The design loads for the shear panels are given in Table 3.2. A frame spacing ( $h_f$ ) of 24 inches was selected for the shear panels since it is representative of actual fuselage structures. The stiffener configuration selection was based on consideration of structural efficiency, manufacturing feasibility and cost (for composites), and current design practice.

In several recent studies hat section stringers have been chosen for composite shear panels because of their superior efficiency. Design application and fabrication studies have shown that, due to their higher torsional stiffness as compared to open sections, hat stiffened panels can be efficiently accommodated in fuselage construction. Thus, a hat section stringer configuration was selected for the composite shear panels. The frame configuration selected was a J-section since it is relatively easy to fabricate, while at the same time providing ease of attachment to other substructure.

For the metal shear panels, Z-section stringers and frames were selected since they offer the best cost and efficiency advantages as demonstrated by their widespread use in many existing aircraft.

The overall shear panel configuration selected consists of three stringers and two frames (rings). Sizing of the composite and metal panels to meet the design criteria was carried out as follows:

- a. Determine the optimum stringer spacing, and web configuration to satisfy design buckling loads.
- b. Size stringers and frames to accommodate ultimate panel load.

Details of the procedure used are given in the following paragraphs.

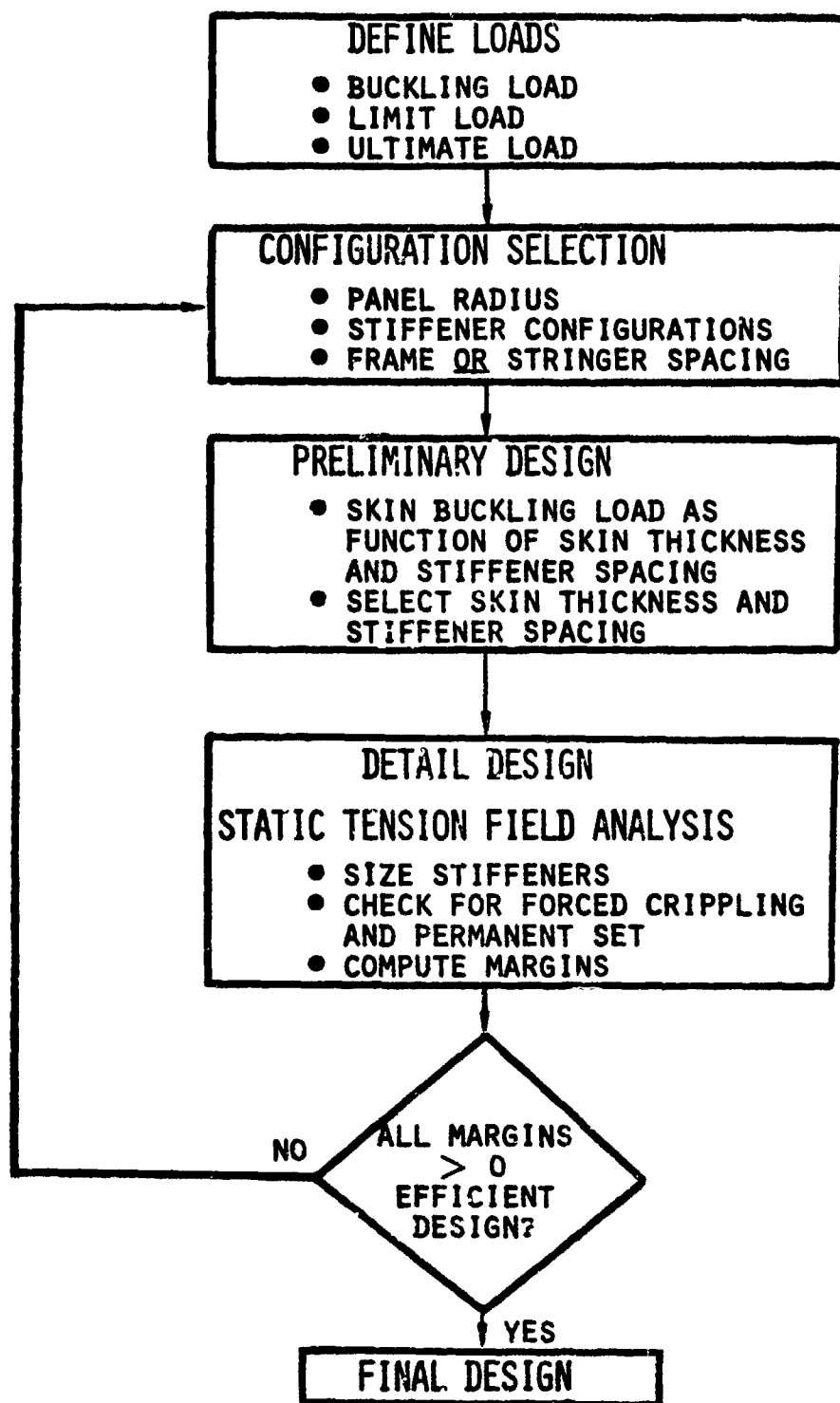


Figure 3.1 Shear Panel Design Procedure.

### Composite Shear Panel

Two possible web configurations (  $45_2, 90, 45_2$  ) and (  $45, 0, 90, 0, 45$  ), which are efficient in the range of design loads being considered, were studied to determine their initial buckling loads. The first configuration consists of four fabric plies and one unidirectional tape ply and has a nominal thickness of 0.0572 inch. The second configuration consists of two fabric plies and three unidirectional tape plies and is 0.0416 inch thick. The second ply skin configuration barely exceeds the minimum gage that is permitted in sound design practice.

The next step in the design procedure was to determine the skin buckling load as a function of skin thickness ( $t_w$ ) and the stiffener spacing ( $h_s$ ) in order to permit a judicious selection of values for these two parameters. For this purpose a buckling parameter  $\lambda$ , equal to the ratio of the calculated buckling load and the design buckling load, was defined. The buckling load was calculated using computer code SS8 (Reference 45) and the previously selected frame spacing of 24 inches.

Plots of buckling parameter " $\lambda$ " for the two web configurations for different widths are presented in Figures 3.2 and 3.3. These plots were obtained clamped and simply supported for boundary conditions as illustrated in the two figures. The cylindrically curved edges for both cases were clamped. In a stiffened panel the exact boundary conditions are not known and it is common practice to assume that the conditions are intermediate between the two above boundary conditions to determine the buckling load of the panel web between the stiffeners. Thus, the stiffener spacing for the two panel configurations to satisfy the design buckling requirements should be 10 and 5.25 inches, respectively.

The panel web configuration with a (  $45_2, 90, 45_2$  ) lay-up and with the larger stiffener spacing is much more desirable than the Figure 3.3 configuration, since it will result in substantial manufacturing cost and weight savings and, therefore, was selected for use in this program.

In order to size the stringers and the frames, tension field theory as applicable to composite panels was used. Details of the tension field theory

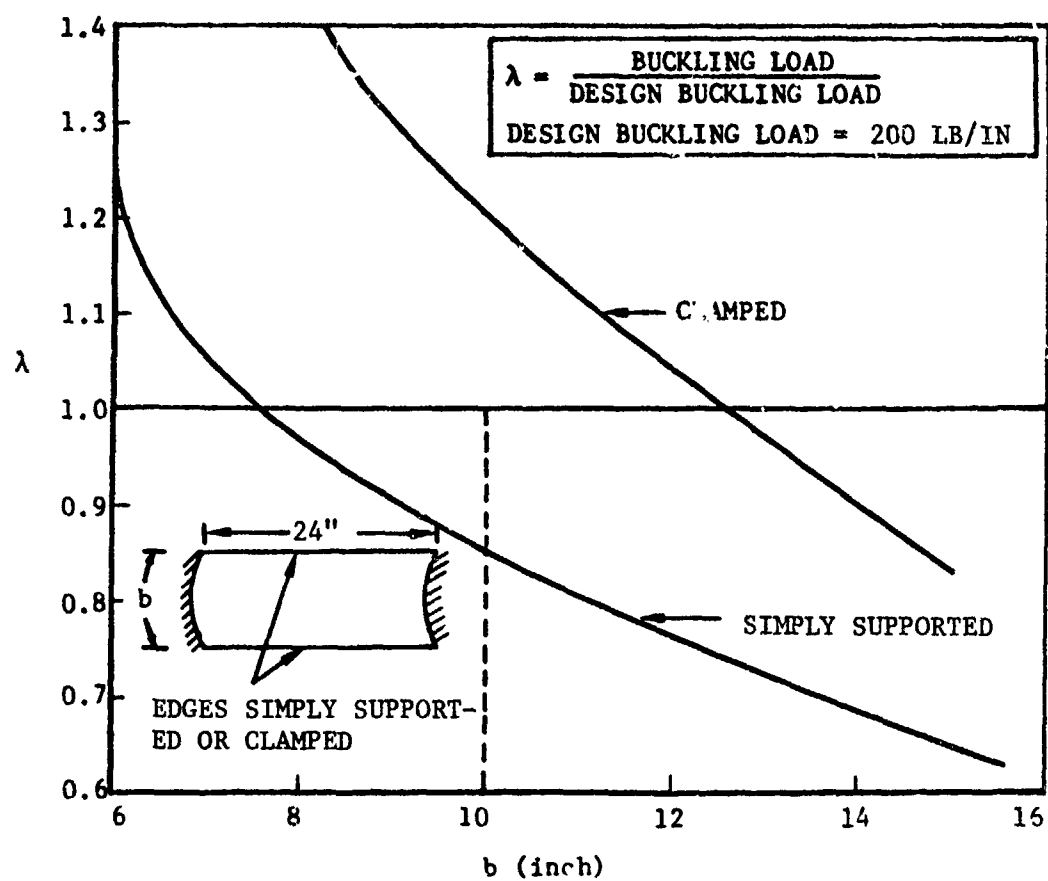


Figure 3.2 Buckling Load of a Curved Graphite-Epoxy Plate  
 ( $\underline{45}_2, 90, \underline{45}_2$ ) Under Shear Loading.

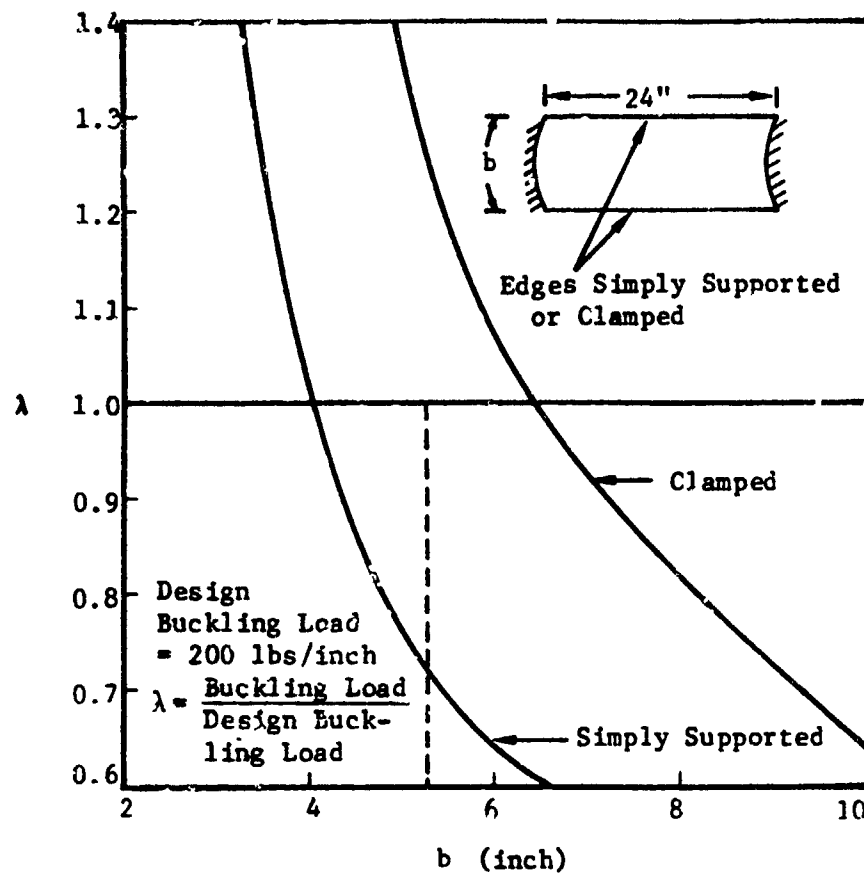


Figure 3.3 Buckling Load of a Curved Graphite/Epoxy Plate Under Shear Loading. (45/90/0/90/45) Layup.



with an accompanying summary flow chart are given in Section 2 (Refer to Figure 2.13). The iterative design procedure was implemented via computer program TENWEB (Section 2 and Reference 91). The program run used to size these test panels is given in Reference 91, Section 3, as Figure 5. The resulting panel design shown in Figure 3.4. The calculated design values and failure modes are summarized in Table 3.4. The panel edges have been increased in thickness to preclude any failures due to load introduction. As mentioned before, the hat section stringers and J-section frames have been used primarily due to their efficiency and lower fabrication costs.

#### Metal Shear Panel

The design of the metal shear panel proceeded exactly along the same lines as that of the composite shear panel described above. The frame and stringer spacing were selected to be the same as for the composite panel ( $h_r = 24"$ ,  $h_s = 10"$ ), the web thickness  $t_w = 0.063"$  was calculated using Figure 3.5 (Reference 34) as necessary to prevent buckling below design buckling load.

The stringers and the frames were sized using computer code TENWEB (Reference 91). The resulting panel configuration is shown in Figure 3.6. The fastener spacing was calculated so as to preclude inter-fastener buckling (Reference 34) and to prevent bearing failure near the fastener holes. HYLOK fasteners were used instead of rivets to reduce fabrication costs. In order to use flush rivets on thin skin (0.063") the skin has to be dimpled, whereas the use of HYLOK fasteners does not necessitate skin dimpling. It should be noted that the panel edges were not initially reinforced since the web thickness is sufficiently large to prevent any static failure due to load introduction. The computer output for the metal shear panel design is included in Appendix A for reference purposes. The additional check required for metal panels where yielding or permanent set in the web is likely due to excessive skin deformation, was performed using Equation 31. The predicted failure mode for the metal panel configuration shown in Figure 3.6 was permanent set in the web. The calculated design values and the failure load predictions for the metal shear panel are summarized in Table 3.4.

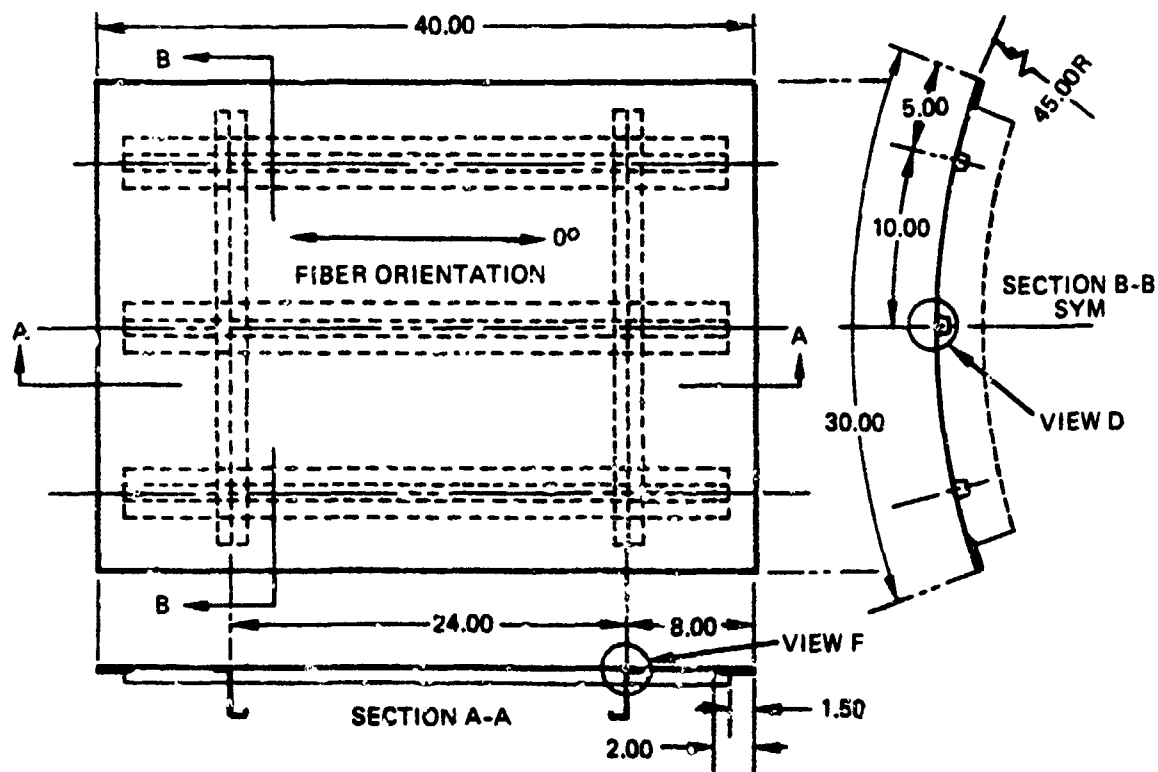
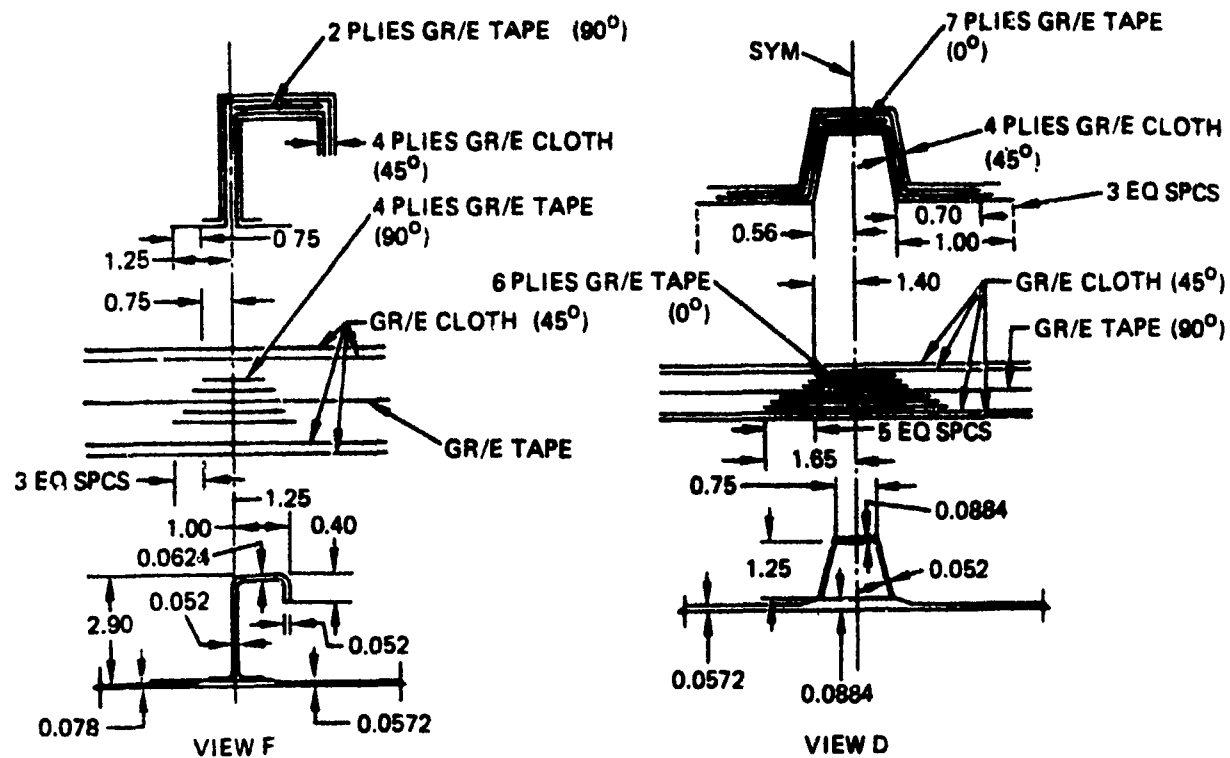


Figure 3.4 Composite Shear Panel Design.

TABLE 3.4. COMPOSITE AND METAL SHEAR PANEL DESIGN SUMMARY

CALCULATED PARAMETER	METAL PANEL	COMPOSITE PANEL
DIAGONAL TENSION ANGLE, $\alpha$	36.9°	29.4°
FAILURE MODE	PERMANENT SET IN WEB	FORCED CRIPPLING OF STRINGER
$\frac{\tau_{ULT}}{\tau_{CR}}$	2.6	4.5
PANEL WEIGHT	2.84 LB.	1.31 LB.

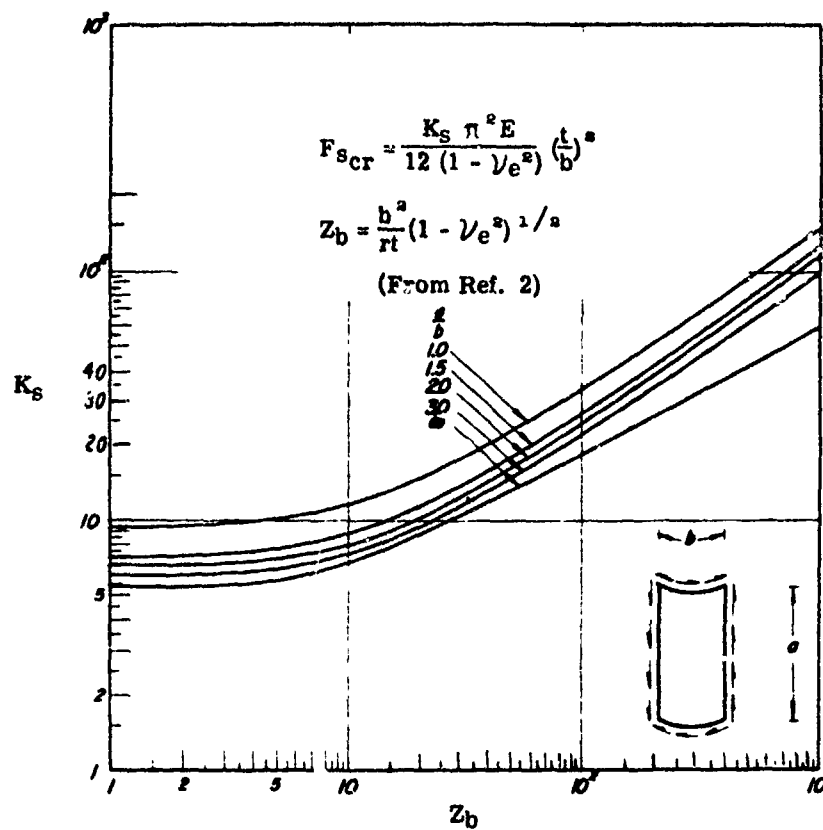


Figure 3.5 Shear Buckling Coefficient for Long Simply Supported Curved Plates (Reference 34).

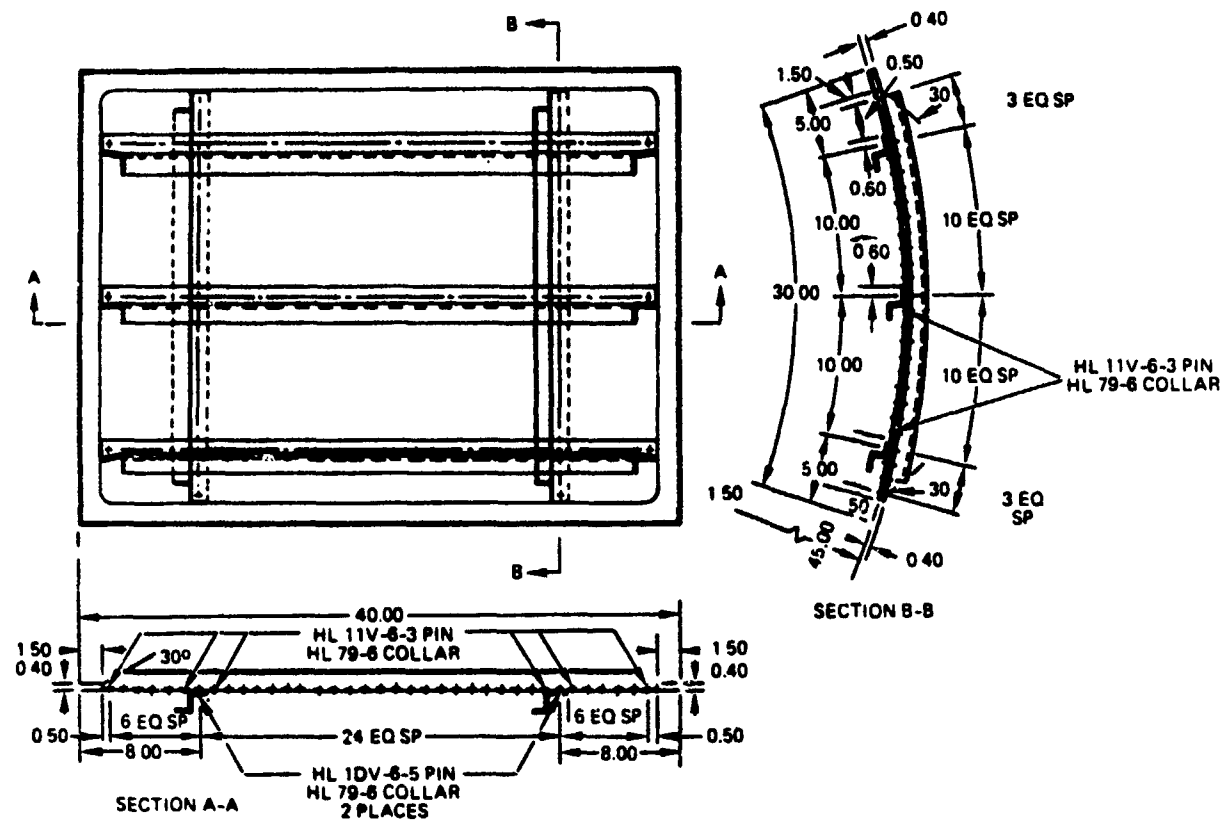


Figure 3.6 Metal Shear Panel Configuration. Stringers are AND10138-1206 and Frames are AND10138-1306 Aluminum Z-Sections.

### 3.2.3 Curved Compression Panel Design

Design of the curved composite and metal compression panels was carried out in accordance with the flowchart shown in Figure 3.7. It is worthwhile to mention here that a curved compression panel can be used to simulate the behavior of a cylindrical built-up fuselage structure provided the cylindrically curved panel is of sufficient width and the appropriate boundary conditions are used. Guidelines for determining the panel width and appropriate boundary conditions, so that the panel buckling load will equal the buckling load of a cylinder loaded in axial compression, have been presented by Sobel and Agarwal (Reference 92). It was shown that a panel enclosed by an angle which is greater than 100 degrees results in a buckling load equal to the complete cylinder load for any arbitrary boundary conditions along the straight edges. At the same time, a panel which is enclosed by less than 20 degrees results in a much higher buckling load than a complete cylinder. A panel enclosed by 30 degrees is able to model a complete cylinder if the appropriate boundary conditions are used along the straight edges, namely SS1 ( $w = M = N_y = N_{xy} = 0$ ), SS3 ( $w = M = u = N_y = 0$ ) or CC1 ( $w = \phi = N_y = N_{xy} = 0$ ). A combination of boundary conditions SS1, SS3, and CC1 can be obtained if one stringer is located at each side of the panel. Thus, for the test program, a cylindrically curved panel enclosed by at least a 30-degree angle with one stiffener at each side was used to simulate the complete cylinder behavior.

Selection of the stringer configuration for the composite panels was based on an experimental and analytical evaluation of several flat compression panels with different stiffener configurations conducted in Reference 44. Figure 3.8 taken from Reference 44 shows that hat stiffeners are the most efficient stiffeners for axially loaded panels (all panels assumed to be buckling resistant). Although the panels in the present program were subjected to loads beyond buckling, the stiffeners carry a major portion of the load in the postbuckling range and, therefore, the efficiency comparison shown in Figure 3.8 should be equally applicable. Thus, hat section stiffener configuration was selected for the composite compression panels. Z-section stiffeners were selected for the metal compression panels due to their

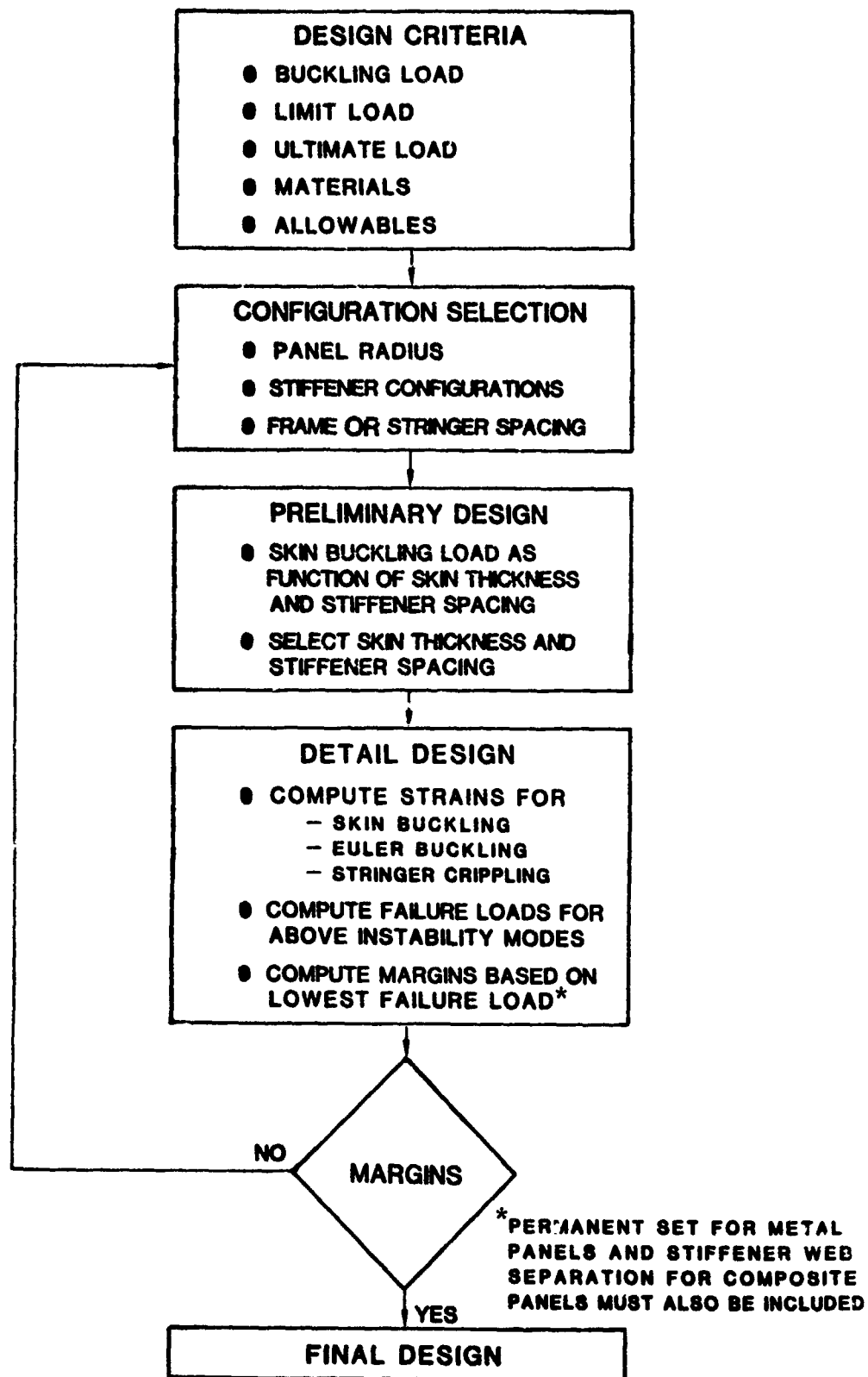


Figure 3.7. Compression Panel Design Procedure

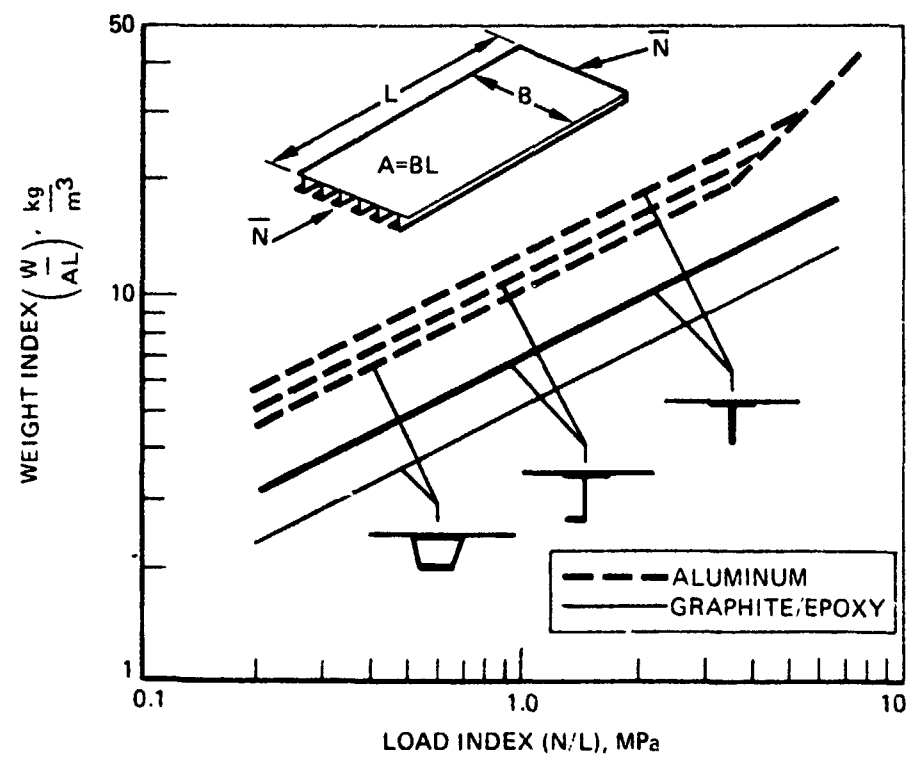


Figure 3.8 Compression Load Structural Efficiency Comparison for Hat-, J-, and Blade Configurations.



widespread use in current design practice. The frame spacing for the compression panels was selected as 20 inches based on the typical spacing of 15-20 inches used in stringer stiffened fuselage shells, and to allow for skin buckling and stiffener crippling at loads reasonably close to the design loads.

A four stiffener, 3-bay configuration was selected for the compression panels based on test data developed in Reference 93, where panels tested with two or three stiffeners resulted in poor agreement with analytical solutions due to distortion of edge stiffeners. However, panels tested with four stiffeners resulted in good agreement with the analytical solutions. The reason for the good correlation in the latter case was that the distortion of the edge stiffeners did not affect the panel center bay.

Design calculations for the composite and metal compression panels are summarized in the following paragraphs.

#### Composite Compression Panel

In selecting the web configuration, design and test studies conducted in References 30 and 31 were used for guidance. In the referenced studies the stiffeners were spaced relatively close together and the panel web was quite thin with a ( $\pm 45$ ,  $\mp 45$ ) lay-up. In the present program the panel web was made slightly thicker and the stiffener spacing was increased to lower manufacturing costs and improve panel efficiency. A skin lay-up of [45 / 0 / 90 / 0 / 45] with a nominal thickness equal to .0416 inch was selected in conjunction with a stiffener spacing of 12.2 inches to meet the design load requirement for skin buckling. The end bays of the four stiffener, 3-bay compression panel were made narrower to preclude early failure in the end bays while at the same time the end bay width was sufficient to ensure skin buckling at loads much lower than the failure load.

The initial buckling load and the Euler buckling load of the composite curved panels were obtained through the use of computer code BUCLASP-2 (Reference 41). Since it is easier to work with strain for composite panels, the following discussion makes extensive use of strain rather than stress.

The buckling strains obtained from the computer code BUCLASP-2 were reduced by 25 percent to accommodate lower buckling strains due to imperfection effects, a common practice for metal panels. However, the percent knockdown is dependent on several design parameters which are not defined for composite panels; therefore, for an initial design estimate, the guidelines for metal panels given in Reference 34 (see also Figure 2.7) were used.

The crippling strain ( $\epsilon_{cc}$ ) is obtained using Equations 5 through 9 and the failure load calculated using Equations 11 through 14. The total load on the panel at stiffener crippling is the sum of the loads carried by the stiffeners and the web. In order to obtain the load in the web the effective width method was used. Equation 13A given in Section 2 was used to obtain the effective width.

Detailed design calculations for the composite compression panel were conducted using computer code CRIP, a sample run for which is included in Reference 91, Section 1, as Figure 3. The panel configuration obtained using the above approach is shown in Figure 3.9. A summary of the initial buckling and final failure strain predictions for the test specimen is shown in Table 3.5.

#### Metal Compression Panel

The metal panel configuration selected for preliminary design was of the following geometry:

Stiffener spacing	$b_s = 10$ inches
Web thickness	$t_w = 0.05$ inch
Panel length	$L = 20$ inches

The local buckling stress for the center bay web between stiffeners was calculated using the equations given in Reference 34. In accordance with Reference 34, the buckling stress  $F_{cr}$  for a curved sheet in compression with simply supported boundary conditions is obtained as

$$F_{cr} = \frac{K_c \pi^2 E}{12(1-\nu^2)} \left( \frac{t_w}{b_s} \right)^2$$

where  $K_c = 13$  (from Figure 2.6)

$$\therefore F_{cr} = 3143 \text{ psi}$$

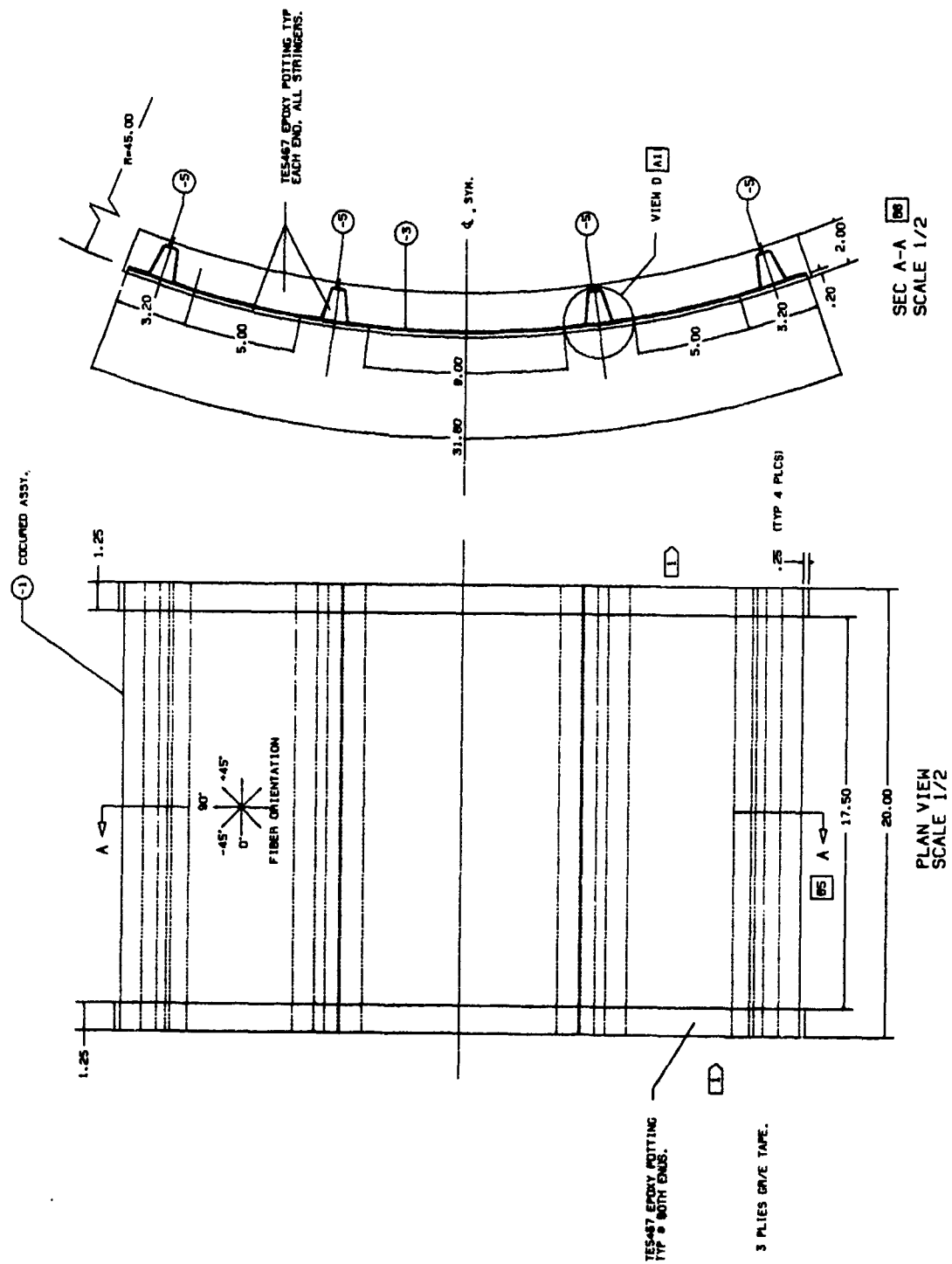


Figure 3.9. Composite Compression Panel Configuration

TABLE 3.5. COMPOSITE AND METAL COMPRESSION PANEL DESIGN SUMMARY

CALCULATED PARAMETER	METAL PANEL	COMPOSITE PANEL
INITIAL BUCKLING -LOAD, $N_x^{cr}$ lb/in	206	--
-STRAIN, $\mu\text{in/in}$	--	870
FAILURE -LOAD, $N_x^F$ lb/in	1050	--
-STRAIN, $\mu\text{in/in}$	--	4956
FAILURE MODE	STIFFENER CRIPPLING	
POSTBUCKLING RATIO	5.1	5.7

The design buckling load ( $N_{x,cr}$ ), however, = 200 lb/in. Hence the stiffener area ( $A_s$ ) required is obtained as follows:

$$A_s = \frac{N_{x,cr} b_s}{F_{cr}} - b_s t_w$$

$$A_s = .1363 \text{ inch}^2$$

Assume the stiffener configuration to be AND 10138-1004 which is shown in Figure 3.10. Thus, the predicted panel buckling load  $N_{xy,cr} = 206 \text{ lb/in}$  which results in a 3 percent margin of safety.

Failure analysis of the panel was carried out in accordance with the procedure outlined in Section 2. Figure 2.6 was used to calculate the crippling stress  $F_{cs}$  for the stiffener and yielded:

$$F_{cs} = 48.9 \text{ ksi}$$

The effective web width at the time of stiffener crippling,  $w$ , was calculated from Equation 13A as:

$$w = 1.2 \text{ inch}$$

The total load at panel failure  $P_{ult}$  is calculated using Equation (14) which yields:

$$P_{ult} = F_{cs} (A_s + w t_w)$$

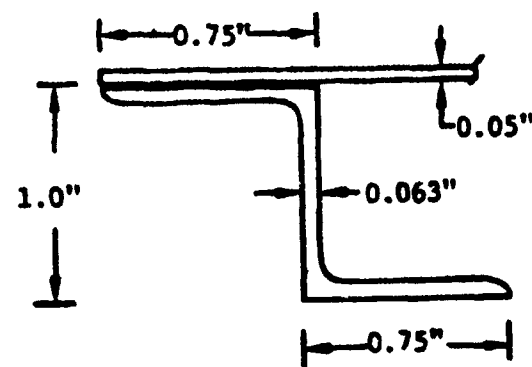
$$= 48900 (.155 + 1.2 \times .05)$$

$$P_{ult} = 10500 \text{ lb.}$$

Hence, the ultimate failure load per unit width ( $N_{x,ult}$ ) is

$$N_{x,ult} = \frac{P_{ult}}{b_s} = 1050 \text{ lb/in}$$

Thus, the panel failure load allows approximately a 15 percent margin of safety.



stiffener area  $A_s = 0.155$  sq. inch

stiffener M.O.I.  $I_{xx_s} = 0.0236$  inch<sup>4</sup>

Figure 3.10 Z-Section 7075-T6 Aluminum Stringer.  
AND 10138-1004 Configuration.

For overall panel instability the Euler buckling stress was calculated using Equation 3 in the following form:

$$\sigma_{\text{Euler}} = \frac{\pi^2 EI_e}{L_e^2 A_t}$$

where,  $L_e$  is the effective length of the panel,  $A_t$  is the total area of the panel and  $I_e$  is the panel moment of inertia about the neutral axis. Since the frame spacing for design purposes was assumed to be 20 inches, the effective length "L" for Euler buckling is 10 inches ( $C = 4$  in Equation 3) assuming fully fixed ends. Thus, the calculated Euler buckling stress for the panel was:

$$\sigma_{\text{Euler}} = 90.63 \text{ ksi}$$

The actual Euler buckling stress will be lower than the value above due to eccentricity effects and yielding, but it is still well in excess of the panel crippling load. Thus, the panel design meets all the required design criteria.

A sketch of the resulting metal compression panel configuration is shown in Figure 3.11. The fastener pitch and other related details shown were obtained to prevent inter-fastener buckling and failures near fastener holes (Reference 34).

### 3.3 TEST PLAN

The selection of a cost-effective and suitable test matrix for the program was made after a review of the gaps in the current technology that are summarized in Table 3.1.

The principle objectives of the curved panel tests were to generate static test data for analysis methodology verification and to conduct fatigue tests for failure mode identification and development of fatigue analysis procedures. One key concern addressed in the program is the fatigue response of curved metal panels. In addition, previous studies have indicated that metal shear panels cannot survive constant amplitude fatigue test at maximum loads much higher than approximately 50 percent of their static

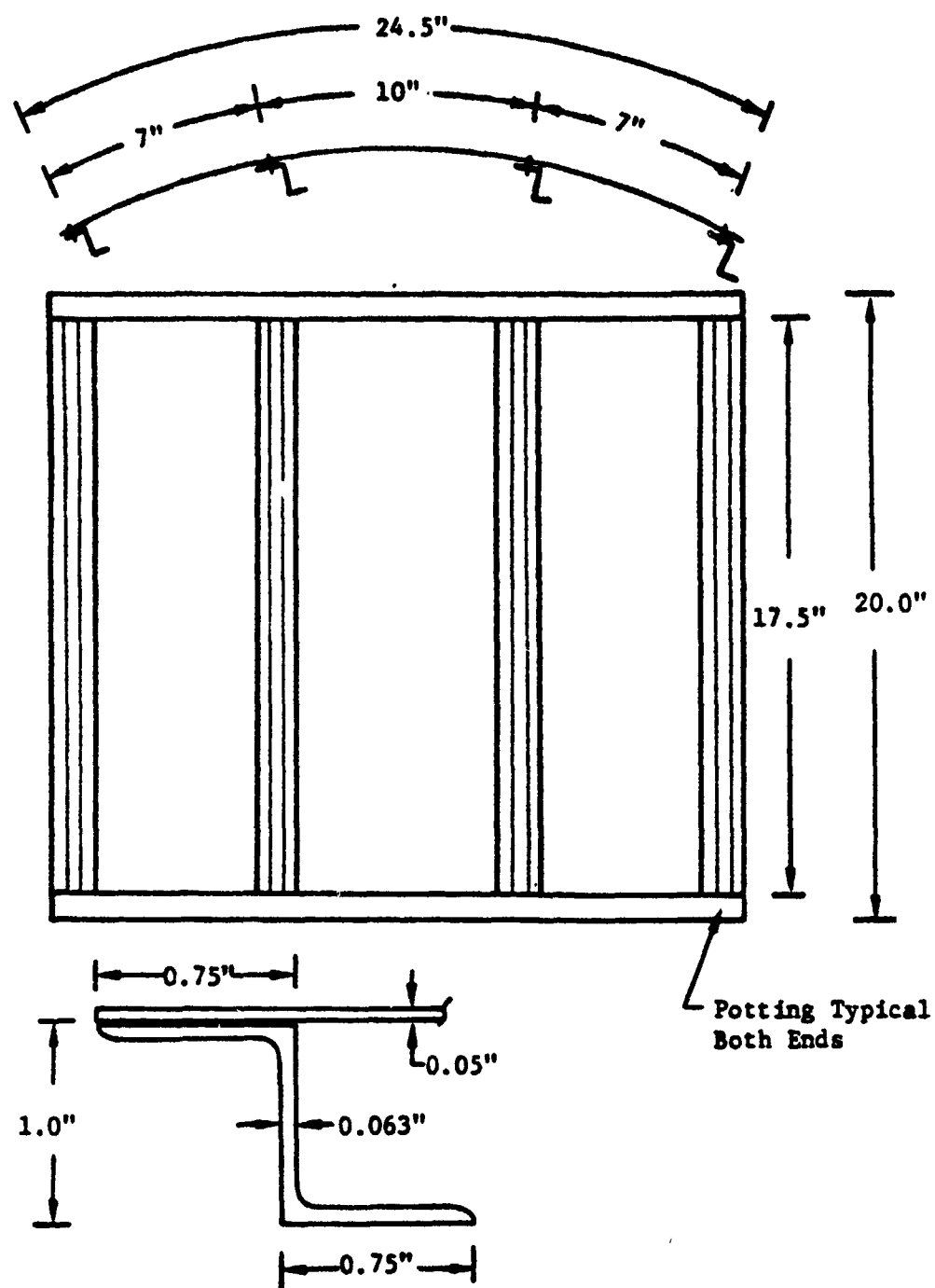


Figure 3.11 Metal Compression Panel Configuration.



ultimate strength. Test data show that composite compression panels, on the other hand, can endure maximum fatigue load amplitudes as high as 70 percent of their static ultimate strength without any strength degradation. However, since fatigue data on composite compression and shear panels are sparse, additional fatigue tests on these panels were required. A greater emphasis was placed on curved shear panels in this program due to their anticipated sensitivity to fatigue loading. Static tests on the curved panels were conducted to obtain skin buckling strains, stiffener crippling strains, skin and stiffener strains at stiffener/web separation, and the strain distribution in the panels as a function of the applied load. These data were required for comparison with predictions made using the semiempirical analysis and the strain distribution in particular for comparison with the non-empirical Rayleigh-Ritz analysis procedure developed in the program. Additional details of the test program are given in the following paragraphs.

#### 3.3.1 Test Matrix

The program test matrix is shown in Table 3.6. As indicated in the table, a total of 26 panels were tested in the program. Four sets of panels were tested to obtain the initial buckling load, postbuckling behavior, ultimate failure load, and mode of failure. The four sets consisted of: aluminum compression, aluminum shear, graphite/epoxy compression, and graphite/epoxy shear panels. All tests were conducted in a room temperature dry (RTD) environment. A greater emphasis is placed on shear panel fatigue tests since fatigue data for curved composite shear panels are not available and those for metal panels are limited in quantity. Each test condition was replicated twice to demonstrate the repeatability of the test and to obtain more reliable test data for analysis verification.

The constant amplitude fatigue tests on compression panels were conducted at an R-ratio ( $\sigma_{\min}/\sigma_{\max}$ ) of 10 with the maximum fatigue load set at 66 percent of the static strength for the first metal panel test and at 70 percent of the static strength for the first composite panel. Selection of the maximum fatigue loads for the subsequent tests was made on the basis of the measured panel response for the first set of tests and the need to obtain a definition of the S-N curve for the panels.

TABLE 3.6. COMPRESSION AND SHEAR PANEL TEST MATRIX

PANEL IDENTIFICATION	MATERIAL/ LOADING	TEST TYPE	R-RATIO	MAXIMUM FATIGUE LOAD AMPLITUDE % STATIC STRENGTH	CONSTANT AMPLITUDE FATIGUE STRAIN SURVEYS AT, N CYCLES		
					0	50K	100K
MC1* MC2* MC3 MC4 IC5**	Aluminum Panel/ Compression Loading	Static	--	--	--	--	--
		Static	--	--	--	--	--
		Fatigue	10	66	✓	✓	✓
		Fatigue	10	55	✓	✓	✓
		Fatigue	10	55	✓	✓	✓
CC1* CC2* CC3 CC4 CC5 CC6	Composite Panel/ Compression Loading	Static	--	--	--	--	--
		Static	--	--	--	--	--
		Fatigue	10	70	✓	✓	✓
		Fatigue	10	70	✓	✓	✓
		Fatigue	10	60	✓	✓	✓
		Fatigue	10	60	✓	✓	✓
MS1 MS2 MS3 MS4 MS5 MS6	Aluminum Panel/ Shear Loading	Static	--	--	--	--	--
		Static	--	--	--	--	--
		Fatigue	0	55	✓	✓	✓
		Fatigue	0	55	✓	✓	✓
		Fatigue	0	45	✓	✓	✓
		Fatigue	0	45	✓	✓	✓
CS1 CS2 CS3 CS4 CS5 CS6 CS7 CS8 CS9 CS10	Composite Panel/ Shear Loading	Static	--	--	--	--	--
		Static	--	--	--	--	--
		Fatigue	-0.25	60	✓	✓	✓
		Fatigue	-0.25	60	✓	✓	✓
		Fatigue	-0.25	70	✓	✓	✓
		Fatigue	-0.25	70	✓	✓	✓
		Fatigue	+0.25	70	✓	✓	✓
		Fatigue	+0.25	70	✓	✓	✓
		Fatigue	+0.25	60	✓	✓	✓
		Fatigue	+0.25	60	✓	✓	✓

\*Out-of-plane displacements measured by LVDT's. \*\*Panel tested as part of Northrop IRAD.

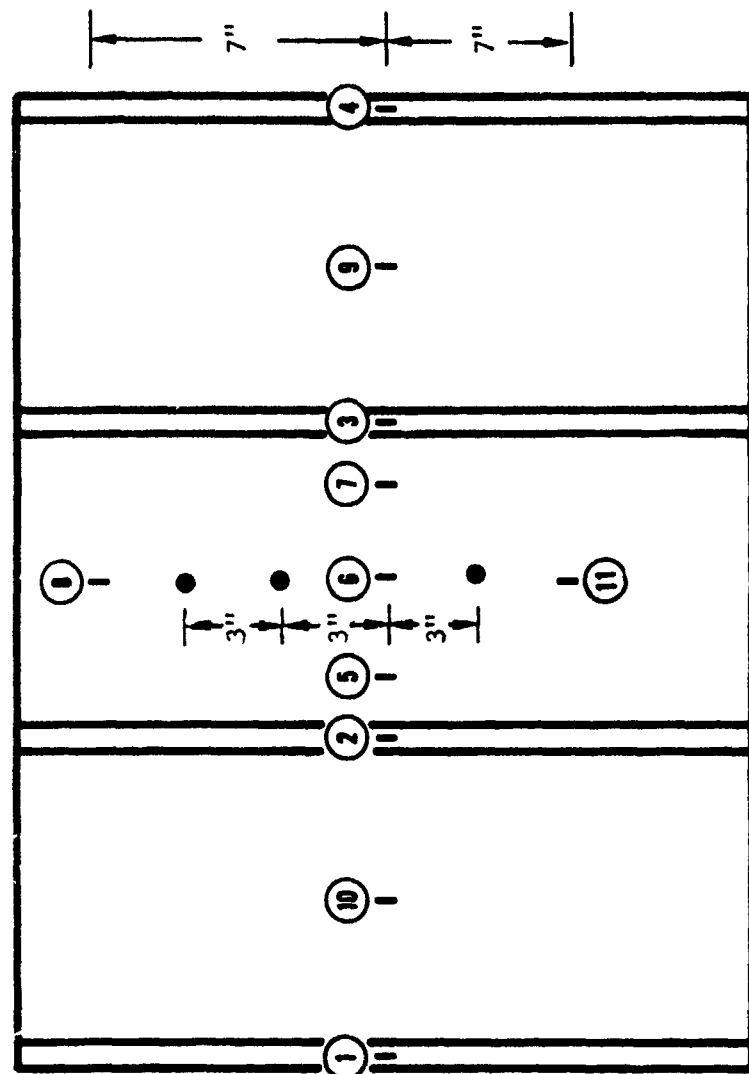
The aluminum shear panel fatigue tests were also conducted under constant amplitude loading with  $R = 0$ . The fatigue load amplitudes selected for these tests were 55 percent and 45 percent of the average static ultimate strength for similar panels. In the case of the composite shear panels the fatigue tests were conducted at  $R = 0.25$  and  $R = -0.25$ , with the latter R-ratio allowing for partial reversal of the shear loading. The fatigue load amplitudes for the composite shear panels were higher than those used for the aluminum panels (70 percent and 60 percent of the average static strength for the panels) due to their much superior fatigue response.

The test panel instrumentation consisted mainly of strain gages and in some select cases of displacement transducers. A more complete description of the instrumentation is given in paragraph 3.3.2. It is noted here, however, that prior to and periodically during the course of the fatigue tests, strain surveys up to the maximum fatigue load were conducted on all fatigue test panels. As indicated in Table 3.1, the intermediate strain surveys during the fatigue tests were conducted at 50,000 and 100,000 cycles.

### 3.3.2 Instrumentation

All panels in the test program were instrumented with strain gages. The static compression test panels were instrumented with LVDT's in addition to the strain gages so that out of plane displacements could be monitored during the course of the tests. Figure 3.12 shows the layout of the strain gages and the locations of the out-of-plane displacement transducers for the compression panels. In this figure the gage layout for the less extensively instrumented compression fatigue panels is also shown. The strain gage layout for the static and fatigue tested shear panels is shown in Figure 3.13. As noted in Figures 3.12 and 3.13, all gages were located back-to-back on the convex and the concave surfaces of the panels in order to determine bending as well as membrane strains due to postbuckling deformations.

In all static tests, a visual indication of the out-of-plane displacements in the postbuckling regime was obtained by means of the Moire' grid technique. For this purpose the composite specimens were painted white and a Moire' grid placed within 0.25 inch of the specimen surface in the case of both metal and composite panels to obtain the fringes associated with the



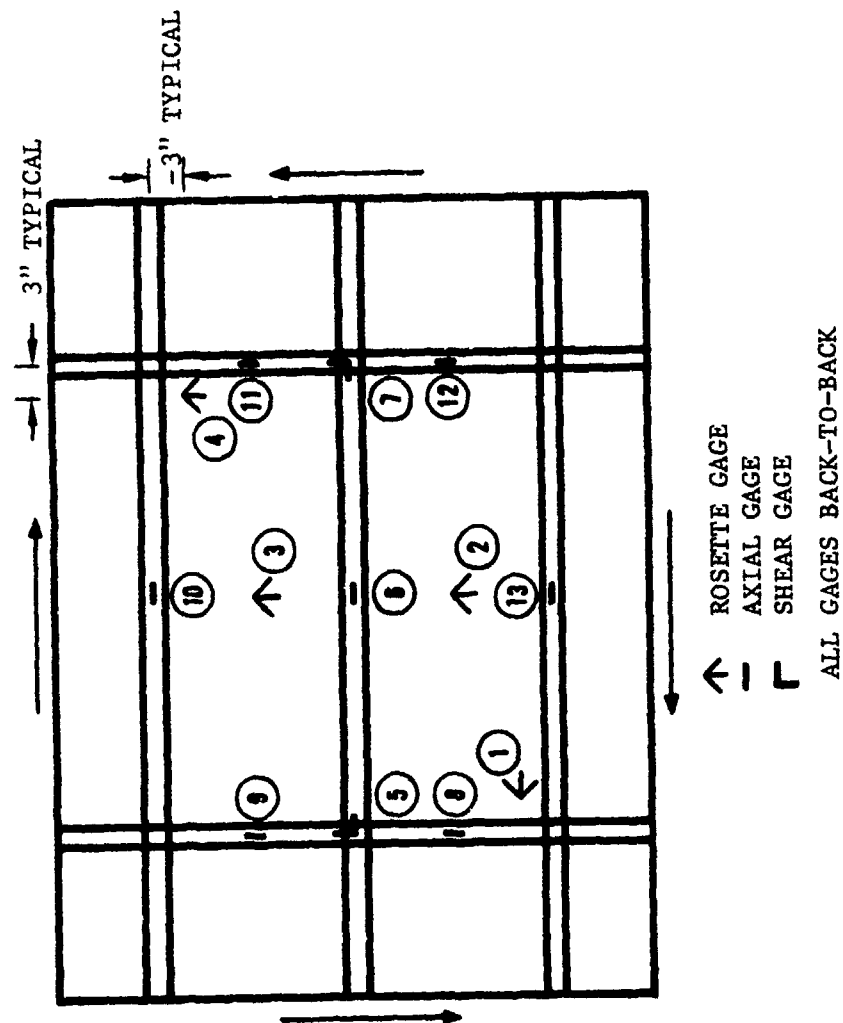
┆ AXIAL GAGE

● DISPLACEMENT TRANSDUCER

ALL GAGES BACK-TO-BACK

- NOTE: 1. Static Test panels MC1, MC2, CC1, and CC2 were instrumented as shown.
2. Fatigue test panels MC3, CC3, and CC4 were instrumented with gages ① through ⑧ only.
3. Fatigue test panels MC4, CC5, and CC6 were instrumented with gages ① through ⑧ only.

Figure 3.12 Compression Panel Instrumentation.



NOTE: 1. Static test panels MS1, MS2, CS1, and CS2 were instrumented as shown.

2. Fatigue test panels were instrumented with gages ① through ⑦ only.

Figure 3.13 Shear Panel Instrumentation

buckle pattern.

During the course of the fatigue tests some of the strain gages were damaged due to fatigue, thus causing loss of some data. However, a majority of the strain gages were not affected and valid data were obtained at the 50,000 cycle and 100,000 cycle strain surveys. The gages that survived and the detailed nomenclature are noted in Appendix A along with the test data.

### 3.3.3 Test Fixture

The static and fatigue tests on the compression panels were conducted in a 100,000 pound capacity Tinius Olsen test machine. The panel ends were potted in an epoxy compound for load introduction. A full view of the test setup, including the Kaye data acquisition system, is shown in the photograph of Figure 3.14. A close-up view of a composite compression panel in the test machine with full instrumentation is shown in Figure 3.15.

The test fixture used for curved shear panel tests is a fixture designed and developed at Northrop under Independent Research and Development funds. This fixture results in the application of extremely uniform shear stress in the panel with no adverse stresses. The loading mechanism and the test fixture are schematically illustrated in Figure 3.16. A view of the test fixture with a metal panel installed for testing is shown in the photograph of Figure 3.17. The glossy appearance of the specimen is due to the Moire' grid which has been positioned close to the specimen surface.

The curved panel is enclosed by two flat dummy panels making up a triangular tube. The two flat panels are considered part of the test fixture and are connected at a point midway between the test panel center of curvature and the test panel. One end of the tube is clamped against all degrees of freedom. The other end is connected to the loading frame plate. Loading frame support plates are slotted to allow free rotation of the loading frame shaft about the tube centroid. The shear load is applied by a torque introduced by two load cylinders moving in opposite directions. The two torque application cylinders are each of 50,000 pound capacity and the torque arm is 74.0 inches. Operation of the test fixture was verified using an aluminum panel which was tested to failure. The fixture design permits

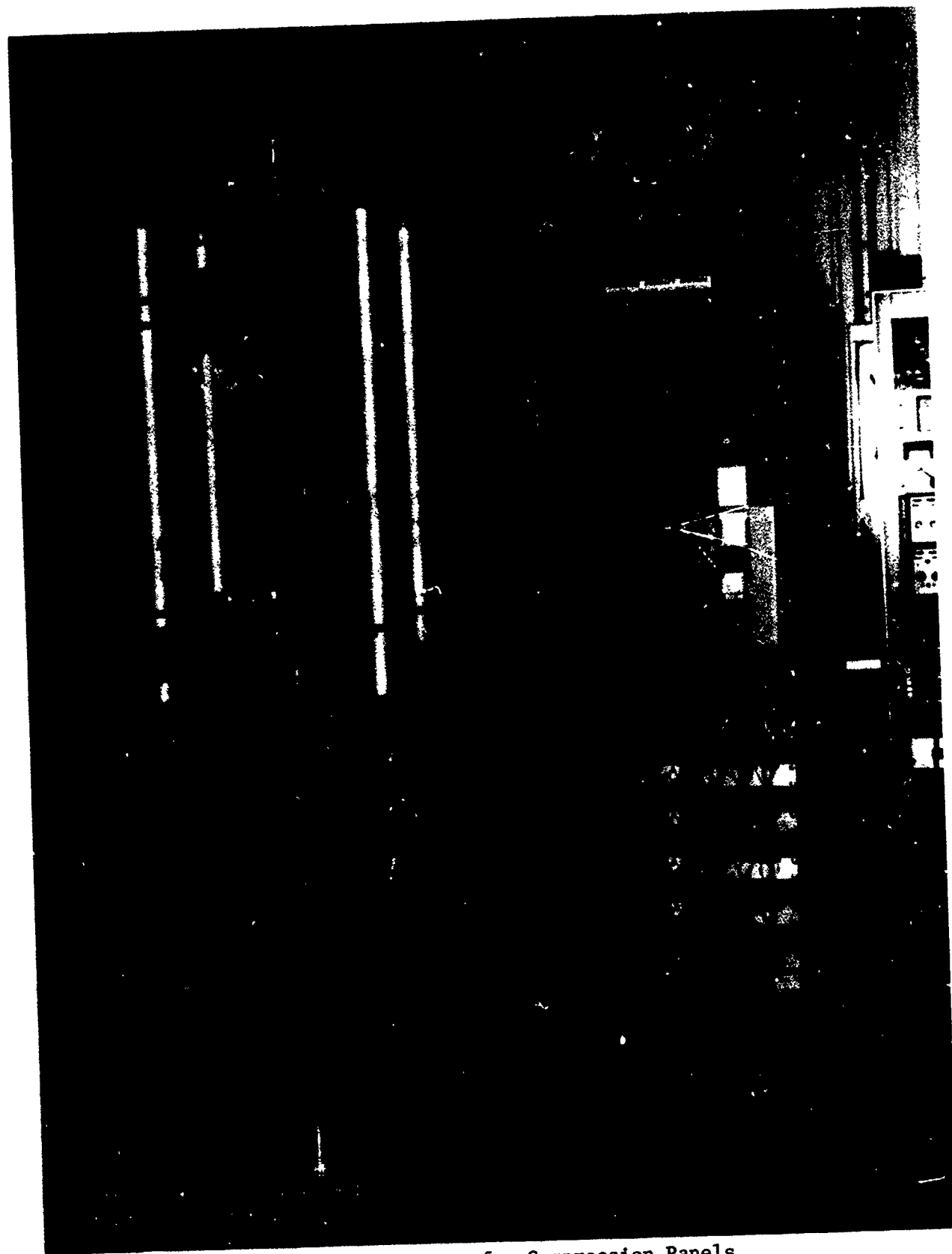


Figure 3.14. Test Setup for Compression Panels



Figure 3.15. Composite Compression Panel Instrumentation and Test Setup



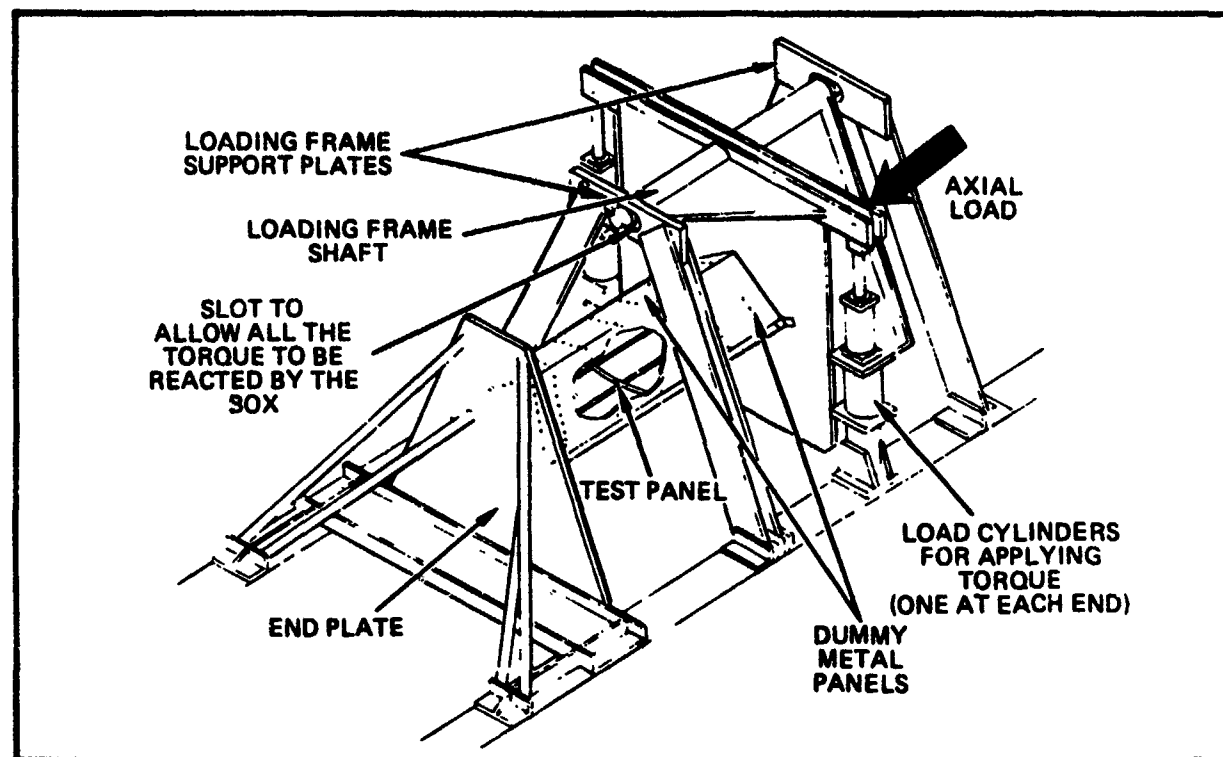


Figure 3.16. Shear Panel Test Fixture Schematic

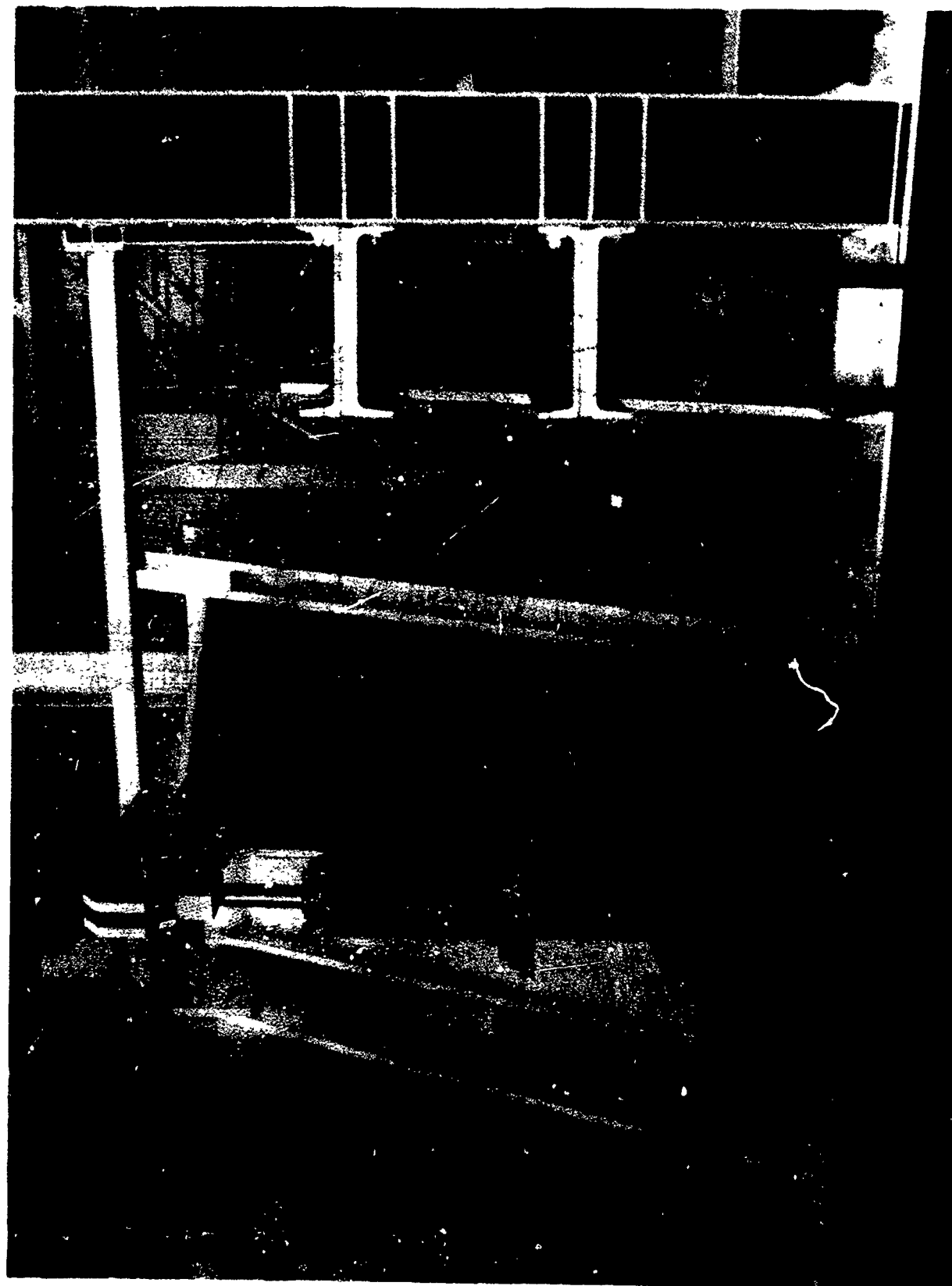


Figure 3.17. View of Test Fixture Showing Loading Arrangement and Test Panel.

testing of curved panels in a wide range of sizes and curvatures with minimal alterations.

### 3.4 FABRICATION OF COMPOSITE TEST PANELS

Special testing and curing fixtures were designed and built to fabricate the composite shear and compression panels. The tooling for the shear panels was more complex due to the curvature of the J-section frames. For the shear panels a steel template formed to a 45-inch radius was used to lay up the skin. The template was marked to indicate the peripheral net trim area; stringer, frame and doubler (edge as well as under the stiffener) locations. An orientation rosette was also marked on the template to ensure angular accuracy of the various plies.

The stiffeners were shaped and fabricated using Dow Corning Silastic-J RTU rubber mandrels. The mandrels themselves were cast in sheet metal molds with the frame mandrel molds designed to allow for opening and shifting of hat cavities when the mandrel is bent into a 45-inch radius after being cast straight. After cure of the frame mandrel, slots were cut into it to allow for expansion of the rubber. The cauls for the stringers were fabricated using two plies of graphite/epoxy sandwiched between two layers of Air-Tech's Airpad black rubber. These cauls were in three pieces of which two were used on the short stringer ends outside of the frames (Refer to Figure 3.4) whereas the third one was used for the portion of a stringer between the frames. The cauls on the stiffeners extended to the surface of the frames and were tapered to prevent excessive mark-off. This kept the hat stiffeners straight, and prevented them from rolling, bowing and distorting during cure. Fiberglass cauls were fabricated for the top of the J-section frames. These kept the frames circumferentially straight, and eliminated wrinkles in the cap of the frame. Figure 3.18 shows the stringer and curved frame mandrels in place on the skin template. The graphite-epoxy cauls used to compact the stringers are also shown in the figure. The cuts in the frame mandrels to accommodate the hat section stringers are illustrated in Figure 3.19 which shows a photograph of the partially laid-up frame mandrel.



Figure 3.18. Intermediate Step-in Composite Shear Panel Fabrication Illustrating Frame and Stringer Mandrels Located on Skin Template



Figure 3.19. Detail View of Frame Mandrels

The panel fabrication procedure consisted of laying up the skin and the stringers separately on a flat template and then locating the preformed stringers onto the skin. The subassembly was debulked under vacuum for 30 minutes, then placed on the curved steel template used as the curing fixture and taped in place to avoid movement in subsequent operations. The frames were laid up on their mandrels and located over the subassembly in the curing fixture. The stringer cauls were then installed, followed by installation of the frame cauls. The panel assembled up to this stage is illustrated in Figure 3.20. This assembly was then covered with bleeder and breather plies as required and bagged for cure. The panel was cured and postcured in accordance with Northrop specification MA-133. The cured composite shear panel is shown in Figure 3.21.

Fabrication of the composite compression panel was considerably simpler due to the absence of the curved frames. The procedure followed in fabricating these four stringer panels (Refer to Figure 3.9) was identical to that used for the shear panels up to the stringer/skin subassembly stage. The finished composite compression panel is shown in Figure 3.22. The panels then are potted for compression load application.

The composite compression and shear panels were nondestructively inspected by means of ultrasonic C-scan to ensure defect-free panels.

### 3.5 TEST RESULTS

#### 3.5.1 Compression Panel Static Tests

The composite and metal compression panel static test results are summarized in Table 3.7. The metal compression panels MC1 and MC2 failed due to stiffener crippling. Web buckling and inter-rivet buckling was observed in some areas prior to failure. These static test results are compared against predictions in Section 5. Development and progression of the buckle pattern for the metal panels is illustrated in Figure 3.23a through e where Moire grid pattern photographs for panel MC1 are shown. Just beyond the initial buckling load the web is seen to have buckled in two half waves along the load axis as well as across the width. This pattern becomes more easily visible as the load is increased further. However,

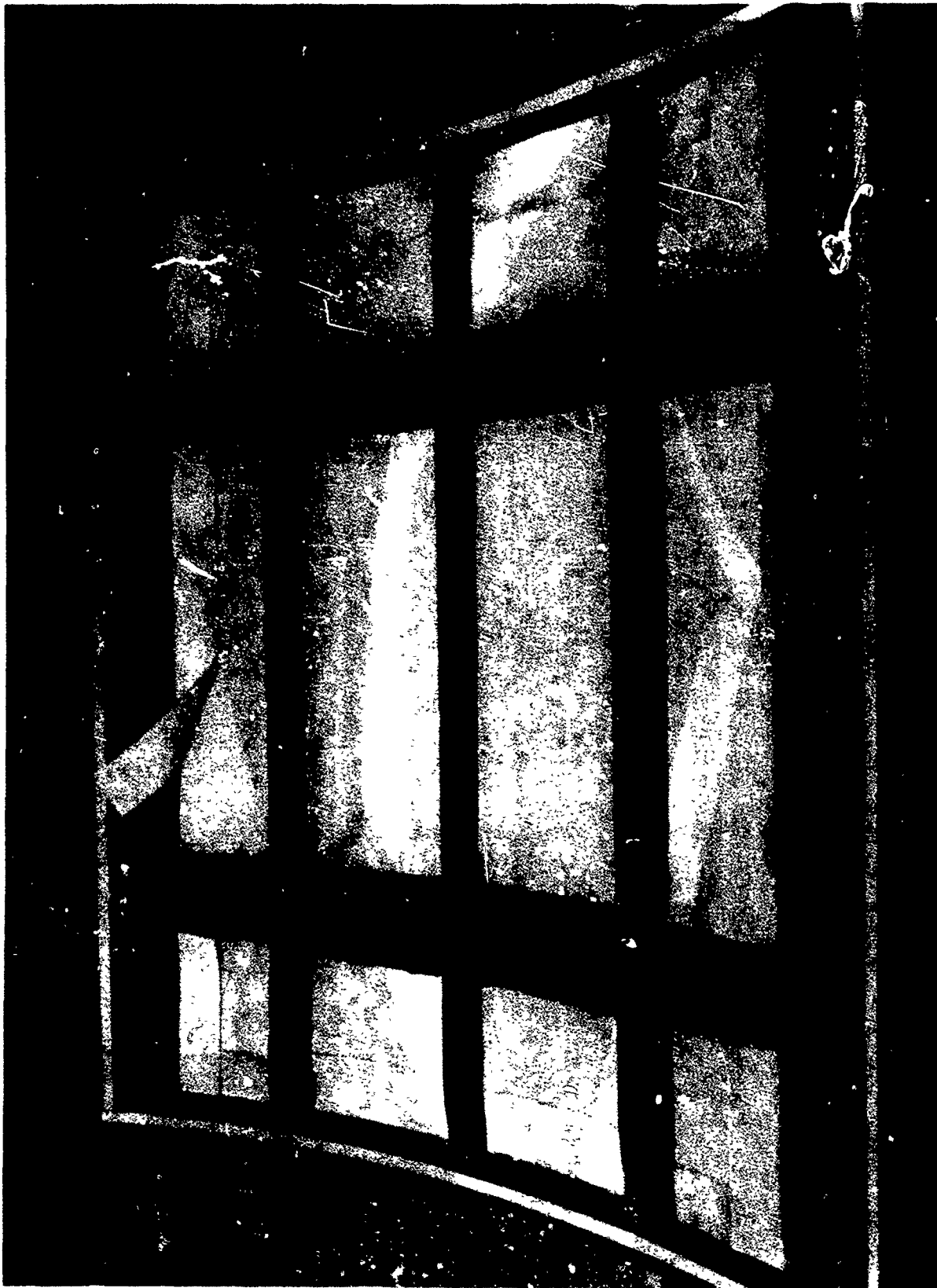


Figure 3.20. Shear Panel Assembly Prior to Cure



Figure 3.21. Cured Composite Shear Panel



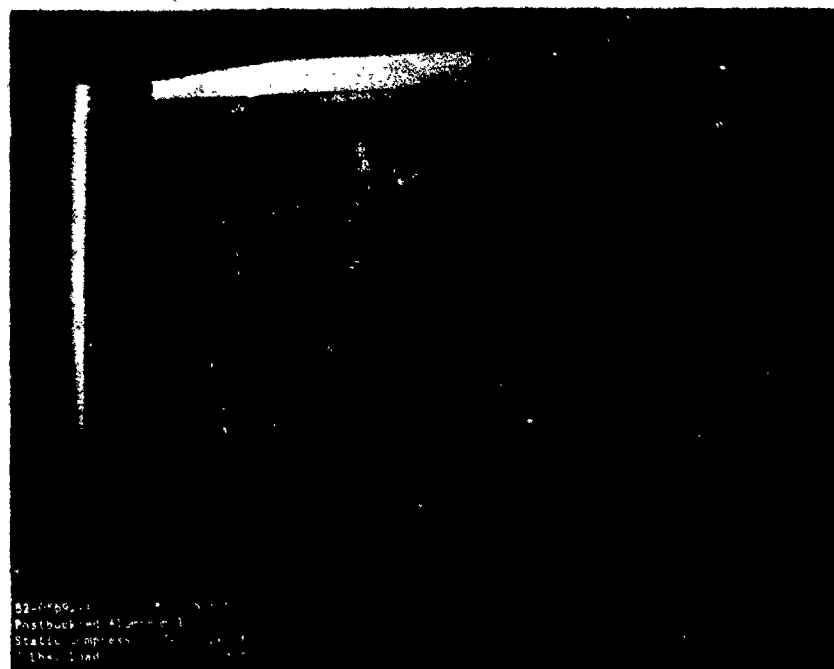


Figure 3.22. Graphite/Epoxy Compression Panel Ready for Potting of the Ends

TABLE 3.7. COMPOSITE AND METAL COMPRESSION PANEL STATIC TEST RESULTS

PANEL NUMBER*	BUCKLING LOAD, KIPS	FAILURE LOAD, KIPS	REMARKS
MC1	12.0	42.0	Panels failed due to stiffener crippling as predicted. See Section 4 for discussion of results.
MC2	14.0	43.6	
CC1	18.0	84.6	Panels failed due to stiffener/web separation.
CC2	16.0	82.0	

\*Prefix M in panel number denotes metal panel and prefix C denotes graphite/epoxy panel.

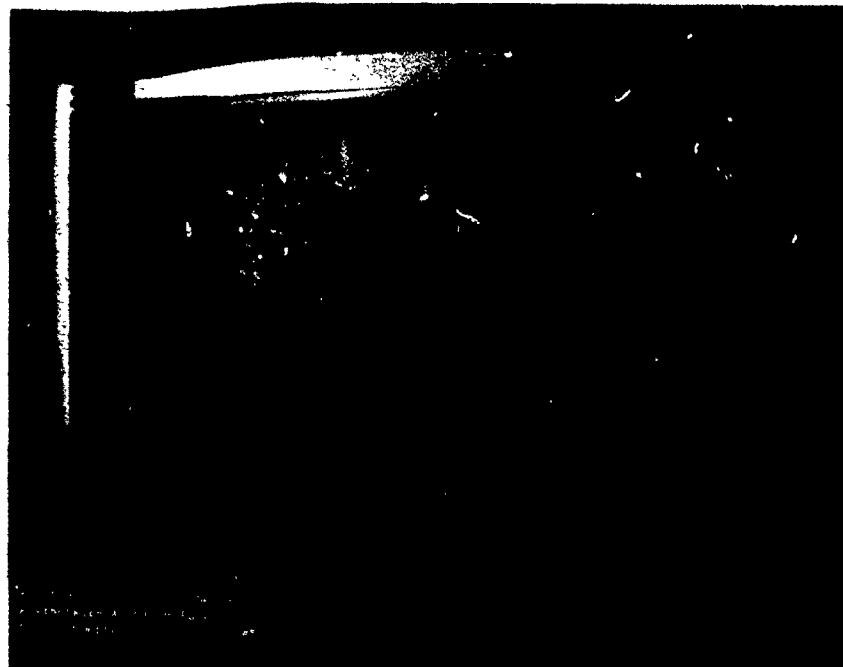


(a) Load - 0 lb



(b) Load = 16K lb

Figure 3.23. Progression of Buckle Pattern with Load for Metal Compression Panel MC1

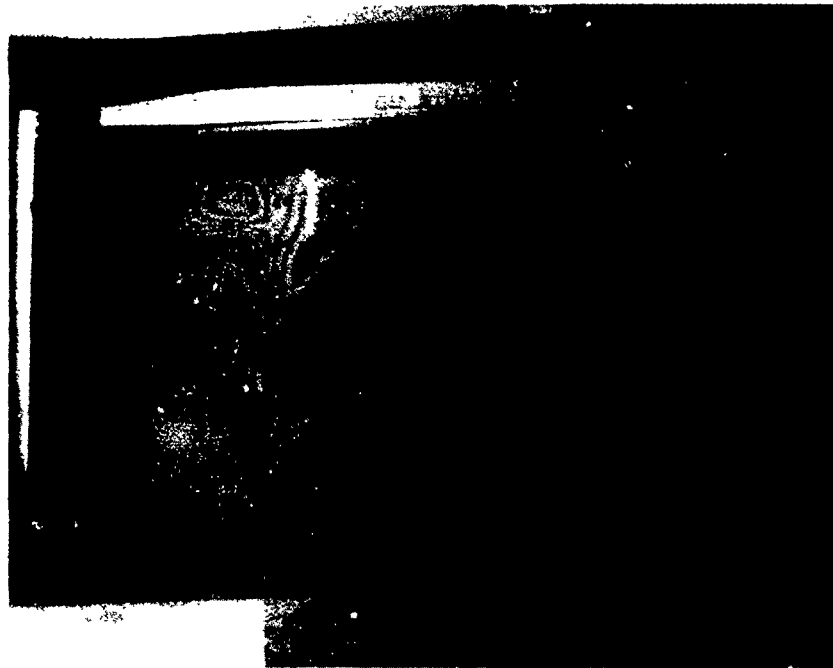


(c) Load = 25K lb



(d) Load = 30K lb

Figure 3.23. Progression of Buckle Pattern with Load for Metal Compression Panel MCl (Continued)



(e) Load = 35K lb

Figure 3.23. Progression of Buckle Pattern with Load for Metal Compression Panel MC1 (Concluded)

between 25,000 and 30,000 lbs the pattern changes to one-half wave across the width of the panel which remains unchanged to failure. A photograph illustrating the final failure mode of the panel by stiffener crippling is shown in Figure 3.24. Strain data for the two metal panels are given in Appendix A and were used to determine the buckling loads given in Table 3.8.

The composite compression panels CC1 and CC2 failed by stiffener/web separation. Final failure was abrupt and resulted in the separation of all stiffeners from the skin and in secondary rupture of all stiffeners. Development and progression of the buckle pattern in panel CC1 is shown in Figure 3.25a through f. Panel CC2 also displayed the same buckle pattern. The strain data given in Appendix A were used to determine the panel buckling loads. The failure mode for these panels is illustrated in Figure 3.26.

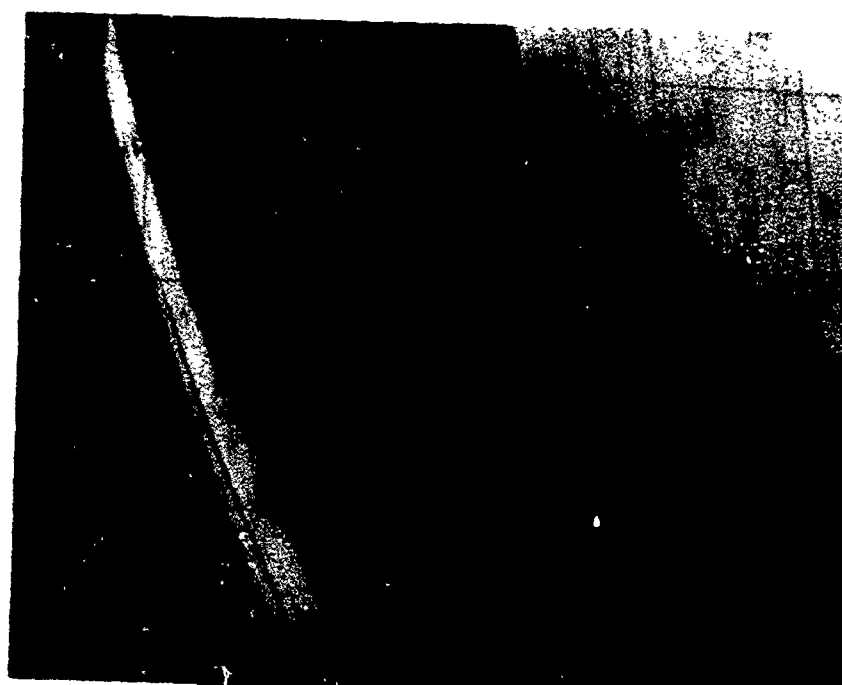
#### 3.5.2 Compression Panel Fatigue Tests

The metal and composite compression panel fatigue tests were conducted at an R-ratio of 10. The test data are summarized in Table 3.8. Metal panel MC3 tested under constant amplitude loading with the maximum fatigue load set at 61 percent of the average static strength, developed sizeable cracks (~2.5 in) after 16,000 cycles. The cracks in the skin were parallel to the stiffener and appeared to be caused by the web bending against the stiffener. Unlike the failure mode shown in Figure 2.2 for flat compression panels, the skin cracks in the curved panel were located along the stiffener edge away from the fasteners.

Panel MC4 tested at a load amplitude equal to 51 percent of the average static strength also developed cracks in the skin along the stiffeners at 43,000 cycles. The panel, however, retained its fatigue load carrying capacity to 100,000 cycles. The initial 2.5-inch crack grew to 4.75 inches in the last 57,000 cycles. The panel was statically tested for residual strength but did not show an appreciable loss in strength. The statically failed panel with the initial fatigue cracks marked is shown in Figure 3.27.



(a) Skin Rupture



(b) Stiffener Crippling

Figure 3.24. Failed Metal Compression Panel MC1

TABLE 3.8. COMPOSITE AND METAL COMPRESSION PANEL FATIGUE TEST RESULTS, R = 10

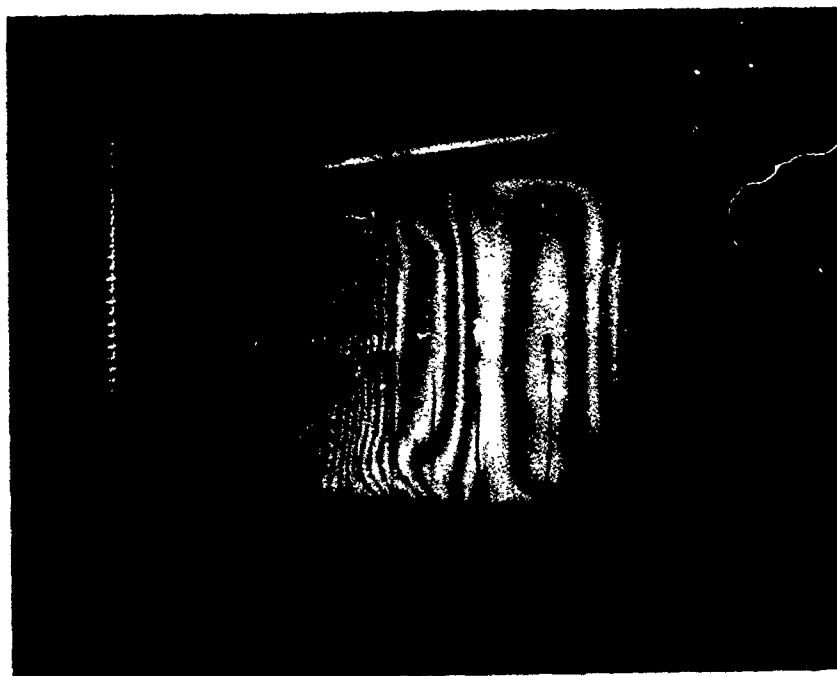
PANEL NO. +	SKIN BUCKLING LOADS, KIPS	MAXIMUM FATIGUE LOAD, KIPS	MAXIMUM FATIGUE LOAD, % AVG. STATIC STRENGTH	FATIGUE LIFE, N CYCLES	RESIDUAL STRENGTH, KIPS	STRAIN SURVEYS AT N, CYCLES			REMARKS
						0	50K	100K	
MC3	10.0	26.0	61	16,430	-	X	-	-	Fatigue crack in skin. Parallel and adjacent to stiffener.
MC4	12.0	22.0	51	100,000**	40.8	X	X	X	5-in Fatigue Crack in skin parallel to stiffener.
IC1++	13.0	22.0	51	100,000R	4.11	-	-	-	Stringer edge in contact with skin, founded to prevent knife edging of skin. 5-in crack in skin at run-out.
CC3	14.0	58.1	70	61,640	-	X	X	-	Failure due to stiffener/web separation.
CC4	12.0	58.1		12,758	-	X	-	-	
CC5	12.0	49.8	60 65	100,000R 100,000	84.5	X	X	X*	After-first 100K cycles load increased to 65% of static strength
CC6	16.0	49.8	60 65	100,000R 5,900	-	X	X	X	After first 100K cycles load increased to 65% of static strength.

\* Additional strain surveys at 150K and 200K cycles.

\*\* R denotes run-out. ++ Panel tested under Northrop IRAD

T Prefix M in panel number denotes metal panel and prefix C denotes graphite/epoxy level.



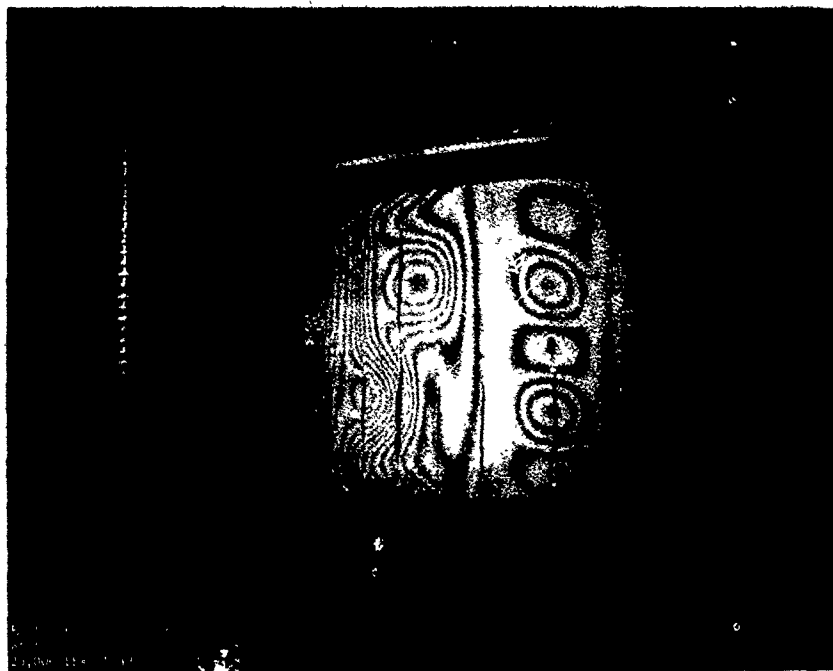


(a) Load = 14K lb

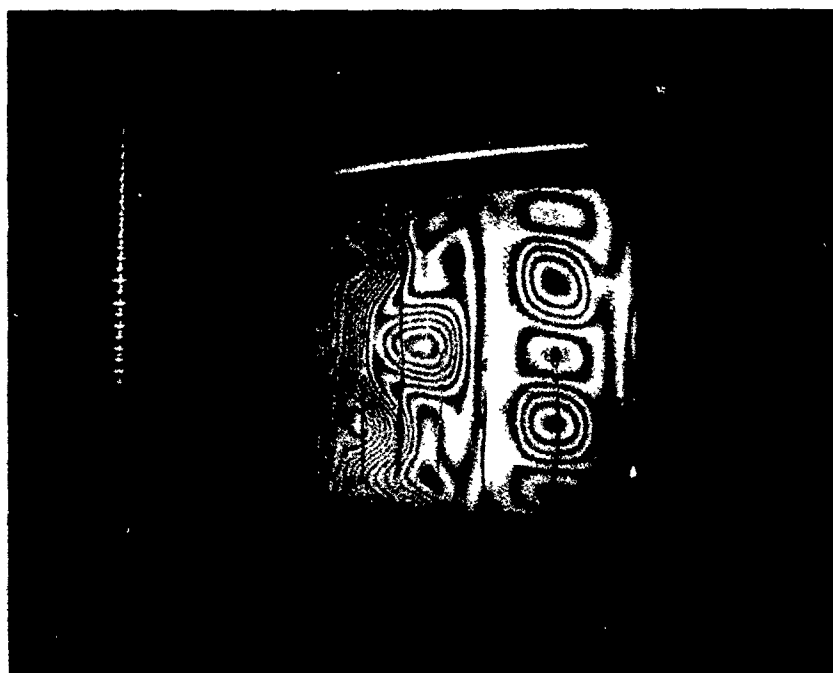


(b) Load = 18K lb

Figure 3.25. Progression of Buckle Pattern with Load for Composite Compression Panel CCl



(c) Load = 25K lb



(d) Load = 35K lb

Figure 3.25. Progression of Buckle Pattern with Load for Composite Compression Panel CCl (Continued)

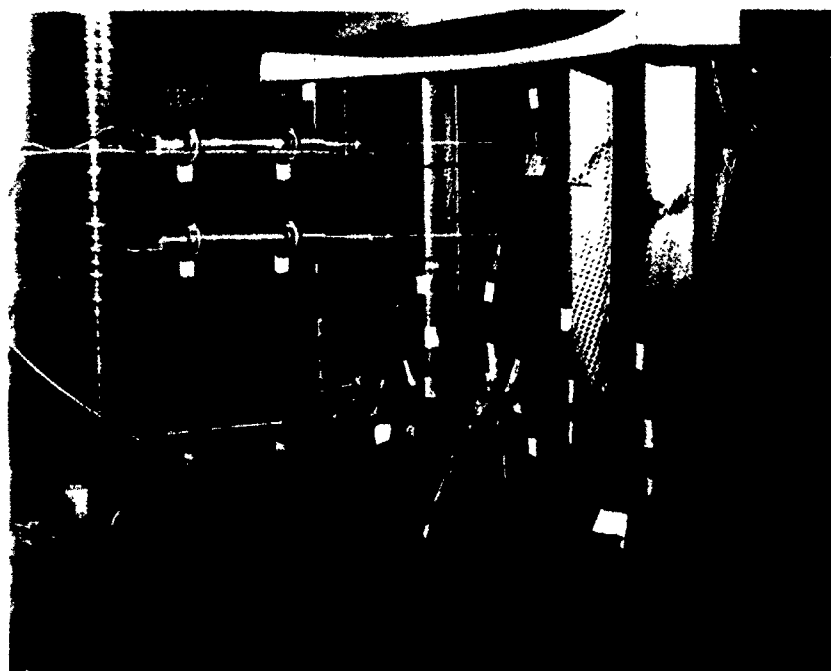


(e) Load = 60K lb



(f) Load = 80K lb

Figure 3.25. Progression of Buckle Pattern with Load for Composite Compression Panel CC1 (Concluded)



(a) Stiffener/Web Separation and Failure



(b) Skin Failure

Figure 3.26. Composite Compression Panel CCl Failure Mode

A curved metal compression panel with rounded stiffener edges (IC1) was fatigue-tested under constant amplitude loading with  $R = 10$  and at a load amplitude equal to 51 percent of the ultimate static strength. Panel IC1 was tested under Northrop's IRAD program to determine if rounding of stiffener edges is effective in improving the panel fatigue life. The stiffener edges were rounded to eliminate crack initiation adjacent to the stiffeners due to web bending against sharp stiffener edges which was observed during fatigue tests on panels MC3 and MC4. The rounded stiffener edges were effective in eliminating crack initiation at the two center stiffeners. Crack initiation at one of the edge stiffeners, however, occurred after approximately the same number of cycles (40,000) as in the case of panels MC3 and MC4 although the initial crack length was smaller (.15 inch versus 2.5 inches). Panel IC1 completed 100,000 cycles of fatigue loading without catastrophic failure. During these 100,000 cycles, the crack at the edge stiffener grew to a length of 4.75 inches. The panel was residual strength-tested and failed by stiffener crippling at 41,000 lbs. showing no reduction from the ultimate static strength. An additional observation from these tests was that just prior to failure, a sizeable crack did appear at one of the center stiffeners indicating that rounded stiffener edges were effective in reducing the web bending stresses and thus, delaying crack initiation.

Curved composite panels CC3 and CC4 were tested in fatigue with the maximum load set at 70% of the average static strength determined from panels CC1 and CC2. The panels failed due to separation of the stiffeners from the skin after 61,640 and 12,758 cycles, respectively. In the case of panel CC3 a single stiffener separated whereas for panel CC4 the damage was more extensive and resulted in the failure of three stiffeners. Panels CC5 and CC6 were fatigue-tested at 60 percent of the average static strength and both survived the first 100,000 cycles of fatigue. The load was subsequently increased to 65 percent of the static strength and the fatigue test continued. Panel CC5 survived an additional 100,000 cycles at this load without any significant loss in residual strength. Panel CC6, however, failed after approximately 6,000 cycles at the increased load. The results for panels CC3 through CC6 are discussed in Section 4.

### 3.5.3 Shear Panel Static Tests

The test results for curved metal and composite shear panels are summarized in Table 3.9. The load values shown in the table are the loads applied by the torque/cylinder. Metal panel static failure was due to permanent buckling of the web. The failure load was well above the design ultimate and the panel was able to sustain loads higher than the loads at which permanent set in the web occurred. The diagonal buckle pattern representative of out-of-plane skin displacements for the metal shear panels is shown in Figure 3.28.

The composite shear panels CS1 and CS2 failed at nearly identical loads by stiffener web separation. Panel CS1 failed at a torque cylinder load of 16,000 lbs. A photograph of the failed panel is shown in Figure 3-29 with a close-up view of the failure area shown in Figure 3.30. The buckle pattern for composite shear panels was similar to that shown in Figure 3.28.

Due to the nature of the test set up for the shear panels direct measurement of the shear flow  $N_{xy}$  in the test area is not possible. The cross-sectional area of the torque box cannot be directly measured due to the presence of attachment hardware at the corners. In addition, friction inherent in the test arrangement means that all the applied torque is not converted to shear flow in the test panel. Hence, the first metal shear panel static test was used to calibrate the applied torque to panel shear flow relationship. Since the properties of 7075-T6 aluminum are well established, this calibration can be carried out by plotting the measured shear strain in the panel web prior to web buckling versus the applied torque as shown in Figure 3.31. Using this plot, the calibration proceeds as follows:

$$N_{xy} = \frac{T}{2A} = \frac{74 P_T}{2A} = G \gamma_{xy} t$$

where,  $T$  is the applied torque,  $A$  the cross-sectional area of the torque tube,  $P_T$  the applied cylinder load, the torque arm is 74 inches,  $t$  is skin thickness and  $\gamma_{xy}$  is the measured shear strain in the web. From the above equation

$$A = \frac{T}{2G \gamma_{xy} t}$$

TABLE 3.9. COMPOSITE AND METAL SHEAR PANEL STATIC TEST RESULTS

PANEL NUMBER*	BUCKLING LOAD, LBS	FAILURE LOAD, LBS	REMARKS
MS1	3820	22800	Panel failed due to permanent set in skin
MS2	4123	14600	Panel failed due to permanent set in skin
CS1	4497	15760	Panels failed due to stiffener web
CS2	4492	16500	separation.

\* Prefix M in panel number denotes metal panel and prefix C denotes graphite/epoxy panel.

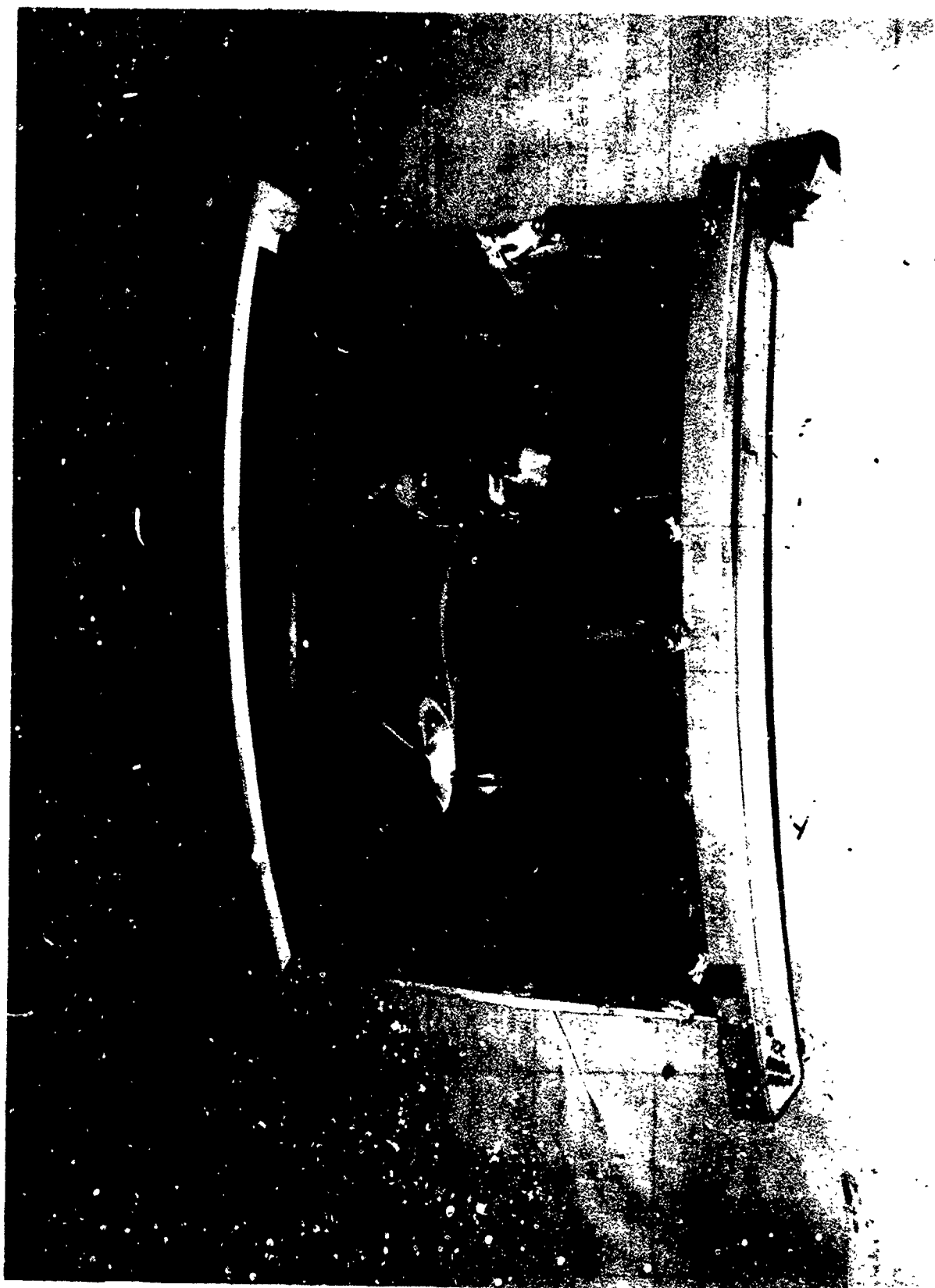


Figure 3.27. Fatigue Cracks in Metal Compression Panel MC4





Figure 3.28. Diagonal Buckle Pattern in Metal Shear Panels

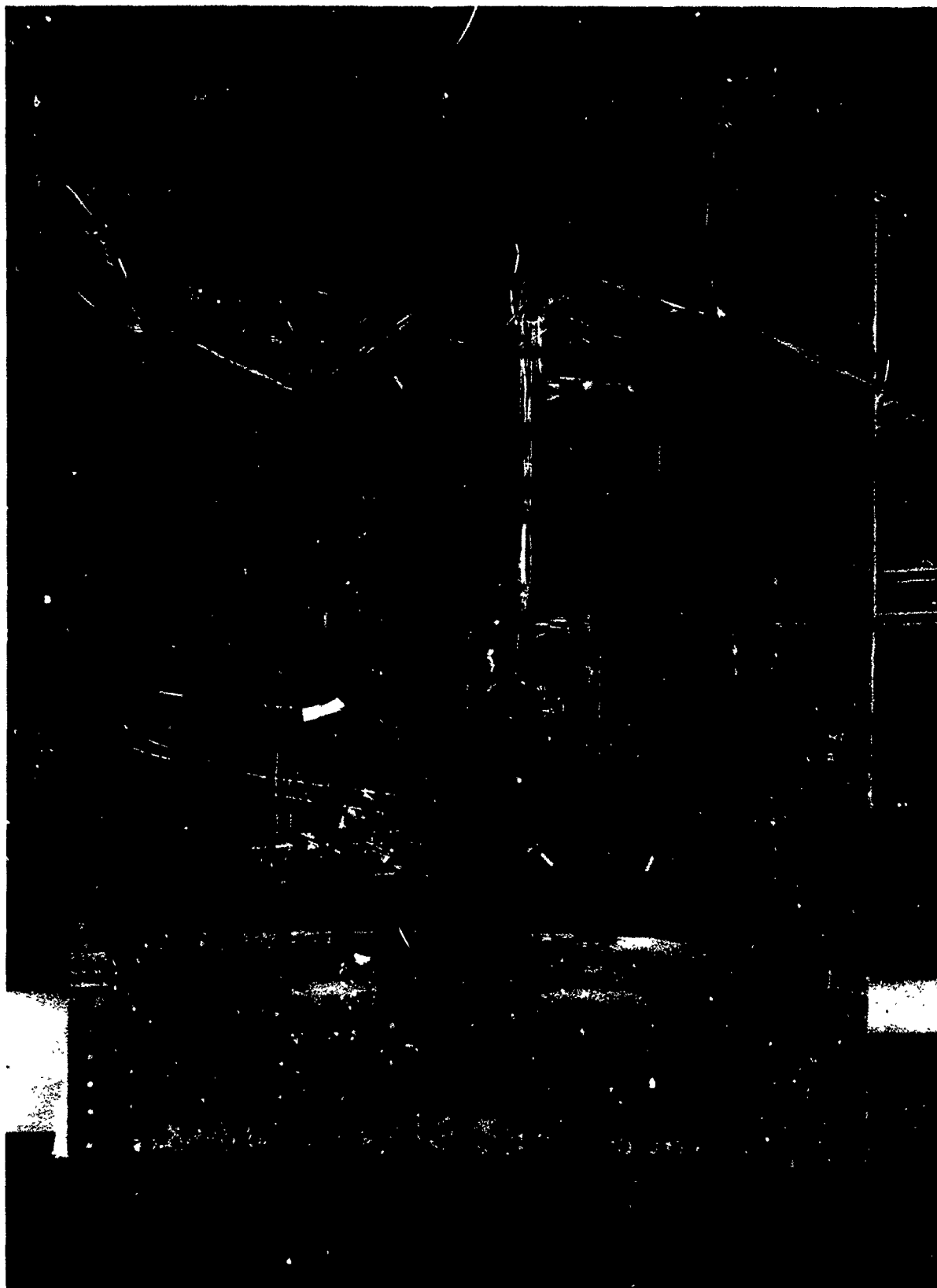


Figure 3.29. Static Failure Mode of Curved Composite Shear Panel CS1



Figure 3.30. Close-Up of Composite Shear Panel Failure by Stiffener/Web Separation

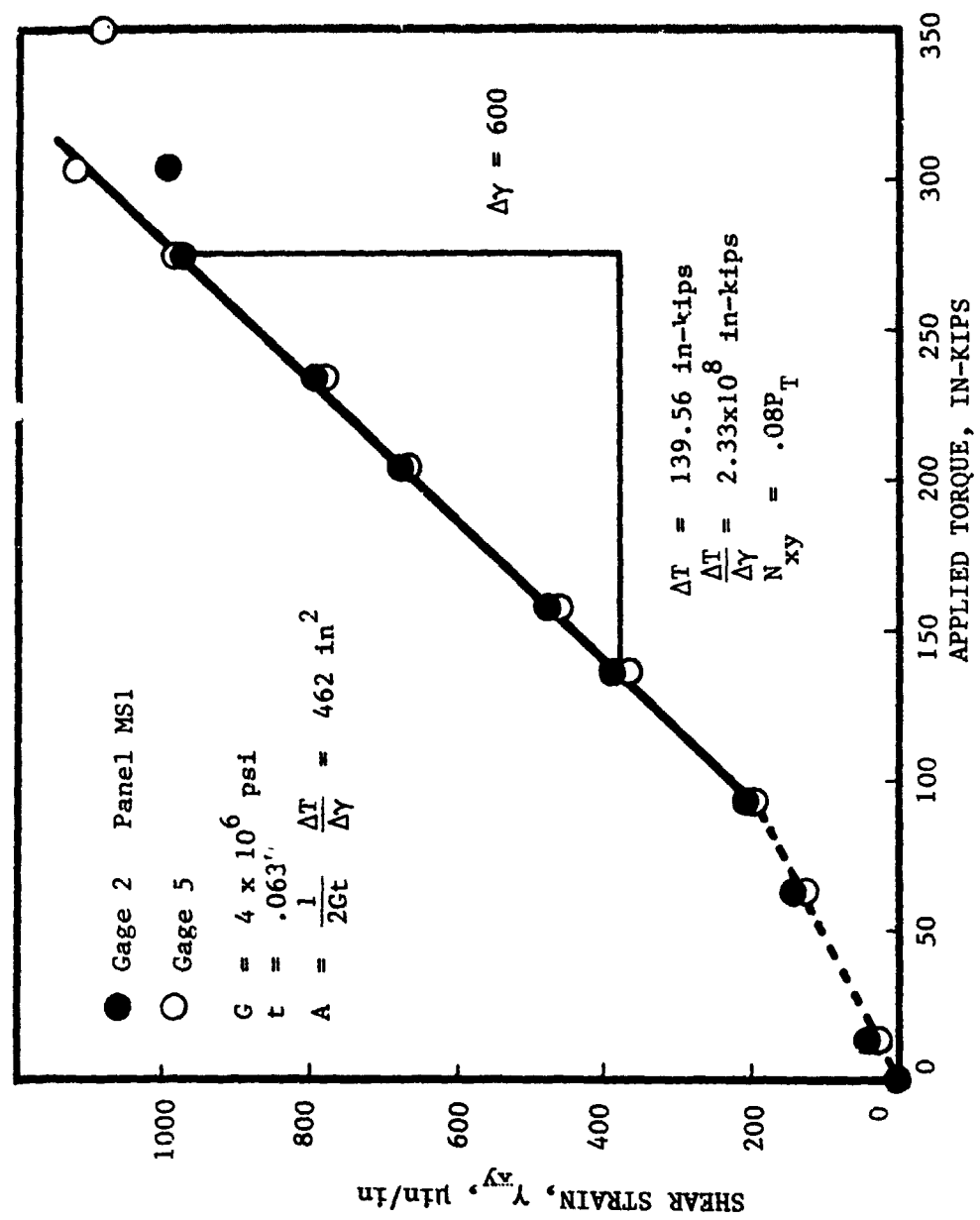


Figure 3.31. Applied Torque to Panel Shear Flow Conversion Calibration

or, using the data shown in Figure 3.31,

$$A = \frac{1}{2Gt} \frac{\Delta T}{\Delta \gamma}$$

Thus the cross-sectional area was determined from Figure 3.31 to be 462 in<sup>2</sup>. This yields the following conversion from cylinder load to panel shear flow

$$N_{xy} = 0.08 P_T$$

where,  $N_{xy}$  is in lb/in and  $P_T$  in lb. The strain data for all statically tested shear panels is given in Appendix A.

#### 3.5.4 Shear Panel Fatigue Tests

The shear panel fatigue test data are summarized in Table 3.10. Metal panels MS3 and MS4 were tested at a maximum fatigue load equal to 80 percent of the design ultimate strength since the wide scatter in the static strength of MS1 and MS2 made it difficult to define a meaningful average static strength.

In panel MS3 test the bolt in the corner of the test bay failed after 7,200 cycles. Fatigue cracks grew soon after the fastener failure in the panel web adjacent to the corner hole as well as at the corner hole. The panel failed due to web rupture after 8,700 cycles. The rupture was caused by cracks which grew normal to the direction of diagonal tension.

In panel MS4 the corner fastener which failed during the specimen MS3 tests was replaced by a higher strength fastener. Panel MS4 sustained 12,500 cycles before any cracks were visible. The first crack appeared in the stringer near the intersection of the frames, where significant stringer bending was observed. The crack was located in the stiffener heel and ran along the length. A second crack developed in the panel web due to bending of the web after 14,800 cycles. The location of this crack was at the point where the buckles stop in the diagonal tension corner. This crack resulted in panel failure after additional 1200 cycles.

TABLE 3.10. COMPOSITE AND METAL SHEAR PANEL FATIGUE TEST RESULTS

PANEL NO. *	BUCKLING LOAD, LB	R-RATIO	MAXIMUM FATIGUE LOAD		FATIGUE LIFE N CYCLES	RESIDUAL STRENGTH KIPS	STRAIN SURVEY, N CYCLES			REMARKS
			KIPS	% AVG STATIC STRENGTH			0	50K	100K	
MS3	4453	0	10.0	54	8,698	---	X	--	--	Cracks at stiffener attach fastener holes led to failure by web rupture.
MS4	3848	0	10.0	54	16,578	---	X	--	--	
MS5	2894	0	8.0	43	51,975	---	X	--	--	
MS6	3811	0	8.0	43	28,789	---	X	--	--	
CS3	3970	-0.25	9.7	60	100,000R	15.2	X	†	†	Stiffener/web separation mode of failure.
CS4	3533	-0.25	9.7	60	100,000R	16.8	X	†	†	
CS5	3945	-0.25	11.3	69	62,000	---	X	†	†	
CS6	3897	-0.25	11.3	69	19,351	---	X	†	†	
CS7	3461	0.25	9.7	60	8,737	---	X	†	†	
CS8	3993	0.25	9.7	60	100,000R	14.5	X	†	†	
CS9	4434	0.25	11.3	69	100,000R	15.8	X	†	†	
CS10	3476	0.25	11.3	69	69,100	---	X	†	†	

\* Prefix M in panel number denotes metal panel and prefix C denotes graphite/epoxy panel.

\*\* R denotes run out.

† Significant number of gages damaged due to fatigue.

Another crack was observed after 15,000 cycles along the stiffener edge similar to the cracks in the compression panels. Complete web rupture occurred at about 16,600 cycles.

Metal shear panels MS5 and MS6 were subjected to constant amplitude fatigue with  $R = 0$  and at a maximum fatigue load equal to 45 percent of the average static strength obtained from static tests on panels MS1 and MS2. The absolute fatigue shear load amplitude was 8,000 lbs. as compared with 10,000 lbs. for panels MS3 and MS4. The edges of panels MS5 and MS6 were thickened by means of an externally (convex side) bonded aluminum doubler to facilitate load introduction and avoid premature cracking of the web at the panel corners. Addition of the doubler did not affect the panel response as manifested by the initial buckling loads of 2,894 lbs. and 3,811 lbs. for panels MS5 and MS6, respectively. As shown in Table 3.10 these buckling loads are in the same range as those for panels MS1 through MS4 where bonded edge doublers were not used.

Panels MS5 and MS6 showed very similar modes of failure although there was some scatter in their fatigue life. In panel MS5, web cracks were first observed at 37,000 cycles parallel to the mid-bay longitudinal stiffener and transverse to the tension field at the vertical frame fastener holes as illustrated in Figure 3.32. Final failure of panel MS5 occurred by web rupture due to propagation of a dominant crack in a direction transverse to the tension field after 52,000 cycles. The dominant crack initiated in the lower bay and propagated across the second bay as shown in Figure 3.32. Fatigue cracks in panel MS6 were first observed at 22,000 cycles and final rupture of the web occurred at 29,000 cycles.

Panels CS3 and CS4 were tested under constant amplitude fatigue loading ( $R = -0.25$ ). The maximum fatigue load was set equal to 60% of the static ultimate failure load. The panels completed 100,000 cycles of fatigue loading without any detectable damage. The panels failed at loads of 15,200 and 16,400 lbs., respectively, during the residual strength test. The failure load and mode of failure were almost identical to the static tests.

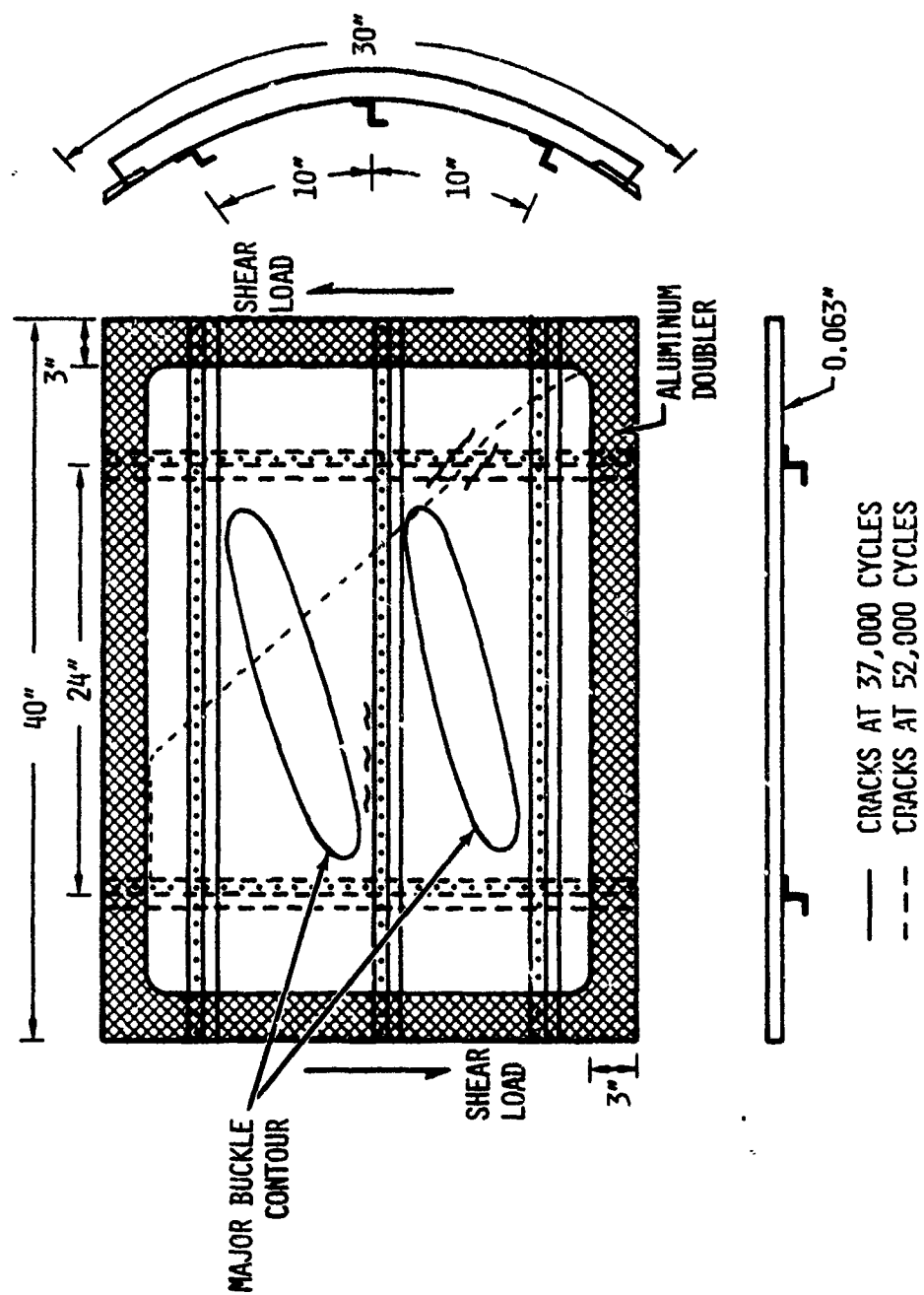


Figure 3.32. Fatigue Failure Mode of Aluminum Shear Panel MS5



The maximum load amplitude for panels CS5 and CS6 was increased to 70% of the static ultimate load. Panels were loaded under constant amplitude fatigue loading ( $R = -0.25$ ). Both panels failed during fatigue after 72,000 cycles and 19,500 cycles, respectively. The failures were sudden and not detected during the inspection periods which were set to 10,000 cycles. Thus the time of damage initiation to final failure was quite rapid. The fatigue failures at such high load magnitudes are to be expected and the data continue to demonstrate excellent durability of composite shear panels.

Panel CS7 was subjected to constant amplitude fatigue loading ( $R = +0.25$ ). No load reversal for this panel was chosen. The maximum load amplitude was set at 70 percent of the static ultimate load. The panel developed stiffener/web separation over a 0.5-inch length after 7,000 cycles. This disband grew rapidly resulting in total panel failure after 8,700 cycles. The slightly lower life with less severe fatigue loading points towards a weakly-bonded region at the stiffener/skin interface.

Panel CS8 was tested at a fatigue load amplitude equal to 70% of the average static strength measured for similar panels. The panel survived 100,000 cycles of fatigue loading without any detectable damage. The residual strength of panel CS8 was 14,500 lbs. which is 10% lower than the average static strength. The failure mode of the panel was identical to that seen in the static tests and was by separation at the stringer/web interface. This test was identical in all respects to that conducted on panel CS7.

The fatigue test results for the two panels show significant scatter although the failure modes are identical. However, the reason for this scatter can be deduced from the observation that panel CS7 developed stiffener/web separation very early in the fatigue test at approximately 7,000 cycles and thereafter this disbond propagated very rapidly. In the case of panel CS8, no such stiffener/web separation was observed even after 100,000 cycles. This suggests that in panel CS7 a flaw in the form of a

void or incomplete resin cure at the stiffener/web interface was inadvertently introduced during fabrication and was the direct cause of the reduced fatigue life.

The last set of curved composite shear panels (CS9 and CS10) were also tested under constant amplitude fatigue loading at an R-ratio of 0.25. The fatigue load amplitude for these two panels, however, was 60% of the average static strength for similar panels. Panel CS9 completed 100,000 cycles of fatigue and survived. The residual strength of this panel was not significantly reduced from the average static strength. Panel CS10 failed by stiffener/web separation after 69,100 cycles of fatigue. The scatter in the fatigue test results for these two panels is suspected to be due to variability in fabrication of the panels.

The significance of the test results presented in this section is discussed in Section 4.

## SECTION 4

### DEVELOPMENT OF ANALYSIS METHODE

#### 4.1 INTRODUCTION

The semiempirical analysis of postbuckled panels presented in Section 2 was done in steps due to the complexity of the solution process. These analyses, although useful for design purposes, do not yield the stress and displacement fields required for a fatigue analysis of the panels. Furthermore, with the semiempirical analyses, the complex mechanisms of load transfer before and after buckling such as the interaction forces between the stiffeners and the web, and the effect of stiffness changes in the postbuckling range, cannot be modelled. Most of these analysis methods were developed before the advent of high-speed computers and result in designs that are conservative by as much as 50 percent. The current technology and recent advances in computation methods make it feasible to model all significant aspects of postbuckled panels in a single analysis with increased accuracy, thereby reducing the conservatism in the final design. Thus, development of such an analysis to accurately predict the postbuckling behavior of the panel as a whole, including the web and the stiffeners, was undertaken.

It was envisioned that the analysis methodology would be used as a design tool. Therefore, ease of application and low computational costs were prime considerations in its development. Based on the survey of nonempirical static analysis methods presented in Section 2, the total postbuckling behavior of stiffened panels loaded in compression or in shear was modelled using the principle of minimum potential energy. The analysis methodology for each loading case is generic in that it applies to curved, flat, metal and composite panels. Details of the analysis for compression and shear panels are discussed in the following paragraphs.

#### 4.2 COMPRESSION PANEL ANALYSIS

The governing equations in this formulation were derived for orthotropic laminates that are balanced and symmetric. It is assumed that

the webs between adjacent stringers deform in an identical fashion. The analysis is also applicable to isotropic materials provided the appropriate constitutive relations are used.

#### 4.2.1 Geometry and Boundary Conditions

The relationship between the compression panel configuration tested in the program and the panel geometry used in the analysis is shown in Figure 4.1. Since adjacent bays are assumed to deform in an identical fashion, a single bay was analyzed. As shown in Figure 4.1, one curved edge of the panel is assumed to be fixed with compression load applied to the other curved edge. At the loaded edge, due to the presence of the stiff frames, the displacement in the Z-direction ( $w$ ) is restricted to zero and no displacement is permitted in the Y-direction ( $v = 0$  at this edge). The latter boundary condition is a realistic representation of the edge conditions in panels under pure compression. The stringer deformations determine the boundary conditions at the straight edges of the panel. The stringers are assumed to be initially straight and deformation relative to the mid-surface of the panel in the Z-direction ( $w$ ) occurs only due to stiffener crippling or Euler buckling of the panel which results in catastrophic failure. The  $u$ , and  $v$  displacements at the straight edges are not restricted.

#### 4.2.2 Strain Energy Expressions

The analysis employs the principle of minimum potential energy. The method is ideally suited for this analysis since it simplifies the handling of discrete stiffeners and imposition of the boundary conditions.

According to the principle of minimum potential energy, a solution of the present problem renders the total potential a relative minimum. The total potential energy,  $\Pi$ , is the sum of the strain energy stored in the web,  $U_w$ , in the stringers,  $U_s$ , in the frame,  $U_f$ , and the potential of the external load,  $\Omega$ , i.e.

$$\Pi = U_w + U_s + U_f + \Omega \quad (32)$$

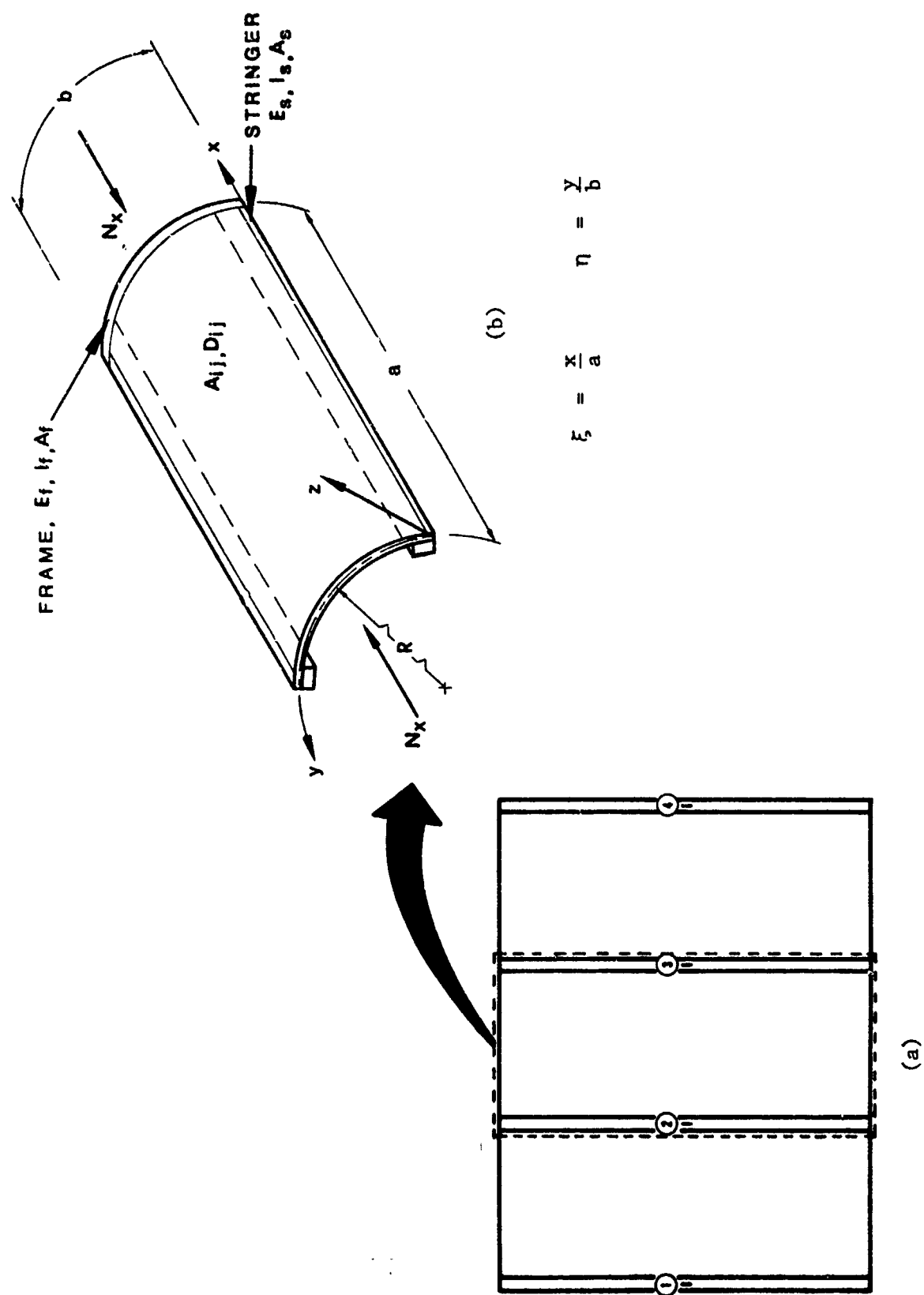


Figure 4.1.1. Curved Compression Panel Geometry and Coordinate System

In applying the principle of minimum potential energy, the first step is to assume kinematically admissible displacement functions with unknown coefficients. These displacement functions are selected to satisfy the geometric boundary conditions. The total potential energy is computed next as a function of the unknown coefficients. The governing equations are then obtained in terms of the unknown coefficients by minimizing the total potential energy with respect to these coefficients. Finally, the set of non-linear equations obtained by minimization of the total potential energy are numerically solved to determine the displacement coefficients.

The strain energy stored in the skin and the stiffeners can be expressed in terms of the assumed displacements  $u$ ,  $v$  and  $w$  using nonlinear strain-displacement relations for curved laminates as:

Strain Energy of the Skin:

$$\begin{aligned}
 U_w = & \frac{ab}{2} \left[ \int_0^1 \int_0^1 A_{11}^* \left( \frac{1}{a^2} u_{,\xi}^2 + \frac{1}{4a^4} w_{,\xi}^4 + \frac{1}{a^3} u_{,\xi} w_{,\xi}^2 \right) d\xi d\eta \right. \\
 & + \int_0^1 \int_0^1 A_{12}^* \left( \frac{2}{ab} u_{,\xi} v_{,\eta} + \frac{1}{ab^2} u_{,\xi} w_{,\eta}^2 + \frac{1}{a^2 b} v_{,\eta} w_{,\xi}^2 \right. \\
 & \quad \left. \left. + \frac{1}{2a^2 b^2} w_{,\xi}^2 w_{,\eta}^2 + \frac{2}{Ra} w u_{,\xi} + \frac{1}{a^2 R} w w_{,\xi}^2 \right) d\xi d\eta \right. \\
 & + \int_0^1 \int_0^1 A_{22}^* \left( \frac{1}{b^2} v_{,\eta}^2 + \frac{1}{4b^4} w_{,\eta}^4 + \frac{w^2}{R^2} + \frac{2}{Rb} w w_{,\eta} + \frac{1}{b^3} v_{,\eta} w_{,\eta}^2 \right. \\
 & \quad \left. \left. + \frac{w}{b^2 R} w_{,\eta}^2 \right) d\xi d\eta \right. \\
 & \left. + \int_0^1 \int_0^1 A_{66}^* \left( \frac{1}{b^2} u_{,\eta}^2 + \frac{1}{a^2} v_{,\xi}^2 + \frac{1}{a^2 b^2} w_{,\xi}^2 w_{,\eta}^2 + \frac{2}{ab} u_{,\eta} v_{,\xi} + \text{cont'd.} \right) d\xi d\eta \right]
 \end{aligned}$$

$$\begin{aligned}
& + \frac{2}{ab^2} u_{,\eta} w_{,\xi} w_{,\eta} + \frac{2}{ab^2} v_{,\eta} w_{,\xi} w_{,\eta} \Big) d\xi d\eta \\
& + \int_0^1 \int_0^1 \left( \frac{1}{a^4} D_{11}^* w_{,\xi\xi}^2 + \frac{2}{a^2 b^2} D_{12}^* w_{,\xi\xi} w_{,\eta\eta} + \frac{4}{a^3 b} D_{16}^* w_{,\xi\xi} w_{,\xi\eta} \right. \\
& + \left. \frac{1}{b^4} D_{22}^* w_{,\eta\eta}^2 + \frac{4}{b^3 a} D_{26}^* w_{,\eta\eta} w_{,\xi\eta} + \frac{4}{a^2 b^2} D_{66}^* w_{,\xi\eta}^2 \right) d\xi d\eta \Big]
\end{aligned}
\tag{33}$$

where,  $\xi$  and  $\eta$  are normalized variables as shown in Figure 4.1, and  $u$ ,  $v$  and  $w$  are displacements in the  $x$ ,  $y$  and  $z$  directions, respectively.  $A_{ij}^*$  are the elements of the laminate axial stiffness matrix and  $D_{ij}^*$  are the elements of the flexural stiffness matrix. Commas denote differentiation with respect to the subscripted variables. The strain energy due to shear and stretching coupling is ignored since the laminate is balanced and symmetric about the midplane, i.e.,  $A_{16} = A_{26} = 0$ .

Strain energy in the stringer:

$$U_s = \frac{A_s E_s}{2a} \int_0^1 u_{,\xi}^2(\xi, 0) d\xi + \frac{I_s E_s}{2a^3} \int_0^1 v_{,\xi\xi}^2(\xi, 0) d\xi \tag{34}$$

where,  $A_s$  is the cross-sectional area of the stringer,  $E_s$  is the modulus and  $I_s$  is the equivalent moment of inertia of the stringer about the  $z$ -axis.

Strain energy in the frames:

$$U_f = \frac{A_f E_f}{2b} \int_0^1 v_{,\eta}^2(1, \eta) d\eta + \frac{I_f E_f}{2b^3} \int_0^1 u_{,\eta\eta}^2(1, \eta) d\eta \tag{35}$$

where,  $A_f$  is the cross-sectional area of the frame,  $E_f$  is the average modulus and  $I_f$  is the equivalent moment of inertia of the frame about the  $z$ -axis.

The potential of the external load is expressed as:

$$\Omega = -\lambda \bar{P} \int_0^1 u(1, \eta) d\eta \quad (36)$$

where,  $\bar{P}$  is a reference load and  $\lambda$  is an unknown load control parameter.

#### 4.2.3 Governing Equations

The governing equations are obtained by substituting a set of assumed displacement functions with unknown coefficients into the expressions for the total potential  $\Pi$  and then minimizing it with respect to the unknown coefficients. As discussed in Section 4.2.1, the boundary conditions that the assumed displacement functions must satisfy are:

$$\begin{array}{lll} u(x,0) \neq 0 & v(x,0) \neq 0 & w(x,0) = 0 \\ u(x,b) \neq 0 & v(x,b) \neq 0 & w(x,b) = 0 \\ u(0,y) = 0 & v(0,y) \neq 0 & w(0,y) = 0 \\ u(a,y) \neq 0 & v(a,y) \neq 0 & w(a,y) = 0 \end{array} \quad (37)$$

where,  $u(x,y)$ ,  $v(x,y)$  and  $w(x,y)$  are the displacements in the  $x$ ,  $y$  and  $z$  directions, respectively. The stiffeners along the straight edges are restricted to in-plane deformations.

The admissible displacement functions for the compression panel were assumed in the following form:

$$\begin{aligned} u(\xi, \eta) &= A_{nm} \phi_n^C \psi_m^C (1 - \phi_1^C) + a_1 a \xi \\ v(\xi, \eta) &= b_{nm} \phi_n^S \psi_m^C + b_1 b \eta \\ w(\xi, \eta) &= C_{nm} \phi_n^S \psi_m^S \end{aligned} \quad \left\{ \begin{array}{l} m = 1, \dots, M \\ n = 1, \dots, N \end{array} \right\} \quad (38)$$

where,

$$\begin{aligned} \phi_n^C &= \cos n\pi\xi & \psi_m^C &= \cos m\pi\eta \\ \phi_n^S &= \sin n\pi\xi & \psi_m^S &= \sin m\pi\eta \end{aligned}$$



and

$$x = a\xi \quad y = b\eta$$

The total potential energy for the compression panels takes the form:

$$\Pi = \Pi(A_{ij}, B_{ij}, C_{ij}, a_1, b_1, \lambda) \quad (39)$$

Using the indicial notation where summation over repeated indices is implied, the total potential energy can be written as follows:

$$\begin{aligned} \Pi = \frac{ab}{2} & \left[ \left\{ \frac{A_{11}^*}{a^2} (A_{nm} A_{pq} F_{lnmpq}^{11} + 2A_{nm} a_1 a F_{2nm}^{11} + a_1^2 a^2) \right. \right. \\ & + \frac{A_{11}^*}{4a^4} C_{nm} C_{pq} C_{rs} C_{tu} F_{lnmpqrstu}^{12} \\ & + \frac{A_{11}^*}{a^3} (A_{nm} C_{pq} C_{rs} F_{lnmpqrs}^{13} + a_1 C_{pq} C_{rs} a F_{2pqrs}^{13}) \\ & + \frac{2A_{12}^*}{ab} (A_{nm} B_{pq} F_{lnmpq}^{21} + A_{nm} b_1 b F_{2nm}^{21} + a_1 B_{pq} a F_{3pq}^{21} \\ & + a_1 b_1 ab) \\ & + \frac{A_{12}^*}{ab^2} (A_{nm} C_{pq} C_{rs} F_{lnmpqrs}^{22} + a_1 C_{pq} C_{rs} a F_{2pqrs}^{22}) \\ & + \frac{A_{12}^*}{a^2 b} (B_{nm} C_{pq} C_{rs} F_{lnmpqrs}^{23} + b_1 C_{pq} C_{rs} b F_{2pqrs}^{23}) \\ & \left. + \frac{A_{12}^*}{2a^2 b^2} C_{nm} C_{pq} C_{rs} C_{tu} F_{lnmpqrstu}^{24} \right] \end{aligned}$$

$$+ \frac{2A_{12}^*}{Ra} (C_{nm} A_{pq} F_{lnmpq}^{25} + a_1 C_{nm} a F_{2nm}^{25})$$

$$+ \frac{A_{12}^*}{a^2 R} C_{nm} C_{pq} C_{rs} F_{lnmpqrs}^{26}$$

$$+ \frac{A_{22}^*}{b^2} (B_{nm} B_{pq} F_{lnmpq}^{31} + 2B_{nmb} b_1 b F_{2nm}^{31} + b_1^2 b^2)$$

$$+ \frac{A_{22}^*}{4b^4} C_{nm} C_{pq} C_{rs} C_{tu} F_{lnmpqrstu}^{32} + \frac{2A_{22}^*}{Rb} C_{nm} C_{pq} F_{lnmpq}^{34}$$

$$+ \frac{A_{22}^*}{b^2} C_{nm} C_{pq} F_{lnmpq}^{33}$$

$$+ \frac{A_{22}^*}{b^3} (B_{nm} C_{pq} C_{rs} F_{lnmpqrs}^{35} + b_1 C_{pq} C_{rs} b F_{2pqrs}^{35})$$

$$+ \frac{A_{22}^*}{b^2 K} C_{nm} C_{pq} C_{rs} F_{lnmpqrs}^{36} + \frac{A_{66}^*}{b^2} A_{nm} A_{pq} F_{lnmpq}^{41}$$

$$+ \frac{A_{66}^*}{a^2} B_{nm} B_{pq} F_{lnmpq}^{42} + \frac{A_{66}^*}{a^2 b^2} C_{nm} C_{pq} C_{rs} C_{tu} F_{lnmpqrstu}^{24}$$

$$+ \frac{2A_{66}^*}{ab} A_{nm} B_{pq} F_{lnmpq}^{44} + \frac{2A_{66}^*}{ab^2} A_{nm} C_{pq} C_{rs} F_{lnmpqrs}^{45}$$

$$\frac{2A_{66}^*}{a^2 b} B_{nm} C_{pq} C_{rs} F_{lnmpqrs}^{46} + \frac{D_{11}^*}{a^4} C_{nm} C_{pq} F_{lnmpq}^{51}$$

$$+ \frac{2D_{12}^*}{a^2 b^2} C_{nm} C_{pq} F_{lnmpq}^{52} + \frac{4D_{16}^*}{a^3 b} C_{nm} C_{pq} F_{lnmpq}^{53}$$

$$\begin{aligned}
& + \frac{D_{22}^*}{b^4} C_{nm} C_{pq} F_{lnmpq}^{54} + \frac{4D_{26}^*}{b^3 a} C_{nm} C_{pq} F_{lnmpq}^{55} \\
& + \frac{4D_{66}^*}{a^2 b^2} C_{nm} C_{pq} F_{lnmpq}^{56} \Bigg\} \\
& + \left\{ \frac{2A_s E_s}{a^2 b} (A_{nm} A_{pq} F_{lnmpq}^{S1} + 2A_{nm} a_1 a F_{2nm}^{S1} + a_1^2 a^2) \right. \\
& + \frac{2I_s E_s h_s}{a^4 b} B_{nm} B_{pq} F_{lnmpq}^{S2} \Bigg\} \\
& + \frac{A_f E_f}{ab^2} (B_{nm} B_{pq} F_{lnmpq}^{F1} + 2B_{nm} b_1 b F_{2nm}^{F1} + b_1^2 b^2) \\
& + \left. \frac{I_f E_f h_f}{ab^4} A_{nm} A_{pq} F_{lnmpq}^{F2} \right\} - 2a_1 N_{xx} \Bigg] \quad (40)
\end{aligned}$$

where,

- $A_{ij}^*$  = in-plane stiffness matrix
- $D_{ij}^*$  = bending stiffness matrix
- $E_s$  = axial modulus for the stringer
- $A_s$  = cross-sectional area of the stringer
- $I_s$  = equivalent moment of inertia of the stringer about the z-axis
- $E_f$  = axial modulus for the frame
- $A_f$  = cross-sectional area of the frame
- $I_f$  = equivalent moment of inertia of the frame about the z-axis
- $N_{xx}$  = applied load (lbs/in)

$F_{ijkl}^{\alpha\beta}$  = functions obtained from the evaluation of integrals which appear in the total potential energy expression. Detailed expressions are given in Appendix B.

The conditions for obtaining the values of the coefficients that minimize the total potential energy,  $\Pi$ , are

$$\frac{\partial \Pi}{\partial A_{ij}} = 0, \quad \frac{\partial \Pi}{\partial B_{ij}} = 0, \quad \frac{\partial \Pi}{\partial C_{ij}} = 0, \quad \frac{\partial \Pi}{\partial a_1} = 0, \quad \frac{\partial \Pi}{\partial b_1} = 0. \quad (41)$$

After performing the differentiation operation, the following five nonlinear simultaneous equations are obtained:

$$\begin{aligned} \frac{\partial \Pi}{\partial A_{ij}} = & \frac{2A_{11}^*}{a^2} (A_{nm} F_{lijnm}^{11} + a_1 a F_{2ij}^{11} + \frac{1}{2a} C_{nm} C_{pq} F_{lijnmpq}^{13}) \\ & + \frac{2A_{12}^*}{ab} (B_{nm} F_{lijnm}^{21} + b_1 b F_{2ij}^{21} + \frac{1}{2b} C_{nm} C_{pq} F_{lijnmpq}^{22} \\ & + \frac{b}{R} C_{nm} F_{lnmij}^{25}) \\ & + \frac{2A_{66}^*}{b^2} (A_{nm} F_{lijnm}^{41} + \frac{b}{a} B_{nm} F_{lijnm}^{44} + \frac{1}{a} C_{nm} C_{pq} F_{lijnmpq}^{45}) \\ & + \frac{4E_s A_s}{a^2 b} (A_{nm} F_{lijnm}^{S1} + a_1 a F_{2ij}^{S1}) + \frac{2I_f E_f}{ab^4} A_{nm} F_{lijnm}^{F2} = 0 \end{aligned} \quad (42)$$

$$\begin{aligned} \frac{\partial \Pi}{\partial B_{ij}} = & \frac{2A_{12}^*}{ab} (A_{nm} F_{lnmij}^{21} + a_1 a F_{3ij}^{21} + \frac{1}{2a} C_{nm} C_{pq} F_{lijnmpq}^{23}) \\ & + \frac{2A_{22}^*}{b^2} (B_{nm} F_{lijnm}^{31} + b_1 b F_{2ij}^{31} + \frac{1}{2b} C_{nm} C_{pq} F_{lijnmpq}^{35}) \end{aligned}$$

$$\begin{aligned}
& + \frac{A_{66}^*}{2} (B_{nm} F_{lijnm}^{42} + \frac{a}{b} A_{nm} F_{lnmij}^{44} + \frac{1}{b} C_{nm} C_{pq} F_{lijnmpq}^{46}) \\
& + \frac{4I_s E_s}{a^4 b} B_{nm} F_{lijnm}^{S2} + \frac{2A_f E_f}{ab^2} (B_{nm} F_{lijnm}^{F1} + b_1 b F_{2ij}^{F1}) = 0
\end{aligned} \tag{43}$$

$$\begin{aligned}
\frac{\partial \Pi}{\partial C_{ij}} = & \frac{A_{11}^*}{a^4} (C_{nm} C_{pq} C_{rs} F_{lijnmpqrs}^{12} + 2a A_{nm} C_{pq} F_{lnmijpq}^{13} \\
& + 2a^2 a_1 C_{nm} F_{2ijnm}^{13}) \\
& + \frac{A_{12}^*}{ab} \left[ \frac{2}{b} A_{nm} C_{pq} F_{lnmijpq}^{22} + \frac{2a}{b} a_1 C_{nm} F_{2ijnm}^{22} + \right. \\
& \frac{2}{a} B_{nm} C_{pq} F_{lnmijpq}^{23} + \frac{2b}{a} b_1 C_{nm} F_{2ijnm}^{23} + \\
& \frac{1}{ab} C_{nm} C_{pq} C_{rs} (F_{lijnmpqrs}^{24} + F_{lnmpqijrs}^{24}) \\
& + \frac{2b}{R} A_{nm} F_{lijnm}^{25} + \frac{2ab}{R} a_1 F_{2ij}^{25} \\
& \left. + \frac{b}{aR} C_{nm} C_{pq} (F_{lijnmpq}^{26} + 2F_{lnmijpq}^{26}) \right]
\end{aligned}$$

$$\begin{aligned}
& + \frac{A_{22}^*}{b^4} \left[ C_{nm} C_{pq} C_{rs} F_{lijnpqrs}^{32} + \frac{2b^4}{R^2} C_{nm} F_{lijnm}^{33} \right. \\
& \quad + \frac{2b^3}{R} C_{nm} (F_{lijnm}^{34} + F_{lnmij}^{34}) \\
& \quad + 2b B_{nm} C_{pq} F_{lnmijpq}^{35} + 2b^2 b_1 C_{nm} F_{2ijnm}^{35} \\
& \quad \left. + \frac{b^2}{R} C_{nm} C_{pq} (F_{lijnpq}^{36} + 2F_{lnmijpq}^{36}) \right]
\end{aligned}$$

$$\begin{aligned}
& + \frac{A_{66}^*}{a^2 b^2} \left[ C_{nm} C_{pq} C_{rs} (F_{lijnpqrs}^{24} + F_{lnmpqijrs}^{24}) \right. \\
& \quad + a A_{nm} C_{pq} (F_{lnmijpq}^{45} + F_{lnmpqij}^{45}) \\
& \quad \left. + b B_{nm} C_{pq} (F_{lnmijpq}^{46} + F_{lnmpqij}^{46}) \right] \\
& + \frac{2D_{11}^*}{a^4} C_{nm} F_{lijnm}^{51} + \frac{2D_{12}^*}{a^2 b^2} C_{nm} (F_{lijnm}^{52} + F_{lnmij}^{52}) \\
& + \frac{4D_{16}^*}{a^3 b} C_{nm} (F_{lijnm}^{53} + F_{lnmij}^{53}) + \frac{2D_{22}^*}{b^4} C_{nm} F_{lijnm}^{54} \\
& + \frac{4D_{26}^*}{ab^3} C_{nm} (F_{lijnm}^{55} + F_{lnmij}^{55}) + \frac{8D_{66}^*}{a^2 b^2} C_{nm} F_{lijnm}^{56} = 0 \quad (44)
\end{aligned}$$

$$\frac{\partial \Pi}{\partial a_1} = \frac{A_{11}^*}{a^2} (2a A_{nm} F_{2nm}^{11} + 2a^2 a_1 + C_{nm} C_{pq} F_{2nmpq}^{13})$$

$$\begin{aligned}
& + \frac{A_{12}^*}{ab} (2a B_{nm} F_{3nm}^{21} + 2b_1 ab + \frac{a}{b} C_{nm} C_{pq} F_{2nmpq}^{22} \\
& + \frac{2ab}{R} C_{nm} F_{2nm}^{25}) \\
& + \frac{4A_s E_s}{ab} (A_{nm} F_{2nm}^{S1} + a_1 a) - 2N_{xx} = 0
\end{aligned} \tag{45}$$

$$\begin{aligned}
\frac{\partial \Pi}{\partial b_1} & = \frac{A_{12}^*}{ab} (2b A_{nm} F_{2nm}^{21} + 2a_1 ab + \frac{b}{a} C_{nm} C_{pq} F_{2nmpq}^{23}) \\
& + \frac{A_{22}^*}{b^2} (2b B_{nm} F_{2nm}^{31} + 2b^2 b_1 + C_{nm} C_{pq} F_{2nmpq}^{35}) \\
& + \frac{2A_f E_f}{ab} (B_{nm} F_{2nm}^{F1} + b_1 b) = 0
\end{aligned} \tag{46}$$

The governing equations are obtained by linearizing Equations 42 through 46 by first expressing the total potential energy as:

$$\Pi = \Pi(\underline{q}, \lambda) \tag{47}$$

where  $\underline{q}$  is the vector of the unknown coefficients. The equilibrium equations related to the stationary condition of the total potential energy are:

$$R_i(\underline{q}, \lambda) \equiv \frac{\partial \Pi(\underline{q}, \lambda)}{\partial q_i} = 0 \quad \& \quad R_i(q_j, \lambda) \equiv F_i(q_j) - \lambda \bar{P}_i \tag{48}$$

The resulting equations are a system of nonlinear coupled algebraic equations. Linearization of these equations is required in order to ensure a systematic solution scheme. Expanding these equations about a known position vector  $\underline{q}_0$  and retaining the linear terms in the expansion, the following set of equations is obtained.

$$\frac{\partial \underline{R}}{\partial \underline{q}} \Delta \underline{q} + \frac{\partial \underline{R}}{\partial \lambda} \Delta \lambda + \underline{R}(\underline{q}_0; \lambda_0) = 0 \quad (49)$$

Defining  $\underline{K} = \frac{\partial \underline{R}}{\partial \underline{q}} = \frac{\partial \underline{F}}{\partial \underline{q}}$ , the equation above becomes,

$$\underline{K} \Delta \underline{q} = -\underline{F} \Delta \lambda - \underline{R}(\underline{q}_0, \lambda_0) \quad (50)$$

The matrix  $\underline{K}$  is called the tangent stiffness matrix and it provides information about the stability of the structure. At the bifurcation point  $\underline{K}$  becomes singular.  $\underline{R}$ ,  $\underline{F}$  and  $\underline{q}$  are called the residual internal and external load vectors, respectively. The full set of equations to be solved numerically then appear as follows:

$$\begin{bmatrix} \frac{\partial^2 \Pi}{\partial A_{ij} \partial A_{kl}} & \frac{\partial^2 \Pi}{\partial A_{ij} \partial B_{kl}} & \frac{\partial^2 \Pi}{\partial A_{ij} \partial C_{kl}} & \frac{\partial^2 \Pi}{\partial A_{ij} \partial a_1} & \frac{\partial^2 \Pi}{\partial A_{ij} \partial b_1} \\ \frac{\partial^2 \Pi}{\partial B_{ij} \partial A_{kl}} & \frac{\partial^2 \Pi}{\partial B_{ij} \partial B_{kl}} & \frac{\partial^2 \Pi}{\partial B_{ij} \partial C_{kl}} & \frac{\partial^2 \Pi}{\partial B_{ij} \partial a_1} & \frac{\partial^2 \Pi}{\partial B_{ij} \partial b_1} \\ \frac{\partial^2 \Pi}{\partial C_{ij} \partial A_{kl}} & \frac{\partial^2 \Pi}{\partial C_{ij} \partial B_{kl}} & \frac{\partial^2 \Pi}{\partial C_{ij} \partial C_{kl}} & \frac{\partial^2 \Pi}{\partial C_{ij} \partial a_1} & \frac{\partial^2 \Pi}{\partial C_{ij} \partial b_1} \\ \frac{\partial^2 \Pi}{\partial a_1 \partial A_{kl}} & \frac{\partial^2 \Pi}{\partial a_1 \partial B_{kl}} & \frac{\partial^2 \Pi}{\partial a_1 \partial C_{kl}} & \frac{\partial^2 \Pi}{\partial a_1 \partial a_1} & \frac{\partial^2 \Pi}{\partial a_1 \partial b_1} \\ \frac{\partial^2 \Pi}{\partial b_1 \partial A_{kl}} & \frac{\partial^2 \Pi}{\partial b_1 \partial B_{kl}} & \frac{\partial^2 \Pi}{\partial b_1 \partial C_{kl}} & \frac{\partial^2 \Pi}{\partial b_1 \partial a_1} & \frac{\partial^2 \Pi}{\partial b_1 \partial b_1} \end{bmatrix} \begin{bmatrix} \Delta A_{kl} \\ \Delta B_{kl} \\ \Delta C_{kl} \\ \Delta a_1 \\ \Delta b_1 \end{bmatrix} = \begin{bmatrix} 0 \\ 0 \\ 0 \\ 2 N_{xx} \\ 0 \end{bmatrix} \Delta \lambda - \begin{bmatrix} \frac{\partial \Pi}{\partial A_{ij}} \\ \frac{\partial \Pi}{\partial B_{ij}} \\ \frac{\partial \Pi}{\partial C_{ij}} \\ \frac{\partial \Pi}{\partial a_1} \\ \frac{\partial \Pi}{\partial b_1} \end{bmatrix} \quad (51)$$



The submatrices of the global matrix in Equation. 51 can be expressed as:

$$\frac{\partial^2 \Pi}{\partial A_{kl} \partial A_{ij}} = \frac{2A_{11}^*}{a^2} F_{1ijkl}^{11} + \frac{2A_{66}^*}{b^2} F_{1ijkl}^{41} + \frac{4E_s A_s}{a^2 b} F_{1ijkl}^{S1} + \frac{2I_f E_f h_f}{ab^4} F_{1ijkl}^{F1} \quad (52)$$

$$\frac{\partial^2 \Pi}{\partial B_{kl} \partial A_{ij}} = \frac{2}{ab} (A_{12}^* F_{1ijkl}^{21} + A_{66}^* F_{1ijkl}^{44}) \quad (53)$$

$$\begin{aligned} \frac{\partial^2 \Pi}{\partial C_{kl} \partial A_{ij}} &= \frac{2A_{11}^*}{a^3} C_{nn} F_{ijklnm}^{13} + \frac{2A_{12}^*}{ab^2} C_{nm} F_{ijklrm}^{22} + \frac{2A_{12}^*}{AR} F_{1kl ij}^{25} \\ &+ \frac{2A_{66}^*}{ab^2} C_{nm} (F_{ijklum}^{45} + F_{ijnmkl}^{45}) \end{aligned} \quad (54)$$

$$\frac{\partial^2 \Pi}{\partial a_1 \partial A_{ij}} = \frac{2A_{11}^*}{a} F_{2ij}^{11} + \frac{4E_s A_s}{ab} F_{2ij}^{51} \quad (55)$$

$$\frac{\partial^2 \Pi}{\partial b_1 \partial A_{ij}} = \frac{2A_{12}^*}{a} F_{2ij}^{21} \quad (56)$$

$$\frac{\partial^2 \Pi}{\partial A_{kl} \partial B_{ij}} = \left[ \frac{\partial^2 \Pi}{\partial B_{kl} \partial A_{ij}} \right]^T \quad (57)$$

$$\frac{\partial^2 \Pi}{\partial B_{kl} \partial B_{ij}} = \frac{2A_{22}^*}{b^2} F_{1ijkl}^{31} + \frac{2A_{66}^*}{a^2} F_{1ijkl}^{42} + \frac{4I_s E_s h_s}{a^4 b} F_{1ijkl}^{S2} + \frac{2A_f E_f}{ab^2} F_{1ijkl}^{F1} \quad (58)$$

$$\begin{aligned} \frac{\partial^2 \Pi}{\partial C_{kl} \partial B_{ij}} &= \frac{2A_{12}^*}{a^2 b} C_{nm} F_{ijklnm}^{23} + \frac{2A_{22}^*}{b^3} C_{nm} F_{ijklnm}^{35} \\ &+ \frac{2A_{66}^*}{a^2 b} C_{nm} (F_{ijklnm}^{46} + F_{ijnmkl}^{46}) \end{aligned} \quad (59)$$

$$\frac{\partial^2 \Pi}{\partial a_1 \partial B_{ij}} = \frac{2A_{12}^*}{b} F_{3ij}^{21} \quad (60)$$

$$\frac{\partial^2 \Pi}{\partial b_1 \partial B_{ij}} = \frac{2A_{22}^*}{b} F_{2ij}^{31} + \frac{2A_f E_f}{ab} F_{2ij}^{F1} \quad (61)$$

$$\frac{\partial^2 \Pi}{\partial A_{kl} \partial C_{ij}} = \left[ \frac{\partial^2 \Pi}{\partial C_{kl} \partial A_{ij}} \right]^T \quad (52)$$

$$\frac{\partial^2 \Pi}{\partial E_{kl} \partial C_{ij}} = \left[ \frac{\partial^2 \Pi}{\partial C_{kl} \partial B_{ij}} \right]^T \quad (63)$$

$$\begin{aligned} \frac{\partial^2 \Pi}{\partial C_{kl} \partial C_{ij}} = & \frac{A_{11}^*}{a^4} (3 C_{nm} C_{pq} F_{lijklnmpq}^{12} + 2a A_{nm} F_{lnmijkl}^{13} + 2a^2 a_1 F_{2ijkl}^{13}) \\ & + \frac{A_{12}^*}{ab} \left( \frac{2}{b} A_{nm} F_{lnmijkl}^{22} + \frac{2a}{b} a_1 F_{2ijkl}^{22} + \frac{2}{a} B_{nm} F_{lnmijkl}^{23} \right. \\ & + \frac{2b}{a} b_1 F_{2ijkl}^{23} + \frac{1}{ab} C_{pm} C_{pq} (2F_{lijnmklpq}^{24} + 2F_{lklmijpq}^{24} \\ & + F_{lijklnmpq}^{24} + F_{lnmpqijkl}^{24}) + \frac{2b}{ak} C_{nm} (F_{lijklnm}^{26} + F_{lnmijkl}^{26} \\ & + F_{lklijnm}^{26}) \\ & + \frac{A_{22}^*}{b^4} (3 C_{nm} C_{pq} F_{lijklnmpq}^{32} + \frac{2b^4}{R} F_{lijk}^{33} + \frac{2b^3}{R} (F_{lijk}^{34} \\ & + F_{lklj}^{34}) + 2b E_{nm} F_{lnmijkl}^{35} + 2b^2 b_1 F_{2ijkl}^{35} \\ & + \frac{2b^2}{R} C_{nm} (F_{lijklnm}^{36} + F_{lnmijkl}^{36} + F_{lklijnm}^{36}) \\ & + \frac{2A_{66}^*}{a^2 b^2} C_{nm} C_{pq} (2F_{lijnmklpq}^{24} + 2F_{lklmijpq}^{24} + F_{lijklnmpq}^{24} \end{aligned}$$

$$\begin{aligned}
& + F_{lnmpqijkl}^{24} + a A_{nm} (F_{lnmijkl}^{45} + F_{lnmklij}^{45}) \\
& + b B_{nm} (F_{lnmijkl}^{46} + F_{lnmklij}^{46}) \\
& + \frac{2D_{11}^*}{a^4} F_{lijkl}^{51} + \frac{2D_{12}^*}{a^2 b^2} (F_{lijkl}^{52} + F_{lklij}^{52}) + \frac{4D_{16}^*}{a^3 b} (F_{Fijkl}^{53} \\
& + F_{lklij}^{53}) + \frac{2D_{22}^*}{b^4} F_{lijkl}^{54} + \frac{4D_{26}^*}{ab^3} (F_{lijkl}^{55} + F_{lklij}^{55}) \\
& + \frac{8D_{66}^*}{a^2 b^2} F_{ijkl}^{56}
\end{aligned} \tag{64}$$

$$\frac{\partial^2 \Pi}{\partial a_1 \partial C_{ij}} = \frac{2A_{11}^*}{a^2} C_{nm} F_{2ijnm}^{13} + \frac{2A_{12}^*}{b^2} C_{nm} F_{2ijnm}^{22} + \frac{2A_{12}^*}{R} F_{2ij}^{25} \tag{65}$$

$$\frac{\partial^2 \Pi}{\partial b_1 \partial C_{ij}} = \frac{2A_{12}^*}{a^2} C_{nm} F_{2ijnm}^{23} + \frac{2A_{22}^*}{b^2} C_{nm} F_{2ijnm}^{25} \tag{66}$$

$$\frac{\partial^2 \Pi}{\partial A_{kl} \partial a_1} = \left[ \frac{\partial^2 \Pi}{\partial a_1 \partial A_{ij}} \right]^T \tag{67}$$

$$\frac{\partial^2 \Pi}{\partial B_{kl} \partial a_1} = \left[ \frac{\partial^2 \Pi}{\partial a_1 \partial B_{ij}} \right]^T \tag{68}$$

$$\frac{\partial^2 \Pi}{\partial C_{kl} \partial a_1} = \left[ \frac{\partial^2 \Pi}{\partial a_1 \partial C_{ij}} \right]^T \tag{69}$$

$$\frac{\partial^2 \Pi}{\partial a_1 \partial a_1} = 2A_{11}^* + \frac{4A_s E_s}{b} \quad (70)$$

$$\frac{\partial^2 \Pi}{\partial b_1 \partial a_1} = 2A_{12}^* \quad (71)$$

$$\frac{\partial^2 \Pi}{\partial A_{k1} \partial b_1} = \left[ \frac{\partial^2 \Pi}{\partial b_1 \partial A_{ij}} \right]^T \quad (72)$$

$$\frac{\partial^2 \Pi}{\partial B_{k1} \partial b_1} = \left[ \frac{\partial^2 \Pi}{\partial b_1 \partial B_{ij}} \right]^T \quad (73)$$

$$\frac{\partial^2 \Pi}{\partial C_{k1} \partial b_1} = \left[ \frac{\partial^2 \Pi}{\partial b_1 \partial C_{ij}} \right]^T \quad (74)$$

$$\frac{\partial^2 \Pi}{\partial b_1 \partial t_1} = 2A_{22}^* + \frac{2A_f E_f}{a} \quad (75)$$

Numerical solution of Equations 51 is accomplished using the method described in Section 4.2.4.

#### 4.2.4 Numerical Solution Procedure

Among the variety of numerical solution schemes, the following method described in Reference 94 is used in the calculation of the fundamental and the post-bifurcation paths.

The full set of equations to be solved numerically can be written in the form:

$$\begin{aligned} \underline{K} \Delta \underline{q} - \underline{\bar{P}} \Delta \lambda &= -\underline{R} \\ \underline{t}^T \Delta \underline{x} &= \Delta s \end{aligned} \quad (76)$$

where the unit vector  $\underline{t}$  is colinear with the vector  $\underline{r}$  and is defined as:

$$\left\{ \underline{t} = \underline{r}/|\underline{r}| \right\} \quad \text{and} \quad \underline{r}^{(k-1)} = \sum_{j=1}^{k-1} \Delta \underline{x}^{(j)} \quad (77)$$

where,  $\Delta \underline{x} = \{\Delta q, \Delta \lambda\}$  and  $\underline{r}^{(k-1)}$  is the vector of the total of instantaneous displacements at the  $(k-1)^{\text{th}}$  iteration.

Equation 76 can be rewritten in a condensed form as:

$$\underline{H} \Delta \underline{x} = \underline{s} \quad (78)$$

The matrix  $\underline{H}$  is constructed by addition of the column  $-\bar{\underline{P}}$  and the row  $\underline{t}^T$  to the  $\underline{K}$  matrix as shown below:

$$\left\{ \begin{array}{cc} \underline{K} & -\bar{\underline{P}} \\ \hline \text{---} & \underline{t}^T \end{array} \right\} \left\{ \begin{array}{c} \Delta \underline{q} \\ \vdots \\ \Delta \lambda \end{array} \right\} = \left\{ \begin{array}{c} \underline{R} \\ \vdots \\ \Delta s \end{array} \right\} \quad (79)$$

If one of the components  $q_{\alpha}$  of the vector  $\underline{q}$  is selected as a control parameter, then  $\underline{t}^T$  initially will be:

$$\underline{t}^T = \{0, \dots, 0, 1, \dots, 0\} \quad (80)$$

where, the 1 appears at the  $q_{\alpha}$  position. Assuming  $q_0 = 0$  as the initial equilibrium position for zero applied load ( $\lambda = 0$ ), the extended residual vector is:

$$\begin{aligned} \underline{s}^{(0)} &= \{0, \Delta s\} \\ \underline{s}^{(k)} &= \{q^{(k)}, 0\} \quad \text{for } k \geq 1 \text{ and} \\ \underline{t}^{(0)T} \Delta \underline{x}^{(1)} &= \Delta s \\ \underline{t}^{(k)T} \Delta \underline{x}^{(k+1)} &= 0 \quad \text{for } k \geq 0 \end{aligned} \quad (81)$$

Equation 81 governs the equilibrium on both the fundamental (pre-buckling) and the post-buckling (post-bifurcation) paths. The solution method outlined above can be used for determining equilibrium points on both parts; however, to ensure convergence of the solution procedure to equilibrium points on the post-buckling path, an orthogonality condition has to be imposed. This is achieved, as illustrated in Figure 4.2, by requiring that the vector,  $t_F$ , tangent at point B to the fundamental path, be non-colinear with the vector,  $t_B$ , tangent at point B to the post-buckling path.

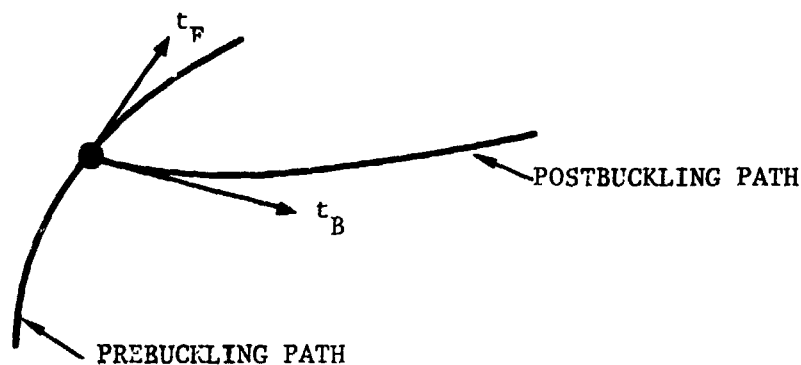


Figure 4.2. Tangent Vectors  $t_F$  and  $t_B$

The vectors  $t_F$  and  $t_B$  can be approximated as:

$$\tilde{t}_f = \Delta \tilde{x}^m / |\Delta \tilde{x}^m| \quad \text{and} \quad \tilde{t}_B = \alpha \{a + \mu \tilde{t}_f\} \quad (82)$$

where,  $\alpha = 1/|t_B|$ ,  $\mu = -a^T t_f$ ,  $a$  is the eigen-vector of the matrix  $K$  at point B.

The imposition of the above condition prevents the solution from returning to the fundamental path of equilibrium in the postbuckling regime. Once the first equilibrium point is obtained on the postbuckling path, the subsequent increments follow the procedure outlined for the fundamental path.

The above procedure is used to first determine the buckling load and the corresponding mode shape. In the postbuckling solution only the unknowns corresponding to the buckle mode shape are retained and the rest are ignored.

#### 4.2.5 Displacement Predictions

The compression panel analysis has been coded in program COMPAN documented in Reference 91 along with the user instructions. The program was used to analyze the metal and composite compression panels described in Section 3. Actual program runs for these two panels are given in Reference 91.

Solutions for the metal and composite panels were obtained by first calculating the buckling load and mode shape and then retaining in the assumed displacements the unknown coefficients corresponding to this mode shape only. Thus, the number of unknowns were significantly reduced from over 20 to 5. The calculated mode shape for composite panels was six half waves along the load direction and one half wave transverse to the load direction. The metal panel was predicted to buckle into five half waves along the load direction and one half wave transverse to the load direction.

The postbuckling predictions consisted of out-of-plane displacements as a function of the applied load, the end shortening, strains in the stringers, and membrane strain distribution in the skin. The predicted end-shortening for the metal and composite panels is shown in Figures 4.3 and 4.4, respectively. These predictions illustrate the nonlinear postbuckling response of the compression panels. End-shortening data were not measured in the test program, therefore, verification was not possible. Comparison of the other predictions with test data is carried out in Section 5, where the accuracy of the predictions is also discussed.

#### 4.3 SHEAR PANEL ANALYSIS

The shear panel analysis closely followed the approach of Denke (Reference 58) and Kudva (Reference 75). In the latter study, Denke's analysis for isotropic flat shear panels was extended to anisotropic flat shear panels.

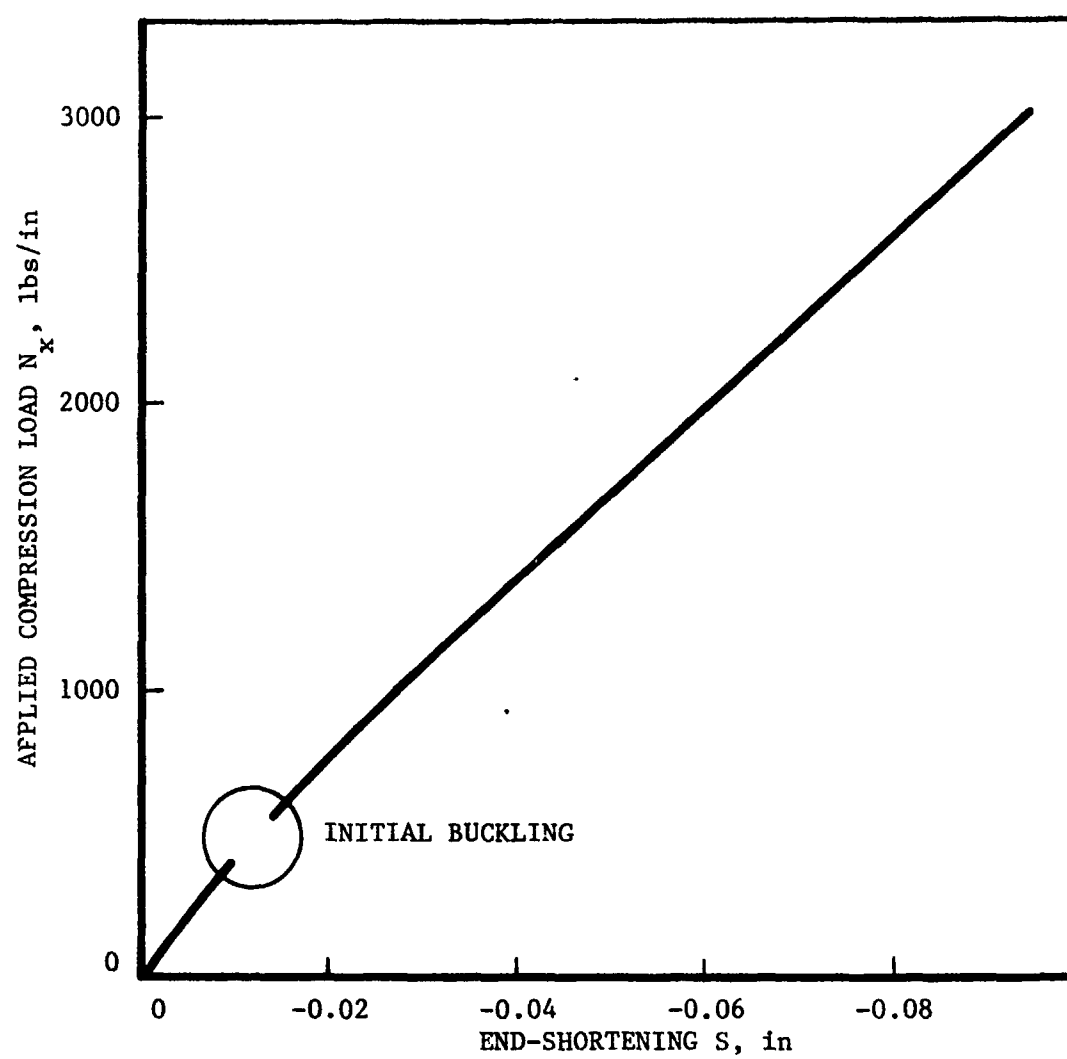


Figure 4.3. End-Shortening for Metal Compression Panels



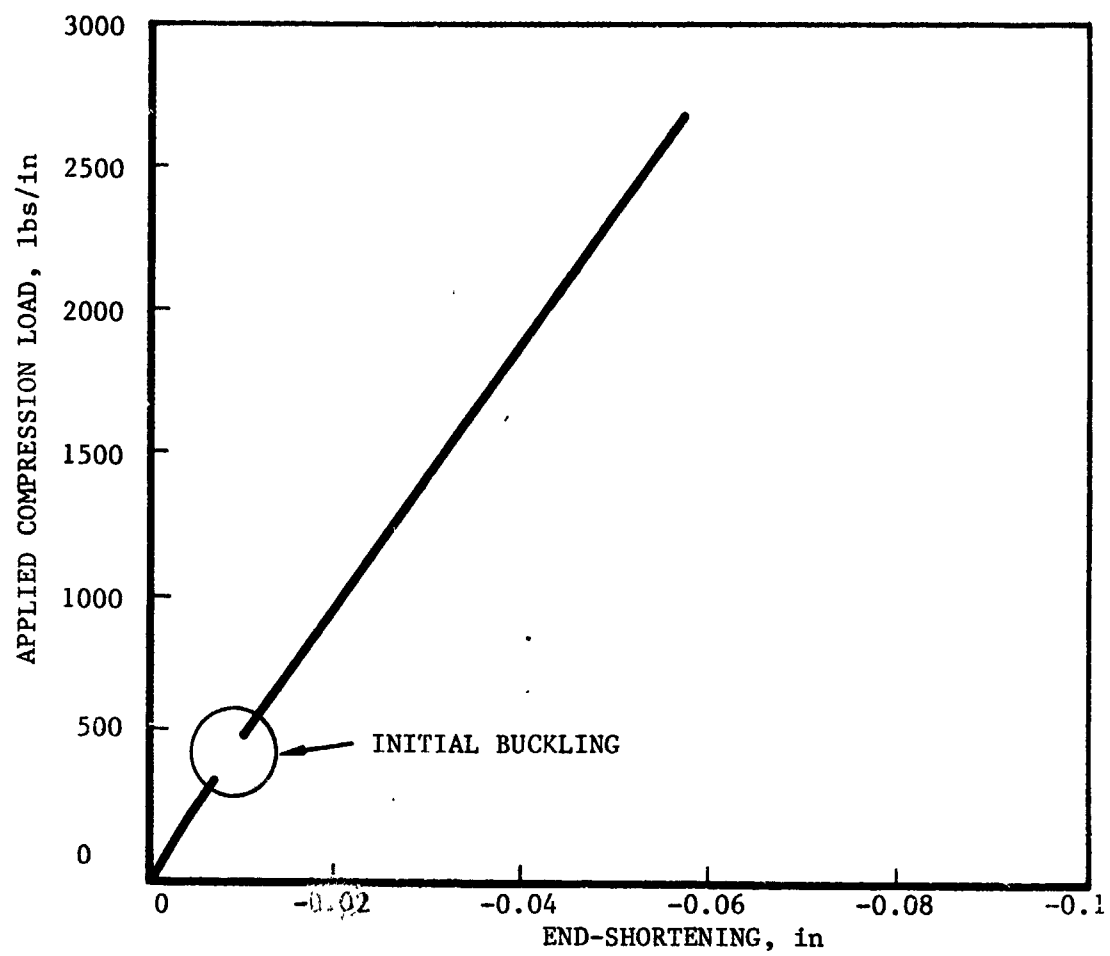


Figure 4.4. End-Shortening for Composite Compression Panels

The present analysis is a further improvement on the Reference 75 analysis in that it applies to curved anisotropic panels. The von-Karman strain displacement relations used in the present analysis include the strain term that accounts for panel curvature.

#### 4.3.1 Panel Geometry and Assumptions

The panel geometry for analysis formulation and its relationship to the three stringer panels tested in the experimental program is shown in Figure 4.5. The horizontal and vertical stiffeners correspond to the stringers and the frames, respectively.

The panel thickness is small compared with the other dimensions of the panel. This allows the use of von Karman plate theory. When subjected to shear loads above the critical load, a stiffened curved panel undergoes large deflection and, to account for this, nonlinear strain-displacement relations are considered.

The nonlinear strain-displacement relations are:

$$\begin{Bmatrix} \epsilon_x \\ \epsilon_y \\ \gamma_{xy} \end{Bmatrix} = \begin{Bmatrix} u_{,x} - w_{,x}^2/2 \\ v_{,y} + w_{,y}^2/2 + w/R \\ u_{,y} + v_{,x} + w_{,x}w_{,y} \end{Bmatrix} + z \begin{Bmatrix} -w_{,xx} \\ -w_{,yy} \\ -2w_{,xy} \end{Bmatrix} \quad \text{or} \quad (83)$$

$$\tilde{\epsilon} = \overset{o}{\epsilon} + z\kappa$$

and  $z$  is the distance from the middle surface. Superscript  $o$  indicates the mid-plane and comma denotes differentiation with respect to the subscript. The solution method employs the concept of principle of minimum potential energy. The total potential energy,  $\Pi$ , is the sum of the strain energy stored in the web,  $U_w$ , in the stringers,  $U_s$ , in the frame,  $U_f$ , and the potential of the external load,  $\Omega$ . i.e.,

$$\Pi = U_w + U_s + U_f + \Omega \quad (84)$$

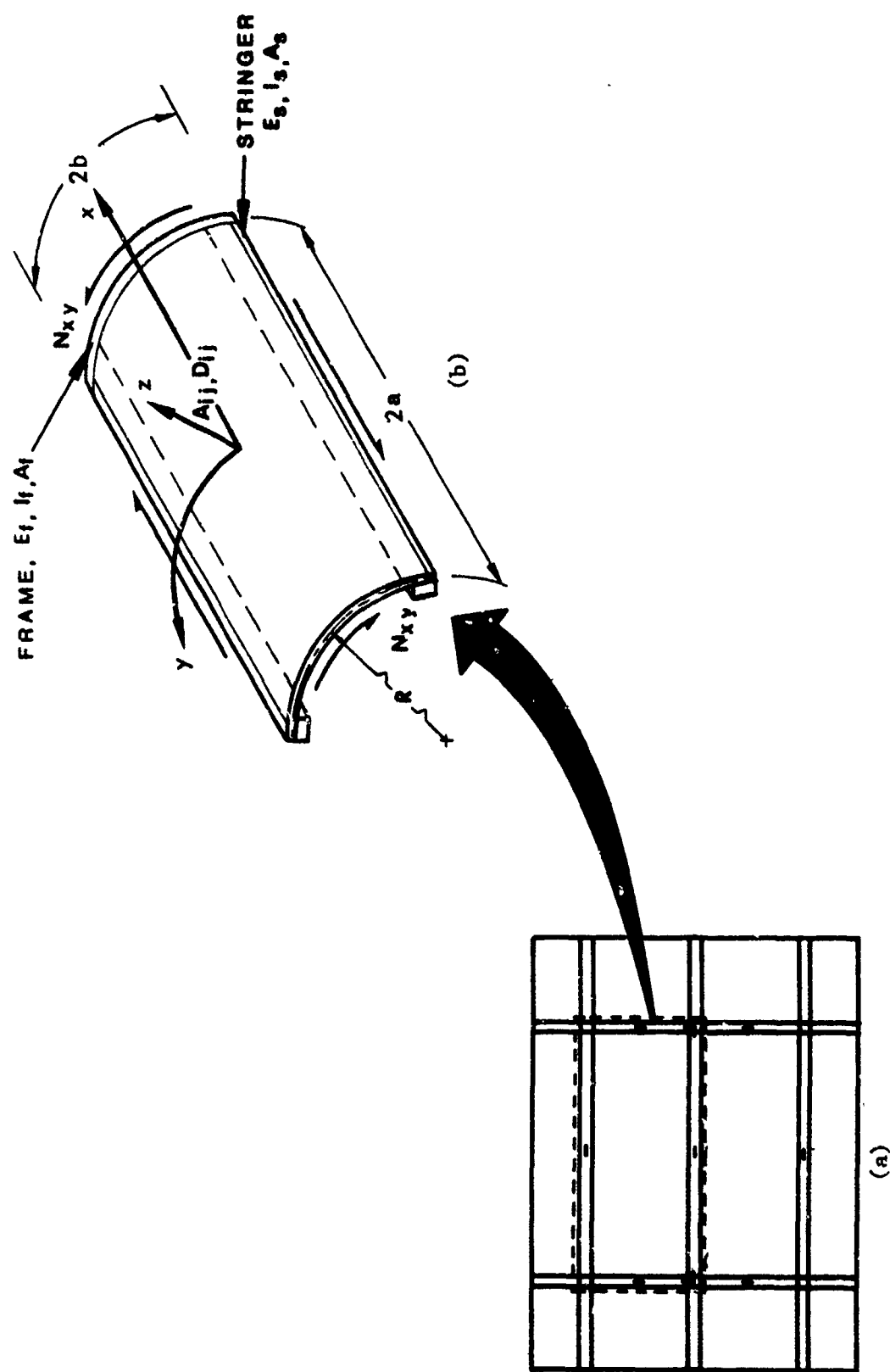


Figure 4.5. Curved Shear Panel Geometry and Coordinate System

The total potential is evaluated in terms of the unknown in-plane and out-of-plane deformation parameters. A two term trigonometric expression is assumed for the out-of-plane displacement. The unknown parameters associated with the assumed displacement function  $w(x,y)$  given in Equation 85 below are  $\bar{m}$ ,  $\bar{n}$  and  $\bar{f}$ .

$$w(x,y) = 8\bar{f} \cos px \cos qy \cos \left( \bar{m} \frac{x}{a} + \bar{n} \frac{y}{b} \right) \quad (85)$$

$$\text{where } \bar{m} = \frac{2\pi}{\lambda_o} a \sin \alpha, \quad \bar{n} = \frac{2\pi}{\lambda_c} b \cos \alpha$$

$$p = \frac{\pi}{2a} \text{ and } q = \frac{\pi}{2b} .$$

$\alpha$  and  $\lambda_o$  are the diagonal tension angle and wave length of the buckles, respectively.  $\bar{f}$  is the amplitude of the buckles. A graphic illustration of the assumed displacement functions is shown in Figure 4.6. The additional in-plane deformation parameters assumed are  $e_h$ ,  $e_y$ ,  $e_v$  and  $\gamma_o$  which are strain quantities with physical significance as illustrated in Figure 4.7. These strain quantities are a result of the following integrations:

$$\begin{aligned} e_h &= -\frac{1}{2a} \int_{-a}^a u_{,x} dx \\ (e_v + e_y) &= -\frac{1}{2b} \int_{-b}^b v_{,y} dy \\ \gamma_o &= \frac{1}{2b} \int_{-b}^b u_{,y} dy \end{aligned} \quad (86)$$

with

$$\int_{-a}^a v_{,x} dx = 0$$

The out-of-plane displacement  $w(x,y)$  is kinematically admissible since  $w(x, \pm b) = w(\pm a, y) = 0$ .

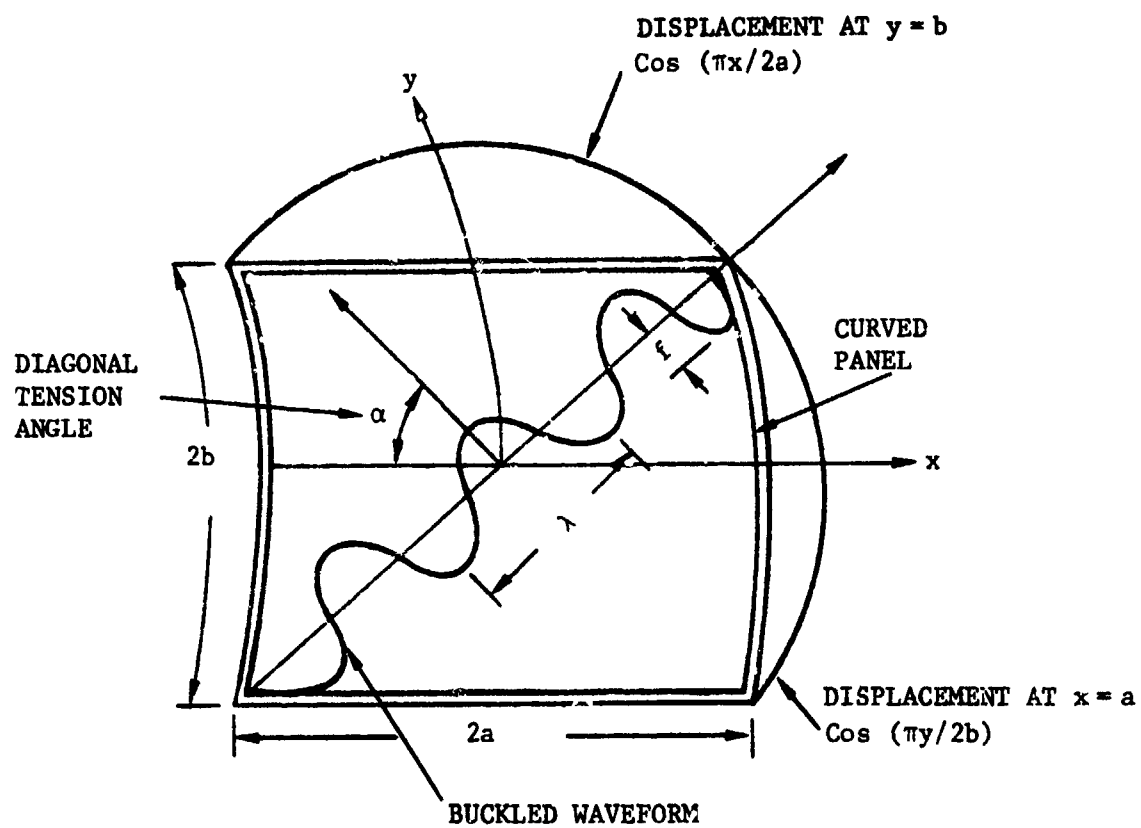
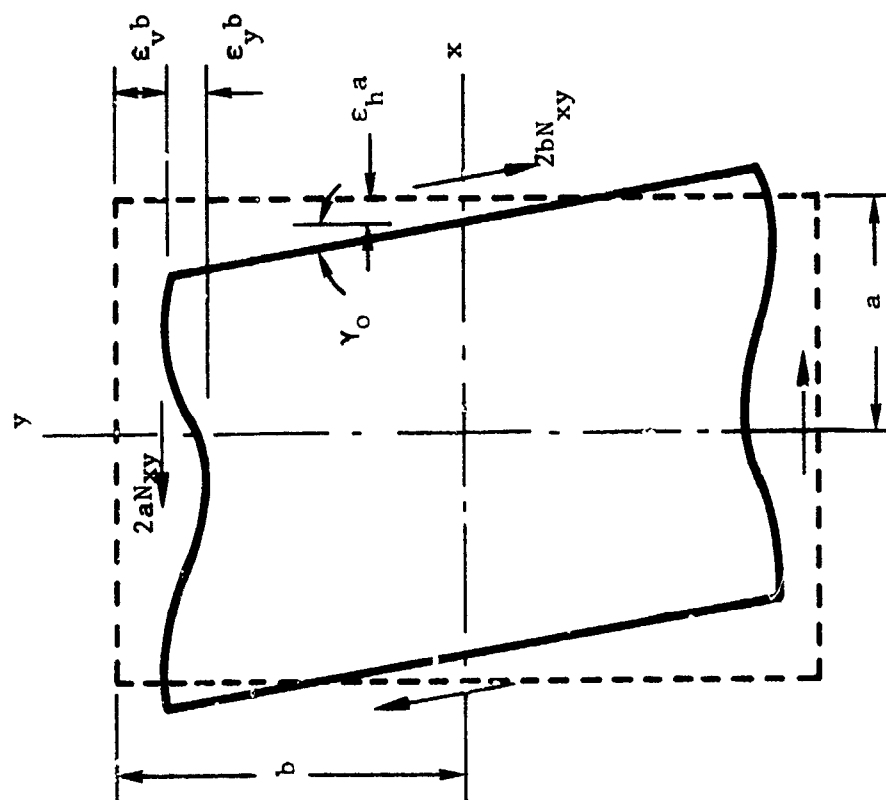


Figure 4.6. Assumed Out-of-Plane Displacement Parameters  $\alpha$ ,  $\lambda$  and  $f$



$\epsilon_v$  = AVERAGE STRAIN IN FRAMES  
 $\epsilon_H$  = AVERAGE STRAIN IN STRINGERS  
 $\epsilon_y^b$  = AVERAGE STRINGER DEFLECTION  
 $\gamma_0$  = AVERAGE SHEAR STRAIN

Figure 4.7. In-Plane Deformation Parameters

In addition to the above assumed displacements, the following are assumed regarding the in-plane stress resultants:

- (A)  $N_{xy}$  is a constant independent of  $x$  and  $y$  and is equal to the externally applied load.
- (B)  $N_x$  is a function of  $y$  only.
- (C)  $N_y$  is a function of  $x$  only.

The latter two assumptions ensure that the in-plane equilibrium equations are satisfied.

#### 4.3.2 Strain Energy Expressions

The strain energies  $U_w$ ,  $U_s$  and  $U_f$  and the potential of the external forces are expressed as shown below.

Strain energy of the web:

$$U_w = \frac{1}{2} \int_{-a}^a \int_{-b}^b \left[ A_{ij} N_i N_j + D_{ij} \kappa_i \kappa_j \right] dx dy \quad (87)$$

The first and the second term of the integrand represent the stored strain energy associated with in-plane, and bending deformations, respectively. The constitutive relations for the panel under consideration are:

$$\begin{Bmatrix} N_x \\ N_y \\ N_{xy} \end{Bmatrix} = \begin{bmatrix} A_{11} & A_{12} & 0 \\ A_{12} & A_{22} & 0 \\ 0 & 0 & A_{66} \end{bmatrix} \begin{Bmatrix} u_{,x} + w_{,x}^2/2 \\ v_{,y} + w_{,y}^2/2 + w/R \\ u_{,y} + v_{,x} + w_{,x} w_{,y} \end{Bmatrix} \quad (88)$$

The average stress resultants  $\bar{N}_x$  and  $\bar{N}_y$  are defined by Equation (89) below. The average shear stress resultant  $\bar{N}_{xy}$  equals the applied shear stress due to assumption (A) above.

$$\bar{N}_x = \frac{1}{2b} \int_{-b}^b N_x(y) dy \quad \text{and} \quad \bar{N}_y = \frac{1}{2a} \int_{-a}^a N_y(x) dx \quad (89)$$

Using the average stress resultants, the constitutive relations can be rewritten as follows:

$$\begin{Bmatrix} \bar{N}_x \\ \bar{N}_y \\ \bar{N}_{xy} \end{Bmatrix} = \begin{bmatrix} A_{11} & A_{12} & 0 \\ A_{12} & A_{22} & 0 \\ 0 & 0 & A_{66} \end{bmatrix} \begin{Bmatrix} \epsilon_1 \\ \epsilon_2 \\ \epsilon_3 \end{Bmatrix} \quad (90)$$

where,

$$\begin{aligned} \epsilon_1 &= \left[ -e_h + \frac{1}{a^2} \bar{f}^2 (\pi^2 + 4\bar{m}^2) \right] \\ \epsilon_2 &= \left[ -(e_v + e_y) + \frac{1}{b^2} \bar{f}^2 (\pi^2 + 4\bar{n}^2) + \right. \\ &\quad \left. \frac{32\pi^2}{R} \bar{f} \frac{\cos \bar{m}}{(\pi^2 - 4\bar{m}^2)} \frac{\cos \bar{n}}{(\pi^2 - 4\bar{n}^2)} \right] \\ \epsilon_3 &= \left[ -\gamma_o + \frac{8}{ab} \bar{f} \bar{m} \bar{n} \right]. \end{aligned} \quad (91)$$

The expressions for  $N_x(y)$  and  $N_y(x)$  can be obtained by performing the integration shown below:



$$\begin{aligned}
N_x(y) &= \frac{1}{a_{11}} \left\{ \int_{-a}^a \left[ u_{,x} + w_{,x}^2/2 - a_{12} N_y(x) \right] dx \right\} \\
N_y(x) &= \frac{1}{a_{22}} \left\{ \int_{-b}^b \left[ v_{,y} + w_{,y}^2/2 + w/R - a_{12} N_x(y) \right] dy \right\}
\end{aligned} \tag{92}$$

Knowing the explicit form of  $N_x(y)$  and  $N_y(x)$ , the strain energy due to in-plane deformation can be obtained from the following:

$$\begin{aligned}
U_I &= \frac{1}{2} \int_{-a}^a \int_{-b}^b \left[ a_{11} N_x^2(y) + 2a_{12} N_x(y) N_y(x) + \right. \\
&\quad \left. a_{22} N_y^2(x) + a_{66} N_{xy}^2 \right] dx dy
\end{aligned} \tag{93}$$

where  $a_{ij} = A_{ij}^{-1}$ . Also, since the laminate is symmetric and balanced about the midplane  $A_{16}$  and  $A_{26}$  are equal to zero.

Performing the integration of Equation (93) leads to the following expression:

$$U_I = 2ab \left[ \epsilon_i A_{ij} \epsilon_j + \frac{1}{2} \left( \frac{1}{a_{11}} \beta^2 + \frac{2}{a_{22}} \mu \right) \right] \tag{94}$$

where,

$$\mu = \frac{1}{2} (\nu - e_y)^2 - 2\phi (\nu - e_y) + \frac{768\pi^4}{R} \bar{f} h(\bar{n}) g(\bar{m}) (\nu - e_y) - \phi^2 + (\text{Continued})$$

$$+ \frac{16\pi^2}{R} \bar{f}^2 h^2(\bar{n}) t(\bar{m}).$$

$$\beta = \frac{1}{a^2} \bar{f}^2 (\pi^2 + 4\bar{m}^2)$$

$$\nu = \frac{1}{b^2} \bar{f}^2 (\pi^2 + 4\bar{n}^2)$$

$$\phi = \frac{32\pi^2}{R} \bar{f} h(\bar{m}) h(\bar{n})$$

$$h(x) = \frac{\cos x}{\pi^2 - 4x^2}$$

$$g(x) = \frac{h(x)}{9\pi^2 - 4x^2}$$

$$t(x) = h(x) \frac{\sin x}{x} \quad (95)$$

The bending strain energy, i.e., the second term in Equation (87) can be rewritten as:

$$U_B = \frac{1}{2} \int_{-a}^a \int_{-b}^b \left[ D_{11} w_{,xx}^2 + 2D_{12} w_{,xx} w_{,yy} + 4D_{66} w_{,xy}^2 + \right. \\ \left. D_{22} w_{,yy}^2 + D_{16} w_{,xx} w_{,xy} + 4D_{26} w_{,yy} w_{,xy} \right] dx dy \quad (96)$$

Substituting the expression for  $w(x,y)$  into Equation (96) and carrying out the integration results in:

$$U_B = ab \bar{f}^2 \left\{ \frac{D_{11}}{a^4} S_1(\bar{m}) + \frac{D_{22}}{b^4} S_1(\bar{n}) + \frac{2D_{12}}{a^2 b^2} S_2(\bar{m}, \bar{n}) + \frac{4D_{66}}{a^2 b^2} S_2(\bar{m}, \bar{n}) \right. \\ \left. + \frac{4D_{16}}{a^3 b} S_3(\bar{m}, \bar{n}) + \frac{4D_{26}}{ab^3} S_3(\bar{n}, \bar{m}) \right\} \quad (97)$$

where,

$$S_1(x) = (\pi^2 + 4x^2)^2 + 16\pi^2 x \\ S_2(x,y) = (\pi^2 + 4x^2)(\pi^2 + 4y^2) + 16\pi^2 xy \\ S_3(x,y) = (\pi^2 + 4x^2)(\pi^2 + 4xy) + 8\pi^2 x(x+y) \quad (98)$$

Strain Energy of the Stringers and Frames:

The axial strain energy of a stringer is given by:

$$U_S = \frac{1}{2} A_S E_S (2a) e_h^2 \quad (99)$$

The axial strain energy of a frame is given by:

$$U_F = \frac{1}{2} A_F E_F (2b) e_v^2 \quad (100)$$

In addition, the deflection shape of the stringer is assumed in the form written below:

$$\delta_y = 2e_y b \cos^2 px \quad (101)$$

The bending strain energy for this deflection shape in a stringer is:

$$U_{SB} = \frac{\pi^4}{2a^3} E_S I_S b^2 e_y^2 \quad (102)$$

where,

$A_S$  = Cross-sectional area of the stringer

$E_S$  = Young's modulus of the stringer

$A_F$  = Cross-sectional area of the frame

$E_F$  = Young's modulus of the frame

$I_S$  = Moment of inertia of the stringer.

Total Potential Energy:

In addition to the strain energy contributions from the various components, the potential of the externally applied shear load needs to be taken into account. This is expressed as:

$$\Omega = -N_{xy} \gamma_o 4 ab \quad (103)$$

where,

$N_{xy}$  = applied in-plane shear load per unit length

Then, the total potential  $\Pi$  is:

$$\Pi = U_I + U_B + U_S + U_{S13} + U_F + \Omega \quad (104)$$

#### 4.3.3 Governing Equations and Solution Procedure

The governing equations are obtained by minimizing the total potential with respect to the deformation parameters. Hence,

$$\frac{\partial \Pi}{\partial \gamma_o} = \frac{\partial \Pi}{\partial \bar{f}} = \frac{\partial \Pi}{\partial \bar{m}} = \frac{\partial \Pi}{\partial \bar{n}} = \frac{\partial \Pi}{\partial e_h} = \frac{\partial \Pi}{\partial e_v} = \frac{\partial \Pi}{\partial e_y} = 0 \quad (105)$$

The seven resulting equations in the seven unknowns  $\gamma_0$ ,  $\bar{f}$ ,  $\bar{m}$ ,  $\bar{n}$ ,  $e_h$ ,  $e_v$  and  $e_y$  are:

$$\frac{\partial \Pi}{\partial \gamma_0} = 0 \rightarrow A_{3j} \epsilon_j + N_{xy} = 0 \quad (106a)$$

$$\frac{\partial \Pi}{\partial e_h} = 0 \rightarrow A_{1j} \epsilon_j - E_S \frac{\Lambda_S}{b} e_h = 0 \quad (106b)$$

$$\frac{\partial \Pi}{\partial e_v} = 0 \rightarrow A_{2j} \epsilon_j - E_F \frac{A_F}{2a} e_v = 0 \quad (106c)$$

$$\begin{aligned} \frac{\partial \Pi}{\partial e_y} = 0 \rightarrow & A_{2j} \epsilon_j - \frac{1}{4ab} \left\{ \frac{1}{2a_{22}} + 2\pi^4 \frac{b^2}{a^3} E_S I_S \right\} e_y \\ & + \frac{1}{4ab} \frac{1}{2a_{22}} \left\{ -v + 2\phi - \frac{768\pi^4}{R} \bar{f} h(\bar{n}) g(\bar{m}) \right\} = 0 \end{aligned} \quad (106d)$$

$$\frac{\partial \Pi}{\partial \bar{f}} = 0 \rightarrow 4ab \left\{ A_{1j} \epsilon_j \frac{\partial \epsilon_j}{\partial \bar{f}} \frac{\beta}{2a_{11}} \frac{\partial \beta}{\partial \bar{f}} + \frac{1}{2a_{22}} \frac{\partial \mu}{\partial \bar{f}} \right\} + \frac{\partial U_B}{\partial \bar{f}} = 0 \quad (106e)$$

$$\frac{\partial \Pi}{\partial \bar{m}} = 0 \rightarrow 4ab \left\{ A_{1j} \epsilon_j \frac{\partial \epsilon_j}{\partial \bar{m}} \frac{\beta}{2a_{11}} \frac{\partial \beta}{\partial \bar{m}} + \frac{1}{2a_{22}} \frac{\partial \mu}{\partial \bar{m}} \right\} + \frac{\partial U_B}{\partial \bar{m}} = 0 \quad (106f)$$

$$\frac{\partial \Pi}{\partial \bar{n}} = 0 \rightarrow 4ab \left\{ A_{1j} \epsilon_j \frac{\partial \epsilon_j}{\partial \bar{n}} + \frac{1}{2a_{22}} \frac{\partial \mu}{\partial \bar{n}} \right\} + \frac{\partial U_B}{\partial \bar{n}} = 0 \quad (106g)$$

The above seven equations are the governing algebraic equations of equilibrium. They are highly nonlinear due to the coupling of in-plane and bending energy terms arising from panel curvature.

Equations (106) were numerically solved using standard mathematical library routines. The specific library was IMSL and the solution routine used was ZSPOW.

#### 4.3.4 Displacement Predictions

The shear panel analysis was coded in a computer program called SHRPAN1 which is documented in Reference 91 along with user instructions. The metal and composite shear panel designs of Section 3 were analyzed using SHRPAN1. Actual program runs for these two panels are given in Reference 91.

The shear panel solutions provide out-of-plane displacements, skin strains, buckle wavelength, and diagonal tension angle as a function of the applied loads. The solution is initiated above the buckling load at some pre-selected value of the displacement. The predicted out-of-plane displacements as a function of the applied load are shown in Figures 4.8 and 4.9 for the metal and composite panels, respectively. The out-of-plane displacement contours at a constant load for the metal and composite panels are shown in Figures 4.10 and 4.11, respectively. These postbuckling displacement contours illustrate the diagonal buckling pattern. Verification of the out-of-plane displacements was not possible since these displacements were not measured during the tests. However, the predicted strains and the diagonal tension angle are compared with the test data in Section 5 where the accuracy of the solution is also discussed.

#### 4.4 FATIGUE ANALYSIS APPROACH

The fatigue tests conducted on metal and composite panels in this program were useful in identifying the panel failure modes. Based on this evidence and on test data from other sources such as Reference 80, approaches to performing fatigue life analyses of metal and composite panels were developed. These approaches utilize the results of the nonempirical analysis developed in this program and in addition require some fracture property data. These fatigue life prediction methodologies are outlined in the following paragraphs.

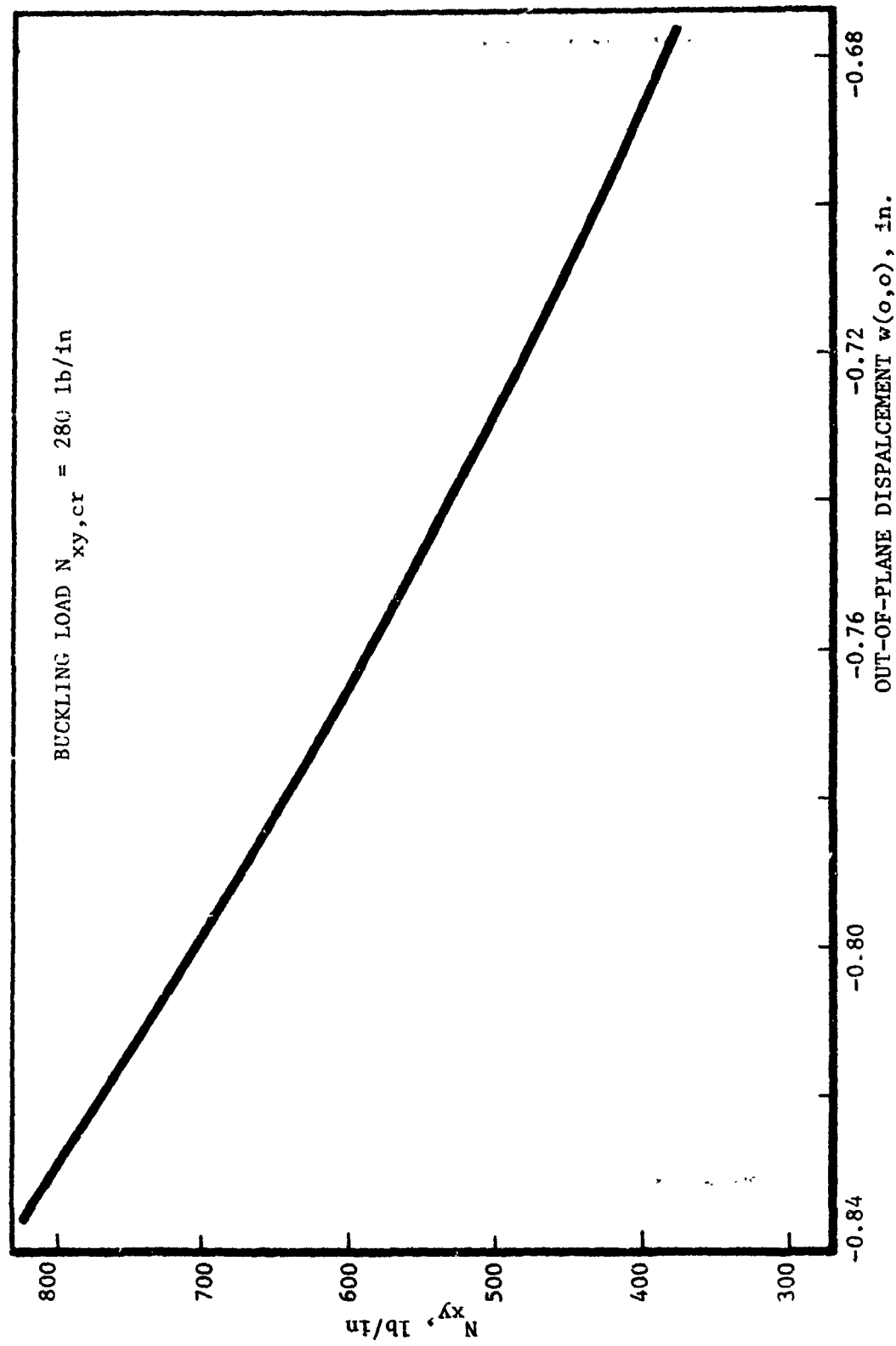


Figure 4.8. Out-of-Plane Displacement at Panel Center as a Function of Applied Shear Load for Metal Panel. SHRPAN1 Predictions

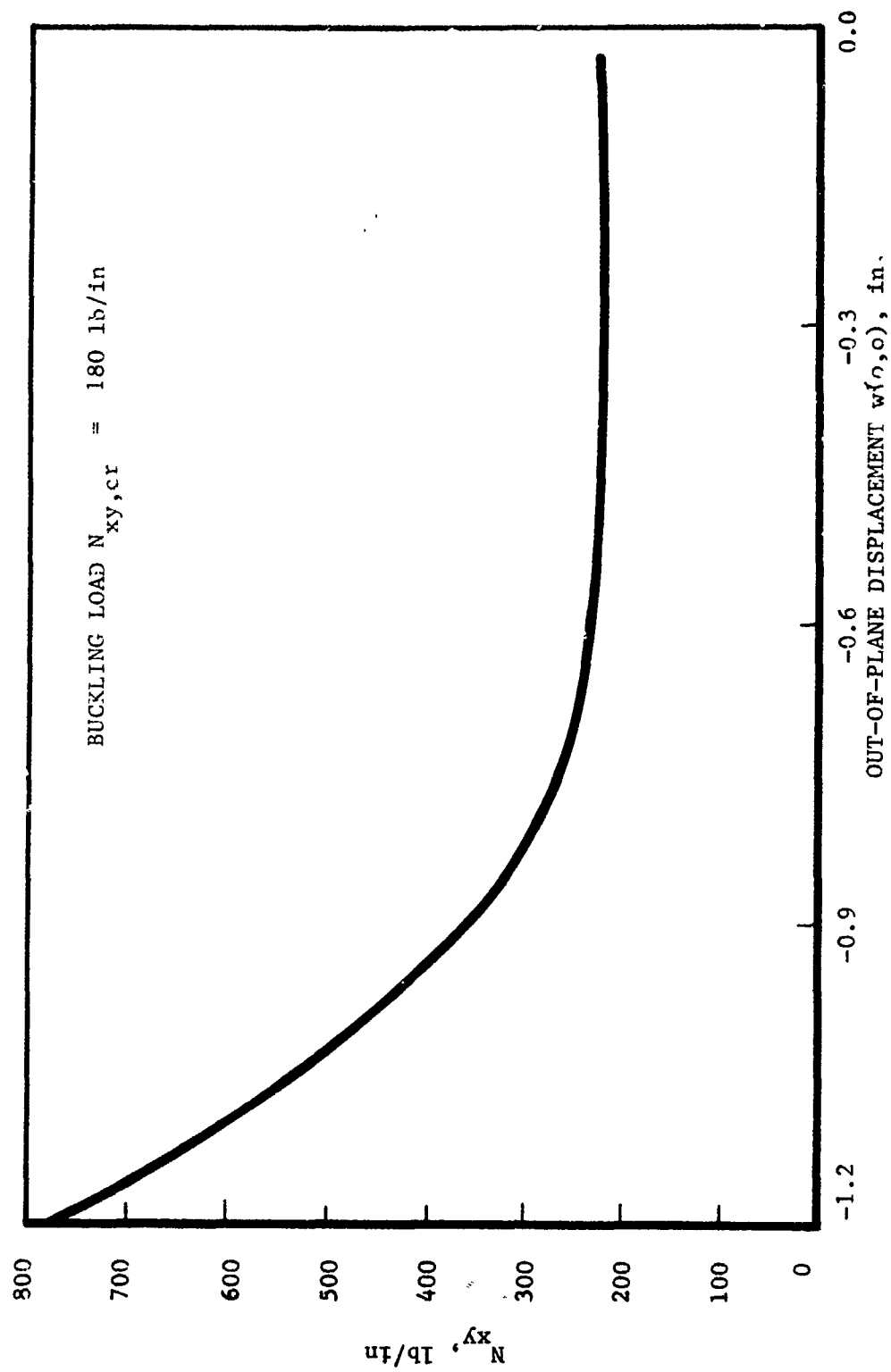


Figure 4.9. Out-of-Plane Displacement at Panel Center as a Function of Applied Shear Load for Composite Panel. SHRPAN1 Predictions



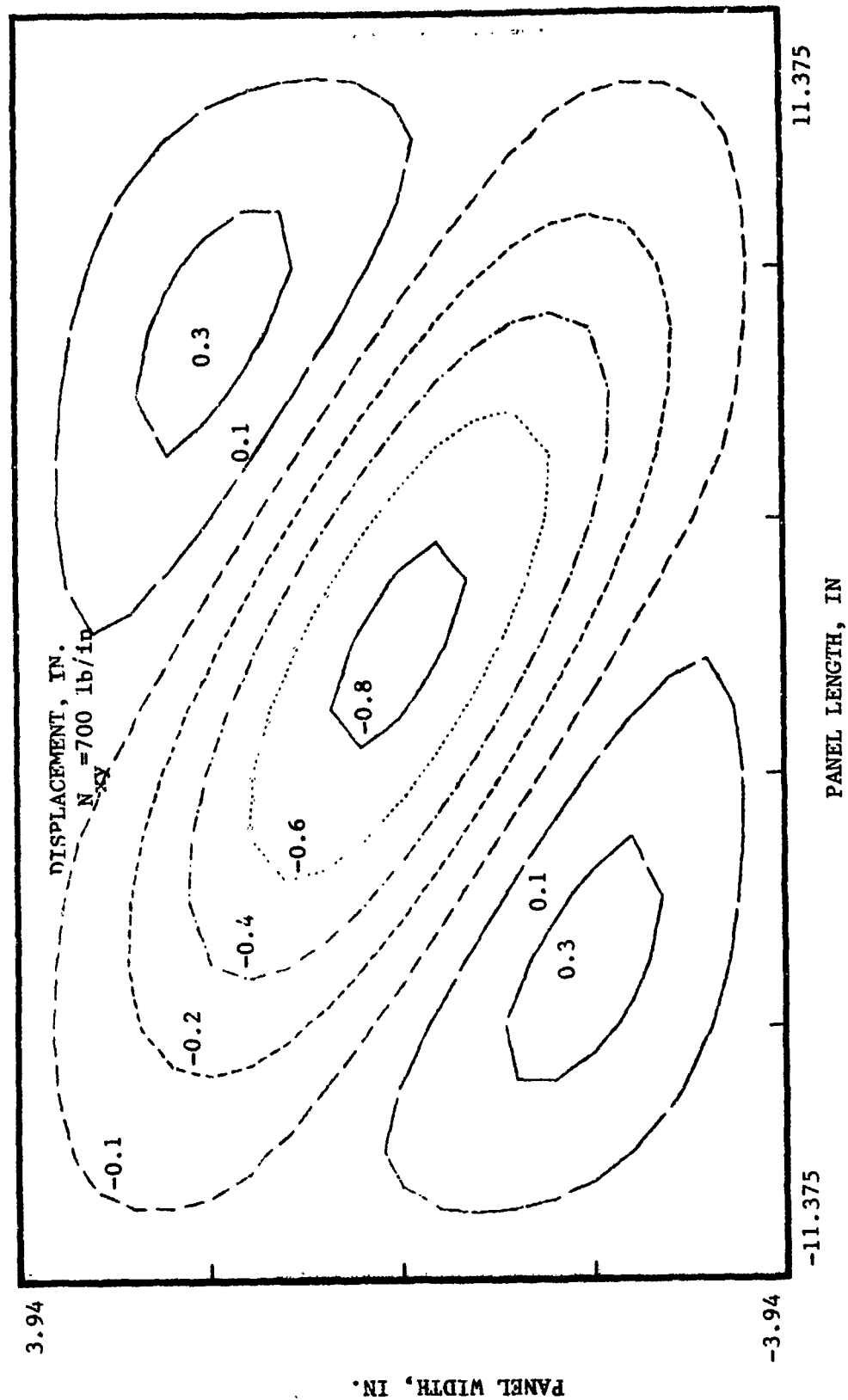


Figure 4.10. Out-of-Plane Displacement Contours for Metal Shear Panel  
 SHRPAM1 Predictions

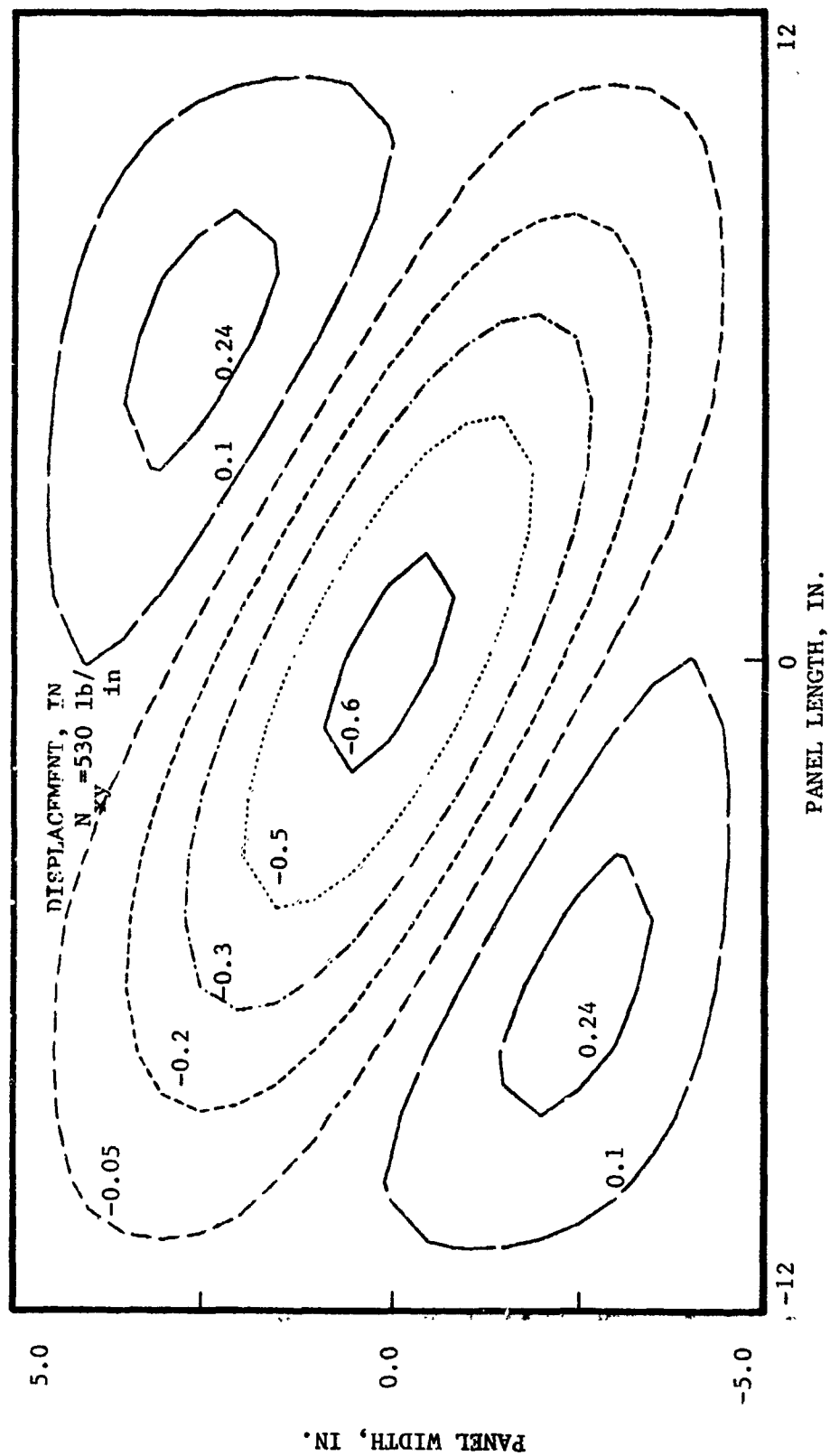


Figure 4.11. Out-of-Plane Displacement Contours for Composite Shear Panel  
SHRPANI Predictions

#### 4.4.1 Metal Panels

The fatigue life prediction methodology for metal panels loaded in compression or shear is summarized in Figure 4.12. The observed failure modes for metal compression panels are cracks in the skin parallel to the stringers, but away from fastener holes, or cracks in the stringer or skin itself at fastener holes (see Figure 2.2). In the case of metal shear panels, the dominant cracks are those that initiate in the skin at stiffener to skin attach fastener holes and propagate transverse to the diagonal tension direction. For fatigue failures initiating at fastener holes, the analysis approach is the same for shear and compression panels with the fatigue life being governed by crack growth at the fastener holes. In the case of skin cracks parallel to the stringers and away from fastener holes, the analysis approach, is somewhat different and the fatigue life is governed by crack initiation and growth in the skin.

As shown in Figure 4.12, a durability rather than a damage tolerance approach is adopted in the analysis of fatigue failures initiating at fastener holes. An initial 0.01-inch corner flaw is assumed to exist at the hole. The stress intensity factors for this initial flaw are computed using available analysis methods. Flaw growth in shear panels occurs due to diagonal tension stresses and, therefore, the principal tensile stress in the skin is used for computing the stress intensity factor. In compression panels transverse tensile stresses are caused at the apex of the fastener hole by the remotely applied compression stress and are equal to it in magnitude. This stress is used in computing the stress intensity factor for the initial flaw.

Once the stress intensity factors have been determined, the Forman crack growth equation (Reference 95) can be used to determine the crack growth life for the metal panels.

In the case of skin cracks parallel to the stringers, the local skin stresses have to be computed using the nonempirical analysis described in the preceding paragraphs. The fatigue life is estimated as the sum of crack initiation life and the crack growth life. The crack initiation life (to 0.01") can be predicted using the cumulative damage analysis of

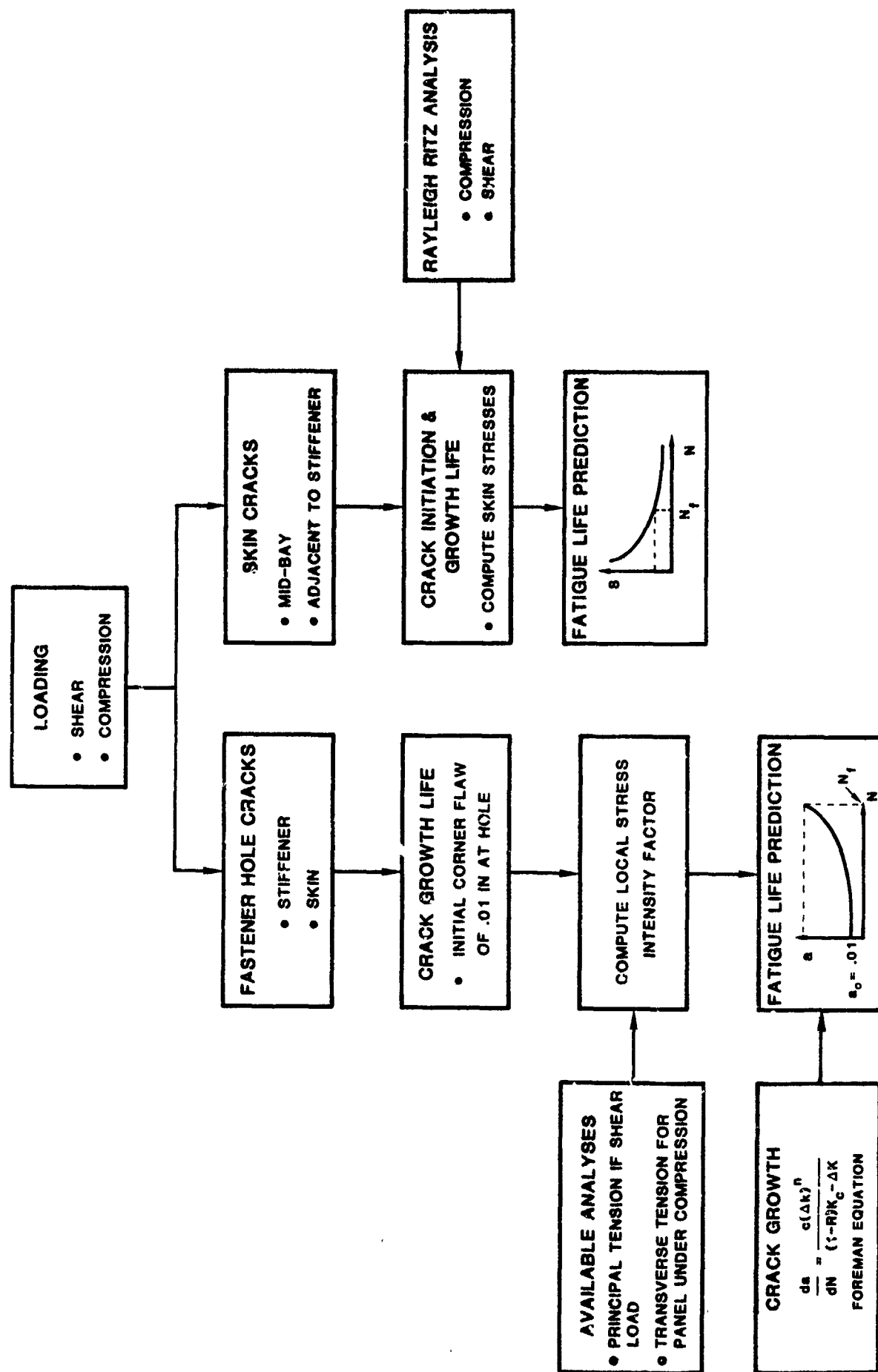


Figure 4.12. Life Prediction Methodology for Postbuckled Metal Panels

Reference 96. Crack growth life can be predicted using the Forman equation (Reference 95). A bending correction may have to be used to obtain the effective stress intensity factor.

#### 4.4.2 Composite Panels

The predictive methodology for composite panels is more complex due to the lack of a static analysis method that can predict the stresses at the stiffener/skin interface. The life prediction approach for composite panels shown in Figure 4.13 addresses the stiffener/web separation mode of failure observed in panel fatigue failures by way of the nonempirical static analysis developed in this program and simple beam model of the stiffener/web attach area.

The approach shown in Figure 4.13 applies to both shear and compression panels and is based on computing the strain energy release rate at the stiffener/web interface. In this approach the nonempirical analysis is used to determine the maximum skin deflection in the postbuckling regime due to fatigue. This maximum deflection is then applied to the beam model shown which represents a strip between the stiffener and the center of the skin. An initial delamination of length  $b_0$  is assumed to exist at the interface of the doubler and the skin laminate in the beam model. The applied maximum displacement is then used to compute the strain energy release rate at the top of the initial delamination. This strain energy release rate  $G$  is the driving force for delamination growth and can be used to predict delamination growth under static as well as fatigue loading. Fatigue life prediction is accomplished by using the nonlinear growth law.

$$\frac{db}{dN} = C(\Delta G - \Delta G_{th})^n$$

where,  $C$ ,  $n$  and  $\Delta G_{th}$  are constants determined from fatigue tests on simple specimens as shown in the box on the extreme right hand side of Figure 4.13. Static failure prediction requires a knowledge of the critical strain energy release rate  $G_c$  which can be determined from static tests on specimens identical to the fatigue test specimens.

The essential requirements for this life prediction approach are the development of an analysis for the beam model and the appropriate fracture properties. These developments are needed to establish a fatigue life prediction methodology for postbuckled composite panels.

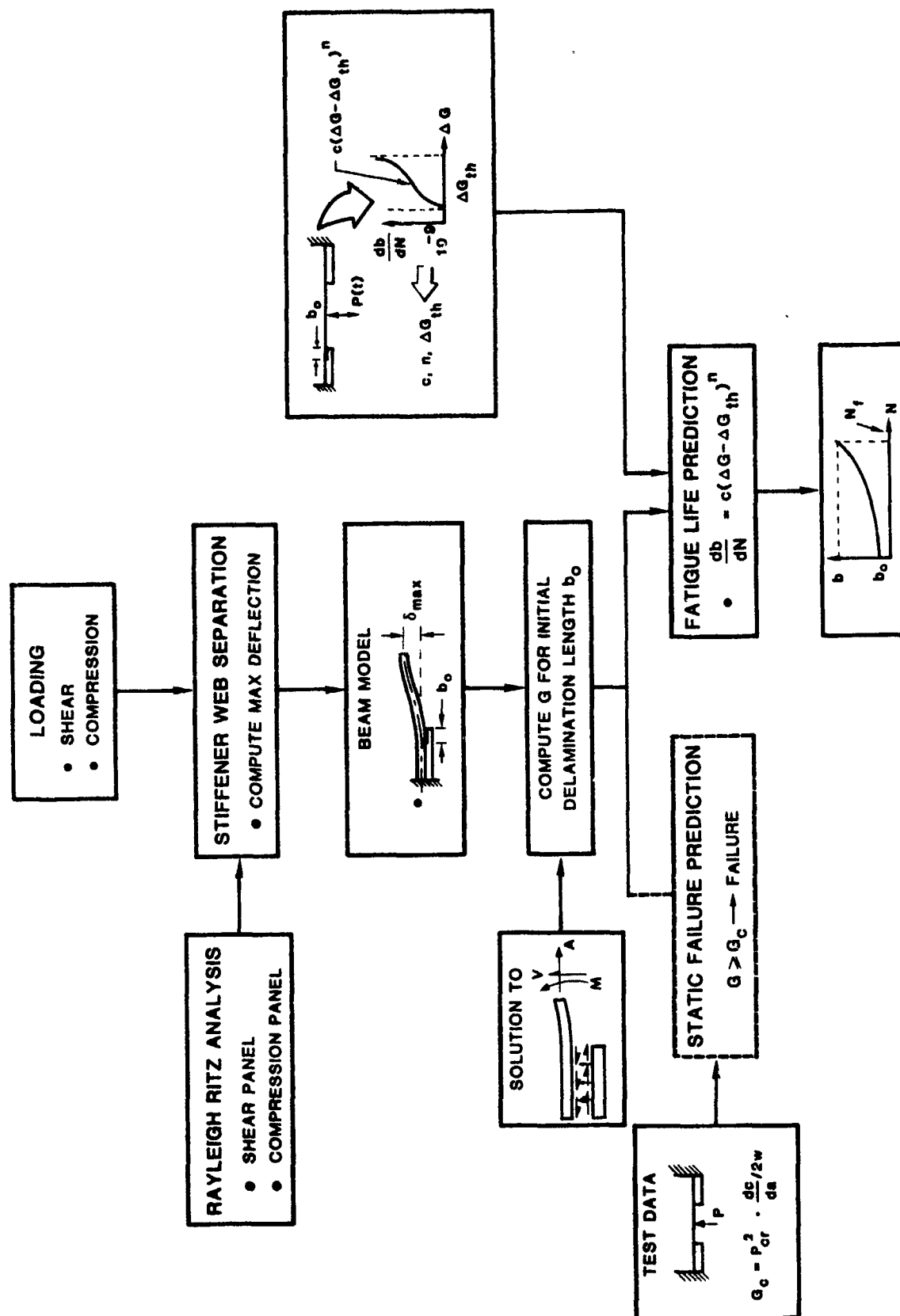


Figure 4.13 Life Prediction Methodology for Postbuckled Composite Panels

## SECTION 5

### DISCUSSION OF RESULTS

#### 5.1 INTRODUCTION

The static and fatigue test data presented in Section 3 and Appendix B were analyzed to correlate the measured initial buckling and ultimate strength, and strain values with predictions. The static test data were also used to determine panel stiffness change due to postbuckling. The fatigue life data were utilized to establish S-N curves for metal and composite panels. These results are discussed in the following paragraphs.

#### 5.2 CURVED PANELS UNDER STATIC COMPRESSION LOAD

Metal compression panel static test results and their correlation with the semiempirical analysis given in Section 2 are summarized in Table 5.1. In this table, the skin buckling data obtained from the fatigue test specimens are pooled together with the static test data. As can be seen from Table 5.1 the local skin buckling predictions which were based on the use of the empirical correction factor  $K_c$  in the expression

$$F_{cr} = \frac{K_c \pi^2 E}{12(1-\nu^2)} \left( \frac{t_w}{b_w} \right)^2$$

with  $K_c$  determined from Figure 2.6, are quite conservative. The modified values of  $K_c$  account for the imperfection sensitivity of curved panels. A reexamination of the equivalent  $K_c$  for the data in Table 5.1 showed that the present data are much closer to predictions based on the theoretical  $K_c$  value of 30. Thus, the theoretical curve shown in Figure 2.6 is reasonably accurate for use in predicting the local skin buckling loads and strains. The comparison of the theoretical and the semiempirical predictions is shown in Figure 5.1. The semiempirical predictions take into account the influence of  $r/t$  ratio on the buckling load. Metal panel failure under static load occurred primarily due to stiffener crippling and as a consequence the failure data shown in Figure 5.1 agree very well with predictions which were based on the calculated stiffener crippling loads.

TABLE 5.1. CURVED METAL COMPRESSION PANEL STATIC DATA\*

Specimen Number	P <sub>cr</sub> , Kips	F <sub>cr</sub> , Ksi	F <sub>xcr</sub> , lbs/in	ε <sub>cr</sub> (Avg), μin/in	ε <sub>cr</sub> /ε <sub>ct</sub> <sup>0</sup>	P <sub>cr</sub> /P <sub>cr</sub> <sup>0</sup>	Equivalent K <sub>c</sub>	P <sub>cs</sub> , Kips	F <sub>cs</sub> , Ksi	N <sub>x</sub> , lbs/in	ε <sub>cs</sub> , μin/in	P <sub>cs</sub> /P <sub>cs</sub> <sup>0</sup>	ε <sub>cs</sub> /ε <sub>cs</sub> <sup>0</sup>
MC1	12.0	6.59	432.0	548.3	1.86	2.10	27.3	42.0	50.1	1078.2	3104	1.03	0.67
MC2	14.0	7.69	503.8	637.0	2.17	2.45	31.8	43.6	52.0	1118.3	3859	1.06	0.84
MC3 <sup>+</sup>	10.0	5.49	359.8	624.0	2.12	1.75	22.7	---	---	---	---	---	---
MC4 <sup>+</sup>	12.0	6.59	431.6	614.0	2.09	2.10	27.3	---	---	---	---	---	---
IC1 <sup>+</sup>	13.0	7.14	467.7	---	---	2.27	29.5	---	---	---	---	---	---

\* For nomenclature used see Secn. 2.

+ These panels were fatigue tested. However, their skin buckling data were obtained in a static strain survey prior to the fatigue test.

1) Superscript '0' denotes predicted values. P<sub>cr</sub><sup>0</sup> = 5.72 kips, P<sub>cs</sub><sup>0</sup> = 40.95 kips

2) K<sub>c</sub> is the empirical constant used in  $F_{cr} = \frac{K_c \pi^2 E}{12(1-\nu^2)} \frac{tw}{bw}$  and is given in Reference 3, Figure C9.1 for various panel radius to skin thickness ratios,  $\frac{r}{t}$ .

3) ε<sub>cr</sub> denotes average skin strain measured in the center bay.

4) ε<sub>cs</sub> denotes average stiffener strain obtained from the four stiffener strain gages.

5) This panel was tested under Northrop IRAD program.



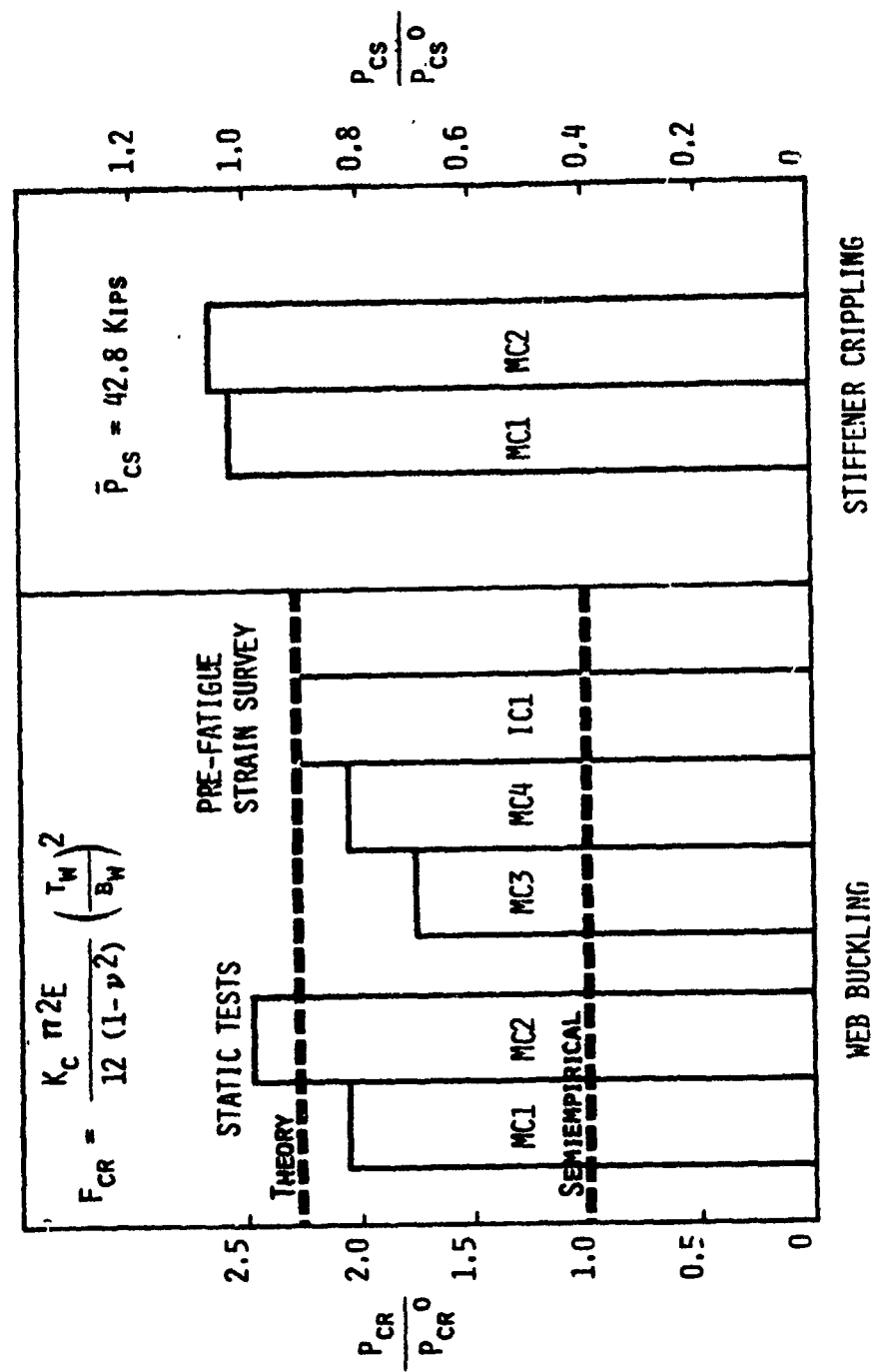


Figure 5.1. Comparison of Metal Compression Panel Test Data with Predictions

The skin buckling loads were determined using mid-bay back-to-back strain gage data. Figure 5.2 shows the typical response of these back-to-back strain gages. These gages were located at the panel centroid and illustrate that there was a change in the buckle wave length at approximately 30 kips. This wave length change in the postbuckled regime is also corroborated by the out-of-plane displacement data shown in Figure 5.3. The actual variation in the number of skin buckles indicated by the strain and displacement data depends on the location of these gages and, therefore, measurement at a single location is not sufficient to fully describe the buckle pattern progression with load. For instance, the displacement plot for  $\delta_3$  in Figure 5.3 shows that the buckle pattern changed thrice prior to attaining the final configuration shown in Figure 3.23e. In Figure 5.3 the out-of-plane displacements predicted using program COMPAN are also shown for comparison. The displacement corresponding to  $\delta_1$  in the figure is in reasonable agreement with the test data in the low postbuckling range. However, with increasing load the test data indicate changes in buckle mode shapes which are not accounted for in the analysis. Thus, the discrepancy between test data and predictions is significant. For displacements at  $\delta_2$  and  $\delta_3$  which were symmetrically located with respect to panel centerline, the disparity in the test data and predictions is significant. In addition to changes in the buckle mode shapes, another reason for this discrepancy could be the extreme sensitivity of the out-of-plane displacements to variations in the location of measurement on the panel. From these comparisons it is apparent that the compression panel analysis for metal panels needs additional refinement.

The axial strain in the stiffeners was approximately bilinear up to failure with a distinct change in the slope after skin buckling. Axial strain variation with applied load for the four stringers of metal panel MC1 is shown in Figure 5.4. The average of the four stringer strains was used in determining the panel gross stiffness change due to skin buckling. Panel MC1 showed a postbuckled stiffness that was 64 percent of the prebuckling stiffness, whereas, for panel MC2 this number was 56 percent.

Correlation of buckling and failure strain data for composite compression panels with theoretical and semiempirical predictions is shown in

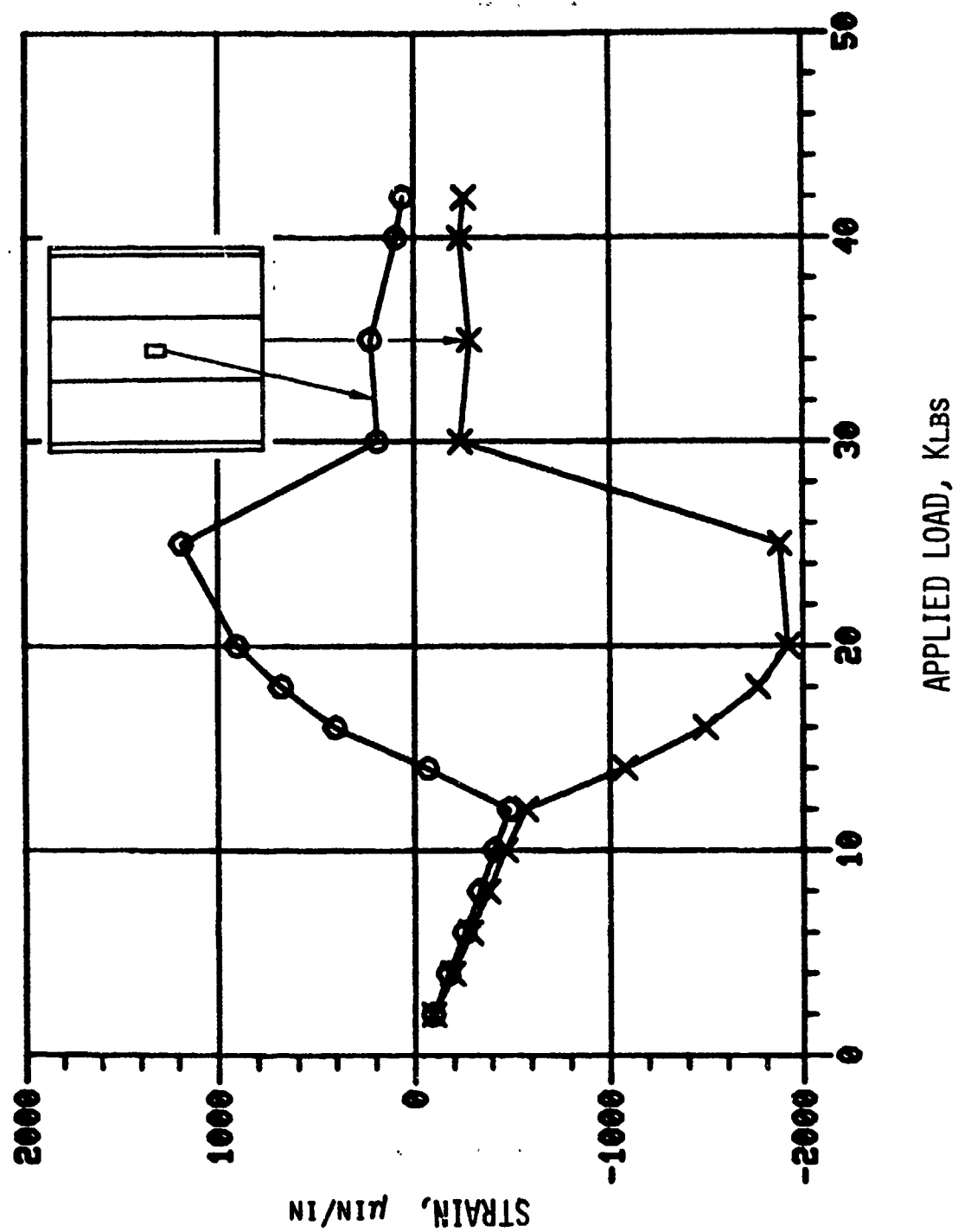


Figure 5.2. Metal Compression Panel Web Static Strain Response

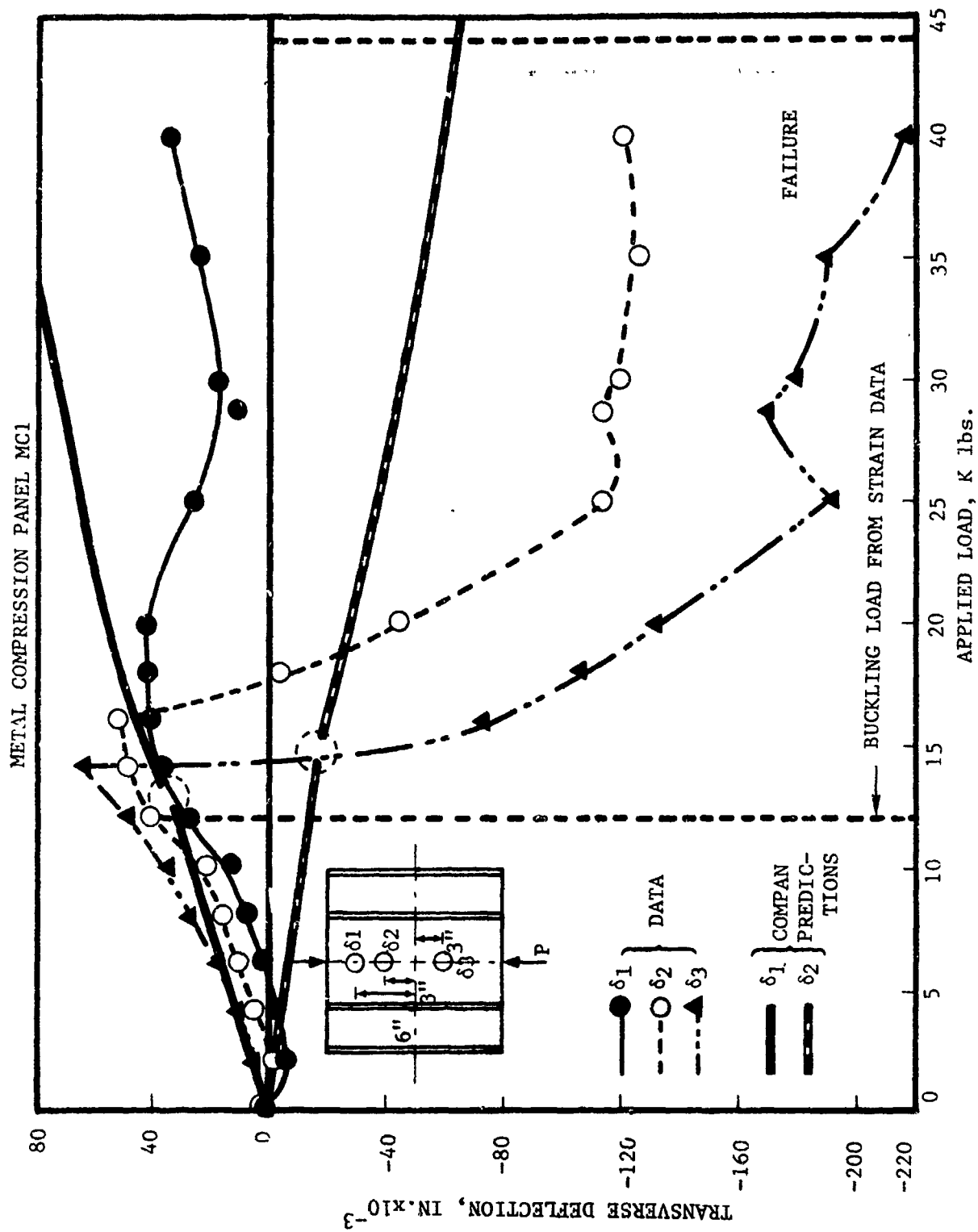


Figure 5.3. Out-of-Plane Displacements for Metal Compression Panels

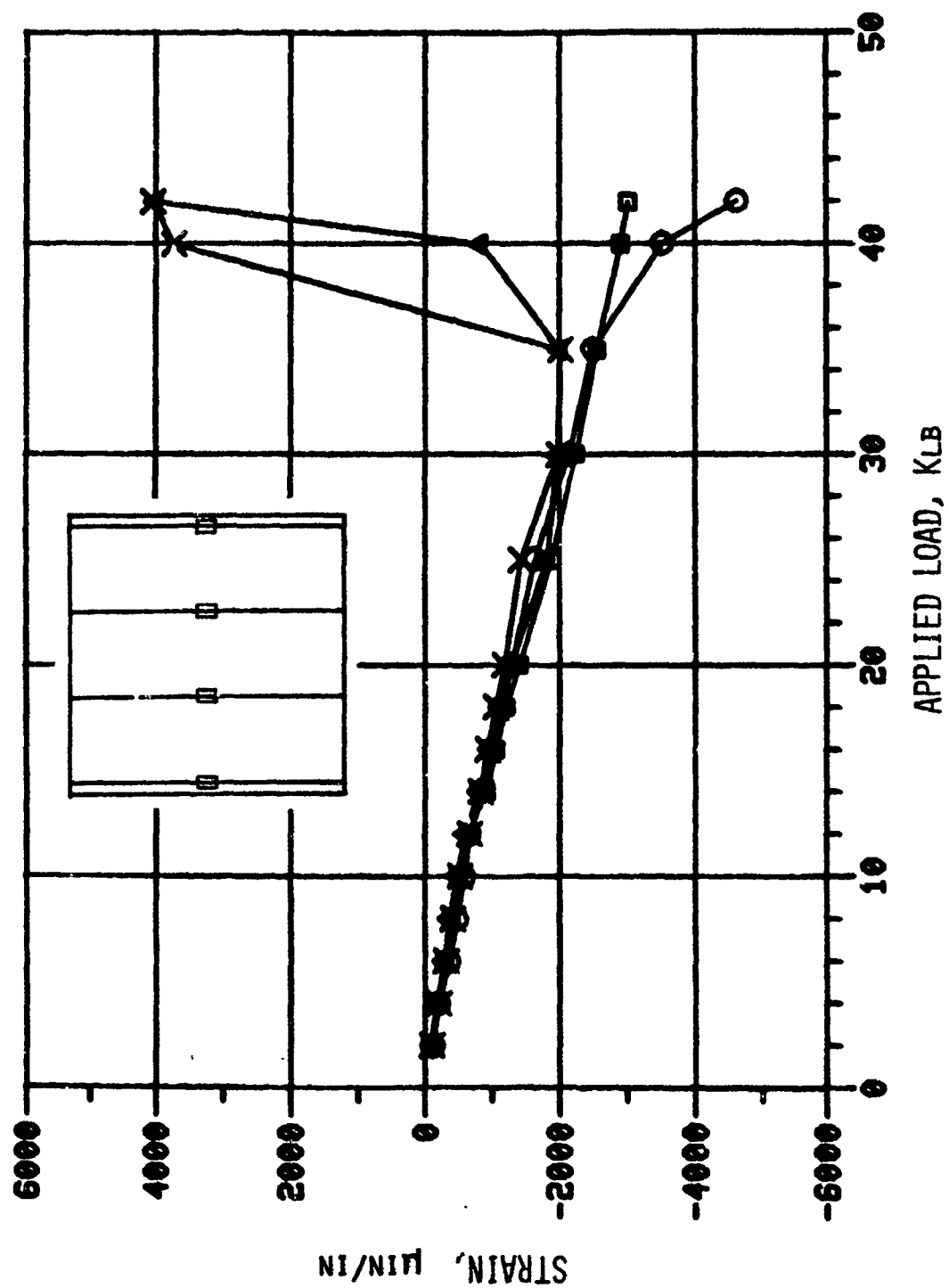


Figure 5.4. Stiffener Axial Strains for Metal Compression Panels

Table 5.2 and Figure 5.5. The measured web buckling strains are considerably lower than the predicted values. This, however, was not surprising since the effective width of the web was not known a priori and was assumed as the distance between the adjacent stiffener flanges as shown by "CURRENT" in Figure 5.5. The test data indicate that this assumption is unconservative. An effective width equal to the distance between the centers of adjacent stiffener flanges, indicated by "PROPOSED" in Figure 5.5, yields excellent correlation between the predictions and the test data.

Composite compression panel strength measurements closely agree with semiempirical predictions based on the stiffener crippling mode of failure. Thus, the stiffener/web separation mode of failure seen in the static tests is induced by stiffener crippling.

Figure 5.6 shows the back-to-back mid-bay strain gage response for composite panel CCl and is typical of that observed for the other five panels. The buckle pattern changes shown are significant from the point of view of developing a nonempirical analysis. The regions where the buckle pattern changes are apt to cause numerical difficulties in predicting the postbuckled response and the nonlinear analysis may have to be performed piecewise with the regions selected so that no change occurs in the buckle pattern. The out-of-plane displacement data for composite panel CCl are shown in Figure 5.7. These data corroborate the buckle pattern progression indicated by the strain gages. For comparison, the predicted values of out-of-plane displacements are also shown in Figure 5.7. The trends in the predicted displacements at  $\delta_2$  and  $\delta_3$  match the test data. However, numerically there is a significant amount of discrepancy.

The stiffener axial strain response for composite panel CCl is shown in Figure 5.8 and is representative of that seen for the remaining composite compression panels. In Figure 5.8, COMPAN predictions of stringer strains are also shown. As opposed to the skin displacements the stringer strain variation with applied loads is reasonably well matched. The strain values predicted, however, are considerably higher than the test data. The stiffener strain data were used to determine the panel stiffness changes due to buckling shown

TABLE 5.2. COMPOSITE COMPRESSION PANEL STATIC TEST DATA CORRELATION WITH PREDICTIONS

PANEL NO.	BUCKLING LOAD $P_{cr}$ kips	BUCKLING STRAIN $\epsilon_{cr}$ , $\mu\text{in}/\text{in}$	$\epsilon_{cr}/\epsilon_{cr}^0$ *	$P_{cs}$ , * kips	$\epsilon_{cs}$ $\mu\text{in}/\text{in}$	$\epsilon_{cs}/\epsilon_{cs}^0$	$\epsilon_{cs}/\epsilon_{ss}^0$	POSTBUCKLING STIFFNESS, % INITIAL STIFFNESS
CC1	18.0	862	0.75	84.6	5281	1.07	1.61	62
CC2	16.0	756	0.66	82.0	5291	1.07	1.62	64
CC3**	14.0	543	0.47	----	----	----	----	
CC4	12.0	603	0.52	----	----	----	----	
CC5	12.0	638	0.55	----	----	----	----	
CC6	16.0	815	0.71	----	----	----	----	

NOTES:

- \*  $\epsilon_{cr}^0$  = 1153  $\mu\text{in}/\text{in}$  - Predicted skin buckling strain.  
 $\epsilon_{cu}$  = 15000  $\mu\text{in}/\text{in}$  - Compression ultimate strain for skin laminate.  
 $P_{cs}$  = Panel failure load.  
 $\epsilon_{cs}$  = Average stiffener strain at panel failure.  
 $\epsilon_{cs}^0$  = 4956  $\mu\text{in}/\text{in}$  - Predicted stiffener crippling strain.  
 $\epsilon_{ss}^0$  = 3276  $\mu\text{in}/\text{in}$  - Predicted stiffener/web separation strain.

\*\* Panels CC3 through CC6 were fatigue test specimens

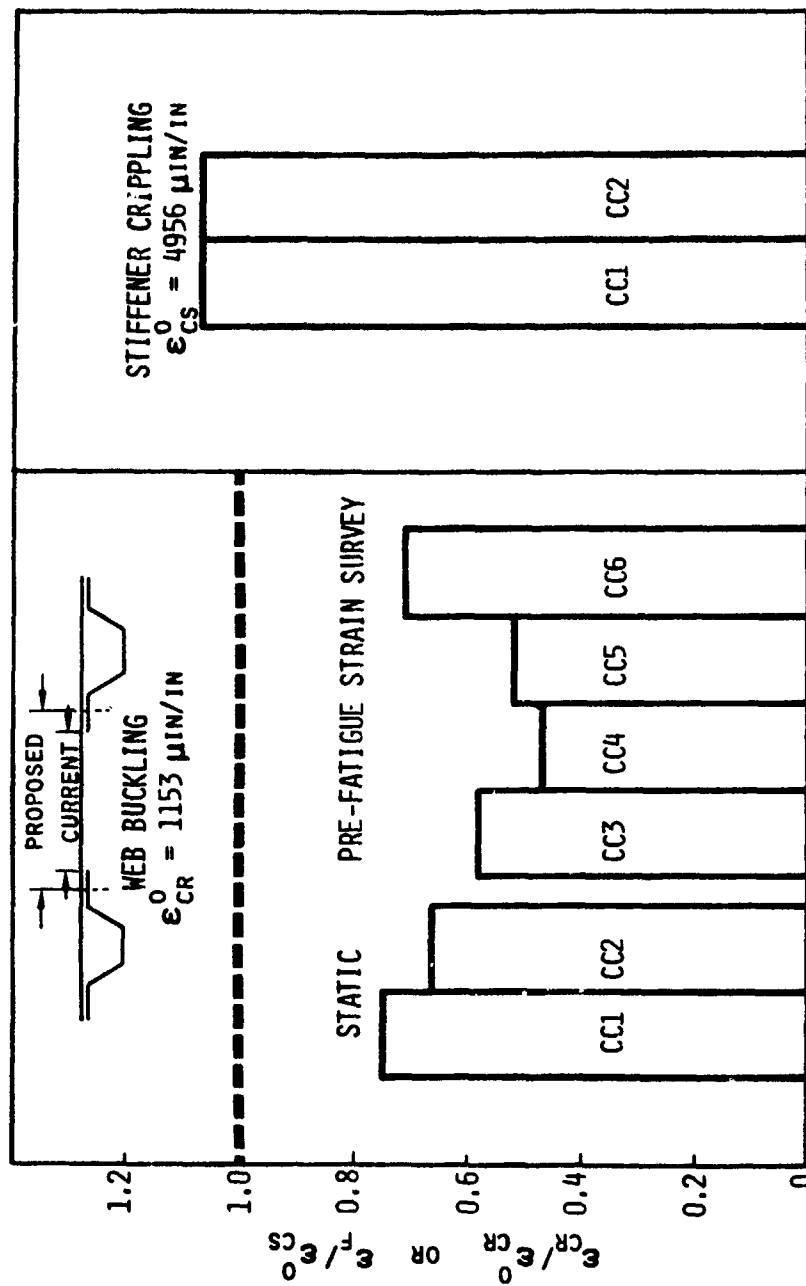


Figure 5.5. Comparison of Composite Compression Panel Test Data with Predictions



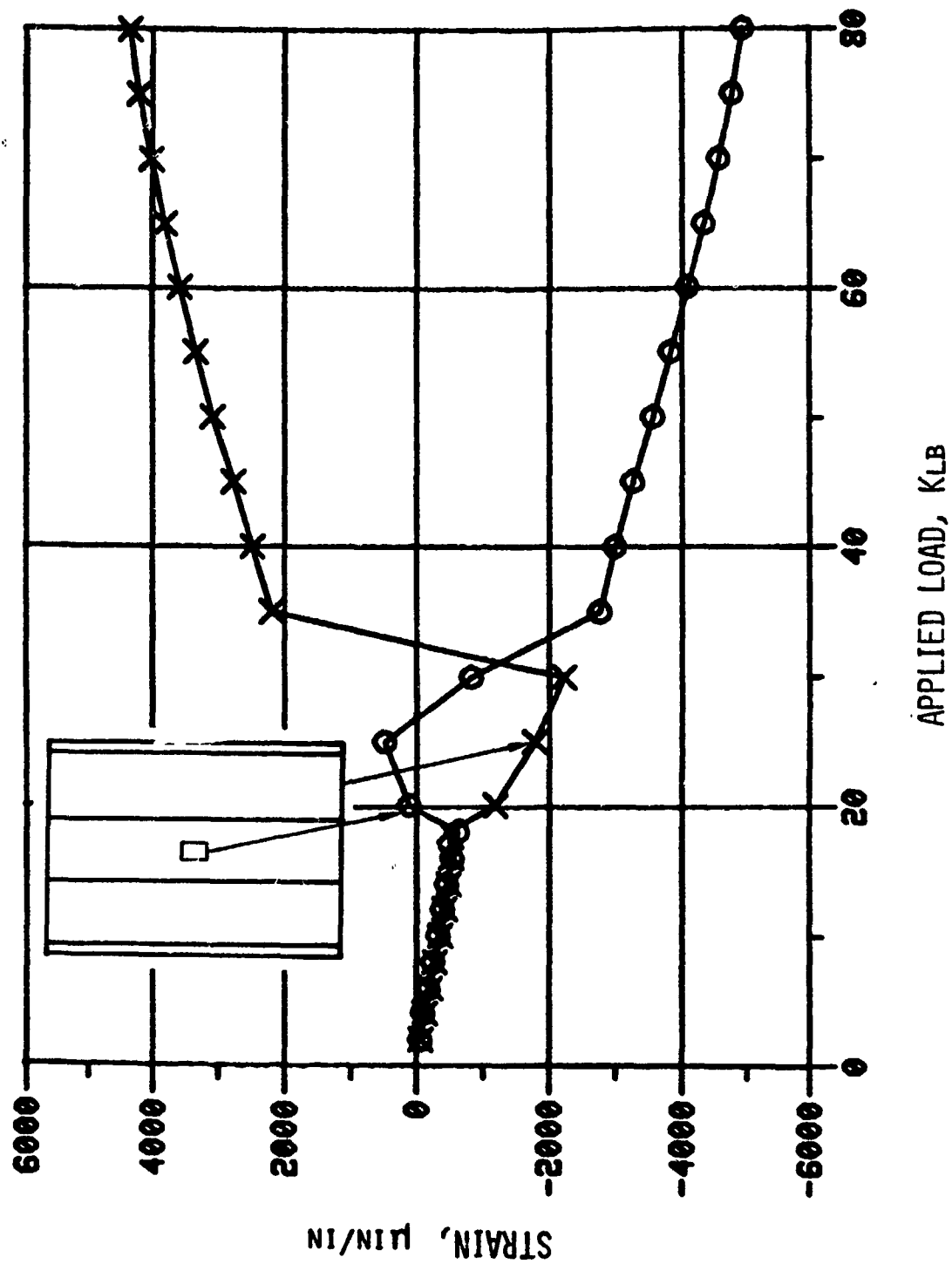


Figure 5.6. Composite Compression Panel CCl Web Strain Response

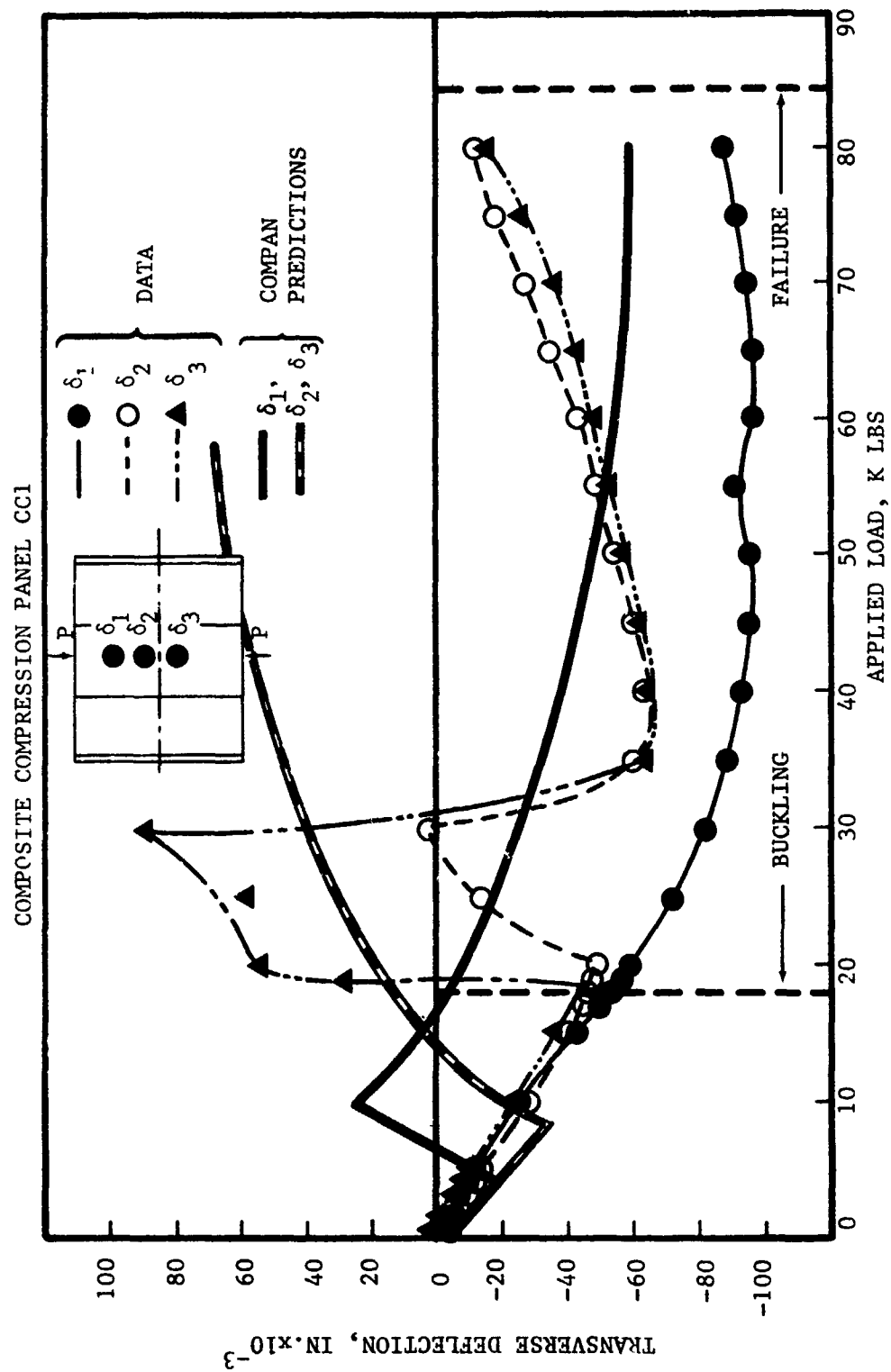


Figure 5.7. Out-of-Plane Displacements for Composite Compression Panel CCl

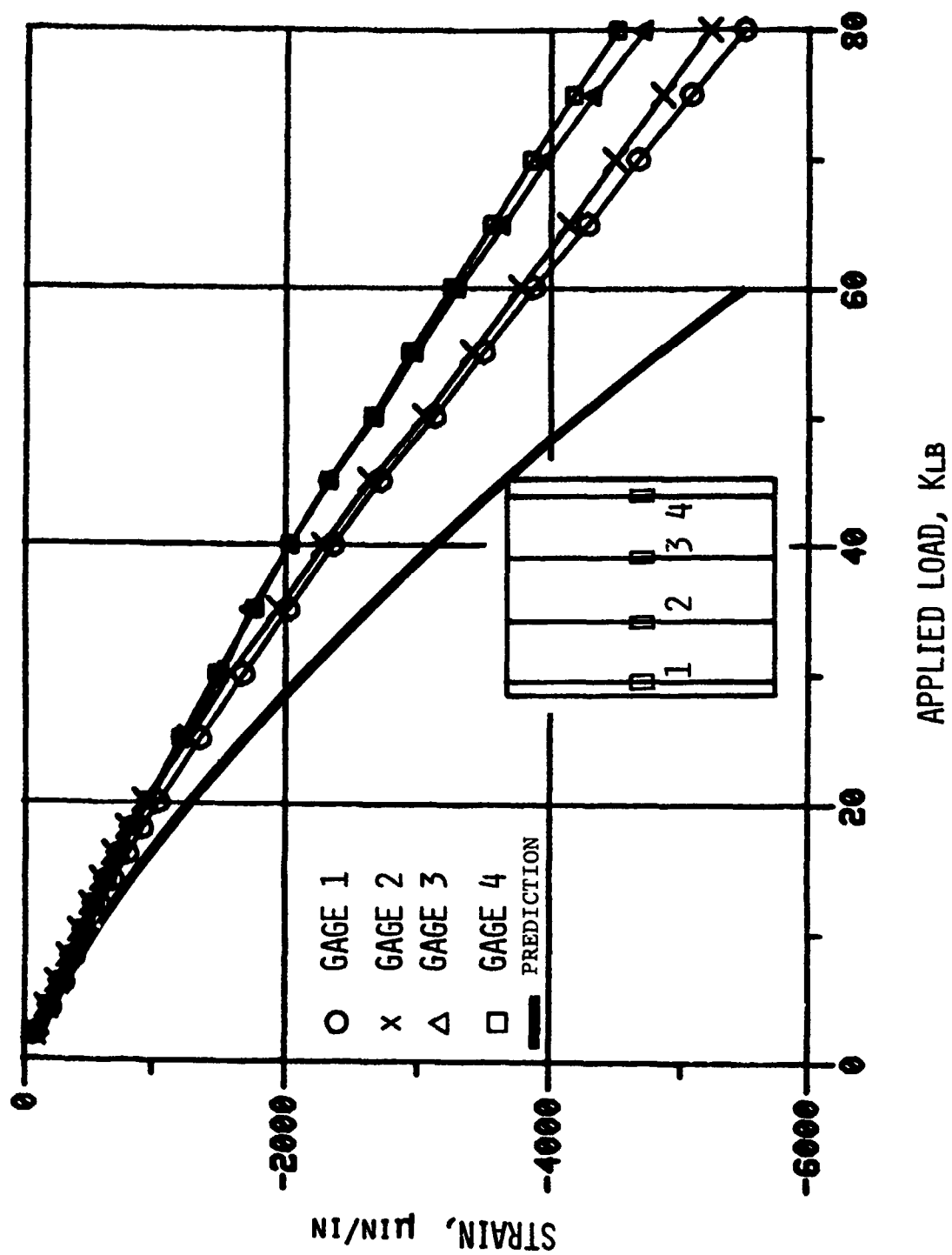


Figure 5.8. Stiffener Axial Strains for Composite Panel CCl

in Table 5.2. The reduction in stiffness after buckling for composite panels is similar to that for metal panels and is approximately 40 percent.

### 5.3 CURVED PANELS UNDER COMPRESSION FATIGUE LOADING

The fatigue data for metal and composite compression panels are shown in the S-N diagram of Figure 5.9. The curves were faired to represent the data trend and due to the limited number of data points a definitive threshold for 100,000 cycles of constant amplitude fatigue cannot be established. The data for composite compression panels, however, are consistent with those obtained from other tests and summarized in Figure 2.4. Therefore, composite compression panel fatigue does not appear to be a concern in the 2500-3500  $\mu\text{in/in}$  operating strain level typically seen in postbuckled structures.

The metal panel fatigue tests were useful in identifying the failure mode that needs to be accounted for in developing a fatigue life prediction methodology (see Section 4.4). The fatigue data also show that the metal panels are quite sensitive to fatigue and, as illustrated in Figure 5.10, are inferior to composite panels designed to the same loading conditions. Additional metal panel tests, however, should be conducted to accurately define their S-N response.

The periodic strain surveys conducted during the fatigue tests were used to determine if repeated buckling of the panels influenced the initial buckling load or panel stiffness. The data showed that repeated loading did not influence the initial buckling load or the panel stiffness.

### 5.4 CURVED PANELS UNDER SHEAR LOADING

The metal shear panel test data analysis is summarized in Table 5.3. Comparison of the data with predictions is shown in Figure 5.11. The predictions were based on Figure 3.5 (Reference 34) assuming the skin width  $b_w$  equal to the stiffener pitch. The data show that with this definition of the skin width, the buckling load predictions are reasonable estimates considering the scatter in the initial buckling loads, and the semiempirical approach of Reference 34 can be readily used for design purposes. The failure load predicted for metal shear panels ( $N_{xy}^{\text{ult}} = 900 \text{ lbs/in}$ ) was based on the

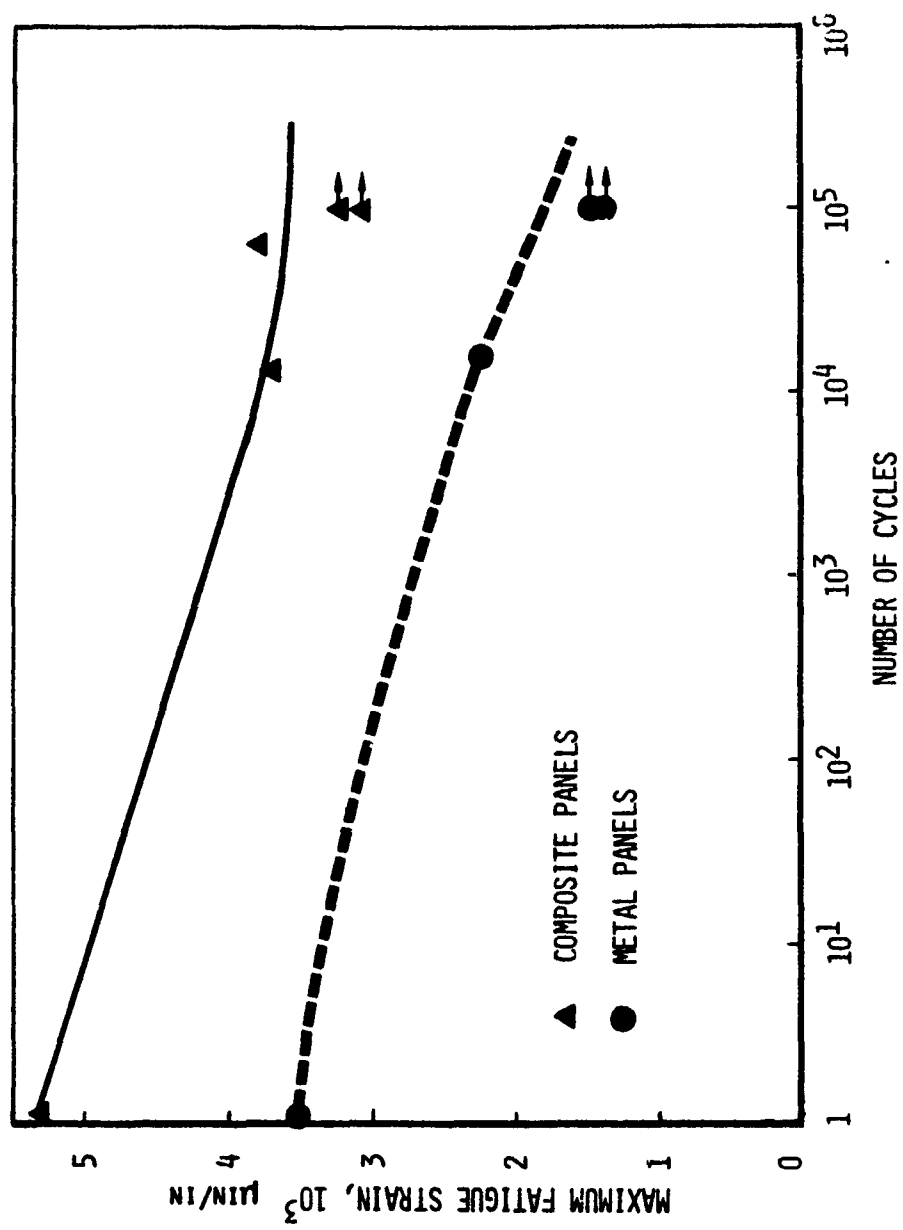


Figure 5.9. Comparison of S-N Data for Metal and Composite Compression Panels

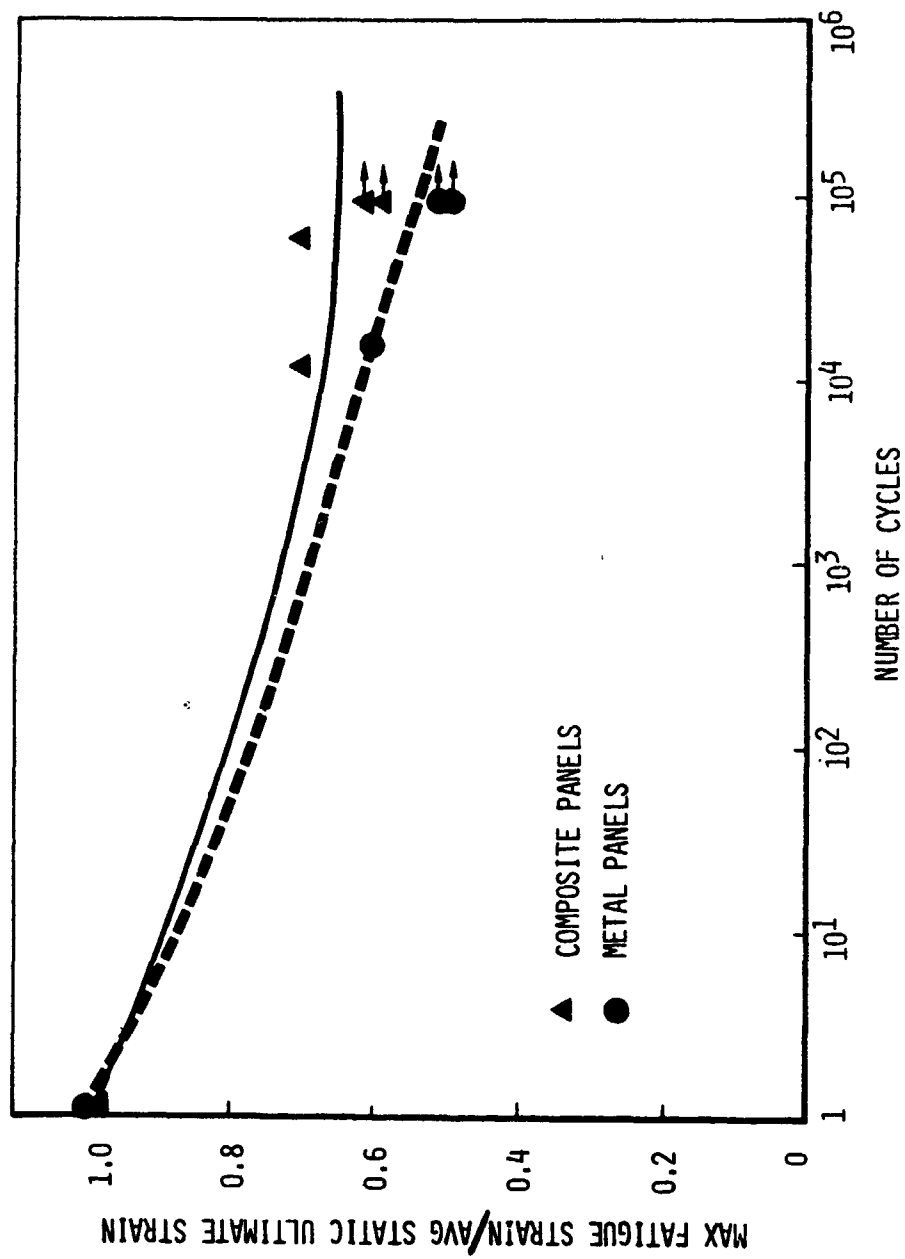


Figure 5.10. Normalized Fatigue Response of Compression Panels

TABLE 5.3. METAL SHEAR PANEL STATIC TEST DATA CORRELATION WITH PREDICTIONS

PANEL NO.	LOAD CELL READING AT BUCKLING, LB	WEB BUCKLING SHEAR STRAIN $\gamma_{xy}^{cr} + \mu_{in/in}$	$N_{xy}^{cr*} = G\tau_{xy}^{cr}$ lbs/in	$\frac{(N_{xy}^{cr})}{(N_{xy}^{cr})_0}$	$\gamma_{xy}^{ult}$ $\mu_{in/in}$	$N_{xy}^{ult} = G\tau_{xy}^{ult}$ lb/in	$\frac{N_{xy}^{ult}}{(N_{xy}^{ult})_0}$	DIAGONAL TENSION ANGLE	POSTBUCKLING STIFFNESS, % INITIAL STIFFNESS
MS1	3820	963	242	0.83	4800	1210	1.34	28°	83
MS2	4123	1118	282	0.97	4200	1058	1.18	26°	89.5
MS3**	4453	1341	338	1.17	---	---	---	---	---
MS4	3848	1298	327	1.13	---	---	---	---	---
MS5	2895	1007	254	0.88	---	---	---	---	---
MS6	3811	1414	356	1.23	---	---	---	---	---

\*  $G = 4 \times 10^6$  psi

\*\* Panels MS3 through MS6 were fatigue test panels

+ Lowest buckling shear strain as measured from Gages 2 and 5 in Figure 3.13

++ Quantities with subscript '0' denote predicted values

$$(N_{xy}^{cr})_0 = 290 \text{ lbs/in (From Figure 3.5)}$$

$$(N_{xy}^{ult})_0 = 900 \text{ lbs/in}$$

§ Predictions based on stiffener forced crippling mode of failure

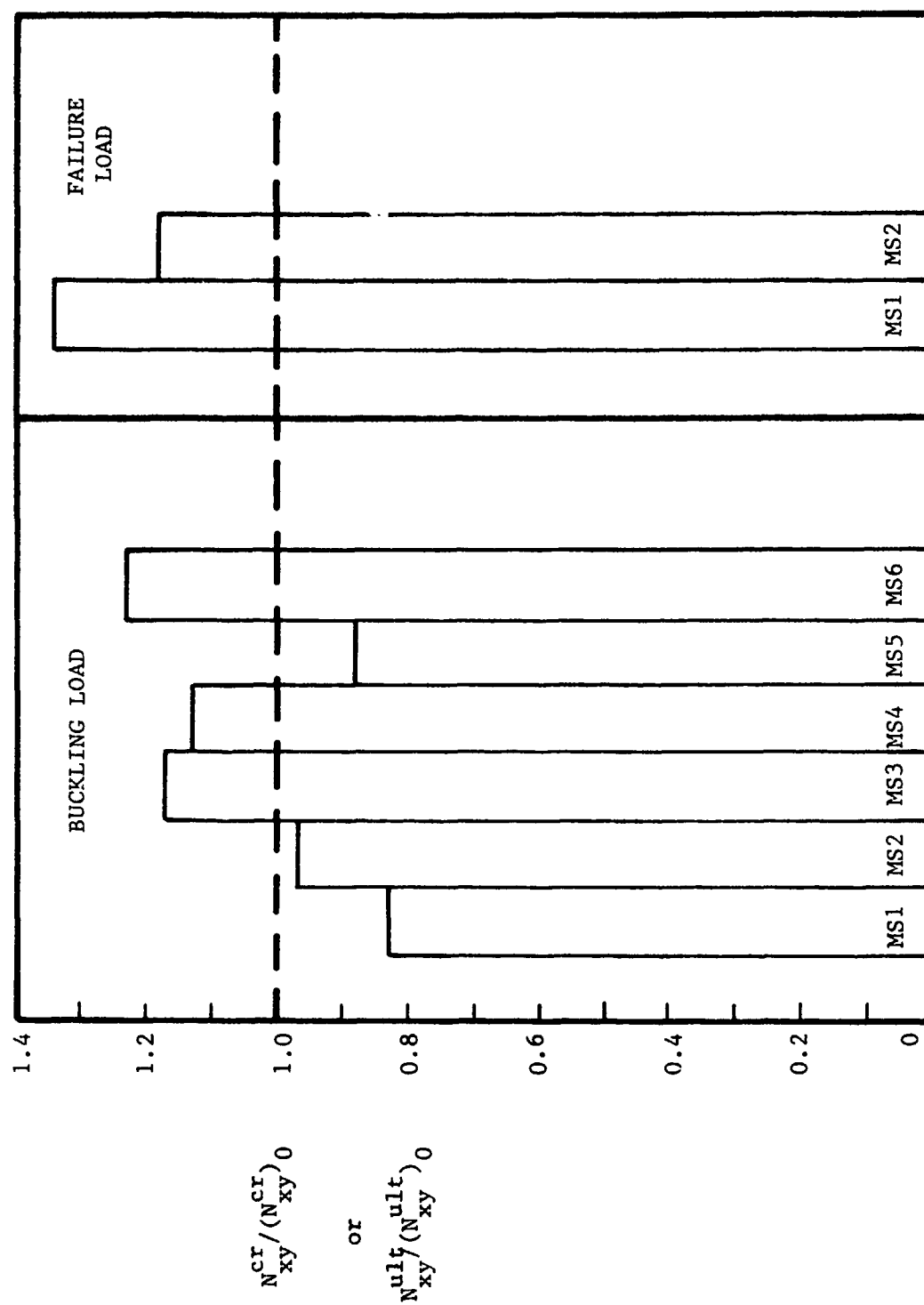


Figure 5.11. Comparison of Metal Shear Panel Static Test Data With Predictions.



stringer forced crippling mode of failure. The ultimate shear flow calculated for shear panels MS1 and MS2 using web-maximum shear strain data at failure, compares well with these predictions. A comparison of the measured stringer axial strains with that predicted for stringer forced crippling, however, shows that the measured strains are considerably less than the predicted crippling values. The actual failure of the metal shear panels was by permanent set in the skin. This was confirmed by an examination of the measured principal strains (Gage 5 in Figure 3.13) in the skin which showed that the 6500  $\mu\text{in/in}$  yield strain for 7075-T6 aluminum had been exceeded. Thus, it is not surprising that the measured stringer axial strains did not exceed the predictions for forced crippling.

In order to verify if permanent set can be predicted using the flat metal panel criterion, the allowable diagonal tension factor for the present panels was calculated with the aid of Equation 31. The maximum value of  $k$  was calculated to be 0.554 which translated into an ultimate load to initial buckling load ratio of 2.2. However, the data show that for these panels, the ratio is of the order of 4. Thus, the flat metal panel permanent set criterion is very conservative for curved panels. A criterion needs to be developed for curved panels by additional testing.

The web shear strain variation with applied load is shown in Figure 5.12. These data were used to compute the change in panel stiffness after buckling. As shown in Table 5.3, the metal panels retain a large percentage of their initial stiffness in the postbuckling range. The maximum reduction in stiffness was approximately 17 percent. The stringer and ring axial strain variations with applied load are shown in Figures 5.13 and 5.14. For comparison, predictions from SHRPAN1 are also shown. The reasons for the large discrepancies are explained in Section 5.6. The measured diagonal tension angle was approximately  $27^\circ$  and is less than that predicted by tension field theory but is larger than the  $20^\circ$  angle predicted by SHRPAN1. A plot of the diagonal tension angle, calculated using the mid-bay strain rosettes (Gages 2 and 5), versus the applied cylinder load is shown in Figure 5.15, along with the predictions from SHRPAN1. The predicted values agree reasonably well with the test data.

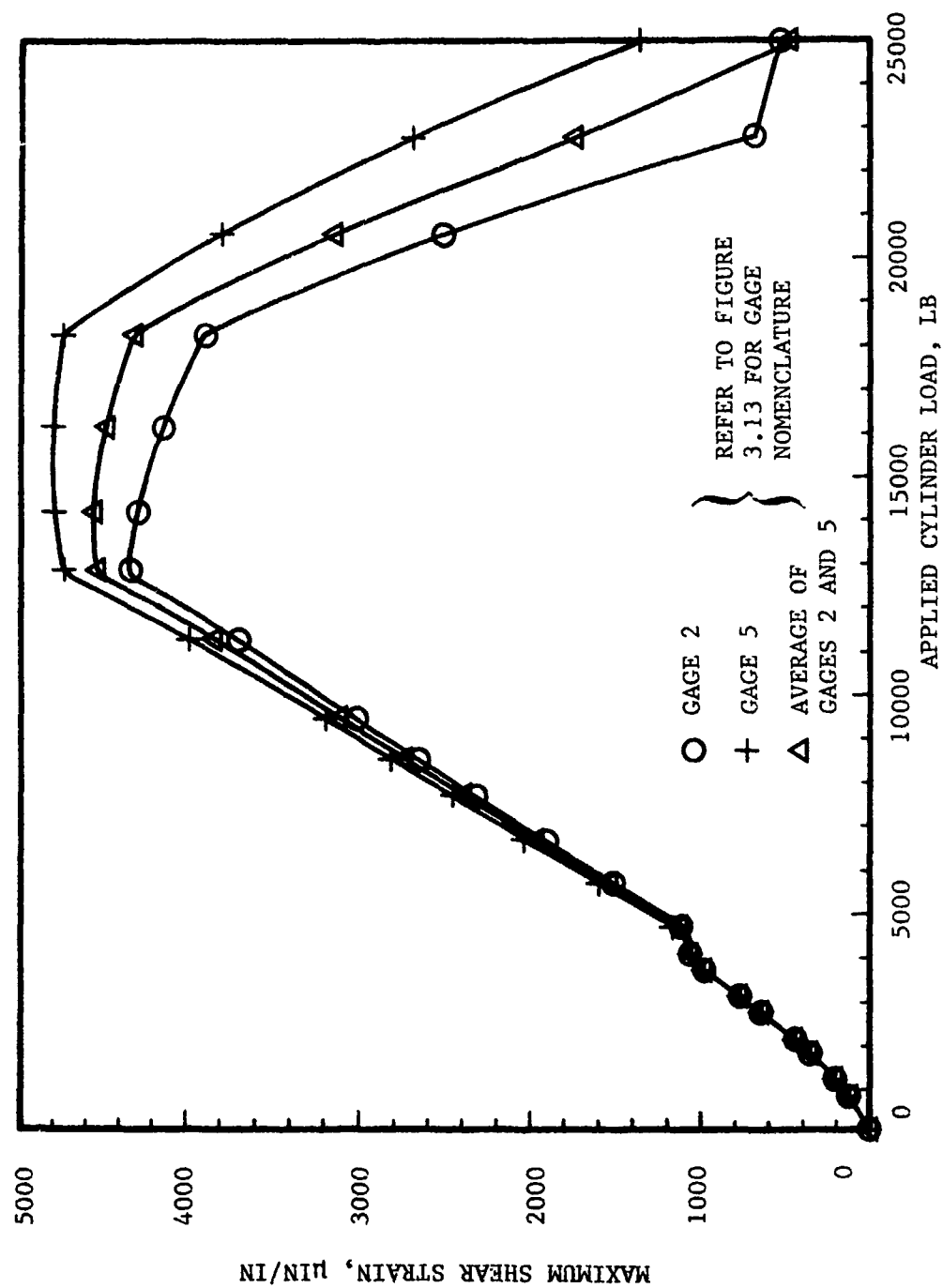


Figure 5.12. Metal Panel Web Maximum Shear Strains as a Function of Applied Load

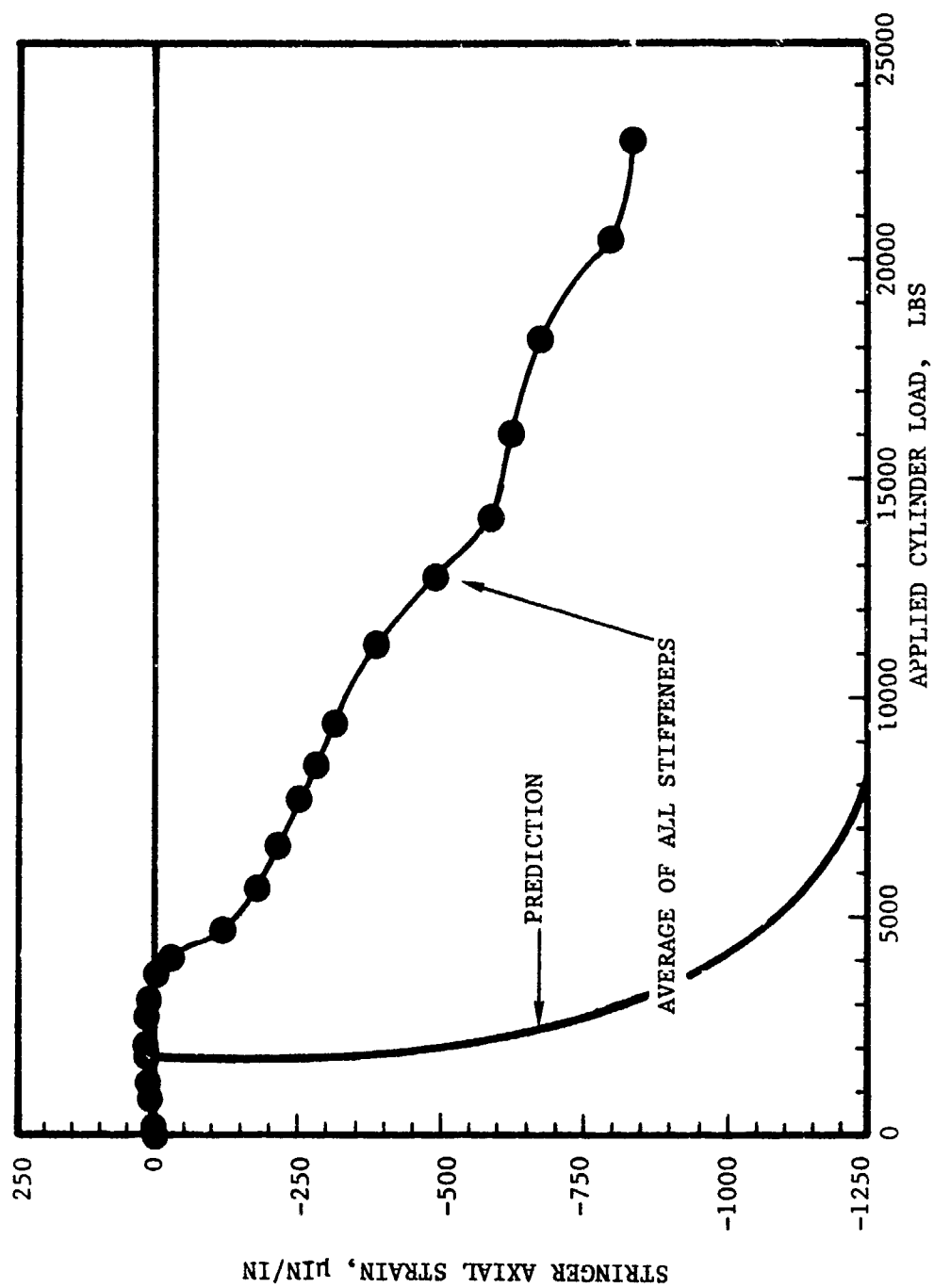


Figure 5.13. Stringer Strains for Metal Shear Panels

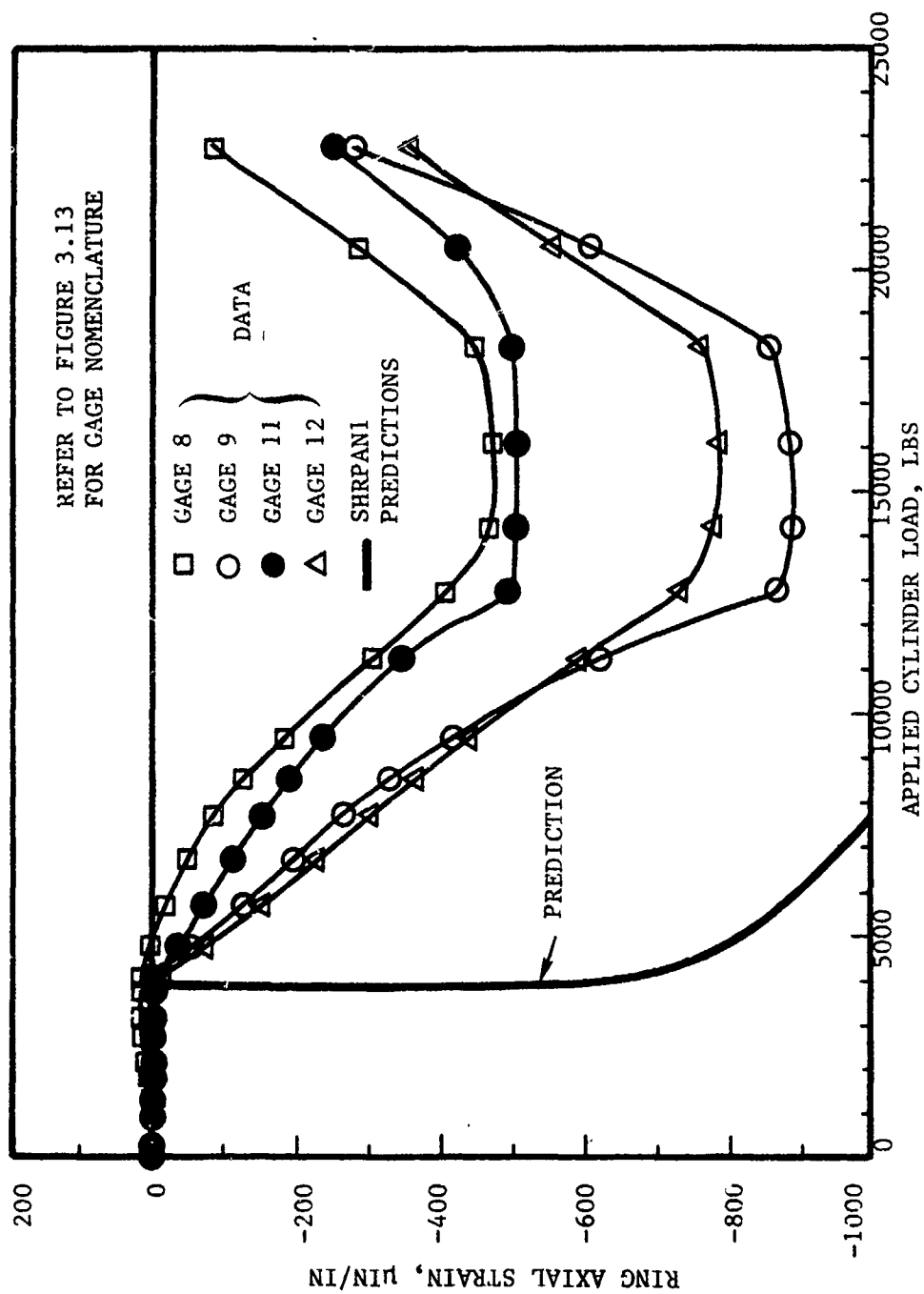


Figure 5.14. Ring Strains for Metal Shear Panels

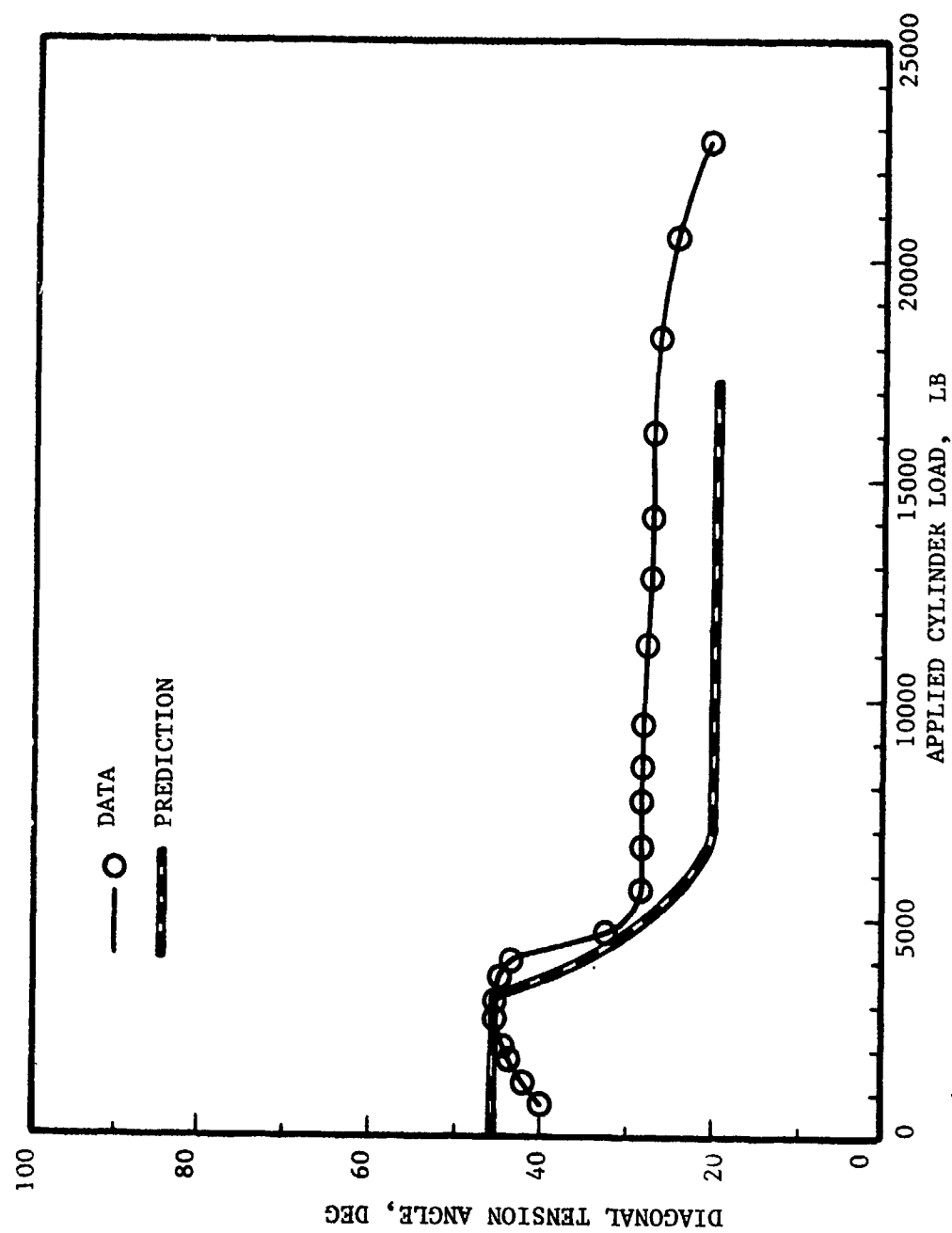


Figure 5.15. Diagonal Tension Angle as a Function of Applied Load for Metal Shear Panels

The composite shear panel test data analysis is summarized in Table 5.4. Comparison of the initial buckling and failure strain data with predictions is shown in Figure 5.16. The predictions were based on a skin width equal to the stringer spacing and are unconservative. In the case of composite shear panels, a more realistic definition of the skin width is the distance between adjacent stiffener flanges. Use of this definition yields better correlation between the test data and the predictions. Failure of the composite panels was predicted by forced crippling of the rings. In Section 2 it was also noted that forced crippling strains for the stiffeners correspond to stiffener/skin separation strains. The data comparison in Figure 5.16 along with the ring/web separation mode of failure observed in composite shear panels CS1 and CS2 substantiate the above hypothesis. The failure predictions made using the modified tension field theory are on the conservative side by approximately 35 percent. The measured maximum shear strains in the composite panel web shown in Figure 5.17 were used to determine panel stiffness change in the postbuckling regime. The composite shear panels show a dramatic loss in stiffness after initial buckling of the skin. As indicated in Table 5.4 the postbuckled stiffness for these panels is approximately 45 percent of the initial stiffness. These data are of significance in the design of postbuckled composite panels since the stiffness has a direct influence on the aeroelastic response of the panels. Therefore, for composite shear panels verification of the design for aeroelastic response criteria will be essential.

The hat section stringers showed significant bending during the static tests. The back-to-back strain gages were placed on the stiffener skin flange and the crown flange and due to the local bending of the crown flange, separation of axial and bending strains for the hat section stringers was not possible. In Figure 5.18 and 5.19, the stringer and ring strains measured on the skin flange of these stiffeners are shown. These data do not indicate the true axial strains due to the reasons cited above; however, they do show the buildup of strain in the stiffeners with increasing load after diagonal buckling. The stiffener strain predictions shown in Figure 5.18 were obtained from SHRPAN1.

The diagonal tension angle variation with load for the composite panels is shown in Figure 5.20. The predictions are in reasonable agreement with test

TABLE 5.4. COMPOSITE SHEAR PANEL STATIC TEST DATA CORRELATION WITH PREDICTIONS

PANEL NO.	WEB BUCKLING SHEAR STRAIN $\gamma_{cr}$ $\mu\text{in/in}^{**}$	$\frac{\gamma_{cr}}{\gamma_{cr0}}^{\dagger}$	WEB SHEAR STRAIN AT FAILURE $\gamma_{ult}$ , $\mu\text{in/in}$	$\frac{\gamma_{ult}}{\gamma_0}$	STRINGER STRAIN AT FAILURE $\epsilon_{os}$ , $\mu\text{in/in}$	$\frac{\epsilon_{os}}{(\epsilon_{os})_0}$	RING STRAIN AT FAILURE $\epsilon_{or}$ , $\mu\text{in/in}$	$\frac{\epsilon_{or}}{(\epsilon_{or})_0}$	POSTBUCKLING STIFFNESS % INITIAL STIFFNESS
CS1	1115	1.45	5200	1.49	-2662	0.83	-3563	1.31	43
CS2	1229	1.6	6100	1.74	-2971	0.93	-3770	1.39	46
CS3*	1244	1.62	---	---	---	---	---	---	---
CS4	1083	1.41	---	---	---	---	---	---	---
CS5	1381	1.79	---	---	---	---	---	---	---
CS6	1407	1.83	---	---	---	---	---	---	---
CS7	1270	1.65	---	---	---	---	---	---	---
CS8	1420	1.84	---	---	---	---	---	---	---
CS9	1577	2.05	---	---	---	---	---	---	---
CS10	1213	1.58	---	---	---	---	---	---	---

\* Panels CS3 through CS10 were fatigue tested.

\*\* Lowest shear strain as measured by gages 2 and 5 in Figure 3.13.

† Quantities with subscript '0' denote predicted values.

$$\gamma_{cr0} = 770 \mu\text{in/in}, \gamma_{ult} = 3500 \mu\text{in/in}, (\epsilon_{or})_0 = -2718 \mu\text{in/in}, (\epsilon_{os})_0 = -3192 \mu\text{in/in}$$

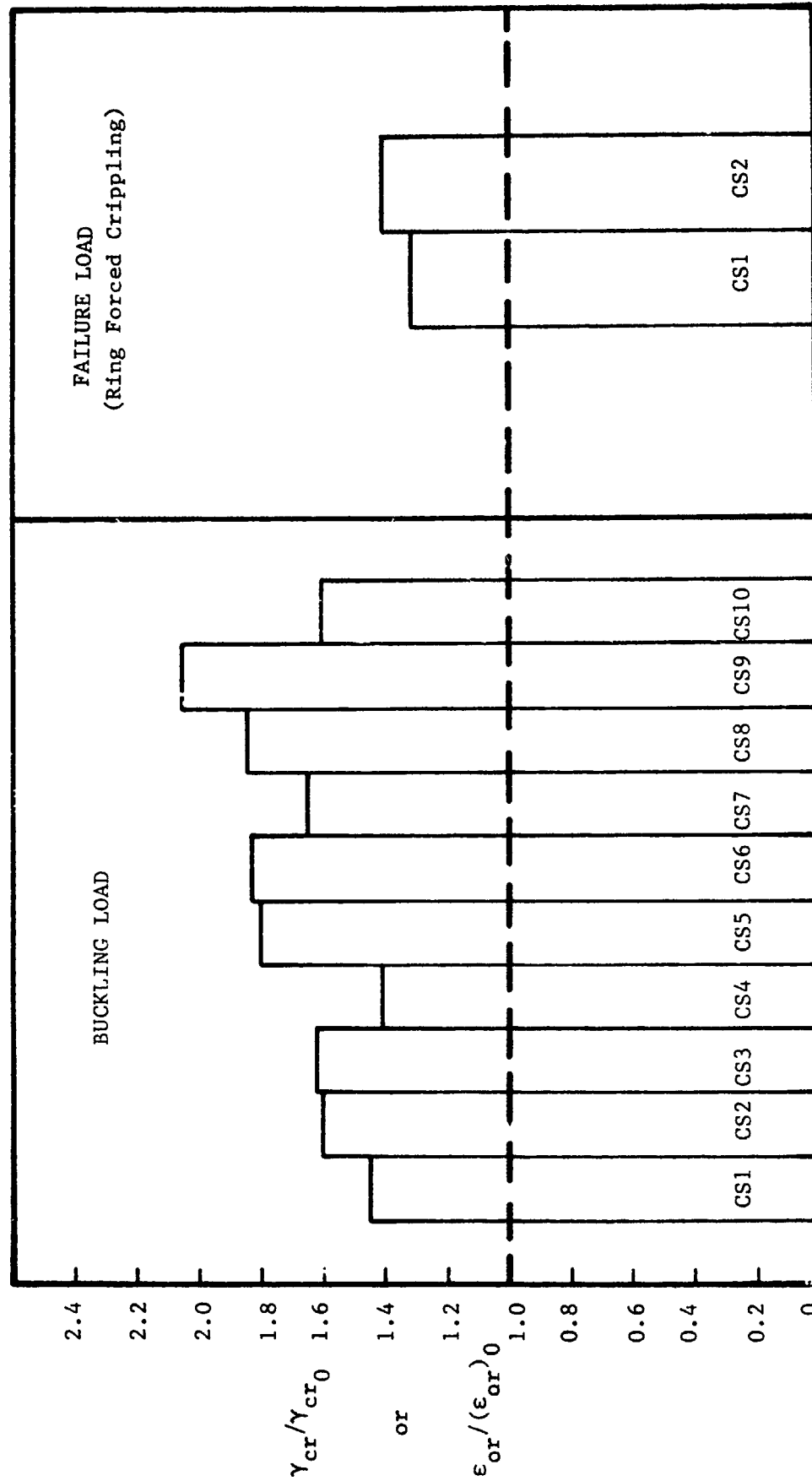


Figure 5.16. Comparison of Composite Shear Panel Static Test Data with Predictions



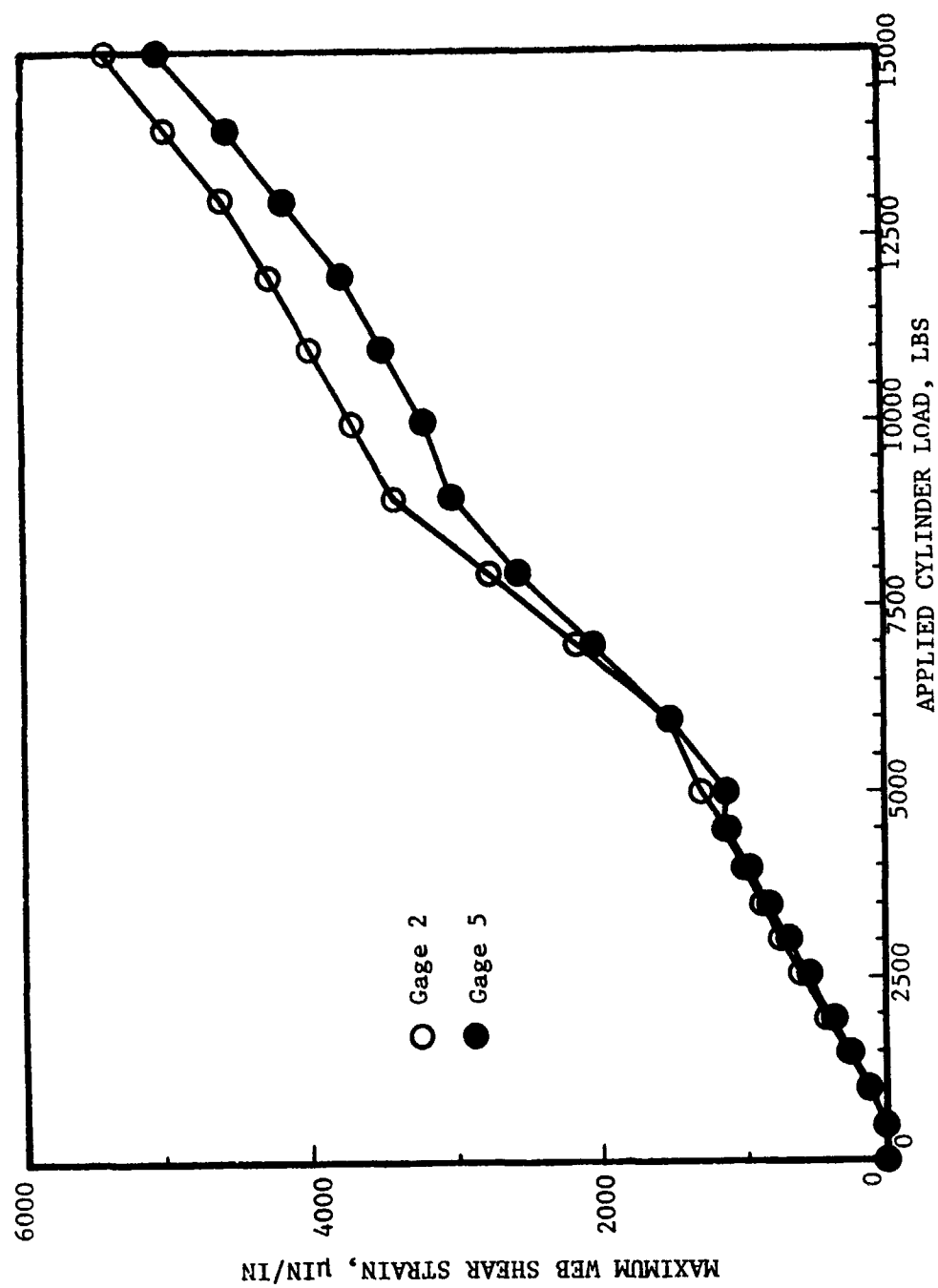


Figure 5.17. Composite Panel Web Maximum Shear Strains as a Function of Applied Load

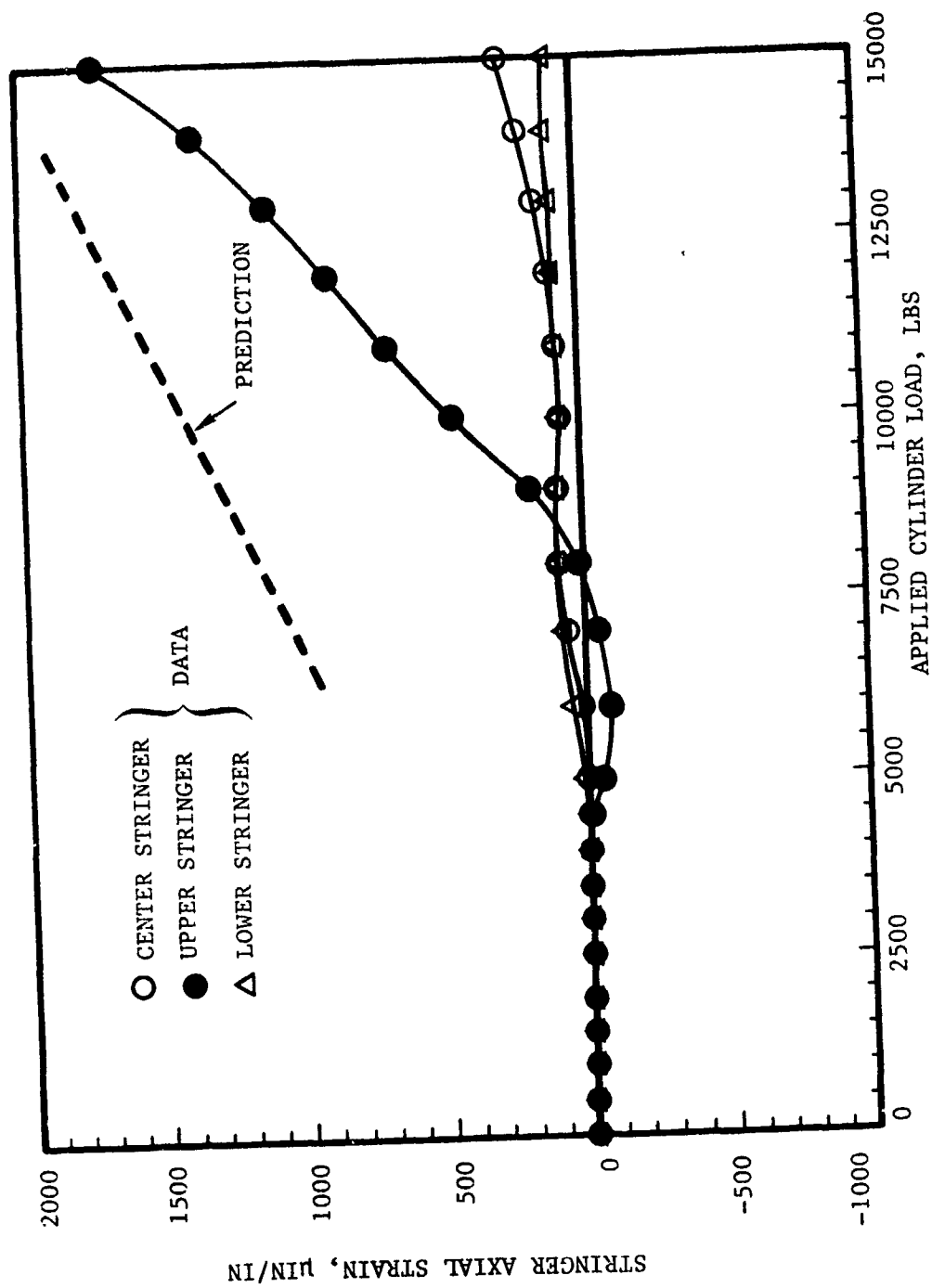


Figure 5.18. Stringer Strains for Composite Shear Panels

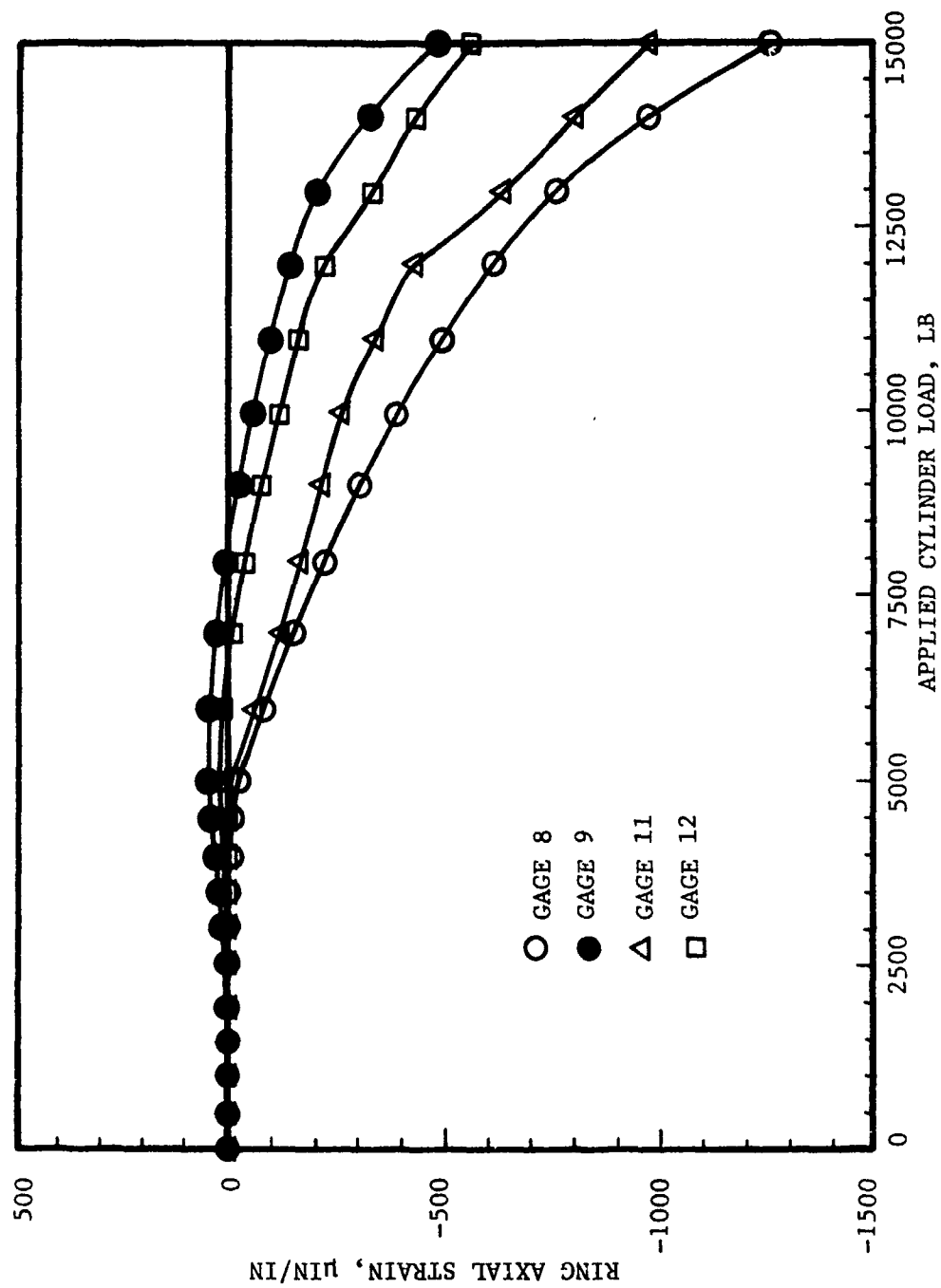


Figure 4.19. Ring Strains for Composite Shear Panels

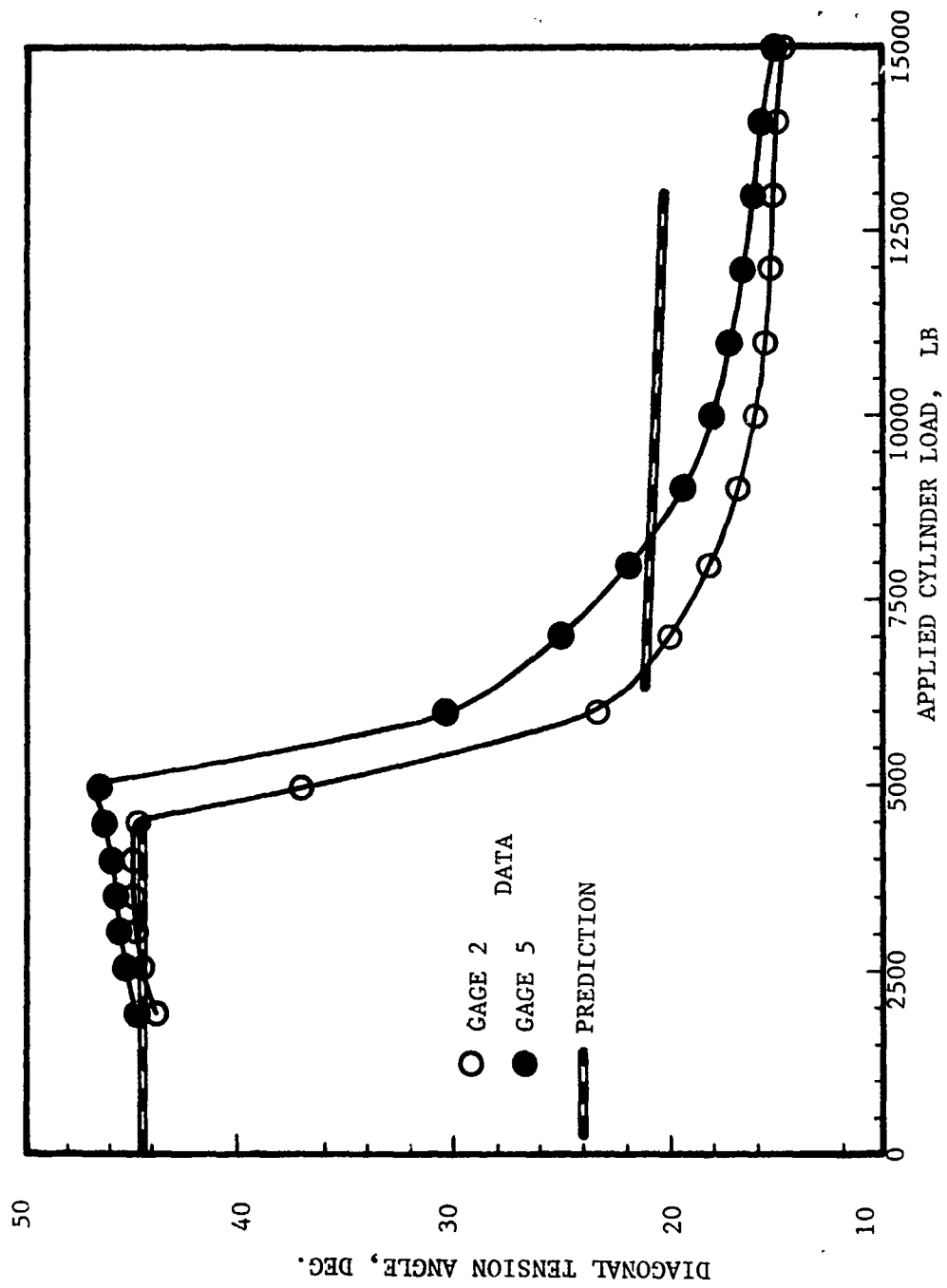


Figure 5.20. Diagonal Tension Angle as a Function of Applied Load for Composite Shear Panels

data. The discontinuity in predictions at an applied cylinder load of 5,000 lbs is due to the instability of SHRPAN1 solution in a close neighborhood of the buckling load. As the load increases, the diagonal tension angle decreases, indicating the tendency of the diagonal buckles to merge and cross over the stringer into the adjacent bay. After buckling the diagonal tension angle is approximately 18 degrees and compares favorably with the predictions.

#### 5.5 CURVED SHEAR PANELS UNDER FATIGUE LOADING

The fatigue test data for metal and composite shear panels are shown plotted as a function of the maximum fatigue load normalized to their respective static strengths in Figure 5.21. The data demonstrate the sensitivity of metal shear panels to fatigue loading and that their response is much inferior to that for composite panels designed for the same loading condition. The composite shear panel fatigue response is not affected by the partial reversal of the shear loading as is evidenced by a comparison of  $R = +0.25$  and  $R = -0.25$  fatigue data in Figure 5.21.

The fatigue tests were also useful in identifying metal and composite panel failure modes. Crack initiation and propagation in the metal panels as shown in Figure 3.32 and stiffener/web separation in composite panels are the critical modes that are addressed in the fatigue analysis methodology proposed in Section 4.4.

Analysis of the periodic strain survey data for the metal panels did not show any influence of repeated loading on initial buckling loads or panel stiffness in the postbuckled range. A majority of the relevant gages on the composite shear panels were lost due to fatigue damage and the data obtained could not be used for a meaningful interpretation of repeated buckling effects. The buckling loads measured in these strain surveys, however, do not show any influence of repeated loading on panel stiffnesses.

#### 5.6 DISCUSSION OF ANALYSIS AND TEST DATA CORRELATION

The out-of-plane displacement and strain predictions from programs COMPAN for compression panels and SHRPAN1 for shear panels are significantly different from the measured values.

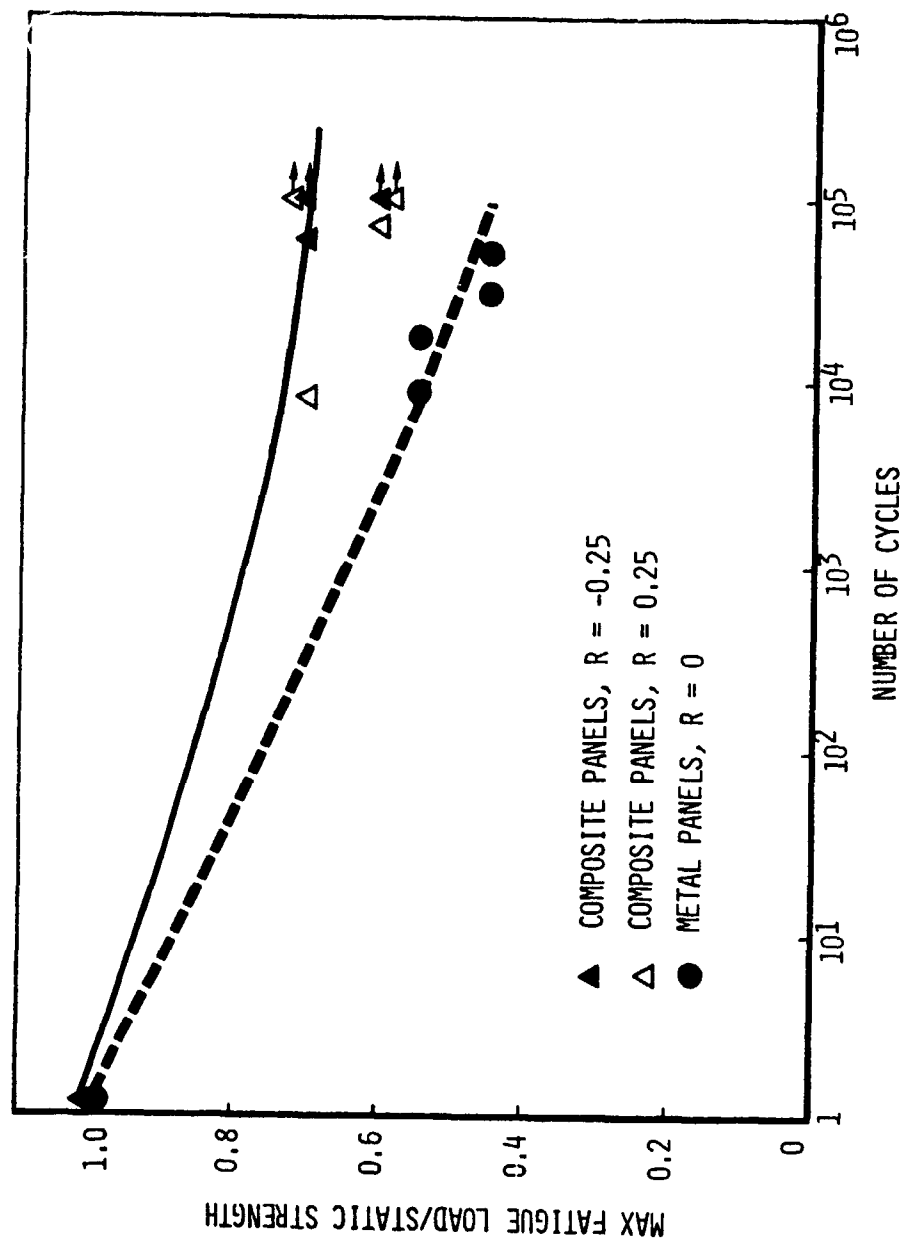


Figure 5.21. Normalized Fatigue Response Metal and Composite of Shear Panels

There are several reasons for these discrepancies. First of all the results of the energy based analyses are very sensitive to the assumed displacement functions. Secondly to account for mode shape changes in the postbuckling path either the assumed displacements should be a superposition of several modes or if a limited number of terms are used, the mode shape parameters should be treated as unknowns. The latter choice is more desirable since assumed displacements with a large number of unknowns inevitably lead to numerical difficulties in the solution of the resulting nonlinear equations.

Several numerical problems were also encountered in solving for the metal and composite compression and shear panels. In the case of compression panels, the solution procedure required that the starting point be zero load and zero displacement. The solution then progressed by marching up the prebuckling path to a load value slightly less than the buckling load and then switching over to the postbuckling path with a mathematical artifice of orthogonal vectors. The multivalued nature of the postbuckling path at bifurcation of equilibrium near the buckling load leads to nonconvergent solutions due to numerical oscillations. Thus, the orthogonal vector approach works only for the simplest of assumed displacement functions. In order to circumvent these problems, a solution scheme that starts from an initially guessed pair of load and displacement values in the vicinity of the postbuckling path, but sufficiently greater than the load and displacement values at bifurcation, should be utilized. In the shear panel analysis this latter scheme was adopted with the buckling loads being computed externally by programs such as SS3. The solution, however, was extremely sensitive to the initially guessed values for the unknowns and considerable expertise was required to select initial values that led to converged solutions. One possible strategy that may be used in selecting the initial displacements is given in Reference 91.

Based on the present experience, it is recommended that in future attempts to model the postbuckling behavior of compression and shear panels the following techniques be used:

- (A) Introduce initial imperfection or a transverse load to eliminate numerical problems in the vicinity of the bifurcation point.

- (B) Treat mode shape or buckle wave length as an unknown in the assumed displacements.
- (C) Evaluate functions other than trigonometric functions for the assumed displacements.



## SECTION 6

### CONCLUSIONS

The significant conclusions from this program are summarized in the following paragraphs.

#### 6.1 DESIGN AND ANALYSIS METHODOLOGY FOR CURVED COMPOSITE POSTBUCKLED PANELS

1. A semiempirical static analysis methodology was developed for curved composite panels loaded in compression or in shear.
2. Experimental verification data provided guidelines for determining the skin dimensions to be used in calculating initial buckling loads for both compression and shear panels.
3. Ultimate load predictions based on the semiempirical analysis for compression panels are very accurate and can be readily used for design purposes.
4. The modified tension field theory is applicable to curved composite shear panels. Ultimate load predictions are conservative by approximately 35 percent.
5. The postbuckled stiffness of compression panels is decreased by approximately 40 percent from the initial stiffness.
6. In shear panels the loss in stiffness after buckling is approximately 55 percent.
7. Stiffener/web separation was the observed failure mode for static and fatigue loading of compression and shear panels.

8. An empirical equation was developed to predict the static stiffener/web separation strain for shear panels.
9. Stringer or ring forced crippling strains correspond to the stiffener/web separation strain for shear panels.
10. Fatigue loading is not a concern for compression or shear panels and sufficient data exist to determine their safe operating strain levels.
11. Based on the fatigue failure modes observed in the tests, an approach to life prediction for compression and shear panels was developed.
12. Repeated buckling had no influence on panel initial buckling.
13. Non-empirical Rayleigh-Ritz analyses of postbuckled compression and shear panels have been developed. The analyses although capable of predicting the detailed displacement and stress field in postbuckled panels require further refinement to ensure numerical accuracy.
14. The program results were used to develop a design guide for compression and shear panels.

6.2

DESIGN AND ANALYSIS METHODOLOGY FOR CURVED METAL POSTBUCKLED PANELS

1. Applicability of the tension field theory to curved shear panels was verified by test data. Skin permanent set was seen to be the primary failure mode in these panels. A need to obtain a permanent set criterion for curved panels was identified.
2. Ultimate load predictions based on the available analysis methods were found to be quite accurate for compression panels.

3. The postbuckled stiffness reduction for compression panels is the same as that for composite panels. In the case of shear panels the stiffness change after buckling was seen to be only about 15 percent.
4. Fatigue sensitivity of compression and shear panels was found to be the greatest concern.
5. Skin cracking parallel to the stringers and away from fastener holes was identified as a failure mode in the compression panels.
6. Skin cracks originating at stiffener attach fastener holes and propagating transverse to the tension field direction was identified as the failure mode in shear panels.
7. Based on these failure modes, a fatigue life prediction approach was formulated for compression and shear panels.
8. Repeated buckling had no influence on the initial buckling load or stiffness of compression or shear panels.
9. The program results were used to develop a design guide.

#### 6.3

#### RECOMMENDATIONS FOR FUTURE WORK

1. Develop a design guide for panels under combined load.
2. Complete the development of the fatigue life prediction methodologies for metal and composite panels and extend the methodology to panels operating under combined loads.

#### REFERENCES

1. Wagner, Herbert, "Flat Sheet Metal Girders with Very Thin Metal Web," Parts I, II, and III, NACA TM 604, 605 and 606, 1931.
2. Kuhn, P.; Peterson, M. P. and Levin, L. R., "Summary of Diagonal Tension," Parts I and II, NACA TN 2661 and 2662, May 1952.
3. Tsongas, A. G. and Ratay, R. T., "Investigation of Diagonal Tension Beams With Very Thin Stiffened Webs," NASA CR 101854, July 1969.
4. Barevics, V. M.; Hoy, J. D. and Sherrer, "SST Technology Follow-On Program, Phase I, Intermediate Shear Beam Analyses," FAA-SS-72-11, May 1972.
5. Peterson, J. P., "Experimental Investigation of Stiffened Circular Cylinders Subjected to Combined Torsion and Compression," NACA TN-2188, 1950.
6. Kaminski, B. E. and Ashton, J. E., "Diagonal Tension Behavior of Boron-Epoxy Shear Panels," Journal of Composite Materials, Vol. 5, October 1971, pp. 553-558.
7. Fant, J. A.; Olson, F. O. and Roberts, R. H., "Advanced Composite Technology Fuselage Program," Vol. 6, Technical Report AFML-TR-71-41, October 1973.
8. Pimm, J. H., "Advanced Composite Tension Field Tests and Evaluation," Proceedings of the Twenty-fourth National Symposium and Exhibition, Book 2, of SAMPE, San Francisco, California, May 1979.
9. Bhatia, N. M., "Postbuckling Fatigue Behavior of Advanced Composite Shear Panels," presented at the Army Symposium on Solid Mechanics, 1976 - Composite Materials: The Influence of Failure on Design, AMMRC MS 76-3, September 1976.
10. Foreman, C. R., et al, "Advanced Composite Aft Fuselage Study, Phase 1 Results," Naval Air Development Center Report NADC-770-58-30, April 1979.
11. Rich, M. J. and Foye, R. L., "Low Cost Composite Airframe Structures," NASA TM X-3377, Third Conference on Fibrous Composites in Flight Vehicle Design, Williamsburg, Virginia, November 1975.
12. Lehman, G. M., "Development of an Advanced Composite Rudder for Flight Service on the DC-10," NASA TM X-3377, Third Conference on Fibrous Composites in Flight Vehicle Design, Williamsburg, Virginia, November 1975.

13. Agarwal, B. L., "Postbuckling Behavior of Composite Shear Webs," a paper presented at the Twentieth AIAA/ASME/SAE, Structures, Structural Dynamics, and Materials Conference, Seattle, Washington, May 1980.
14. Agarwal, B. L., "Flat Stiffened Graphite/Epoxy Tension Field Panels Under Constant-Amplitude Fully-Reversed Fatigue Loading," Report No. NADC-81169-60, Final Report on NADC Contract N62269-79-C-0461, August 1981.
15. Ostrom, R. B., "Postbuckling Fatigue Behavior of Flat, Stiffened Graphite/Epoxy Panels Under Shear Loading," Report No. NADC-78137-60, Final Report on Navy Contract N62269-79-C-0462, May 1981.
16. Renieri, M. P. and Garrett, R. A., "Postbuckling Fatigue Behavior of Flat Stiffened Graphite/Epoxy Panels Under Shear Loading," NADC Report No. NADC-78137-60, Final Report for Contract N62269-79-C-0463, August 1980.
17. Dastin, S., et al, "Advanced Composite Center Fuselage Structure V/STOL A - Phase II, Prototype Design," June 1980. (Navy Contract recently completed by Grumman and Northrop.)
18. Surdenas, J. and Van Putten, D. J., "Advanced Composite Center Fuselage Structure - V/STOL A - Phase I, Task 3, Element Design, Manufacture, and Test," Northrop Corporation Report NOR 80-49, March 1980. (Work done under subcontract to Grumman on a recent Navy Contract.)
19. Foreman, C. R., "Design Concepts for Composite Fuselage Structures," presented at Fourth Conference on Fibrous Composites in Structural Design, San Diego, California, November 1980.
20. Agarwal, B. L., "Design Concepts to Improve the Stiffener/Web Interface Strength of Postbuckled Panels," results of IR&D at Northrop, to be published.
21. Bhatia, N. M. and Van Putten, D. J., "Postbuckling Behavior of Cross-Stiffened Advanced Composites Panel Under Combined Loads," paper presented at Fifth DOD/NASA Conference on Fibrous Composites in Structural Design, New Orleans, Louisiana, January 1981.
22. Grimes, G. C. and Dusablon, E., "Structural Evaluation of Organic Matrix Filamentary Materials for Use at Elevated Temperatures," study completed at Northrop under NADC Contract N62269-80-C-0810.
23. Agarwal, B. L. and Van Etten, C. D., "Effect of Spectrum Loading on Postbuckling Fatigue of Advanced Composite Flat Shear Panels," Report No. NADC-80117-60, Final Report on NADC Contract N62269-81-C-0321, December 1981.

24. Garrett, R. A., et al, "Structural Analysis and Design Demonstration for Composite Shear Panels," study completed at McDonnell Douglas Corporation under NADC sponsorship.
25. Eves, J. J., et al, "Composite Wing/Fuselage Program," study being conducted at Northrop under Air Force Contract F33615-79-C-3203.
26. Starnes, J. H.; Knight, N. F. and Rouse, M., "Postbuckling Behavior of Selected Flat Stiffened Graphite/Epoxy Panels Loaded in Compression," AIAA paper No. 82-0777.
27. Garrett, R. A., "Postbuckling of Flat Stiffened Composite Panels Under Combined Loads," a study in progress under Navy Contract N62269-81-C-0384.
28. Ho, T., "Postbuckling of Kevlar/Epoxy Composite Shear Panels," paper presented at the Fifth DOD/NASA Conference on Fibrous Composites in Structural Design, New Orleans, Louisiana, January 1981.
29. Agarwal, B. L., "Postbuckling Behavior of Composite Stiffened Curved Panels Loaded in Compression," a paper presented at the Fourth SESA International Congress on Experimental Mechanics, Boston, Massachusetts, May 1980.
30. Agarwal, B. L., "Postbuckling Behavior of Hat-Stiffened Flat and Curved Composite Compression Panels," Report No. NOR 81-187, Final Report on Navy Contract N00019-79-C-0549, October 1981.
31. Hinkle, T. V.; Sorensen, J. P. and Garrett, R. A., "Compression Postbuckling Behavior of Stiffened Curved Graphite/Epoxy Panels," a paper presented at the Fifth DOD/NASA Conference on Fibrous Composites in Structural Design, held in New Orleans, Louisiana, January 1981.
32. Garrett, R. A., "Postbuckling of Curved Stiffened Composite Panels Under Combined Loads," a study in progress under Navy Contract N62269-81-C-0385.
33. Structural Design Manual, Northrop Corporation, Aircraft Division.
34. Bruhn, E. F., Analysis and Design of Flight Vehicle Structures, 1973.
35. Gerard, G. and Becker, H., "Handbook of Structural Stability," NACA TN 3781 through 3785, 1957.

36. Timoshenko, S. P. and Gere, J. M., Theory of Elastic Stability, McGraw-Hill, 1961.
37. "Advanced Composites Structural Manual," Northrop Corporation, Aircraft Division
38. "DOD/NASA Advanced Composites Design Guide," Prepared by Rockwell International Corporation under Contract F33615-78-C-3203, July 1983.
39. Steinbacher, F. R. and Gerard, G., Aircraft Structural Mechanics, Pittman Aeronautical Engineering Series, Pittman Publishing Corporation, New York, 1952.
40. Reed, D. L., "Laminated Sandwich Panel Analysis," General Dynamics Convair Aerospace Division, Report FZM-5590, October 1971.
41. Viswanathan, A. V. and Tamekuni, M., "Elastic Buckling Analysis for Composite Stiffened Panels and Other Structures Subjected to Biaxial Inplane Loads," NASA CR-2216, 1973.
42. Wittrick, W. H. and Williams, F. W., "Buckling and Vibration of Anisotropic or Isotropic Plate Assemblies Under Combined Loadings," International Journal of Mechanical Sciences, Vol. 16, No. 4, April 1974.
43. Williams, J. G. and Mikulas, M. M., Jr., "Analytical and Experimental Study of Structurally Efficient Composite Hat-Stiffened Panels Loaded in Axial Compression, AIAA Paper 75-754, Denver, Colorado, 1975 (also available as NASA TM X-72813).
44. Williams, J. G. and Stein, M., "Buckling Behavior and Structural Efficiency of Open-Section Stiffened Composite Compression Panels," AIAA Journal, Vol. 14, No. 11, November 1976.
45. Wilkins, D. J., "Anisotropic Curved Panel Analysis," General Dynamics, Convair Aerospace Division Report FZM-5567, May 1973.
46. Spier, E. E. and Klouman, F. L., "Empirical Crippling Analysis of Graphite/Epoxy Laminated Plates," in Composite Materials: Testing and Design (Fourth Conference), ASTM STP 617, 1977, pp. 255-271.
47. Spier, E. E., "Stability of Graphite/Epoxy Structures with Arbitrary Symmetrical Laminates," Experimental Mechanics, Vol. 18, No. 11, pp. 401-408, November 1978.
48. Renieri, M. P. and Garrett, R. A., "Investigation of the Local Buckling, Postbuckling and Crippling Behavior of Graphite/Epoxy Short Thin-Walled Compression Members," Report No. MDC A7091, Final Report on NAVAIR Contract N00019-80-C-0175, July 1981.

49. Sharifi, P., "Nonlinear Buckling Analysis of Composite Shells," AIAA Journal, Vol. 13, No. 6, June 1975, pp. 729-734.
50. Turney, G. J. and Wittrick, W. H., "The Large Deflection and Postbuckling Behavior of Some Laminated Plates," Aeronautical Quarterly, May 1973, pp. 77-86.
51. Rushton, K. R., "Postbuckling of Rectangular Plates with Various Boundary Conditions," Aeronautical Quarterly, May 1970, pp. 163-181.
52. Schmit, L. A. and Monforton, G. R., "Finite Deflection Discrete Element Analysis of Sandwich Plates and Cylindrical Shells with Laminated Faces," AIAA Journal, Vol. 8, No. 8, August 1970, pp. 1454-1461.
53. Stein, M. and Starnes, J. H., Jr., "Numerical Analysis of Stiffened Shear Webs in the Postbuckling Range," Numerical Solution of Nonlinear Structural Problems, ASME, Vol. 6, 1973, pp. 211-223.
54. Vestergren, P. and Knutsson, L., "Theoretical and Experimental Investigation of the Buckling and Postbuckling Characteristics of Flat Carbon Fiber Reinforced Plastic Panels Subjected to Compression on Shear Loads," presented at Eleventh International Council of the Aeronautical Sciences Congress, Lisbon, Portugal, September 1978.
55. Rothwell, A. and Allahyasi, H., "The Compressive Stiffness of a Thin Plate Buckled in Shear," Journal of Strain Analysis, Vol. 15, No. 4, 1980.
56. Noor, Ahmed, K.; Mathers, M. D. and Anderson, M. S., "Exploiting Symmetries of Efficient Postbuckling Analysis of Composite Plates," Proceedings, AIAA/ASME/SAE Seventeenth SDM Conference, Pennsylvania, May 1976.
57. Cristfield, M. A., "A Combined Rayleigh-Ritz Finite Element Method for the Nonlinear Analysis of Stiffened Plate Structures," Journal of Computers and Structures, Vol. 8, No. 6, June 1978.
58. Denke, P. H., "Strain Energy Analysis of Incomplete Tension Field Web-Stiffener Combinations," Journal of the Aeronautical Sciences, January 1944.
59. Levy, S.; Fienup, K. L. and Wooley, R. M., "Analysis of Square Shear Web Above Buckling Load," NACA TN 962, February 1945.
60. Levy, S.; Fienup, K. L. and Wooley, R. M., "Analysis of Deep Rectangular Shear Webs Above the Buckling Load," NACA TN 1009, 1946.



61. Mayers, J. and Budiansky, B., "Analysis of Behavior of Simply Supported Flat Plates Compressed Beyond the Buckling Load into the Plastic Range," NACA TN-3368, 1955.
62. Chia, C. Y. and Prabhakara, M. K., "Postbuckling Behavior of Unsymmetrically Layered Anisotropic Plates," Journal of Applied Mechanics, March 1974, pp. 155-162.
63. Harris, G. Z., "The Buckling and Postbuckling Behavior of Composite Plates Under Biaxial Loading," International Journal of Mechanical Sciences, Vol. 17, 1975, pp. 187-202.
64. Harris, G. Z., "Buckling and Postbuckling of Orthotropic Laminated Plates," Paper No. 75-813, AIAA/ASME/SAE Sixteenth Structures, Structural Dynamics, and Materials Conference, Denver, Colorado, May 27-29, 1975.
65. Chan, D. P., "An Analytical Study of the Postbuckling Behavior of Laminated, Anisotropic Plates," PhD Thesis, Case Western Reserve University, 1971.
66. Djubeck, J., "Deformation of Rectangular Slender Web Plates with Boundary Members Flexible in the Web Plate Plane," Aeronautical Quarterly, November 1966, pp. 371-394.
67. Mello, R. M.; Sherrer, R. E. and Musgrove, M. D., "Intermediate Diagonal Tension Field Shear Beam Development for the Boeing SST," J. Aircraft, Vol. 9, No. 9, September 1971, pp. 470.
68. Khot, N. S., "On the Effect of Fiber Orientation and Nonhomogeneity on Buckling and Postbuckling Behavior of Fiber-Reinforced Cylindrical Shells Under Uniform Axial Compression, AFFDL-TR-68-19, May 1968.
69. Khot, N. S., "On the Influence of Initial Geometric Imperfections on the Buckling and Postbuckling Behavior of Fiber-Reinforced Cylindrical Shells Under Uniform Axial Compression," AFFDL-TR-68-136, October 1968.
70. Dickson, J. N.; Cole, R. T. and Wang, J. T., "Design of Stiffened Composite Panels in the Postbuckling Range," Proceedings of the Fourth Conference on Fibrous Composites in Structural Design, San Diego, November 1978.
71. Dickson, J. N. and Biggers, S. B., "Design and Analysis of a Stiffened Composite Fuselage Panel," NASA CR-159302, August 1980.
72. Dickson, J. N. and Biggers, S. B., "POSTOP: Postbuckled Open Stiffener Optimum Panels - Theory and Capability," NASA CR-172259, January 1984.

73. Wang, J. T. S. and Biggers, S. B., "Skin/Stiffener Interface Stresses in Composite Stiffened Panels," NASA CR-172261, January 1984.
74. Kudva, N. J. and Agarwal, B. L., "Postbuckling Analysis of Stiffened Composite Shear Panels - Theoretical Analysis and Comparison with Experiments," paper presented at the Winter Annual Meeting of the ASME, Washington, D.C., November 1981.
75. Kudva, N. J., "On the Postbuckling Analysis of Flat, Stiffened Composite Shear Panels," Northrop Report No. NOR 80-186, January 1981.
76. Feng, M., "An Energy Theory for Postbuckling of Composite Plates Under Combined Loading," Computers and Structures, Vol. 16, No. 1-4, pp. 423-431, 1983.
77. Zhang, Y. and Matthews, F. L., "Postbuckling Behavior of Anisotropic Laminated Plates Under Pure Shear Combined With Compressive Loading," AIAA Journal, Vol. 22, No. 2, February 1984.
78. Arnold, R. R. and Mayers, J., "Buckling, Postbuckling, and Crippling of Materially Nonlinear Laminated Composite Plates," International Journal of Solids and Structures, Vol. 20, No. 9/10, September 1984, pp. 863-880.
79. Forman, R. G.; Kearney, V. E. and Engle, R. M., "Numerical Analysis of Crack Propagation in Cyclic-Loaded Structures," J. Bas. Engng. Trans. ASME, Ser. D, 89, 459 (1967).
80. Salvetti, A. et al, "Theoretical and Experimental Research on the Fatigue Behavior of Cracked Stiffened Panels," U.S. Army Contract DAJA 37-72-C-1783, European Research Office, AD 769 948, February 1973.
81. Salvetti, A. and Casarosa, C., "Fatigue Behavior of Hat Section Stringer Stiffened Panels Compressed in the Postbuckling Range," U.S. Army Contract DAJA 37-72-C-1280, European Research Office, AD 773 672, July 1973.
82. Salvetti, A. and Casarosa, C., "Fatigue Behavior of Hat Section Stringer Stiffened Panels Compressed in the Postbuckling Range," U.S. Army Contract DAJA 37-71-C-1147, AD 748 855, March 1972.
83. Renieri, M. P. and Garrett, R. A., "Stiffener/Skin Interface Design Improvements for Postbuckled Composite Shear Panels," Report No. NADC-80134-60, Final Report, NADC Contract No. N62269-81-C-0333.

84. Tsai, H. C., "Solution Method for Stiffener-Skin Separation in Composite Tension Field Panel," Report No. NADC-82171-60, October 1982.
85. McCarty, J. E. and Ratwani, M. M., "Damage Tolerance of Composites," First Interim Report (March 1983), AFWAL Contract F33615-82-C-3213.
86. Wilkins, D. J. et al, "Characterizing Delamination Growth in Graphite Epoxy," ASTM STP 775, 1982, pp. 168.
87. Block, D. L., Card, M. F., and Mikulas, M. M., Jr., "Buckling of Eccentrically Stiffened Orthotropic Cylinders." NASA TND-29601, August 1965.
88. "Advanced Composites Structural Manual - Volume II," Northrop Corporation, Aircraft Division.
89. Spier, E. E., "Local Buckling, Postbuckling, and Crippling Behavior of Graphite-Epoxy Short Thin Walled Compression Members," Final Technical Report NASC Contract N00019-80-C-0174, July 1981.
90. Hinkle, T. V., and Garrett, R. A., "Examination of Postbuckled Compression Behavior of Curved Panels," Final Technical Report, NASC Contract N00019-79-C-0204, August 1982.
91. Deo, R. B., Agarwal, B. L., and Madenci, E., "Design Methodology and Life Analysis of Postbuckled Metal and Composite Panels, Volume 2 - Automated Software Documentation for Programs CRIP and TENWEB," AFWAL Contract F33615-81-C-3208, March 1985.
92. Sobel, H., and Agarwal, B. L., "Buckling of Eccentrically Stringer-Stiffened Cylindrical Panels Under Axial Compression," Journal of Computers and Structures, Volume 6, 1976.
93. Sechler, E., and Dunn, L., Airplane Structural Analysis and Design, John Wiley and Sons, Inc., New York, 1942.
94. Waszczyszyn, Z., "Numerical Problems of Nonlinear Stability Analysis of Elastic Structures," Computers and Structures, Volume 17, No. 1, pp. 13-24. 1983.
95. Forman, R. G., "Study of Fatigue Crack Initiation From Flaws Using Fracture Mechanics Theory," Engineering Fracture Mechanics Theory," Engineering Fracture Mechanics, 1972, Volume 4, pp. 333-345.
96. Porter, P. G. and Liu, A. F., "A Rapid Method to Predict Fatigue Crack Initiation," NADC Report 81010-60, February 1983.

## APPENDIX A

### COMPRESSION AND SHEAR PANEL STRAIN DATA

#### A.1 COMPRESSION PANEL STRAIN DATA

The strain data obtained from all compression panel static tests and fatigue strain surveys are tabulated in this section of the appendix. Correspondence Table A-1 should be used to correlate the gage numbers in the strain data tables with the locations shown in Figure 3.12. All gages were axial gages.

TABLE A-1. GAGE NUMBER CORRESPONDENCE TABLE FOR STATIC COMPRESSION TEST PANELS

GAGE NO. IN FIGURE 3.12*	GAGE NO. IN DATA TABLE*
1E	1
1I	2
2E	3
2I	4
3E	5
3I	6
4E	7
4I	8
5E	9
5I	10
6E	11
6I	12
7E	13
7I	14
8E	15
8I	16
9E	17
9I	18
10E	19
10I	20
11E	21
11I	22
12E**	23
12I**	24

\*Fatigue panel MC3 instrumented with gages 1 through 8.  
 Fatigue panels MC4, CC3 and CC4 instrumented with gages 1 through 6.  
 Fatigue panels CC5 and CC6 instrumented with gages 1 through 4 and 6.  
 Gage 6 data corresponds to column numbers 9 and 10 in the data table.

\*\*Gage on midbay stringer of panel CC2.

# COMPRESSION PANEL STRAIN DATA

## STRAIN DATA FOR PANEL CCI

LOAD	GAGE 1	GAGE 2	GAGE 3	GAGE 4	GAGE 5	GAGE 6	GAGE 7	GAGE 8	GAGE 9	GAGE 10	GAGE 11	GAGE 12	GAGE 13	GAGE 14	GAGE 15
2	-92	-86	-93	-65	-99	-82	-64	-45	-77	-79	-64	-71	-83	-84	-8
4	-223	-225	-183	-174	-199	-188	-197	-182	-151	-155	-119	-138	-155	-161	-32
6	-323	-319	-271	-260	-291	-281	-298	-276	-229	-236	-190	-212	-234	-244	-60
8	-413	-409	-352	-341	-384	-370	-395	-367	-308	-317	-261	-289	-314	-330	-75
10	-515	-494	-444	-432	-476	-461	-490	-458	-389	-401	-334	-365	-391	-415	-73
12	-618	-593	-533	-523	-566	-547	-578	-545	-468	-479	-404	-436	-467	-488	-51
14	-721	-694	-631	-613	-653	-642	-672	-639	-552	-554	-479	-499	-545	-580	-8
16	-833	-796	-711	-711	-744	-734	-762	-733	-645	-610	-561	-536	-629	-644	63
18	-968	-906	-802	-827	-857	-836	-874	-834	-731	-610	-635	-515	-748	-658	173
20	-1078	-1022	-910	-959	-1009	-954	-1001	-949	-774	-830	-82	-1102	-188	-1248	212
25	-1425	-1319	-1240	-1240	-1331	-1251	-1211	-1253	-533	-1236	472	-1810	-144	-1619	315
30	-1757	-1616	-1522	-1522	-1515	-1527	-1493	-1491	-423	-1528	-854	-2249	-9	-1853	543
35	-2114	-1936	-1846	-1846	-1732	-1776	-1784	-1768	-330	-1735	-2790	-2173	-2018	-1853	1018
40	-2469	-2253	-2163	-2163	-1997	-2076	-2001	-2076	-203	-191	-3018	-2776	-2136	-1396	1394
45	-2830	-2586	-2786	-2497	-2306	-2661	-2272	-2371	-289	-317	-3283	-2771	-2211	-1458	1891
50	-3273	-2974	-3216	-2887	-2672	-2692	-2580	-2725	-330	-330	-3584	-3076	-2314	-1640	1891
55	-3669	-3318	-3586	-3236	-2995	-2985	-2863	-3030	-423	-330	-3843	-3076	-2434	-1818	2340
60	-4093	-3680	-3953	-3609	-3341	-3285	-3149	-3355	-617	-388	-4107	-3572	-2530	-2020	2360
65	-4529	-4055	-4292	-4092	-3690	-3590	-3435	-3639	-842	-1029	-4361	-3808	-2797	-2259	2360
70	-4924	-4417	-4695	-4385	-4058	-3894	-3705	-4015	-1312	-1118	-4581	-4012	-3071	-2530	2372
75	-5353	-4808	-5025	-4799	-4454	-4222	-3995	-4388	-1812	-1531	-4790	-4203	-3464	-2898	2361
80	-5892	-5204	-5218	-5239	-4892	-4572	-4256	-4740	-2419	-1325	-4961	-4360	-3973	-3329	3187

LOAD IN KIPS

STRAIN IN  $\mu$ in/in

LOAD	GAGE 16	GAGE 17	GAGE 18	GAGE 19	GAGE 20	GAGE 21	GAGE 22
2	-58	-84	-86	-79	-84	-53	-51
4	-175	-217	-223	-180	-188	-107	-100
6	-319	-318	-329	-268	-280	-186	-176
8	-409	-418	-434	-354	-369	-271	-240
10	-563	-517	-532	-448	-467	-365	-295
12	-663	-574	-592	-523	-557	-465	-334
14	-827	-722	-702	-637	-688	-572	-345
16	-1027	-875	-894	-833	-865	-693	-325
18	-1332	-1277	-1263	-1151	-1241	-831	-269
20	-1627	-1508	-1511	-1403	-1481	-119	-967
25	-1924	-1702	-1710	-1543	-1619	-193	-948
30	-2358	-2112	-2178	-1938	-2146	-31	-985
35	-2807	-2479	-271	-2408	-2506	-2399	-1227
40	-3255	-2834	2683	1602	-2363	-2405	1534
45	-3972	-3132	2871	1623	-2375	-2550	1918
50	-4420	-3276	3059	1506	-2279	-2784	2301
55	-4798	-3432	3213	1191	-2014	-2945	2582
60	-5157	-3587	3373	526	-1429	-3085	2810
65	-5538	-3751	3543	-137	-820	-3218	3007
70	-5899	-3914	3717	-430	-539	-3331	3174
75	-6252	-4077	3928	-606	-387	-3472	3346
80	-6598	-4302	4156	-750	-330	-3674	3590

STRAIN DATA FOR PANEL CC2

LOAD	GAGE 1	GAGE 2	GAGE 3	GAGE 4	GAGE 5	GAGE 6	GAGE 7	GAGE 8	GAGE 9	GAGE10	GAGE11	GAGE12	GAGE13	GAGE14	GAGE15
2	-151	-73	-72	-82	-109	-101	-102	-141	-82	-80	-67	-61	-89	-84	-97
4	-238	-170	-154	-106	-202	-188	-204	-251	-163	-160	-147	-132	-173	-163	-227
6	-308	-262	-242	-156	-307	-293	-317	-357	-252	-240	-237	-215	-372	-357	-382
8	-375	-349	-326	-256	-400	-389	-413	-474	-336	-330	-318	-280	-365	-343	-545
10	-454	-444	-413	-433	-488	-483	-509	-574	-416	-412	-391	-363	-450	-424	-731
12	-534	-540	-502	-526	-578	-578	-596	-676	-495	-498	-456	-431	-532	-502	-949
14	-617	-636	-591	-618	-671	-674	-694	-778	-552	-593	-495	-526	-590	-602	-1190
16	-700	-733	-681	-711	-766	-773	-804	-879	-550	-717	-463	-552	-591	-627	-1465
18	-788	-844	-808	-855	-905	-954	-933	-1029	-1138	-275	-1229	-93	-1127	-363	-1377
20	-903	-977	-924	-1005	-1020	-1082	-1053	-1150	-1286	-206	-1482	345	-1279	-324	-1534
22	-1177	-1293	-1210	-1333	-1297	-1420	-1353	-1439	-1602	-100	-1943	709	-1680	-164	-1912
24	-1465	-1596	-1508	-1591	-1582	-1747	-1652	-1772	-1944	65	-2332	1190	-2061	73	-2315
26	-1759	-1880	-1824	-2036	-1816	-1964	-1910	-2121	-208	-350	1632	-2823	-2061	-2124	-3166
28	-2051	-2220	-2131	-2406	-2100	-2298	-2214	-2477	-783	-312	2134	-3202	-2124	-2180	-3619
30	-2359	-2593	-2446	-2841	-2390	-2646	-2527	-2852	-788	-279	2540	-3702	-2540	-2244	-4021
32	-2713	-3135	-2819	-3267	-2720	-3046	-2893	-3296	-706	-271	2868	-4071	-271	-2333	-4442
34	-3035	-3662	-3149	-3651	-3027	-3416	-3266	-376	-815	-357	3124	-4370	-357	-2438	-4777
36	-3398	-4011	-3527	-4026	-3344	-3700	-3544	-4123	-851	-640	3304	-4586	-640	-2582	-5080
38	-3754	-4442	-3903	-4383	-3570	-4166	-3926	-4533	-802	-1051	3333	-4614	-1051	-2327	-5358
40	-4119	-4886	-4233	-4780	-4094	-4457	-4300	-4917	-1592	-182	-223	-457	-182	-1072	-5716
42	-4500	-5337	-4607	-5163	-4516	-4967	-4691	-5303	-1802	45	-2527	-567	-1319	-788	-5844
44	-4886	-5770	-5002	-5465	-4919	-5506	-5091	-5669	-2001	197	-3455	2702	-2223	1485	-6278

LOAD	GAGE16	GAGE17	GAGE18	GAGE19	GAGE20	GAGE21	GAGE22	GAGE23	GAGE24
2	-28	-112	-113	-72	-71	-50	-46	78	44
4	-66	-202	-204	-160	-159	-137	-128	36	6
6	-99	-303	-308	-251	-250	-222	-230	-22	-43
8	-108	-394	-410	-339	-341	-287	-326	-84	-95
10	-97	-481	-510	-434	-437	-374	-428	-150	-145
12	-56	-582	-650	-532	-533	-363	-542	-222	-190
14	18	-661	-739	-626	-643	-332	-666	-299	-254
16	127	-748	-831	-712	-750	-258	-803	-373	-305
18	190	-861	-919	-806	-834	-703	-917	-356	404
20	287	-926	-1019	-880	-938	-714	-962	-396	544
22	476	-1772	-1746	-154	-137	-515	-308	-537	615
24	742	-2934	-2913	-154	-137	-600	-285	-594	889
26	1157	-4055	-4013	-501	-326	1100	-1829	-725	-691
28	1423	-5139	-5093	-1035	-751	1438	-2090	-727	-676
30	1556	-6149	-6088	-1228	-1211	1740	-2348	-724	-615
32	1802	-7031	-6958	-2238	-2238	2439	-2589	-747	-558
34	2066	-8132	-7950	-2238	-2238	2883	-2819	-802	-476
36	2303	-9337	-9036	-1316	-1316	3557	-3057	-863	-315
38	2584	-1077	-1037	-1144	-1144	4557	-4557	-919	-103
40	2703	-1274	-1219	-1623	-1623	5295	-5295	-840	1147
42	2703	-1483	-1393	-2031	-2031	6571	-6571	-366	1400

STRAIN DATA FOR PANEL CC3 (BEFORE FATIGUE)

LOAD	GAGE 1	GAGE 2	GAGE 3	GAGE 4	GAGE 5	GAGE 6	GAGE 7	GAGE 8	GAGE 9	GAGE 10	GAGE 11	GAGE 12
2	-174	-80	-112	-99	-70	-148	-159	-159	-93	-87	-145	-64
4	-246	-164	-200	-191	-152	-110	-245	-245	-176	-165	-262	-80
6	-302	-247	-286	-280	-234	-302	-319	-319	-267	-251	-406	-94
8	-359	-336	-331	-395	-323	-430	-386	-386	-368	-344	-575	-97
10	-434	-424	-417	-495	-408	-556	-468	-468	-465	-437	-754	-89
12	-500	-507	-588	-591	-486	-679	-540	-540	-544	-524	-935	-80
14	-626	-584	-679	-691	-571	-804	-613	-613	-583	-563	-1160	-28
16	-755	-659	-835	-832	-665	-823	-637	-637	-583	-563	-1240	-10
18	-879	-733	-998	-931	-845	-863	-780	-780	-649	-621	-1239	22
20	-1004	-802	-1170	-1065	-962	-1063	-872	-872	-672	-641	-1412	110
25	-1344	-1027	-1616	-1466	-1257	-1514	-1078	-1078	-1290	458	-1934	402
30	-1622	-1243	-2027	-1804	-1547	-1857	-1283	-1283	-1367	672	-2351	816
35	-2054	-1473	-2488	-2157	-1900	-2230	-1680	-1680	-1874	700	-1957	921
40	-2440	-1739	-2920	-2545	-2257	-2612	-1858	-1858	-2072	1103	-2037	1074
45	-2828	-2025	-3350	-2868	-2615	-2951	-2113	-2113	-2242	1267	-2103	1202
50	-3210	-2293	-3803	-3348	-2930	-3267	-2373	-2373	-2719	1397	-2136	1292
55	-3610	-2567	-4251	-3742	-3359	-3710	-2638	-2638	-2710	1454	-2158	1340
58	-3850	-2736	-4534	-3985	-3596	-3990	-2801	-2801	-2710	1425	-2172	1350



STRAIN DATA FOR PANEL CC3 AFTER 50,000 CYCLES OF FATIGUE

LOAD	GAGE 1	GAGE 2	GAGE 3	GAGE 4	GAGE 5	GAGE 6	GAGE 7	GAGE 8	GAGE 9	GAGE 10	GAGE 11	GAGE 12
2	-274	-178	-30	-65	-147	9	-386	-188	-74	-86	-24	-143
4	-386	-265	-145	-164	-246	-47	-550	-290	-151	-160	-93	-162
6	-521	-341	-242	-252	-326	-115	-602	-374	-236	-230	-213	-190
8	-555	-418	-365	-333	-511	-180	-821	-57	-325	-319	-332	-208
10	-786	-494	-481	-428	-641	-286	-574	-349	-415	-397	-491	-215
12	-102	-564	-604	-513	-772	-343	-1013	-615	-506	-474	-686	-207
14	-1026	-643	-743	-618	-914	-436	-1170	-780	-591	-563	-955	-160
16	-1140	-713	-843	-736	-1056	-508	-125	-774	-977	-187	-1077	-37
18	-1268	-802	-972	-828	-1241	-572	-1704	-801	-1137	-315	-1255	-45
20	-1375	-895	-1072	-931	-1385	-784	-1947	-900	-1138	-410	-1487	126
25	-1661	-1073	-1312	-1171	-1772	-1114	-1782	-1205	-1259	-693	-2067	323
30	-1983	-1277	-1511	-1326	-2174	-1391	-2475	-1416	-1426	-718	-2162	1040
35	-2267	-1488	-1723	-1502	-2539	-1748	-2950	-1648	-1715	-960	-1906	1124
40	-2574	-1713	-2081	-2002	-2906	-2110	-3637	-1895	-1951	-1168	-1988	1206
45	-2888	-1960	-2304	-2428	-3410	-2480	-4366	-2066	-2179	-1354	-1970	1280
50	-3175	-2170	-2595	-2802	-3746	-2872	-5239	-2359	-2324	-1455	-1871	1245
55	-3503	-2455	-3038	-3233	-4263	-3285	-6302	-2515	-2423	-1503	-1864	1255
58	-3696	-2617	-3300	-3586	-4520	-3536	-6750	-2666	-2443	-1483	-1854	1253

# STRAIN DATA FOR PANEL CC4 BEFORE FATIGUE

LOAD	GAGE 1	GAGE 2	GAGE 3	GAGE 4	GAGE 5	GAGE 6	GAGE 7	GAGE 8	GAGE 9	GAGE 10	GAGE 11	GAGE 12
2	-171	-61	-127	-126	-112	-71	-123	-123	-112	-108	-47	8
4	-245	-138	-214	-218	-182	-151	-201	-201	-180	-166	-94	12
6	-328	-222	-314	-317	-259	-248	-286	-286	-259	-239	-122	22
8	-410	-305	-406	-420	-355	-343	-368	-368	-347	-311	-162	33
10	-491	-382	-489	-528	-413	-445	-449	-449	-425	-389	-212	44
12	-575	-460	-563	-640	-508	-550	-550	-550	-491	-487	-276	49
14	-657	-536	-633	-794	-582	-655	-666	-666	-714	-566	-304	47
16	-742	-612	-711	-933	-652	-820	-785	-785	-880	-775	-345	57
18	-821	-685	-822	-1063	-712	-953	-890	-890	-1042	-842	-391	56
20	-903	-754	-902	-1197	-772	-1094	-1071	-1071	-1158	-842	-463	42
25	-1029	-884	-1056	-1673	-1131	-1450	-1057	-1070	-1250	-762	-886	67
30	-1153	-1009	-1180	-2076	-1543	-1787	-1307	-1278	-1322	-762	-1439	256
35	-1273	-1127	-1300	-2399	-1944	-2162	-1507	-1583	-1379	-762	-1901	397
40	-1393	-1251	-1420	-2765	-2397	-2790	-1902	-1828	-2343	-762	-1585	1005
45	-1510	-1367	-1540	-3050	-2837	-3290	-2198	-2088	-2376	-762	-1886	1190
50	-1628	-1481	-1650	-3483	-3234	-3793	-2501	-2366	-2452	-762	-2094	1332
55	-1742	-1595	-1763	-3966	-3720	-4313	-2828	-2664	-2452	-762	-2343	1482
60	-1858	-1708	-1873	-4481	-4180	-4619	-3044	-2851	-2354	-762	-2428	1581

STRAIN DATA FOR PANEL C05 (BEFORE FATIGUE)

LOAD	GAGE 1	GAGE 2	GAGE 3	GAGE 4	GAGE 5	GAGE 6	GAGE 7	GAGE 8	GAGE 9	GAGE 10
2	-88	-74	-91	-93	-88	-110	-62	-112	-98	-96
4	-190	-170	-201	-182	-189	-201	-161	-219	-184	-177
6	-303	-263	-313	-289	-294	-290	-273	-321	-271	-258
8	-411	-359	-423	-357	-404	-382	-389	-424	-361	-336
10	-522	-455	-537	-417	-517	-474	-506	-526	-447	-412
12	-632	-551	-649	-537	-631	-566	-626	-630	-512	-494
14	-754	-655	-809	-633	-796	-659	-753	-738	-34	-204
16	-874	-756	-954	-735	-951	-782	-885	-874	129	-142
18	-1007	-887	-1098	-875	-1099	-905	-1018	-1001	62	-27
20	-1127	-993	-1234	-985	-1247	-1027	-1148	-1151	349	-243
25	-1463	-1316	-1600	-1203	-1620	-1328	-1490	-1492	759	-691
30	-1772	-1611	-1939	-1601	-1961	-1632	-1813	-1817	816	-638
35	-2133	-1945	-2303	-2116	-2305	-2216	-2178	-2166	-1976	1433
40	-2460	-2272	-2664	-2492	-2674	-2610	-2521	-2517	-2175	1601
45	-2796	-2608	-3030	-2869	-3053	-3011	-2871	-2876	-2353	1740
50	-3132	-2940	-3398	-3235	-3433	-3411	-3220	-3236	-2509	1853

# STRAIN DATA FOR PANEL C06 AFTER 50,000 CYCLES OF FATIGUE

LOAD	GAGE 1	GAGE 2	GAGE 3	GAGE 4	GAGE 5	GAGE 6	GAGE 7	GAGE 8	GAGE 9	GAGE 10
2	-195	-110	-121	-45	-89	-59	-153	-159	-53	-63
4	-328	-215	-243	-123	-124	-130	-278	-273	-138	-142
6	-459	-321	-367	-189	-302	-221	-412	-373	-224	-221
8	-573	-410	-472	-257	-305	-297	-525	-404	-300	-282
10	-691	-508	-585	-308	-500	-378	-548	-501	-388	-347
12	-805	-611	-709	-437	-611	-468	-669	-596	-502	-301
14	-935	-713	-861	-539	-765	-565	-804	-813	-504	-133
16	-1055	-816	-1003	-644	-907	-691	-1037	-944	-401	-266
18	-1177	-939	-1149	-779	-1050	-826	-1165	-1086	-430	-300
20	-1295	-1054	-1277	-901	-1194	-949	-1296	-1218	-421	-278
22	-1422	-1168	-1403	-1032	-1347	-1214	-1420	-1376	-400	-308
24	-1526	-1258	-1502	-1137	-1472	-1335	-1519	-1496	-1571	-388
26	-1628	-1379	-1621	-1216	-1572	-1447	-1623	-1596	-1823	-388
28	-1728	-1490	-1719	-1303	-1690	-1535	-1721	-1623	-1823	-388
30	-1828	-1590	-1819	-1373	-1776	-1639	-1821	-1623	-1823	-388
32	-1928	-1690	-1919	-1446	-1876	-1734	-1921	-1623	-1823	-388
34	-2028	-1790	-2019	-1516	-1976	-1834	-2021	-1623	-1823	-388
36	-2128	-1890	-2119	-1586	-2076	-1934	-2121	-1623	-1823	-388
38	-2228	-1990	-2219	-1656	-2176	-2034	-2221	-1623	-1823	-388
40	-2328	-2090	-2319	-1726	-2276	-2134	-2321	-1623	-1823	-388
42	-2428	-2190	-2419	-1796	-2376	-2234	-2421	-1623	-1823	-388
44	-2528	-2290	-2519	-1866	-2476	-2334	-2521	-1623	-1823	-388
46	-2628	-2390	-2619	-1936	-2576	-2434	-2621	-1623	-1823	-388
48	-2728	-2490	-2719	-2006	-2676	-2534	-2721	-1623	-1823	-388
50	-2828	-2590	-2819	-2076	-2776	-2634	-2821	-1623	-1823	-388

STRAIN DATA FOR PANEL CCS (AFTER 100,000 CYCLES)

LOAD	GAGE 1	GAGE 2	GAGE 3	GAGE 4	GAGE 5	GAGE 6	GAGE 7	GAGE 8	GAGE 9	GAGE 10
2	-34	-58	-79	-92	-70	-112	-56	-62	-129	-133
4	-153	-158	-195	-180	-162	-197	-162	-178	-216	-211
6	-271	-256	-310	-261	-261	-280	-288	-203	-301	-282
8	-402	-363	-432	-353	-367	-369	-409	-394	-396	-351
10	-515	-456	-539	-441	-476	-463	-538	-503	-495	-402
12	-651	-566	-704	-535	-622	-548	-665	-607	-451	-439
14	-780	-673	-850	-633	-757	-546	-800	-710	-341	-281
16	-909	-794	-986	-761	-889	-785	-934	-851	-493	-381
18	-1035	-908	-1118	-870	-1021	-903	-1060	-979	-410	-376
20	-1160	-1028	-1257	-1001	-1157	-1023	-1190	-1113	-250	-292
25	-1527	-1365	-1643	-1380	-1534	-1429	-1564	-1493	-789	-680
30	-1867	-1672	-2011	-1757	-1871	-1828	-1895	-1819	-1687	-1176
35	-2196	-1970	-2355	-2086	-2209	-2172	-2226	-2151	-1912	-1374
40	-2545	-2288	-2727	-2443	-2575	-2543	-2578	-2508	-2115	-1554
45	-2885	-2617	-3080	-2821	-2941	-2937	-2924	-2882	-2303	-1715
50	-3213	-2934	-3453	-3198	-3302	-3331	-3254	-3244	-2463	-1837
54	-3492	-3205	-3752	-3512	-3605	-3662	-3534	-3556	-2568	-1910

STRAIN DATA FOR PANEL CUS AFTER 150,000 CYCLES OF FATIGUE

LOAD	GAGE 1	GAGE 2	GAGE 3	GAGE 4	GAGE 5	GAGE 6	GAGE 7	GAGE 8	GAGE 9	GAGE 10
1	-66	-77	-183	-86	-88	-93	-94	-88	-127	-120
5	187	-184	-253	-165	-178	-177	-190	-205	-217	-199
6	-314	-290	-339	-242	-281	-258	-312	-318	-308	-263
8	-439	-394	-453	-315	-380	-335	-434	-424	-409	-300
10	558	-492	-577	-393	-498	-412	-556	-526	-707	122
12	-718	-624	-741	-500	-648	-524	-716	-558	-736	330
14	-844	-728	-866	-595	-774	-622	-852	-767	-715	424
16	-975	-851	-997	-715	-903	-759	-986	-900	-800	526
18	-1114	-980	-1142	-844	-1048	-892	-1129	-1045	-753	565
20	-1265	-1118	-1293	-983	-1196	-1049	-1284	-1201	-879	646
25	-1617	-1439	-1673	-1344	-1559	-1439	-1643	-1549	-1373	918
30	-1955	-1755	-2035	-1684	-1900	-1788	-1982	-1881	-1608	1134
35	-2294	-2057	-2377	-2005	-2248	-2134	-2316	-2218	-1757	1282
40	-2633	-2386	-2732	-2349	-2621	-2500	-2662	-2573	-1842	1367
45	-2972	-2715	-3098	-2718	-2990	-2903	-3006	-2939	-2000	1519
50	-3300	-3042	-3454	-3082	-3340	-3209	-3335	-3288	-2148	1619
54	-3550	-3303	-3740	-3378	-3640	-3516	-3601	-3590	-2238	1684

STRAIN DATA FOR PANEL C05 AFTER 200,000 CYCLES OF FATIGUE

LOAD	GAGE 1	GAGE 2	GAGE 3	GAGE 4	GAGE 5	GAGE 6	GAGE 7	GAGE 8	GAGE 9	GAGE 10
2	-66	-85	-98	41	-75	-95	-81	-97	-138	-136
4	-199	-199	-216	7	-159	-179	-182	-206	-218	-206
6	-329	-307	-342	-18	-289	-256	-320	-336	-310	-278
8	-448	-408	-454	-198	-379	-332	-442	-470	-395	-328
10	-564	-506	-555	-394	-477	-406	-566	-530	-518	-337
12	-707	-619	-722	-277	-631	-501	-711	-646	-685	256
14	-846	-722	-863	6	-768	-601	-854	-761	-648	359
16	-991	-864	-1005	77	-911	-738	-990	-890	-739	483
18	-1138	-998	-1153	-702	-1059	-869	-1148	-1037	-724	533
20	-1272	-1119	-1233	-1020	-1201	-1004	-1288	-1185	-880	541
25	-1630	-1438	-1552	-1384	-1549	-1382	-1651	-1535	-1365	858
30	-1996	-1765	-1940	-1735	-1919	-1751	-2015	-1882	-1637	1121
35	-2344	-2080	-2297	-2100	-2272	-2101	-2363	-2223	-1833	1306
40	-2676	-2392	-2745	-2451	-2620	-2463	-2637	-2564	-2014	1470
45	-3028	-2723	-3117	-2833	-2996	-2866	-3052	-2930	-2183	1617
50	-3364	-3064	-3488	-3214	-3369	-3270	-3396	-3310	-2303	1713
55	-3701	-3414	-3847	-3569	-3766	-3665	-3743	-3685	-2306	1696
60	-4051	-3832	-4245	-3943	-4154	-4087	-4113	-4093	-2400	1755
65	-4399	-4202	-4632	-4304	-4540	-4474	-4474	-4475	-2458	1767
70	-4808	-4576	-5043	-4702	-4958	-4862	-4866	-4860	-2440	1719
75	-5203	-4955	-5483	-5127	-5309	-5241	-5279	-5243	-2364	1617
80	-5605	-5322	-5938	-5550	-5830	-5600	-5703	-5599	-2226	1462

STRAIN DATA FOR SPECIMEN CCB BEFORE FATIGUE

LOAD	GAGE 1	GAGE 2	GAGE 3	GAGE 4	GAGE 5	GAGE 6	GAGE 7	GAGE 8	GAGE 9	GAGE 10
2	-85	-74	-122	-28	-107	-104	-66	-79	-115	-124
4	-193	-165	-217	-200	-194	-190	-168	-176	-188	-207
6	-280	-254	-293	-280	-268	-267	-255	-274	-253	-280
8	-384	-377	-384	-408	-360	-367	-362	-377	-320	-359
10	-487	-502	-472	-525	-440	-468	-469	-491	-392	-430
12	-584	-623	-555	-634	-532	-559	-565	-592	-458	-502
14	-681	-758	-647	-754	-624	-633	-669	-708	-537	-552
16	-800	-897	-779	-899	-724	-786	-781	-843	-648	-519
18	-946	-1030	-944	-1034	-821	-913	-870	-950	-112	-1035
20	-1043	-1154	-1063	-1163	-919	-1058	-938	-1103	180	-1185
25	-1301	-1500	-1428	-1514	-1366	-1368	-1322	-1426	574	-1749
30	-1711	-1823	-1771	-1851	-1718	-1695	-1620	-1757	909	-2079
35	-2048	-2152	-2033	-2222	-1958	-1869	-1935	-2078	-2619	1925
40	-2377	-2478	-2311	-2581	-2301	-2287	-2254	-2411	-2674	2063
45	-2710	-2804	-2689	-2942	-2637	-2591	-2566	-2731	-2687	2115
50	-3070	-3158	-3382	-3331	-2995	-2821	-2990	-3083	-2699	2037



STRAIN DATA FOR SPECIMEN C06 AFTER 50,000 CYCLES OF FATIGUE

LOAD	GAGE 1	GAGE 2	GAGE 3	GAGE 4	GAGE 5	GAGE 6	GAGE 7	GAGE 8	GAGE 9	GAGE 10
2	-113	-145	0	-114	-77	-100	-105	-129	0	-70
4	-209	-263	0	-219	-157	-184	-204	-235	0	-147
6	-316	-396	0	-338	-246	-280	-315	-350	0	-230
8	-426	-532	0	-460	-336	-379	-427	-470	0	-315
10	-516	-644	0	-560	-413	-467	-518	-588	0	-379
12	-625	-777	0	-680	-500	-572	-621	-722	0	-457
14	-719	-892	0	-784	-579	-671	-713	-843	0	-500
16	-818	-1031	0	-915	-669	-780	-812	-970	0	-507
18	-992	-1176	0	-1068	-832	-932	-944	-1117	0	-1206
20	-1119	-1304	0	-1198	-960	-1054	-1058	-1245	0	-1415
25	-1428	-1621	0	-1514	-1204	-1381	-1324	-1577	0	-1724
30	-1753	-1953	0	-1856	-1516	-1707	-1630	-1907	0	-1911
35	-2081	-2279	0	-2210	-1929	-2010	-2001	-2229	0	-1805
40	-2413	-2598	0	-2539	-2186	-2286	-2307	-2544	0	-1405
45	-2752	-2923	0	-2896	-2531	-2598	-2632	-2872	0	-1587
50	-3089	-3246	0	-3259	-2907	-2929	-2954	-3201	0	-963

STRAIN DATA FORT SPECIMEN CCG AFTER 100,000 CYCLES OF FATIGUE

LOAD	GAGE 1	GAGE 2	GAGE 3	GAGE 4	GAGE 5	GAGE 6	GAGE 7	GAGE 8	GAGE 9	GAGE 10
2	-78	-99	0	-94	-93	-90	-78	-98	0	-93
4	-175	-210	0	-187	-177	-183	-175	-197	0	-176
6	-273	-326	0	-286	-262	-269	-277	-296	0	-257
8	-379	-458	0	-426	-386	-384	-388	-395	0	-342
10	-477	-584	0	-535	-413	-452	-486	-505	0	-417
12	-575	-676	0	-645	-510	-546	-578	-621	0	-481
14	-678	-795	0	-760	-621	-650	-678	-744	0	-513
16	-811	-929	0	-894	-724	-782	-783	-872	0	-779
18	-934	-1054	0	-1038	-888	-914	-908	-1010	0	-1425
20	-1076	-1186	0	-1177	-1017	-1035	-1021	-1135	0	-1517
25	-1406	-1514	0	-1519	-1342	-1355	-1313	-1463	0	-1790
30	-1725	-1830	0	-1849	-1597	-1692	-1607	-1801	0	-1967
35	-2054	-2156	0	-2196	-1985	-1981	-1969	-2122	0	-1417
40	-2391	-2490	0	-2530	-2252	-2264	-2283	-2451	0	-1403
45	-2749	-2846	0	-2910	-2612	-2597	-2626	-2809	0	-1365
50	-3103	-3196	0	-3280	-3000	-2946	-2962	-3162	0	-836
54	-3394	-3479	0	-3590	-3312	-3220	-3235	-3448	0	679

STRAIN DATA FOR SPECIMEN PNC1

LOAD	GAGE 1	GAGE 2	GAGE 3	GAGE 4	GAGE 5	GAGE 6	GAGE 7	GAGE 8	GAGE 9	GAGE 10	GAGE 11	GAGE 12	GAGE 13	GAGE 14	GAGE 15
2	-136	-117	-124	-125	-88	-122	-54	-134	-107	-129	-98	-103	-91	-96	-52
4	-223	-210	-214	-222	-185	-230	-174	-220	-190	-216	-180	-195	-188	-194	-100
6	-356	-359	-331	-330	-267	-323	-271	-330	-276	-320	-358	-287	-274	-281	-143
8	-469	-491	-422	-434	-352	-421	-373	-430	-354	-421	-336	-376	-263	-370	-102
10	-569	-612	-523	-538	-442	-523	-474	-547	-420	-523	-413	-468	-456	-461	-221
12	-556	-782	-757	-592	-584	-656	-617	-579	-424	-625	-488	-576	-588	-578	-270
14	-738	-971	-912	-760	-781	-849	-617	-688	-21	-994	-72	-1084	-582	-753	-201
16	-883	-1144	-985	-933	-926	-1038	-1183	-843	-215	-994	-397	-1084	-371	-753	-253
18	-1004	-1310	-1097	-1071	-1078	-1350	-1474	-982	-1168	-1168	-676	-1761	-220	-1010	-253
20	-1122	-1480	-1199	-1208	-1278	-1695	-1760	-1988	-1258	-1592	-902	-1922	-154	-1353	-107
25	-1397	-1929	-1341	-1578	-2018	-2172	-2592	-1824	-1353	-1778	-182	-1881	-46	-1951	52
30	-1666	-2637	-1704	-2337	-1893	-2172	-3453	-1524	-1353	-1778	-182	-243	614	-1193	407
35	-1808	-3216	-1352	-2716	-1822	-2443	-3453	-1702	-1353	-1778	-182	-292	868	-1326	397
40	-3320	-3757	9999	-2544	1687	-2700	-3824	-1924	-1353	-1778	-182	-237	1108	-1427	706
42	-5409	-3886	9999	-1931	9999	-1989	-3741	-2321	-2470	-3089	54	-259	1554	-2085	523

LOAD	GAGE 16	GAGE 17	GAGE 18	GAGE 19	GAGE 20	GAGE 21	GAGE 22
2	-96	-193	-193	-91	-96	-52	-96
4	-218	-22	-195	-188	-184	-100	-218
6	-344	-34	-287	-274	-281	-143	-344
8	-477	-47	-376	-363	-370	-182	-477
10	-626	-62	-468	-456	-461	-221	-626
12	-871	-617	-701	-634	-634	-583	-871
14	-1067	-1402	-1161	-131	-260	-210	-1114
16	-1156	-346	-751	-187	-458	-78	-1156
18	-1327	-670	-566	-490	-718	78	-1088
20	-1516	-774	-745	-587	-762	120	-1088
25	-2053	-1448	1419	-940	-796	154	-1088
30	-2011	-1068	916	-1316	-901	216	-828
35	-2434	-1045	790	-1460	-1453	517	-904
40	-2743	-1177	812	-1456	-1537	591	-904
42	-2341	-1958	1209	-1037	-1370	928	-1258
						888	-1025

# STRAIN DATA FOR SPECIMEN NC2

LOAD	GAGE 1	GAGE 2	GAGE 3	GAGE 4	GAGE 5	GAGE 6	GAGE 7	GAGE 8	GAGE 9	GAGE 10	GAGE 11	GAGE 12	GAGE 13	GAGE 14	GAGE 15
2	-183	-143	-88	-93	-185	-115	-88	-224	-89	-120	-182	-189	-105	-89	-48
4	-189	-145	-180	-195	-282	-203	-191	-316	-193	-239	-203	-208	-202	-193	-198
6	-284	-259	-294	-309	-281	-288	-284	-494	-293	-345	-292	-306	-282	-293	-166
8	-355	-358	-397	-401	-359	-405	-395	-504	-388	-459	-375	-398	-355	-388	-210
10	-474	-462	-497	-508	-432	-497	-486	-508	-473	-547	-417	-483	-355	-474	-286
12	-472	-501	-544	-559	-525	-612	-544	-762	-565	-687	-526	-570	-478	-562	-323
14	-473	-583	-622	-659	-714	-612	-591	-893	-567	-749	-625	-670	-478	-698	-376
16	-646	-695	-729	-769	-779	-735	-716	-1064	-688	-757	-625	-633	-478	-819	-268
18	-792	-796	-821	-855	-858	-803	-787	-1248	-674	-724	-452	-436	-197	-1119	-92
20	-921	-943	-958	-1021	-958	-893	-857	-1417	-87	-724	-452	-436	-197	-1243	-268
22	-1166	-1145	-1285	-1285	-1243	-1021	-1021	-1832	-110	-1366	-710	-613	-230	-1434	-465
24	-1763	-2338	-1609	-1609	-3565	-2374	-249	-1832	-369	-2398	-203	-284	-351	-2768	59
26	-2632	-3285	-1407	-1834	-4305	-2081	-2386	-2140	-3789	-2129	-2452	-2894	-2894	-3357	77
28	-3471	-3867	-6555	-1835	-4733	-2666	-3654	-2760	-4515	-1871	-3237	-2425	-2326	-4070	171
30	-7209	-3760	-3844	-2721	-4173	-2116	-446	-3221	-6425	-2192	-3699	-3870	-2782	5516	172

LOAD	GAGE 16	GAGE 17	GAGE 18	GAGE 19	GAGE 20	GAGE 21	GAGE 22
2	-37	-115	-205	-98	-112	-133	-174
4	-149	-246	-312	-309	-236	-243	-288
6	-269	-353	-375	-316	-351	-339	-483
8	-308	-432	-463	-439	-489	-430	-557
10	-376	-502	-538	-529	-615	-617	-622
12	-482	-644	-679	-693	-836	-682	-822
14	-1054	-1559	-1833	-1828	-1898	-833	-830
16	-1165	-1605	-1787	-1850	-1716	-1227	-829
18	-1123	-1616	-1737	-1837	-1605	-168	-683
20	-1356	-2144	-2334	-2366	-284	-261	-380
22	-1590	-2444	-2634	-2666	-318	-231	-454
24	-1811	-2708	-2898	-2930	-370	-231	-545
26	-2027	-3022	-3212	-3244	-418	-231	-641
28	-2252	-3332	-3522	-3554	-463	-231	-742

STRAIN DATA FOR SPECIMEN MC3 BEFORE FATIGUE

LOAD	GAGE 1	GAGE 2	GAGE 3	GAGE 4	GAGE 5	GAGE 6	GAGE 7	GAGE 8	GAGE 9	GAGE 10	GAGE 11	GAGE 12
2	-99	-106	-115	-96	-92	-78	-68	-80	-112	-117	-113	-112
4	-181	-187	-219	-216	-192	-189	-139	-157	-226	-235	-241	-231
6	-265	-271	-324	-342	-300	-309	-204	-243	-345	-359	-370	-349
8	-349	-361	-433	-474	-410	-431	-266	-335	-486	-486	-509	-484
10	-431	-433	-569	-616	-533	-561	-304	-424	-607	-627	-630	-583
12	-543	-630	-760	-793	-657	-771	-344	-512	21	-912	-603	-549
14	-633	-757	-883	-880	-929	-895	-459	-716	552	-1685	-809	-461
16	-854	-1095	-1237	-1017	-1107	-1395	-964	-825	-1751	-1702	-455	-708
18	-987	-1314	-2711	-1016	-1412	-1473	-1126	-992	-1849	1726	565	-919
20	-1117	-1514	-3006	-1042	-1797	-1567	-1275	-1139	-1954	1775	624	-997
22	-1238	-1780	-3262	-1083	-1993	-1540	-1417	-1258	-2047	1822	676	-1072
24	-1364	-1892	-3492	-1083	-2294	-1733	-1562	-1388	-2137	1856	733	-1151
26	-1480	-2071	-3734	-1086	-2765	-1989	-1843	-1746	-2429	2035	682	-1243
28	-1623	-2273	-3893	-1107	-3080	-2622	-2007	-1909	-2528	2087	736	-1331

STRAIN DATA FOR SPECIMEN NC4 BEFORE FATIGUE

LOAD	GAGE 1	GAGE 2	GAGE 3	GAGE 4	GAGE 5	GAGE 6	GAGE 7	GAGE 8	GAGE 9	GAGE 10
2	-102	-100	-118	-108	-90	-77	-97	-153	-128	-117
4	-205	-199	-217	-206	-190	-185	-187	-247	-232	-215
6	-325	-318	-325	-330	-306	-311	-286	-352	-348	-321
8	-436	-433	-424	-448	-411	-428	-378	-453	-455	-416
10	-539	-550	-516	-563	-500	-538	-462	-555	-555	-498
12	-639	-670	-608	-675	-602	-644	-537	-663	-656	-572
14	-870	-870	-738	-943	-753	-834	-693	-771	129	-1240
16	-994	-1068	-1025	-1110	-1088	-987	-749	-1086	555	-1724
18	-1031	-1255	-1191	-1306	-1272	-1148	-888	-1267	857	-1930
20	-1114	-1368	-1313	-1448	-1429	-1260	-980	-1308	1050	-2054
22	-1207	-1551	-1482	-1634	-1687	-1396	-1095	-1567	1256	-2176

# MS1 STATIC TEST

LOAD	GAGE 29	GAGE 30	GAGE 31	GAGE 32	GAGE 33	GAGE 34	GAGE 35	GAGE 36	GAGE 37	GAGE 38	GAGE 39	GAGE 40	GAGE 41	GAGE 42
0.	0.	0.	0.	0.	0.	0.	0.	0.	0.	0.	0.	0.	0.	0.
183.	1.	-4.	-1.	7.	-4.	-7.	-4.	-7.	0.	-7.	0.	-4.	9.	-4.
878.	0.	-4.	14.	0.	0.	-19.	0.	-4.	7.	-4.	0.	-4.	0.	-8.
1257.	-4.	-4.	22.	11.	4.	-22.	-4.	0.	11.	0.	-4.	0.	19.	-11.
1837.	-4.	4.	30.	11.	7.	-22.	0.	0.	15.	0.	0.	0.	27.	-8.
2127.	-4.	11.	30.	11.	11.	-22.	4.	11.	11.	0.	4.	0.	34.	-11.
2756.	-11.	19.	30.	0.	11.	-30.	0.	15.	0.	-7.	11.	0.	38.	-19.
3143.	-19.	29.	28.	-7.	11.	-37.	0.	19.	-4.	-7.	15.	-4.	30.	-23.
3723.	-30.	30.	30.	-25.	18.	-44.	-7.	26.	-11.	-11.	27.	-15.	30.	-27.
4110.	-37.	37.	41.	-57.	22.	-56.	-7.	33.	-17.	-11.	49.	-30.	30.	-30.
4720.	-59.	-19.	-15.	-100.	93.	-345.	-56.	59.	-302.	105.	51.	-72.	-27.	-209.
5706.	-81.	-67.	-63.	-30.	126.	-441.	-74.	15.	-323.	233.	15.	-90.	-152.	-582.
6373.	-104.	-114.	-53.	19.	137.	-593.	-81.	-33.	-48.	218.	-49.	-84.	-327.	-1031.
7633.	-133.	-163.	-104.	52.	137.	-723.	-85.	-36.	-370.	167.	-137.	-9.	-545.	-1571.
8477.	-163.	-211.	-107.	56.	104.	-853.	-96.	-70.	-426.	164.	-136.	-116.	-780.	-2062.
9204.	-204.	-233.	-107.	44.	33.	-909.	-107.	-256.	-478.	0.	-384.	-221.	-1042.	-2651.
11275.	-259.	-441.	-70.	-23.	-144.	-1030.	-137.	-463.	-526.	-237.	-833.	-175.	-1655.	-3019.
12785.	-311.	-689.	18.	-167.	-144.	-1330.	-174.	-530.	-583.	-611.	-1636.	-1156.	-2556.	-5658.
14267.	-359.	-678.	93.	-208.	-126.	-1434.	-209.	-834.	-222.	-690.	-1965.	-1145.	-2911.	-5766.
16101.	-374.	-634.	133.	-252.	-160.	-1464.	-278.	-663.	-284.	-782.	-1887.	-1095.	-2713.	-5898.
18177.	-459.	-534.	137.	-322.	-52.	-1401.	-263.	-645.	-1310.	-785.	-1837.	-1095.	-2659.	-4994.
19550.	-507.	-337.	-378.	-548.	30.	-1152.	-243.	-322.	-1018.	-577.	-1566.	-533.	-2126.	-3916.
20774.	-515.	-315.	-633.	-1623.	15.	-725.	-178.	-1.	-580.	-696.	-871.	-23.	-1548.	-3916.
24550.	-448.	-340.	-622.	-1375.	-231.	-156.	63.	-30.	-218.	-1129.	-730.	-33.	-1445.	-3322.

LOAD	GAGE 43	GAGE 44	GAGE 45	GAGE 46
0.	0.	0.	0.	-4.
183.	0.	0.	0.	-4.
878.	4.	0.	15.	-11.
1257.	0.	-7.	23.	-19.
1837.	16.	-4.	30.	-23.
2127.	16.	-4.	27.	-23.
2756.	12.	0.	22.	-34.
3143.	12.	0.	11.	-43.
3723.	12.	6.	11.	-43.
4110.	16.	0.	4.	0.
4720.	-12.	-91.	-04.	49.
5706.	-151.	-221.	-217.	-49.
6373.	-358.	-316.	-234.	-46.
7633.	-365.	-434.	-475.	-48.
8477.	-435.	-544.	-653.	-160.
9204.	-505.	-617.	-814.	-183.
11275.	-617.	-871.	-1104.	-182.
12785.	-730.	-1042.	-1712.	-1879.
14267.	-761.	-1045.	-2043.	-3163.
16101.	-815.	-1081.	-2107.	-3163.
18177.	-887.	-1075.	-2184.	-3633.
19550.	-971.	-1061.	-1910.	-3481.
20774.	-1032.	-80.	-636.	-1910.
24550.	-1005.	30.	-702.	100.

SHEAR PANEL STRAIN DATA

RS1 STATIC TEST

LOAD	GAGE 1	GAGE 2	GAGE 3	GAGE 4	GAGE 5	GAGE 6	GAGE 7	GAGE 8	GAGE 9	GAGE 10	GAGE 11	GAGE 12	GAGE 13	GAGE 14
0	0	0	0	0	0	0	0	0	0	0	0	0	0	0
192	-3	-4	-4	-4	4	8	4	0	-3	34	-4	-8	8	-4
178	0	0	-8	68	19	-8	64	-11	-61	64	-4	-57	68	-5
157	57	7	-68	106	22	-53	99	-15	-95	102	-4	-91	102	-22
157	91	11	-106	201	22	-53	186	-15	-178	193	4	-171	186	-39
157	167	7	-205	254	22	-159	235	-15	-178	243	7	-216	227	-33
2137	214	0	-662	254	22	-201	330	-26	-334	335	15	-315	315	-56
2756	397	0	-662	384	22	-251	383	-33	-304	388	19	-376	363	-82
3143	353	-7	-455	425	26	-342	481	-48	-500	503	33	-471	413	-167
3723	434	-11	-569	531	30	-414	546	-85	-595	576	52	-516	281	-594
4118	489	-4	-622	603	30	-474	546	-177	-595	576	143	-1051	27	-2536
4739	777	200	-629	907	-141	-850	83	-177	-1967	886	143	-1051	27	-2536
5706	1000	571	-731	1270	-521	-1199	152	-2050	-3044	1478	3023	-2144	216	-3419
6673	917	619	-1258	1478	-419	-823	326	-3446	-3895	1895	3023	-2721	413	-3459
7608	679	245	-1258	1698	141	315	542	-3076	-4132	2274	3443	-3159	613	-3851
8510	537	-74	-3468	1837	619	1306	735	-4401	-4401	2562	3688	-3300	830	-4174
8477	751	-234	-4454	2067	1063	2372	959	-4384	-4568	2854	3344	-3527	1061	-4520
11456	1150	-245	-5040	2315	1823	3624	1406	-4307	-4598	3324	3873	-3252	1516	-5091
12765	1706	-171	-7346	2572	2727	4778	1834	-4181	-4458	3787	3758	-3252	1945	-5627
14167	1702	-308	-7706	3578	2931	5228	1859	-4186	-4333	3753	3717	-3214	1933	-5916
16101	1595	-364	-7706	3472	2653	5214	1766	-4302	-4302	3650	3717	-3214	1933	-5916
18277	1421	-453	-7530	3059	2716	5159	1536	-4022	-4022	3480	3717	-3214	1835	-5986
20950	403	-842	-8128	2130	1741	4478	644	-3043	-3043	2487	3561	-3313	1126	-5942
23774	-402	-1024	-3783	701	437	2846	-455	-3251	-3978	1141	2965	-2903	406	-5537
24850	-70	-657	-802	-102	-178	391	76	-406	-3978	1141	2965	-182	-167	-3826

CYLINDER LOAD IN KIPS, STRAIN IN  $\mu$  in/in, TORQUE ARM = 74 in

LOAD	GAGE 15	GAGE 16	GAGE 17	GAGE 18	GAGE 19	GAGE 20	GAGE 21	GAGE 22	GAGE 23	GAGE 24	GAGE 25	GAGE 26	GAGE 27	GAGE 28
0	0	0	0	0	0	0	0	0	0	0	0	0	0	0
123	-4	-4	-4	-4	-4	-4	-4	-4	-4	-4	-4	-4	-4	-4
178	-15	68	-7	-11	8	-15	-78	8	0	-11	-4	-4	0	-4
157	-70	110	-4	-65	68	-22	-110	114	4	-65	15	4	4	-7
157	-114	198	0	-95	106	-30	-197	197	26	-99	22	7	4	-4
2127	-295	247	11	-175	186	-33	-246	250	41	-182	28	7	11	-4
2756	-558	346	19	-216	235	-52	-349	361	67	-228	26	-4	15	0
3143	-463	403	45	-307	330	-52	-406	426	85	-402	33	-15	11	-4
3723	-628	488	63	-357	387	-63	-478	543	123	-531	63	-41	11	-4
4118	-828	558	120	-53	402	-80	-559	568	143	-687	63	-180	11	-11
4739	-1053	558	435	-53	569	-85	-559	594	111	-687	63	-174	19	-145
5706	-1259	1253	2175	-2009	710	-11	311	1195	-63	-1901	-22	-137	33	-385
6673	-1622	1622	2658	-2414	654	-163	345	1366	-115	-1932	-307	-33	48	-437
7608	-1991	1991	3006	-2804	626	-178	288	1571	-111	-1885	-600	104	78	-597
8510	-2359	2359	3003	-3499	858	-170	227	1765	-108	-1890	-789	233	114	-767
9477	-2659	2659	3003	-3944	858	-163	182	2007	-130	-1939	-1023	397	144	-975
11456	-3094	3094	4142	-4444	1063	-115	167	2407	-139	-2129	-1518	756	185	-1416
12765	-3590	3590	4695	-5058	1503	-150	462	2402	-550	-2654	-2097	1115	185	-1868
14167	-4156	4156	5231	-5658	1919	-189	553	3055	-605	-2706	-2375	1186	120	-1897
16101	-4808	4808	5306	-5739	2342	-260	590	3053	-635	-2728	-2409	1160	100	-1850
18277	-5398	5398	5413	-5939	2842	-280	614	3043	-654	-2728	-2423	1009	74	-1794
20950	-6006	6006	5458	-5908	3323	-280	614	3043	-654	-2728	-2423	1009	104	-1323
23774	-6708	6708	5276	-5408	3823	-274	227	2448	-253	-1939	-2183	578	155	-715
24850	-7413	7413	4822	-4899	4371	-713	-1440	1878	-230	-568	-1645	-37	274	-663
	-3499	-1891	3517	3112	421	-1705		1579	977	516	-1412	619		



# STRAIN DATA FOR SPECIMEN NO.4 AFTER 50,000 CYCLES OF FATIGUE

LOAD	GAGE 1	GAGE 2	GAGE 3	GAGE 4	GAGE 5	GAGE 6	GAGE 7	GAGE 8	GAGE 9	GAGE 10
2	-117	-126	-118	-132	-16	-104	-93	-109	-125	-129
4	-118	-222	-212	-228	-108	-312	-179	-254	-223	-215
6	-328	-334	-317	-349	-317	-338	-276	-358	-329	-317
8	-549	-462	-417	-472	-424	-459	-372	-468	-445	-499
10	-543	-580	-507	-582	-521	-554	-455	-579	-552	-491
12	-797	-776	-656	-747	-643	-668	-524	-687	-662	-589
14	-816	-953	-882	-972	-952	-861	-611	-965	-375	-1554
16	-946	-1117	-1040	-1143	-1112	-1099	-738	-1123	1018	-1817
18	-1056	-1261	-1182	-1295	-1262	-135	-844	-1255	1217	-2948
20	-1168	-1413	-1339	-1452	-1447	-1261	-854	-1411	1325	-2188
22	-1279	-1563	-1592	-1613	-1673	-1381	-1062	-1551	1361	-2291

STRAIN DATA FOR SPECIMEN MC4 AFTER 100,000 CYCLES OF FATIGUE										
LOAD	GAGE 1	GAGE 2	GAGE 3	GAGE 4	GAGE 5	GAGE 6	GAGE 7	GAGE 8	GAGE 9	GAGE 10
2	-115	-56	-108	-123	-107	-90	-107	-168	1572	-111
4	-223	-210	-204	-241	-217	-211	-204	-264	-142	-211
6	-322	-334	-290	-357	-315	-221	-244	-357	-331	-301
8	-426	-463	-400	-477	-419	-435	-388	-476	-414	-354
10	-520	-584	-492	-590	-518	-539	-470	-525	-547	-454
12	-733	-801	-671	-755	-645	-653	-530	-671	-660	-577
14	-875	-1013	-907	-1000	-1000	-860	-594	-963	-809	-1535
16	-1097	-1173	-1050	-1168	-1163	-994	-594	-1105	-899	-1762
18	-1140	-1347	-1207	-1345	-1357	-1131	-818	-1257	-746	-1931
20	-1271	-1521	-1350	-1522	-1580	-1261	-820	-1406	-1244	-2053
22	-1381	-1653	-1487	-1668	-1824	-1361	-1025	-1520	-1482	-2122
24	-1672	-2001	-1776	-2026	-2845	-1556	-1550	-1825	-1512	-2381
26	-2013	-2417	-1786	-2516	-1740	-2436	-2063	-2165	-313	-309
28	-2451	-2784	-1810	-2757	-1857	-2601	-2442	-2463	-380	-190
30	-3762	-3250	-1536	-3151	-1535	-2318	-3483	-3074	20	-145

A.2      SHEAR PANEL STRAIN DATA

The strain data obtained from all shear panel static tests and fatigue strain surveys are tabulated in this appendix. The nomenclature for the strain gages in the following tables differs from that shown in Figure 3.13. The correspondence Table A-2 below should be used to correlate the gage numbers in the strain data tables with the locations shown in Figure 3.13.

TABLE A-2. SHEAR PANEL GAGE CORRESPONDENCE TABLE. GAGES ORIENTED AS SHOWN IN FIGURE 3.13.

GAGE NO. IN FIGURE 3.13	TYPE OF GAGE	GAGE NO. IN DATA TABLES
1E	Rosette	1
		2
		3
1I	Rosette	4
		5
		6
2E	Rosette	7
		8
		9
2I	Rosette	10
		11
		12
3E	Rosette	13
		14
		15
3I	Rosette	16
		17
		18
4E	Rosette	19
		20
		21
4I	Rosette	22
		23
		24
6E	Axial	25
6I	Axial	26
8E	Axial	27
8I	Axial	28
9E	Axial	29
9I	Axial	30
10E	Axial	31
10I	Axial	32
11E	Axial	33
11I	Axial	34
12E	Axial	35
12I	Axial	36
13E	Axial	37
13I	Axial	38
5E	Shear	39
		40
5I	Shear	41
		42
7E	Shear	43
		44
7I	Shear	45
		46

- NOTES: (1) Gages 8 through 13 omitted from fatigue test panels and gages 5 and 7 assigned numbers 27 through 34 in the data tables.
- (2) After 50,000 cycles of fatigue on specimen CS4, gages 3E, 3I and the first kg of 2E were lost. All remaining strain channels numbered consecutively.

METAL SHEAR PANEL RS2 STATIC TEST

LOAD	GAGE 1	GAGE 2	GAGE 3	GAGE 4	GAGE 5	GAGE 6	GAGE 7	GAGE 8	GAGE 9	GAGE 10	GAGE 11	GAGE 12	GAGE 13	GAGE 14
-24.	-7.	-3.	-7.	-7.	-11.	-7.	-11.	-11.	-3.	-7.	-3.	-7.	-7.	-7.
300.	34.	3.	-61.	45.	6.	-42.	34.	-14.	-46.	45.	-15.	-42.	38.	-11.
597.	106.	3.	-144.	120.	14.	-102.	118.	-18.	-118.	120.	-22.	-114.	114.	-4.
1063.	163.	-3.	-217.	183.	19.	-156.	186.	-18.	-178.	180.	-15.	-174.	182.	11.
1563.	235.	-19.	-327.	284.	19.	-228.	274.	-22.	-269.	327.	-25.	-269.	277.	22.
2000.	305.	-37.	-410.	341.	19.	-277.	331.	-26.	-330.	342.	-27.	-341.	338.	33.
2500.	361.	-59.	-543.	440.	26.	-345.	489.	-22.	-421.	440.	-30.	-341.	432.	45.
3000.	419.	-82.	-650.	512.	30.	-376.	566.	-7.	-478.	516.	-33.	-527.	497.	56.
3465.	467.	-125.	-821.	643.	48.	-476.	612.	37.	-516.	622.	-30.	-527.	506.	82.
4022.	517.	-182.	-1000.	817.	178.	-808.	857.	-985.	-797.	1078.	1675.	1285.	789.	212.
4463.	563.	-137.	-1231.	1160.	257.	-979.	979.	-1786.	-1715.	1389.	2254.	1937.	930.	383.
5015.	609.	-137.	-1587.	1391.	390.	-1069.	217.	-2382.	-2994.	1704.	2544.	2237.	304.	-122.
5633.	659.	-78.	-2041.	1531.	545.	-1489.	388.	-3261.	-3541.	1935.	2715.	2534.	323.	-2262.
6000.	703.	-145.	-2491.	1787.	845.	-1560.	577.	-3695.	-3927.	2224.	3019.	2710.	493.	-3060.
6465.	752.	-267.	-2973.	2017.	939.	-1826.	764.	-4147.	-4227.	2512.	3353.	3032.	706.	-3543.
6950.	804.	-363.	-3473.	2271.	1174.	-2505.	963.	-4855.	-4474.	3227.	3740.	3415.	952.	-4197.
7450.	853.	-464.	-4071.	2504.	1534.	-3036.	1185.	-4855.	-4607.	3199.	4215.	3916.	1211.	-4516.
7950.	903.	-378.	-4589.	2771.	1946.	-3567.	1463.	-4840.	-4622.	3620.	4735.	4458.	1510.	-4909.
8450.	953.	-508.	-5109.	3000.	2336.	-4011.	1712.	-4143.	-4539.	3986.	5169.	4901.	1788.	-5221.
8950.	1003.	-593.	-5639.	3268.	2874.	-4563.	1926.	-4143.	-4459.	4516.	5704.	5424.	2133.	-5574.
9450.	1053.	-700.	-6159.	3536.	3405.	-5023.	2090.	-3900.	-4492.	4762.	5946.	5648.	2284.	-5697.
9950.	1103.	-811.	-6679.	3804.	3945.	-5483.	2279.	-3810.	-4345.	5081.	6228.	5992.	2501.	-5856.
10450.	1153.	-922.	-7199.	4072.	4453.	-5943.	2515.	-3791.	-4250.	5329.	6533.	6228.	2812.	-6061.
10950.	1203.	-1033.	-7719.	4340.	4963.	-6403.	2751.	-3641.	-4853.	5607.	6833.	6565.	3138.	-6239.
11450.	1253.	-1144.	-8239.	4608.	5473.	-6863.	2987.	-3524.	-5310.	5897.	7015.	6805.	3465.	-6395.
11950.	1303.	-1255.	-8759.	4876.	5983.	-7323.	3223.	-3407.	-5741.	6187.	7372.	7176.		

LOAD	GAGE 15	GAGE 16	GAGE 17	GAGE 18	GAGE 19	GAGE 20	GAGE 21	GAGE 22	GAGE 23	GAGE 24	GAGE 25	GAGE 26	GAGE 27	GAGE 28
-24.	-3.	-7.	-3.	-46.	0.	0.	-11.	-7.	-3.	-7.	-3.	-7.	-7.	-7.
300.	-42.	34.	-7.	-46.	45.	-7.	-49.	34.	0.	-49.	15.	-7.	-3.	-11.
593.	-106.	106.	-19.	-118.	121.	-3.	-118.	114.	-11.	-118.	30.	3.	3.	-11.
1454.	-155.	160.	-37.	-182.	186.	-4.	-171.	175.	-22.	-277.	44.	-11.	7.	-26.
1563.	-231.	236.	-63.	-235.	277.	-3.	-354.	258.	-22.	-334.	44.	-11.	7.	-30.
2000.	-300.	300.	-83.	-353.	334.	-4.	-387.	312.	-30.	-437.	44.	-11.	7.	-37.
2500.	-368.	368.	-93.	-455.	436.	0.	-436.	403.	-45.	-509.	48.	-11.	11.	-44.
2700.	-368.	368.	-93.	-455.	436.	0.	-436.	403.	-45.	-509.	48.	-11.	11.	-44.
3465.	-421.	441.	-108.	-527.	500.	4.	-509.	460.	-52.	-569.	48.	-11.	11.	-52.
4022.	-485.	528.	-130.	-626.	599.	15.	-599.	647.	-74.	-615.	44.	-11.	11.	-100.
4458.	-602.	669.	-167.	-733.	686.	134.	-686.	634.	-153.	-851.	44.	-11.	11.	-100.
5016.	-675.	735.	-178.	-873.	800.	200.	-800.	843.	-175.	-1106.	44.	-11.	11.	-100.
5633.	-739.	830.	-212.	-1022.	1060.	268.	-1060.	1064.	-219.	-1877.	4.	-11.	11.	-100.
6000.	-803.	820.	-234.	-1287.	1118.	398.	-1118.	1120.	-285.	-2371.	348.	-11.	11.	-100.
6465.	-867.	894.	-256.	-1422.	1178.	466.	-1178.	1180.	-320.	-3301.	348.	-11.	11.	-100.
6950.	-931.	955.	-278.	-1557.	1238.	534.	-1238.	1240.	-355.	-3586.	348.	-11.	11.	-100.
7450.	-995.	1000.	-300.	-1692.	1298.	602.	-1298.	1300.	-390.	-3931.	348.	-11.	11.	-100.
7950.	-1059.	1060.	-322.	-1827.	1358.	670.	-1358.	1360.	-425.	-4286.	348.	-11.	11.	-100.
8450.	-1123.	1123.	-344.	-1962.	1418.	738.	-1418.	1420.	-460.	-4631.	348.	-11.	11.	-100.
8950.	-1187.	1187.	-366.	-2097.	1478.	806.	-1478.	1480.	-495.	-4986.	348.	-11.	11.	-100.
9450.	-1251.	1251.	-388.	-2232.	1538.	874.	-1538.	1540.	-530.	-5331.	348.	-11.	11.	-100.
9950.	-1315.	1315.	-410.	-2367.	1598.	942.	-1598.	1600.	-565.	-5686.	348.	-11.	11.	-100.
10450.	-1379.	1379.	-432.	-2502.	1658.	1010.	-1658.	1660.	-600.	-6031.	348.	-11.	11.	-100.
10950.	-1443.	1443.	-454.	-2637.	1718.	1078.	-1718.	1720.	-635.	-6386.	348.	-11.	11.	-100.
11450.	-1507.	1507.	-476.	-2772.	1778.	1146.	-1778.	1780.	-670.	-6731.	348.	-11.	11.	-100.
11950.	-1571.	1571.	-498.	-2907.	1838.	1214.	-1838.	1840.	-705.	-7086.	348.	-11.	11.	-100.
12450.	-1635.	1635.	-520.	-3042.	1898.	1282.	-1898.	1900.	-740.	-7431.	348.	-11.	11.	-100.
12950.	-1699.	1699.	-542.	-3177.	1958.	1350.	-1958.	1960.	-775.	-7806.	348.	-11.	11.	-100.
13450.	-1763.	1763.	-564.	-3312.	2018.	1418.	-2018.	2020.	-810.	-8151.	348.	-11.	11.	-100.
13950.	-1827.	1827.	-586.	-3447.	2078.	1486.	-2078.	2080.	-845.	-8506.	348.	-11.	11.	-100.
14450.	-1891.	1891.	-608.	-3582.	2138.	1554.	-2138.	2140.	-880.	-8851.	348.	-11.	11.	-100.
14950.	-1955.	1955.	-630.	-3717.	2198.	1622.	-2198.	2200.	-915.	-9206.	348.	-11.	11.	-100.
15450.	-2019.	2019.	-652.	-3852.	2258.	1690.	-2258.	2260.	-950.	-9551.	348.	-11.	11.	-100.
15950.	-2083.	2083.	-674.	-3987.	2318.	1758.	-2318.	2320.	-985.	-9906.	348.	-11.	11.	-100.
16450.	-2147.	2147.	-696.	-4122.	2378.	1826.	-2378.	2380.	-1020.	-10251.	348.	-11.	11.	-100.
16950.	-2211.	2211.	-718.	-4257.	2438.	1894.	-2438.	2440.	-1055.	-10606.	348.	-11.	11.	-100.
17450.	-2275.	2275.	-740.	-4392.	2498.	1962.	-2498.	2500.	-1090.	-10651.	348.	-11.	11.	-100.
17950.	-2339.	2339.	-762.	-4527.	2558.	2030.	-2558.	2560.	-1125.	-10706.	348.	-11.	11.	-100.
18450.	-2403.	2403.	-784.	-4662.	2618.	2098.	-2618.	2620.	-1160.	-10751.	348.	-11.	11.	-100.
18950.	-2467.	2467.	-806.	-4797.	2678.	2166.	-2678.	2680.	-1195.	-10806.	348.	-11.	11.	-100.
19450.	-2531.	2531.	-828.	-4932.	2738.	2234.	-2738.	2740.	-1230.	-10851.	348.	-11.	11.	-100.
19950.	-2595.	2595.	-850.	-5067.	2798.	2302.	-2798.	2800.	-1265.	-10906.	348.	-11.	11.	-100.
20450.	-2659.	2659.	-872.	-5202.	2858.	2370.	-2858.	2860.	-1300.	-10951.	348.	-11.	11.	-100.
20950.	-2723.	2723.	-894.	-5337.	2918.	2438.	-2918.	2920.	-1335.	-11006.	348.	-11.	11.	-100.
21450.	-2787.	2787.	-916.	-5472.	2978.	2506.	-2978.	2980.	-1370.	-11051.	348.	-11.	11.	-100.
21950.	-2851.	2851.	-938.	-5607.	3038.	2574.	-3038.	3040.	-1405.	-11106.	348.	-11.	11.	-100.
22450.	-2915.	2915.	-960.	-5742.	3098.	2642.	-3098.	3050.	-1440.	-11151.	348.	-11.	11.	-100.
22950.	-2979.	2979.	-982.	-5877.	3158.	2710.	-3158.	3160.	-1475.	-11206.	348.	-11.	11.	-100.
23450.	-3043.	3043.	-1004.	-6012.	3218.	2778.	-3218.	3220.	-1510.	-11251.	348.	-11.	11.	-100.
23950.	-3107.	3107.	-1026.	-6147.	3278.	2846.	-3278.	3280.	-1545.	-11306.	348.	-11.	11.	-100.
24450.	-3171.	3171.	-1048.	-6282.	3338.	2914.	-3338.	3340.	-1580.	-11351.	348.	-11.	11.	-100.
24950.	-3235.	3235.	-1070.	-6417.	3398.	2982.	-3398.	3400.	-1615.	-11406.	348.	-11.	11.	-100.
25450.	-3299.	3299.	-1092.	-6552.	3458.	3050.	-3458.	3060.	-1650.	-11451.	348.	-11.	11.	-100.
25950.	-3363.	3363.	-1114.	-6687.	3518.	3118.	-3518.	3120.	-1685.	-11506.	348.	-11.	11.	-100.
26450.	-3427.	3427.	-1136.	-6822.	3578.	3186.	-3578.	3188.	-1720.	-11551.	348.	-11.	11.	-100.
26950.	-3491.	3491.	-1158.	-6957.	3638.	3254.	-3638.	3256.	-1755.	-11606.	348.	-11.	11.	-100.
27450.	-3555.	3555.	-1180.	-7092.	3698.	3322.	-3698.	3324.	-1790.	-11651.	348.	-11.	11.	-100.
27950.	-3619.	3619.	-1202.	-7227.	3758.	3390.	-3758.	3392.	-1825.	-11706.	348.	-11.	11.	-100.
28450.	-3683.	3683.	-1224.	-7362.	3818.	3458.	-3818.	3460.	-1860.	-11751.	348.	-11.	11.	-100.
28950.	-3747.	3747.	-1246.	-7497.	3878.	3526.	-3878.	3528.	-1895.	-11806.	348.	-11.	11.	-100.
29450.	-3811.	3811.	-1268.	-7632.	3938.	3594.	-3938.	3596.	-1930.	-11851.	348.	-11.	11.	-100.
29950.	-3875.	3875.	-1290.	-7767.	3998.	3662.	-3998.	3664.	-1965.	-11906.	348.	-11.	11.	-100.
30450.	-3939.	3939.	-1312.	-7902.	4058.	3730.	-4058.	3732.	-2000.	-11951.	348.	-11.	11.	-100.
30950.	-4003.	4003.	-1334.	-8037.	4118.	3798.	-4098.	3792.	-2035.	-12006.	348.	-11.	11.	-100.
31450.	-4067.	4067.	-1356.	-8172.	4178.	3866.	-4098.	3860.	-2070.	-12051.	348.	-11.	11.	-100.
31950.	-4131.	4131.	-1378.	-8307.	4238.	3934.	-4178.	3936.	-2105.	-12106.	348.	-11.	11.	-100.
32450.	-4195.	4195.	-1400.	-8442.	4298.	4002.	-4238.	4004.	-2140.	-12151.	348.	-11.	11.	-100.
32950.	-4259.	4259.	-1422.	-8577.	4358.	4070.	-4298.	4072.	-2175.	-12206.	348.	-11.	11.	-100.
33450.	-4323.	4323.	-1444.	-8712.	4418.	4138.	-4358.	4140.	-2210.	-12251.	348.	-11.	11.	-100.
33950.	-4387.	4387.	-1466.	-8847.	4478.	4206.	-4418.	4208.	-2245.	-12306.	348.	-11.	11.	-100.
34450.	-4451.	4451.	-1488.	-8982.	4538.	4274.	-4478.	4276.	-2280.	-12351.	348.	-11.	11.	-100.
34950.	-4515.	4515.	-1510.	-9117.	4598.	4342.	-4538.	4344.	-2315.	-12406.	348.	-11.	11.	-100.
35450.	-4579.	4579.	-1532.	-9252.	4658.	4410.	-4598.	4412.	-2350.	-12451.	348.	-11.	11.	-100.
35950.	-4643.	4643.	-1554.	-9387.	4718.	4478.	-4658.	4480.	-2385.	-12506.	348.	-11.	11.	-100.
36450.	-4707.	4707.	-1576.	-9522.	4778.	4546.	-4718.	4548.	-2420.	-12551.	348.	-11.	11.	-100.
36950.	-4771.	4771.	-1598.	-9657.	4838.	4614.	-4778.	4616.	-2455.	-12606.	348.	-11.	11.	-100.
37450.	-4835.	4835.	-1620.	-9792.	4898.	4682.	-4838.	4684.	-2490.	-12651.	348.	-11.	11.	-100.
37950.	-4899.	4899.	-1642.	-9927.	4958.	4750.	-4898.	4752.	-2525.	-12706.	348.	-11.	11.	-100.
38450.	-4963.	4963.	-1664.	-10062.	5018.	4818.	-4958.	4820.	-2560.	-12751.	348.	-11.	11.	-100.
38950.	-5027.	5027.	-1686.	-10197.	5078.	4886.	-5018.	4888.	-2595.	-12806.	348.	-11.	11.	-100.
39450.	-5091.	5091.	-1708.	-10332.	5138.	4954.	-5078.	4956.	-2630.	-12851.	348.	-11.	11.	-100.
39950.	-5155.	5155.	-1730.	-10467.	5198.	5022.	-5138.	5024.	-2665.	-12906.	348.	-11.	11.	-100.
40450.	-5219.	5219.	-1752.	-10602.	5258.	5090.	-5198.	5092.	-2700.	-12951.	348.	-11.	11.	-100.
40950.	-5283.	5283.	-1774.	-10737.	5318.	5158.	-5258.	5160.	-2735.	-13006.	348.	-11.	11.	-100.
41450.	-5347.	5347.	-1796.	-10872.	5378.	5226.	-5318.	5228.	-2770.	-13051.	348.	-11.	11.	-100.
41950.	-5411.	5411.	-1818.	-11007.	5438.	5294.	-5378.	5296.	-2805.	-13106.	348.	-11.	11.	-100.
42450.	-5475.	5475.	-1840.	-11142.	5498.	5362.	-5438.	5364.	-2840.	-13151.	348.	-11.	11.	-100.
42950.	-5539.	5539.	-1862.	-11277.	5558.	5430.	-5498.	5432.	-2875.	-13206.	348.	-11.	11.	-100.
43450.	-5603.	5603.	-1884.	-11412.	5618.	5498.	-5558.	5500.	-2910.	-13251.	348.	-11.	11.	-100.
43950.	-5667.	5667.	-1906.	-11547.	5678.	5566.	-5618.	5568.	-2945.	-13306.	348.	-11.	11.	-100.
44450.	-5731.	5731.	-1928.	-11682.	5738.	5634.	-5678.	5636.	-2980.	-13351.	348.	-11.	11.	-100.
44950.	-5795.	5795.	-1950.	-11817.	5798.	5702.	-5738.	5704.	-3015.	-13406.	348.	-11.	11.	-100.
45450.	-5859.	5859.	-1972.	-11952.	5858.	5770.	-5798.	5772.	-3050.	-13451.	348.	-11.	11.	-100.
45950.	-5923.	592												

# RETAL SHEAR PANEL MS2 STATIC TEST

LOAD	GAGE29	GAGE30	GAGE31	GAGE32	GAGE33	GAGE34	GAGE35	GAGE36	GAGE37	GAGE38	GAGE39	GAGE40	GAGE41	GAGE42
-24.	-11.	-11.	-7.	-7.	-3.	7.	-3.	-3.	-11.	-3.	-7.	-7.	6.	-7.
308.	0.	-11.	-4.	-4.	-3.	7.	-3.	-11.	4.	3.	-7.	23.	-8.	4.
893.	0.	-11.	-4.	-11.	-3.	-7.	-3.	-15.	19.	11.	-4.	23.	-4.	15.
1454.	7.	-11.	-15.	-19.	-3.	11.	-3.	-19.	22.	22.	-8.	30.	4.	15.
2309.	4.	-11.	-37.	-44.	-3.	-4.	-15.	-26.	15.	26.	-11.	34.	4.	11.
3453.	7.	-22.	-48.	-52.	-3.	0.	-10.	-39.	30.	30.	-15.	34.	4.	4.
4453.	0.	-11.	-58.	-52.	-3.	0.	-30.	-33.	4.	41.	-11.	42.	8.	4.
5015.	-4.	7.	-59.	-48.	-3.	-7.	-41.	-37.	7.	52.	-4.	53.	8.	4.
5833.	-15.	70.	-59.	-22.	15.	-11.	-59.	-37.	-7.	63.	34.	61.	8.	11.
6833.	-37.	108.	-122.	-44.	33.	-59.	-67.	-32.	85.	122.	61.	23.	-73.	103.
7093.	-70.	41.	-315.	-48.	63.	-107.	-74.	-15.	-67.	130.	76.	-141.	-149.	103.
8029.	-93.	-33.	-308.	-11.	82.	-370.	-81.	-156.	-130.	245.	53.	-228.	-394.	72.
8855.	-111.	-104.	-319.	10.	89.	-518.	-93.	-196.	-174.	289.	15.	-285.	-520.	-107.
9853.	-130.	-174.	-290.	22.	96.	-609.	-93.	-245.	-211.	289.	-42.	-315.	-839.	-91.
10803.	-141.	-260.	-263.	7.	95.	-847.	-85.	-308.	-237.	248.	-141.	-315.	-723.	-57.
11873.	-159.	-371.	-282.	-33.	82.	-1106.	-70.	-397.	-263.	130.	-312.	-247.	-742.	8.
12745.	-159.	-487.	-174.	-33.	7.	-1343.	-63.	-511.	-282.	-11.	-586.	-118.	-757.	87.
13656.	-152.	-608.	-130.	-152.	-88.	-1512.	-59.	-609.	-293.	-163.	-898.	34.	-800.	171.
14587.	-152.	-772.	-59.	-248.	-174.	-1642.	-52.	-671.	-263.	-274.	-1175.	171.	-842.	255.
15798.	-141.	-848.	-53.	-266.	-552.	-1740.	-56.	-730.	-245.	-367.	-1411.	274.	-887.	201.
16702.	-137.	-847.	7.	-363.	-463.	-1071.	-52.	-778.	-204.	-460.	-1677.	388.	-922.	258.
17010.	-137.	-1031.	74.	-456.	-634.	-2141.	-52.	-875.	-156.	-552.	-1997.	581.	-930.	460.
18023.	-133.	-1135.	108.	-553.	-707.	-3233.	-52.	-993.	-85.	-640.	-2453.	889.	-1121.	647.
18787.	-126.	-1232.	233.	-700.	-923.	-2407.	-52.	-1119.	0.	-730.	-2933.	1246.	-1282.	902.
						-3525.	-63.	-1227.	78.	-771.	-3401.	1611.	-1420.	1202.

LOAD	GAGE43	GAGE44	GAGE45	GAGE46
-24.	-7.	-7.	-8.	-7.
308.	-7.	-4.	-11.	-7.
893.	0.	0.	-8.	-4.
1454.	0.	8.	-11.	0.
1953.	15.	8.	-10.	0.
2309.	23.	8.	-27.	-4.
3453.	27.	8.	-38.	-4.
4453.	27.	11.	-48.	4.
5015.	42.	11.	-58.	4.
5833.	27.	76.	-175.	57.
6833.	-38.	133.	-270.	72.
7093.	-61.	213.	-400.	-381.
8029.	-76.	270.	-557.	-855.
8855.	-103.	278.	-773.	-1353.
9853.	-175.	217.	-897.	-1823.
10803.	-308.	89.	-1168.	-2301.
11873.	-518.	-332.	-1401.	-2800.
12745.	-723.	-602.	-1608.	-3366.
13656.	-800.	-1050.	-1849.	-3876.
14587.	-1024.	-1377.	-2046.	-4290.
15798.	-1150.	-1620.	-2246.	-4525.
16702.	-1255.	-1801.	-2421.	-4955.
17010.	-1493.	-2240.	-2813.	-5403.
18023.	-1687.	-2746.	-3308.	-6015.
18787.	-1851.	-3256.	-3843.	-6853.
		-3732.	-4303.	-7393.

PETAL SHEAR PANEL MS3 RESIDUAL STRENGTH TEST

LOAD	GAGE 1	GAGE 2	GAGE 3	GAGE 4	GAGE 5	GAGE 6	GAGE 7	GAGE 8	GAGE 9	GAGE 10	GAGE 11	GAGE 12	GAGE 13	GAGE 14
-24.	-7.	-3.	-7.	-3.	-7.	-4.	-7.	-7.	-7.	-11.	-3.	-11.	-3.	-7.
484.	57.	7.	-63.	61.	7.	-57.	57.	-19.	-61.	53.	-3.	-65.	53.	-18.
982.	110.	15.	-121.	118.	22.	-102.	114.	-33.	-110.	114.	-3.	-106.	98.	-30.
1476.	170.	4.	-212.	197.	19.	-175.	190.	-37.	-194.	194.	-7.	-198.	178.	-37.
1986.	248.	-7.	-311.	273.	19.	-243.	259.	-45.	-281.	274.	0.	-270.	254.	-45.
2489.	314.	-18.	-402.	349.	22.	-304.	346.	-56.	-361.	353.	4.	-342.	330.	-52.
2977.	378.	-33.	-504.	422.	22.	-361.	413.	-59.	-448.	437.	15.	-418.	406.	-56.
3461.	435.	-45.	-606.	502.	30.	-414.	489.	-74.	-527.	517.	22.	-581.	478.	-56.
3959.	515.	-48.	-729.	603.	56.	-455.	589.	-78.	-603.	612.	30.	-680.	565.	-45.
4453.	572.	-74.	-849.	682.	78.	-471.	667.	-74.	-664.	703.	2236.	-684.	649.	-1993.
4937.	627.	-56.	-969.	781.	106.	-1078.	797.	-806.	-874.	1241.	2477.	-1964.	-27.	-2821.
5478.	687.	616.	-1081.	1053.	124.	-1305.	861.	-896.	-9013.	1550.	2715.	-2174.	-11.	-3045.
5970.	748.	727.	-1201.	1153.	153.	-1404.	136.	-3212.	-3271.	1751.	2937.	-2580.	65.	-3365.
6462.	807.	748.	-1327.	1255.	158.	-1532.	284.	-3461.	-3541.	1941.	3138.	-2773.	167.	-3599.
6946.	867.	660.	-1443.	1353.	140.	-1674.	352.	-3685.	-3791.	2124.	3342.	-2773.	273.	-3829.
7435.	911.	660.	-1563.	1443.	149.	-1815.	425.	-3823.	-4069.	2317.	3547.	-2773.	387.	-4067.
7923.	963.	690.	-1673.	1554.	182.	-1958.	500.	-4179.	-4334.	2519.	3728.	-3168.	512.	-4290.
8403.	1015.	83.	-1786.	1673.	182.	-2057.	571.	-4386.	-4584.	2713.	3888.	-3447.	630.	-4502.
8881.	1067.	83.	-1896.	1794.	509.	-2171.	648.	-4590.	-4823.	2893.	3988.	-3503.	751.	-4699.
9361.	1119.	-153.	-2006.	1893.	813.	-2281.	897.	-4800.	-5024.	3092.	4022.	-3636.	880.	-4822.
9845.	1171.	-185.	-2116.	1993.	1022.	-2391.	948.	-4909.	-5229.	3288.	4141.	-3736.	1044.	-4922.

LOAD	GAGE 15	GAGE 16	GAGE 17	GAGE 18	GAGE 19	GAGE 20	GAGE 21	GAGE 22	GAGE 23	GAGE 24	GAGE 25	GAGE 26	GAGE 27	GAGE 28
-24.	0.	-7.	-3.	-7.	0.	-11.	-3.	-3.	-7.	-3.	-3.	-7.	-3.	-7.
484.	-57.	53.	-3.	-61.	53.	-22.	-68.	61.	-7.	-49.	11.	0.	0.	7.
982.	-104.	106.	-3.	-106.	99.	-33.	-121.	114.	-4.	-87.	22.	7.	-3.	23.
1476.	-160.	186.	-3.	-185.	167.	-45.	-216.	190.	11.	-153.	22.	4.	-3.	34.
1986.	-281.	278.	0.	-274.	243.	-59.	-311.	269.	30.	-235.	19.	-4.	-3.	42.
2489.	-356.	346.	0.	-353.	311.	-74.	-408.	345.	41.	-300.	15.	-4.	0.	50.
2977.	-436.	425.	0.	-433.	376.	-93.	-497.	428.	56.	-364.	22.	-7.	0.	61.
3461.	-512.	505.	-3.	-517.	440.	-112.	-588.	504.	71.	-485.	15.	-11.	-3.	84.
3959.	-588.	586.	-3.	-584.	516.	-134.	-694.	595.	93.	-550.	26.	-19.	8.	122.
4453.	-658.	653.	-15.	-659.	584.	-160.	-786.	675.	119.	-604.	33.	-405.	84.	145.
4937.	-730.	723.	1493.	-721.	670.	-185.	-886.	786.	14.	-674.	182.	-349.	61.	199.
5478.	-803.	791.	2501.	-791.	725.	-201.	-981.	881.	52.	-744.	325.	-271.	23.	257.
5970.	-878.	868.	2510.	-868.	788.	-249.	-1071.	971.	63.	-826.	457.	-178.	-80.	0.
6462.	-948.	937.	2520.	-937.	833.	-296.	-1161.	1061.	134.	-917.	575.	-89.	-145.	-61.
6946.	-1018.	1007.	2530.	-1007.	880.	-346.	-1251.	1151.	231.	-1007.	626.	-180.	-145.	-99.
7435.	-1088.	1077.	2540.	-1077.	927.	-396.	-1341.	1241.	341.	-1097.	726.	-180.	-145.	-221.
7923.	-1158.	1147.	2550.	-1147.	974.	-446.	-1431.	1331.	390.	-1187.	817.	-180.	-145.	-266.
8403.	-1228.	1217.	2560.	-1217.	1020.	-496.	-1521.	1421.	439.	-1277.	908.	-180.	-145.	-315.
8881.	-1298.	1287.	2570.	-1287.	1067.	-546.	-1611.	1511.	488.	-1367.	999.	-180.	-145.	-360.
9361.	-1368.	1357.	2580.	-1357.	1113.	-596.	-1701.	1601.	537.	-1457.	1090.	-180.	-145.	-408.
9845.	-1438.	1427.	2590.	-1427.	1160.	-646.	-1791.	1691.	586.	-1547.	1181.	-180.	-145.	-458.

# METAL SHEAR PANEL MS3 RESIDUAL STRENGTH TEST

LOAD	GAGE29	GAGE30	GAGE31	GAGE32	GAGE33	GAGE34
-24.	-4.	-7.	-7.	-7.	-8.	-3.
484.	-8.	11.	-7.	-11.	-4.	-11.
932.	-16.	30.	-15.	-11.	-8.	-7.
1476.	-24.	30.	-23.	-11.	-8.	0.
1985.	-24.	30.	-27.	-15.	0.	-7.
2469.	-23.	30.	-30.	-11.	0.	-4.
2977.	-23.	27.	-30.	-15.	4.	4.
3461.	-36.	30.	-34.	-11.	0.	4.
3960.	-36.	34.	-38.	-15.	0.	15.
4453.	-36.	34.	-34.	-7.	8.	19.
4937.	-263.	-175.	-80.	-427.	-118.	188.
5479.	-364.	-238.	-186.	-724.	-164.	268.
5978.	-473.	-278.	-133.	-988.	-231.	236.
6422.	-570.	-300.	-145.	-1268.	-278.	255.
6946.	-666.	-369.	-160.	-1512.	-312.	255.
7465.	-736.	-407.	-171.	-1775.	-346.	249.
7853.	-829.	-441.	-171.	-2034.	-373.	118.
8423.	-930.	-456.	-152.	-2262.	-386.	-11.
8931.	-1032.	-468.	-179.	-2532.	-407.	-302.
9416.	-1145.	-477.	-205.	-2795.	-386.	-465.
9906.	-1278.	-392.	-247.	-3092.	-382.	



METAL SHEAR PANEL RS4 RESIDUAL STRENGTH TEST

LOAD	GAGE29	GAGE30	GAGE31	GAGE32	GAGE33	GAGE34
-24.	-8.	0.	-3.	0.	-3.	0.
37.	-4.	11.	-11.	-15.	-3.	4.
886.	-4.	11.	-31.	-30.	0.	4.
1889.	-4.	15.	-40.	-40.	3.	0.
2372.	0.	15.	-57.	-88.	3.	0.
2809.	0.	19.	-73.	-87.	8.	4.
3354.	4.	30.	-88.	-90.	0.	11.
3840.	4.	34.	-103.	-118.	0.	8.
4357.	0.	38.	-118.	-133.	-3.	11.
4889.	75.	27.	-180.	-98.	-11.	-30.
5373.	63.	11.	-264.	-60.	-15.	-141.
5857.	59.	-30.	-341.	-34.	-23.	-384.
6341.	29.	-84.	-417.	0.	-42.	-486.
6874.	4.	-177.	-424.	34.	-61.	-676.
7303.	-37.	-183.	-570.	49.	-103.	-874.
7825.	-70.	-227.	-686.	38.	-149.	-1083.
8374.	-141.	-270.	-774.	-15.	-246.	-1296.
8858.	-211.	-312.	-806.	-87.	-270.	-1520.
9357.	-262.	-358.	-1011.	-170.	-331.	-1736.
9875.	-373.	-464.	-1145.	-280.	-407.	-1886.
	-472.		-1283.	-414.	-486.	-2210.

METAL SHEAR PANEL M34 RESIDUAL STRENGTH TEST

LOAD	GAGE 1	GAGE 2	GAGE 3	GAGE 4	GAGE 5	GAGE 6	GAGE 7	GAGE 8	GAGE 9	GAGE 10	GAGE 11	GAGE 12	GAGE 13	GAGE 14
-34.	-7.	-7.	-11.	0.	-3.	-3.	-16.	-3.	-3.	-3.	-7.	-3.	-3.	-3.
387.	57.	11.	-51.	61.	3.	-53.	67.	-7.	-57.	57.	11.	-43.	53.	-11.
896.	144.	15.	-152.	159.	-3.	-144.	144.	-11.	-152.	144.	-11.	-136.	144.	-11.
1386.	238.	16.	-242.	250.	-11.	-235.	228.	-14.	-243.	228.	-11.	-228.	231.	-19.
1888.	319.	17.	-331.	353.	-19.	-334.	319.	-56.	-343.	319.	-11.	-384.	319.	-22.
2372.	410.	37.	-411.	447.	-26.	-425.	407.	-41.	-448.	406.	0.	-478.	406.	-26.
2890.	508.	52.	-487.	553.	-30.	-519.	498.	-59.	-543.	497.	19.	-548.	493.	-37.
3354.	598.	67.	-552.	648.	-45.	-618.	556.	-93.	-648.	581.	41.	-595.	573.	-52.
3848.	693.	80.	-609.	743.	-67.	-722.	619.	-145.	-767.	664.	78.	-546.	641.	-74.
4357.	792.	101.	-682.	843.	-94.	-804.	728.	-185.	-857.	745.	810.	-527.	657.	-2291.
4883.	892.	117.	-761.	944.	-124.	-883.	858.	-236.	-957.	845.	1422.	-592.	715.	-2592.
5373.	995.	133.	-831.	1017.	-152.	-962.	944.	-283.	-1059.	943.	1995.	-533.	91.	-2841.
5877.	1098.	150.	-900.	1111.	-180.	-1038.	1017.	-322.	-1159.	1060.	2280.	-597.	182.	-3168.
6374.	1201.	167.	-961.	1214.	-208.	-1109.	1111.	-363.	-1268.	1166.	2581.	-641.	269.	-3361.
6874.	1304.	184.	-1022.	1317.	-236.	-1180.	1214.	-403.	-1378.	1266.	2841.	-689.	264.	-3554.
7382.	1407.	201.	-1083.	1420.	-264.	-1251.	1317.	-443.	-1489.	1360.	3067.	-737.	259.	-3751.
7897.	1510.	218.	-1144.	1523.	-292.	-1322.	1420.	-483.	-1600.	1459.	3283.	-785.	259.	-3940.
8374.	1613.	235.	-1205.	1626.	-320.	-1393.	1523.	-523.	-1711.	1554.	3480.	-833.	259.	-4122.
8858.	1716.	252.	-1266.	1729.	-348.	-1464.	1626.	-563.	-1822.	1647.	3678.	-881.	259.	-4278.
9357.	1819.	269.	-1327.	1832.	-376.	-1535.	1729.	-603.	-1933.	1732.	3876.	-929.	259.	-4438.
9876.	1922.	286.	-1388.	1945.	-404.	-1606.	1832.	-643.	-2044.	1832.	3962.	-977.	1986.	-4579.

LOAD	GAGE 15	GAGE 16	GAGE 17	GAGE 18	GAGE 19	GAGE 20	GAGE 21	GAGE 22	GAGE 23	GAGE 24	GAGE 25	GAGE 26	GAGE 27	GAGE 28
-24.	-7.	-3.	-7.	0.	0.	-3.	-3.	-3.	-7.	-3.	-3.	-3.	-3.	-3.
387.	-57.	53.	-3.	-140.	57.	-15.	-57.	49.	0.	-49.	11.	-3.	8.	19.
896.	-156.	148.	-3.	-140.	136.	-22.	-153.	148.	7.	-129.	15.	-3.	15.	42.
1386.	-247.	236.	-3.	-228.	219.	-37.	-258.	236.	22.	-239.	27.	-11.	27.	61.
1888.	-337.	327.	0.	-319.	305.	-48.	-364.	331.	37.	-385.	7.	-19.	34.	90.
2372.	-428.	422.	3.	-405.	371.	-53.	-457.	422.	52.	-451.	11.	-22.	42.	103.
2890.	-519.	508.	15.	-485.	461.	-78.	-562.	508.	78.	-542.	11.	-38.	57.	123.
3354.	-610.	604.	22.	-582.	547.	-97.	-640.	604.	100.	-618.	11.	-48.	69.	145.
3848.	-701.	688.	37.	-665.	622.	-123.	-740.	691.	130.	-748.	15.	-74.	88.	160.
4357.	-792.	784.	52.	-744.	701.	-152.	-822.	784.	160.	-822.	0.	-74.	100.	175.
4883.	-883.	871.	67.	-826.	784.	-172.	-904.	871.	190.	-904.	0.	-74.	120.	190.
5373.	-974.	962.	82.	-917.	883.	-192.	-985.	962.	220.	-985.	0.	-74.	141.	215.
5877.	-1065.	1053.	97.	-1008.	984.	-212.	-1065.	1053.	250.	-1065.	0.	-74.	161.	240.
6374.	-1156.	1144.	112.	-1109.	1084.	-232.	-1156.	1144.	280.	-1156.	0.	-74.	181.	265.
6874.	-1247.	1235.	127.	-1190.	1165.	-252.	-1247.	1235.	310.	-1247.	0.	-74.	201.	290.
7382.	-1338.	1326.	142.	-1281.	1256.	-272.	-1338.	1326.	340.	-1338.	0.	-74.	221.	315.
7897.	-1429.	1417.	157.	-1372.	1347.	-292.	-1429.	1417.	370.	-1429.	0.	-74.	241.	340.
8374.	-1520.	1508.	172.	-1463.	1438.	-312.	-1520.	1508.	400.	-1520.	0.	-74.	261.	365.
8858.	-1611.	1599.	187.	-1554.	1529.	-332.	-1611.	1599.	430.	-1611.	0.	-74.	281.	390.
9357.	-1702.	1690.	202.	-1645.	1615.	-352.	-1702.	1690.	460.	-1702.	0.	-74.	301.	415.
9876.	-1793.	1781.	217.	-1736.	1711.	-372.	-1793.	1781.	490.	-1793.	0.	-74.	321.	440.

POSTBUCKLED ALUM. SHEAR PANEL MSS PRE-FATIGUE STRAIN SURVEY

LOAD	GAGE 1	GAGE 2	GAGE 3	GAGE 4	GAGE 5	GAGE 6	GAGE 7	GAGE 8	GAGE 9	GAGE 10	GAGE 11	GAGE 12	GAGE 13	GAGE 14
48.	-7.	3.	-7.	-3.	3.	-3.	-7.	-3.	-3.	0.	-11.	-3.	-7.	-3.
916.	136.	-29.	-220.	189.	7.	-159.	163.	-37.	-216.	170.	18.	-147.	166.	-18.
1881.	289.	-63.	-440.	394.	29.	-895.	382.	-111.	-459.	356.	70.	-273.	333.	-55.
2894.	427.	-92.	-706.	606.	49.	-482.	420.	-304.	-804.	561.	227.	-307.	470.	-129.
3859.	613.	22.	-1067.	1013.	-111.	-565.	224.	-1550.	-2007.	586.	1317.	842.	481.	-445.
4872.	632.	92.	-1717.	1340.	-156.	-462.	305.	-2236.	-2709.	1449.	1972.	1461.	455.	-1149.
5885.	682.	-44.	-2428.	1690.	70.	0.	577.	-2515.	-3134.	1779.	2333.	1764.	538.	-1710.
6898.	643.	-178.	-3065.	1859.	342.	512.	778.	-2915.	-3487.	2087.	2605.	1996.	675.	-2192.
7911.	761.	-263.	-3639.	2090.	587.	967.	972.	-3160.	-3794.	2387.	2836.	2189.	834.	-2630.

LOAD	GAGE 15	GAGE 16	GAGE 17	GAGE 18	GAGE 19	GAGE 20	GAGE 21	GAGE 22	GAGE 23	GAGE 24	GAGE 25	GAGE 26	GAGE 27	GAGE 28
48.	-3.	-3.	3.	-3.	-3.	-7.	-3.	-11.	3.	-3.	0.	0.	-7.	0.
916.	-182.	155.	0.	-159.	-129.	-59.	-107.	205.	62.	-163.	3.	-22.	-30.	-3.
1881.	-372.	322.	29.	-393.	269.	-104.	-394.	425.	122.	-326.	7.	-45.	-57.	-7.
2894.	-581.	527.	89.	-435.	428.	-144.	-584.	668.	196.	-516.	11.	-49.	-76.	-22.
3859.	-832.	796.	363.	-263.	637.	-167.	-721.	230.	270.	-843.	22.	-54.	-190.	-57.
4872.	-1466.	1108.	1017.	-276.	861.	-189.	-717.	1318.	292.	-1363.	34.	-114.	-502.	-38.
5885.	-2351.	1423.	1533.	769.	948.	-245.	-622.	1527.	229.	-1732.	45.	-167.	-830.	34.
6898.	-2593.	1741.	1979.	1201.	994.	-260.	-575.	1686.	151.	-1952.	49.	-213.	-1182.	143.
7911.	-3115.	2066.	2305.	1603.	1062.	-260.	-485.	1834.	96.	-2047.	53.	-247.	-1519.	296.

LOAD	GAGE 29	GAGE 30	GAGE 31	GAGE 32	GAGE 33	GAGE 34
48.	-3.	-3.	3.	-7.	-3.	-3.
916.	7.	7.	-15.	-26.	18.	-3.
1881.	25.	-37.	-34.	-34.	49.	-11.
2894.	55.	-96.	-49.	-45.	98.	-28.
3859.	74.	-259.	-87.	-72.	235.	-87.
4872.	-89.	-286.	-87.	-183.	269.	-121.
5885.	-278.	-196.	-60.	-398.	129.	-129.
6898.	-478.	-89.	-19.	-437.	129.	-133.
7911.	-657.	14.	22.	-552.	18.	-133.

POSTBUCKLED METAL SHEAR PANEL NSS PRE-FATIGUE STRAIN SURVEY

LOAD	GAGE 1	GAGE 2	GAGE 3	GAGE 4	GAGE 5	GAGE 6	GAGE 7	GAGE 8	GAGE 9	GAGE 10	GAGE 11	GAGE 12	GAGE 13	GAGE 14
-48.	-3.	-7.	-7.	3.	-7.	-7.	-7.	-7.	-3.	-3.	-3.	-7.	-7.	0.
-820.	-193.	-39.	148.	-142.	0.	156.	159.	-15.	-183.	156.	0.	-167.	160.	7.
1833.	-422.	-53.	316.	-293.	3.	355.	338.	-34.	-385.	338.	11.	-343.	350.	11.
8700.	-651.	-79.	476.	-411.	19.	642.	517.	-76.	-595.	521.	57.	-492.	526.	11.
3011.	-914.	-99.	625.	-495.	34.	756.	651.	-197.	-866.	716.	152.	-595.	633.	-7.
4521.	-1662.	439.	842.	-873.	-265.	1241.	163.	-2468.	-2817.	1325.	2118.	1599.	331.	-1789.
5789.	-1263.	597.	960.	-1059.	-110.	1478.	373.	-3119.	-3504.	1808.	2727.	2175.	507.	-2880.
6962.	-1491.	643.	1975.	-1614.	121.	1658.	616.	-3609.	-4072.	2220.	3172.	2591.	766.	-3438.
7061.	-1693.	699.	1258.	-949.	365.	1864.	898.	-4058.	-4641.	2639.	3675.	2985.	1067.	-3871.

PLEASE MAKE A COPY AND HIT ON

COMPOSITE SHEAR PANEL CS1 STATIC TEST

LOAD	GAGE 1	GAGE 2	GAGE 3	GAGE 4	GAGE 5	GAGE 6	GAGE 7	GAGE 8	GAGE 9	GAGE 10	GAGE 11	GAGE 12	GAGE 13	GAGE 14
0	-3	-3	-3	0	0	-7	-3	0	0	-7	-3	3	-7	-3
508	19	-15	-23	-31	-11	15	23	0	-23	22	-8	-23	11	-3
1015	76	0	-76	-76	-8	65	76	-4	-69	89	-15	-76	88	-1
1475	133	-34	-141	-145	-27	122	137	11	-137	153	-23	-145	137	-11
1934	202	-57	-214	-217	-42	183	206	0	-206	229	-30	-229	214	-11
2553	274	-84	-301	-301	-61	256	286	27	-286	317	-42	-324	301	-11
3045	342	-103	-378	-370	-76	317	358	42	-351	389	-57	-412	378	-11
3506	403	-122	-439	-431	-87	370	419	61	-401	450	-80	-480	443	-11
3963	463	-145	-515	-506	-95	431	492	91	-443	507	-110	-595	515	-15
4437	523	-164	-595	-587	-99	492	568	160	-450	553	-194	-717	588	-15
4904	581	-205	-700	-693	-8	603	689	237	-488	675	-327	-1530	717	202
5371	641	-255	-826	-818	418	693	789	320	-502	775	-440	-3044	811	2807
5871	701	-317	-986	-978	869	1434	1917	387	-564	175	-5379	-4612	1671	3549
6354	764	-385	-1188	-1180	1144	1625	2367	477	-638	190	-5879	-4893	2156	4009
6805	824	-455	-1375	-1367	2006	1893	2763	594	-736	237	-5291	-4239	2537	4870
7285	885	-537	-1510	-1502	2775	2504	3507	850	-800	294	-4770	-3674	2590	5439
7791	945	-627	-1693	-1685	3431	3239	4387	1915	-877	355	-4295	-3155	2617	5480
8291	1005	-727	-1875	-1867	4166	4023	5387	2638	-957	425	-3777	-2675	2760	5153
8791	1065	-827	-2057	-2049	4895	4752	6767	3458	-1039	495	-3436	-2121	2888	5172
9291	1125	-927	-2239	-2231	5624	5481	8183	4275	-1119	565	-2239	-1507	2808	5199
9791	1185	-1027	-2421	-2413	6353	6210	9593	5093	-1201	635	-2519	-1413	2808	5518
10291	1245	-1127	-2603	-2595	7082	6939	10993	5903	-1283	705	-2519	-1413	2808	5518

LOAD	GAGE 15	GAGE 16	GAGE 17	GAGE 18	GAGE 19	GAGE 20	GAGE 21	GAGE 22	GAGE 23	GAGE 24	GAGE 25	GAGE 26	GAGE 27	GAGE 28
0	-3	-3	-3	3	-7	0	0	-7	0	-7	-3	-3	-7	-3
508	-15	11	-7	-15	11	-4	-19	15	-4	-15	0	-3	-11	0
1015	-64	57	-7	-61	57	-4	-73	72	-8	-57	0	3	3	0
1475	-137	114	-7	-130	118	0	-149	137	0	-118	0	8	0	8
1934	-213	170	-4	-202	170	8	-233	217	8	-187	3	11	8	8
2553	-281	252	-4	-269	252	15	-322	305	11	-262	3	23	-8	11
3045	-351	313	-4	-352	320	23	-416	381	23	-322	3	27	-11	15
3506	-426	374	0	-423	374	27	-485	446	23	-389	3	34	-15	23
3963	-502	439	4	-495	439	34	-555	519	30	-454	3	39	-27	31
4437	-578	495	11	-561	495	38	-645	588	30	-515	-15	42	-31	51
4904	-654	569	22	-647	569	42	-733	675	38	-597	3	49	-34	103
5371	-730	635	33	-723	635	46	-820	762	38	-687	42	54	-34	50
5871	-806	701	44	-800	701	50	-908	850	38	-775	42	59	19	51
6354	-882	767	55	-875	767	54	-996	938	38	-863	84	-111	97	-51
6805	-958	833	66	-951	833	58	-1084	1026	38	-951	153	-111	240	-310
7285	-1034	899	77	-1027	899	62	-1172	1114	38	-1040	245	-111	240	-310
7791	-1110	965	88	-1103	965	66	-1260	1202	38	-1128	317	-111	240	-310
8291	-1186	1031	99	-1179	1031	70	-1348	1280	38	-1216	378	-111	240	-310
8791	-1262	1097	110	-1255	1097	74	-1436	1368	38	-1304	436	-111	240	-310
9291	-1338	1163	121	-1331	1163	78	-1524	1456	38	-1392	493	-111	240	-310
9791	-1414	1229	132	-1407	1229	82	-1612	1544	38	-1480	551	-111	240	-310
10291	-1490	1295	143	-1483	1295	86	-1700	1632	38	-1568	609	-111	240	-310

POSTBUCKLED METAL SHEAR PANEL RS6 PRE-FATIGUE STRAIN SURVEY PLEASE MAKE COPY AND HIT CR

LOAD	GAGE 1	GAGE 2	GAGE 3	GAGE 4	GAGE 5	GAGE 6	GAGE 7	GAGE 8	GAGE 9	GAGE 10	GAGE 11	GAGE 12	GAGE 13	GAGE 14
-48.	-3.	-7.	-7.	3.	-7.	-7.	-7.	-7.	3.	-3.	-3.	-7.	-7.	0.
-829.	-188.	-30.	148.	-148.	0.	156.	159.	-15.	-183.	156.	-3.	-167.	150.	7.
1833.	-423.	-53.	316.	-293.	3.	355.	338.	-13.	-323.	338.	4.	-343.	350.	11.
2798.	-661.	-79.	476.	-411.	19.	542.	517.	-7.	-595.	521.	11.	-482.	526.	11.
3811.	-914.	-99.	625.	-495.	34.	766.	651.	-6.	-886.	716.	57.	-512.	693.	-7.
4631.	-1062.	-430.	842.	-873.	-205.	1241.	153.	-197.	-2817.	1325.	152.	-599.	33.	-1789.
5729.	-1273.	-597.	959.	-1059.	-110.	1478.	172.	-2468.	-757.	1809.	2118.	1599.	507.	-2888.
6893.	-1401.	-643.	1075.	-1014.	121.	1658.	816.	-3119.	-4012.	2779.	2727.	2591.	766.	-3438.
7883.	-1603.	-689.	1253.	-949.	365.	1854.	898.	-4858.	-4641.	2639.	3575.	2985.	1067.	-3871.

LOAD	GAGE 15	GAGE 16	GAGE 17	GAGE 18	GAGE 19	GAGE 20	GAGE 21	GAGE 22	GAGE 23	GAGE 24	GAGE 25	GAGE 26	GAGE 27	GAGE 28
-48.	-7.	0.	-11.	-7.	-7.	-11.	-180.	3.	0.	-7.	-7.	-7.	-3.	-15.
-829.	-171.	152.	-23.	-171.	125.	-46.	-411.	171.	30.	-160.	7.	-19.	19.	-22.
1833.	-363.	334.	-34.	-358.	286.	-81.	-639.	377.	68.	-332.	26.	-36.	40.	-49.
2798.	-546.	517.	-34.	-539.	435.	-129.	-835.	575.	106.	-185.	11.	-15.	61.	-80.
3811.	-726.	711.	-55.	-769.	636.	-159.	-835.	702.	148.	-649.	11.	7.	80.	-118.
4631.	-891.	1283.	-85.	-879.	869.	-110.	-822.	1279.	288.	-1490.	76.	34.	42.	-646.
5729.	-1062.	1859.	-151.	-904.	957.	-134.	-1331.	1614.	1414.	-856.	61.	-75.	91.	-1205.
6893.	-1273.	2297.	-253.	-1044.	591.	-1689.	-2173.	1957.	1633.	-179.	38.	-179.	206.	-1817.
7883.	-1465.	2763.	-367.	-2962.	783.	-2339.	-2779.	2286.	2089.	-53.	7.	-263.	37.	-2491.

LOAD	GAGE 29	GAGE 30	GAGE 31	GAGE 32	GAGE 33	GAGE 34
-48.	0.	-11.	-3.	-11.	-7.	-3.
-829.	7.	-11.	-11.	-3.	-3.	-7.
1833.	11.	-3.	0.	-15.	11.	28.
2798.	18.	-11.	-3.	-19.	15.	57.
3811.	34.	-45.	-3.	-15.	-3.	139.
4631.	-117.	-346.	-103.	18.	-129.	532.
5729.	-338.	-178.	-237.	3.	-84.	452.
6893.	-547.	-118.	-389.	3.	19.	237.
7883.	-75.	89.	-569.	22.	292.	-89.

COMPOSITE SHEAR PANEL C51 STATIC TEST

LOAD	GAGE 29	GAGE 30	GAGE 31	GAGE 32	GAGE 33	GAGE 34	GAGE 35	GAGE 36	GAGE 37	GAGE 38	GAGE 39	GAGE 40	GAGE 41	GAGE 42
0	0	-3	0	-3	3	-3	0	0	0	3	0	0	0	0
508	0	-3	-4	3	11	-3	4	-4	3	-3	0	0	0	0
1015	1	15	-11	10	27	-15	0	-3	0	-3	8	8	0	4
1475	10	8	-11	8	27	-15	0	-11	3	0	11	4	4	-8
1934	10	4	-15	3	27	-19	0	-15	15	0	11	0	4	-8
2563	23	0	-19	0	27	-23	-4	-15	19	3	15	-4	8	-3
3016	23	-8	-23	-3	27	-27	-4	-19	27	3	15	-8	8	-8
3666	15	-11	-27	-8	23	-27	-4	-23	34	8	19	-11	11	-11
3888	15	-15	-27	-8	19	-27	0	-27	42	11	27	-15	15	-11
4477	11	-4	-30	15	-46	-34	4	-31	50	15	34	-19	15	-11
5004	-36	-4	-42	31	-42	23	34	-54	57	27	102	-23	53	-23
5071	-114	-57	-42	42	-42	-34	0	-210	123	-50	102	-76	53	-179
5071	50	-191	-8	-42	42	-34	0	-406	183	-139	221	-114	130	-386
7554	370	-330	42	-157	42	-128	171	-612	244	-237	286	-114	130	-564
8004	955	-603	145	-410	141	-328	293	-888	301	-356	251	-92	374	-895
8365	1880	-880	282	1	321	-670	450	-1221	427	-486	240	-10	561	-1976
11080	3543	-1301	424	-1660	474	-820	632	-1600	484	-773	294	-137	744	-1419
11897	3341	-1579	520	-1297	618	-1104	758	-1822	563	-972	374	-172	892	-1774
13097	4102	-1823	623	-1516	753	-1466	918	-2422	530	-972	460	-183	1618	-2513
13074	4930	-2224	723	-1734	897	-1757	941	-2968	488	-1171	561	-149	1224	-3163
14665	6804	-2652	826	-1950	1005	-2129	105	-3553	-428	-1435	660	-229	-8	-1038
8415	3391	-1831	1033	-2314	160	-1718	-145	-781		-308	93			

LOAD	GAGE 43	GAGE 44	GAGE 45	GAGE 46
0	0	-7	0	-3
508	0	-4	0	15
1015	0	-4	15	15
1475	4	-7	11	15
1934	8	-7	11	11
2563	11	-4	11	11
3016	15	-4	11	15
3666	19	-4	11	11
3888	19	-4	11	11
4477	27	-4	11	27
5004	34	0	0	-80
5071	34	-73	171	-134
7011	109	-100	200	-148
7554	214	-230	240	-111
8004	294	-455	282	-77
8365	381	-634	306	-160
11080	461	-792	444	-134
11897	526	-957	501	-172
13097	607	-1137	578	-150
13074	683	-1350	640	-218
14665	805	-1633	708	-436
8415	3391	-742	-815	

COMPOSITE SHEAR PYLON CS2 STATIC TEST

LOAD	GAGE 1	GAGE 2	GAGE 3	GAGE 4	GAGE 5	GAGE 6	GAGE 7	GAGE 8	GAGE 9	GAGE 10	GAGE 11	GAGE 12	GAGE 13	GAGE 14
0	0	-3	0	-8	0	-46	0	0	0	-46	0	0	0	-8
483	46	-15	-38	31	0	-8	46	8	-38	-46	0	0	31	8
998	99	-8	-88	99	15	-91	-23	-23	-82	114	-8	-84	84	23
1473	168	-23	-168	158	15	-160	160	-38	-168	183	0	-145	153	46
1909	236	-38	-260	250	8	-236	244	-48	-252	282	15	-221	237	69
2463	397	-61	-344	328	8	-395	320	-53	-358	366	30	-290	306	107
2979	373	-76	-435	412	8	-373	395	-81	-412	450	38	-373	388	145
3477	434	-99	-519	483	15	-434	473	-83	-489	524	45	-442	465	213
3985	510	-114	-641	583	23	-510	549	-88	-573	625	53	-526	555	287
4488	578	-129	-771	689	33	-611	649	-98	-611	694	23	-633	687	404
4993	876	-222	-1253	955	366	-412	1349	-38	-1780	99	-2643	-2599	1199	1737
5498	1189	-731	-2016	1451	700	-381	1931	2082	2334	-122	-3930	-3620	1711	2650
6003	1455	-1186	-2512	1856	1089	-564	2424	2655	2676	-38	-4897	-4382	2162	3245
6508	1676	-1318	-2512	1856	1318	-1448	2424	2655	4102	107	-5666	-4946	2557	3594
7013	1892	-1576	-336	208	148	-4557	2738	3731	4026	290	-5849	-4901	2872	3831
7518	2193	-176	336	328	176	-8871	2738	3731	4026	519	-4768	-3735	2758	3193
8023	2354	-3034	625	-844	-745	-9154	2507	1583	2842	800	-4037	-2957	2681	2551
8528	2729	-3282	6940	-23	-623	-9898	2507	1583	2842	1105	-4037	-2957	2681	1828
9033	3033	-4242	7035	204	-449	-10792	2507	1583	2842	1486	-4037	-2957	2681	510
9538	3374	-4573	8576	480	-312	-11332	2639	-385	495	1886	-4037	-2957	2681	653
10043	3779	-5251	9256	777	-167	-12325	2789	-891	61	1886	-4037	-2957	2681	1820
10548	4076	-5682	9782	891	68	-12713	2789	-1615	-617	2073	-4037	-2957	2681	2346

LOAD	GAGE 15	GAGE 16	GAGE 17	GAGE 18	GAGE 19	GAGE 20	GAGE 21	GAGE 22	GAGE 23	GAGE 24	GAGE 25	GAGE 26	GAGE 27	GAGE 28
0	0	8	0	-8	-8	-7	0	0	0	-7	0	0	0	0
483	-23	31	-8	-38	-8	-7	-31	3	0	-34	0	0	0	8
998	-60	84	-23	-107	76	0	-76	14	-8	-76	-8	15	-8	23
1473	-182	237	-46	-182	105	23	-145	145	-8	-145	-8	15	-8	31
1909	-191	237	-61	-288	229	23	-229	229	-8	-221	-8	23	-8	31
2463	-244	306	-76	-397	289	61	-382	290	8	-382	-8	31	-8	38
2979	-365	374	-107	-512	374	76	-451	386	3	-358	-8	31	15	46
3477	-381	435	-145	-618	451	166	-535	494	15	-488	-8	38	15	31
3985	-381	489	-221	-764	649	114	-642	570	38	-518	-15	54	38	23
4488	-389	451	-449	-1001	849	114	-1146	784	385	-183	-15	107	100	69
4993	-409	8	-263	-2400	849	114	-1146	784	385	-183	-15	107	100	69
5498	-409	8	-263	-2400	849	114	-1146	784	385	-183	-15	107	100	69
5993	-409	8	-263	-2400	849	114	-1146	784	385	-183	-15	107	100	69
6498	-409	8	-263	-2400	849	114	-1146	784	385	-183	-15	107	100	69
6993	-409	8	-263	-2400	849	114	-1146	784	385	-183	-15	107	100	69
7498	-409	8	-263	-2400	849	114	-1146	784	385	-183	-15	107	100	69
7993	-409	8	-263	-2400	849	114	-1146	784	385	-183	-15	107	100	69
8498	-409	8	-263	-2400	849	114	-1146	784	385	-183	-15	107	100	69
8993	-409	8	-263	-2400	849	114	-1146	784	385	-183	-15	107	100	69
9498	-409	8	-263	-2400	849	114	-1146	784	385	-183	-15	107	100	69
9993	-409	8	-263	-2400	849	114	-1146	784	385	-183	-15	107	100	69
10498	-409	8	-263	-2400	849	114	-1146	784	385	-183	-15	107	100	69
10993	-409	8	-263	-2400	849	114	-1146	784	385	-183	-15	107	100	69
11498	-409	8	-263	-2400	849	114	-1146	784	385	-183	-15	107	100	69
11993	-409	8	-263	-2400	849	114	-1146	784	385	-183	-15	107	100	69
12498	-409	8	-263	-2400	849	114	-1146	784	385	-183	-15	107	100	69
12993	-409	8	-263	-2400	849	114	-1146	784	385	-183	-15	107	100	69
13498	-409	8	-263	-2400	849	114	-1146	784	385	-183	-15	107	100	69
13993	-409	8	-263	-2400	849	114	-1146	784	385	-183	-15	107	100	69
14498	-409	8	-263	-2400	849	114	-1146	784	385	-183	-15	107	100	69
14993	-409	8	-263	-2400	849	114	-1146	784	385	-183	-15	107	100	69



COMPOSITE SHEAR PANEL C52 STATIC TEST

LOAD	GAGE 29	GAGE 30	GAGE 31	GAGE 32	GAGE 33	GAGE 34	GAGE 35	GAGE 36	GAGE 37	GAGE 38	GAGE 39	GAGE 40	GAGE 41	GAGE 42
0	0	0	0	0	0	0	0	0	0	0	0	0	0	0
483	8	15	-15	8	-8	-7	-8	-7	-7	-8	8	-8	0	0
990	23	31	-31	15	-15	23	-8	-7	0	-8	23	15	0	-8
1473	31	38	-38	23	-23	31	-15	-15	7	-8	30	15	-8	-8
1989	31	31	-46	23	-23	31	-15	-23	23	-8	34	8	-8	-15
2463	38	38	-61	23	-23	23	-15	-30	30	-8	46	8	-8	-15
2974	31	31	-77	31	-31	23	-15	-38	53	-8	53	8	-8	-23
3477	31	38	-84	46	-46	15	-23	-53	64	-8	61	8	0	-30
3985	31	38	-107	61	-61	-61	8	-115	84	-30	137	-30	15	-114
4482	8	46	-122	92	-92	-38	68	-320	129	-122	281	-80	68	-282
4989	8	38	-115	77	-77	0	152	-541	213	-122	418	-122	144	-480
5482	46	-53	-61	38	-38	0	152	-784	297	-114	494	-114	236	-716
5983	137	-183	-8	-30	-30	61	253	-1074	381	-53	471	-53	350	-1036
6483	512	-351	77	-198	-712	181	538	-1356	489	-838	425	0	555	-1379
6982	1854	-641	191	-489	-995	353	859	-1883	579	-1059	471	-8	538	-172
7482	1863	-1039	258	-582	-1271	637	1048	-1973	685	-1659	540	-30	730	-2140
7982	2543	-1359	321	-677	-1200	865	1284	-2470	792	-1283	682	-30	790	-2628
8482	3223	-1665	375	-819	-1522	1053	1554	-3247	929	-1509	845	-144	904	-3266
8985	4049	-2020	489	-964	-2245	1289	1322	-3511	838	-1714	867	-129	965	-3778
9480	4760	-2467	512	-986	-2391	1369	1368	-3770	807	-1790	1036	-129		-3993
9984	5514	-2971	519	-1020										
10483	5903													

LOAD	GAGE 43	GAGE 44	GAGE 45	GAGE 46
0	0	0	0	0
483	0	-7	-8	8
990	0	-7	15	30
1473	0	-7	23	30
1989	0	-7	30	30
2463	0	-7	30	30
2974	15	-7	30	30
3477	15	-7	30	30
3985	23	-7	46	38
4482	30	-7	53	38
4989	30	-7	91	8
5482	68	-46	231	-61
5983	120	-137	305	-87
6483	190	-243	355	-107
6982	244	-357	385	-91
7482	305	-478	451	-107
7982	359	-581	475	-160
8482	434	-739	490	-208
8985	440	-881	550	-303
9480	440	-1087	588	-405
9984	541	-1401	678	-145
10483	526	-1645	745	-122
10982	540	-1781	831	-81

COMPOSITE FATIGUE SHEAR (PAGE), CS3 STRAIN SURVEY

LOAD	GAGE 1	GAGE 2	GAGE 3	GAGE 4	GAGE 5	GAGE 6	GAGE 7	GAGE 8	GAGE 9	GAGE 10	GAGE 11	GAGE 12	GAGE 13	GAGE 14
-84.	-7.	0.	-7.	0.	0.	0.	0.	0.	0.	-7.	0.	-7.	0.	0.
468.	69.	-7.	-84.	61.	-78.	78.	168.	15.	-84.	59.	-15.	-92.	89.	-7.
982.	153.	-2.	-168.	130.	-160.	160.	252.	30.	-168.	153.	-23.	-176.	145.	-7.
1476.	229.	-30.	-244.	199.	-244.	252.	335.	46.	-252.	259.	-38.	-260.	213.	-15.
1968.	305.	-38.	-321.	267.	-328.	335.	427.	68.	-338.	368.	-46.	-344.	282.	-23.
2460.	389.	-53.	-397.	336.	-412.	427.	518.	81.	-412.	451.	-69.	-428.	351.	-38.
2953.	473.	-61.	-466.	426.	-503.	518.	610.	122.	-483.	574.	-91.	-519.	419.	-46.
3451.	565.	-68.	-535.	473.	-602.	709.	789.	182.	-556.	674.	-122.	-619.	488.	-68.
3959.	657.	-84.	-604.	535.	-701.	897.	1087.	282.	-610.	871.	-180.	-741.	556.	-114.
4453.	749.	-107.	-686.	604.	-781.	1087.	1387.	468.	-650.	1087.	-2551.	-807.	945.	780.
4953.	841.	-129.	-741.	674.	-864.	1387.	1687.	650.	-650.	1387.	-3184.	-1087.	1258.	1657.
5470.	933.	-153.	-807.	749.	-944.	1687.	1987.	833.	-650.	1687.	-3886.	-1387.	1562.	2310.
5978.	1025.	-176.	-871.	833.	-1033.	1987.	2287.	1018.	-650.	1987.	-4588.	-1687.	1844.	2812.
6486.	1117.	-199.	-933.	918.	-1133.	2287.	2587.	1199.	-650.	2287.	-5290.	-1987.	2112.	3336.
6986.	1209.	-223.	-1000.	1000.	-1255.	2587.	2887.	1380.	-650.	2587.	-6000.	-2287.	2438.	3867.
7490.	1301.	-246.	-1064.	1087.	-1333.	2887.	3187.	1561.	-650.	2887.	-6702.	-2587.	2658.	4164.
7997.	1393.	-269.	-1129.	1176.	-1418.	3187.	3487.	1742.	-650.	3187.	-7404.	-2887.	2744.	4162.
8497.	1485.	-293.	-1193.	1260.	-1500.	3487.	3787.	1923.	-650.	3487.	-8106.	-3187.	2729.	3952.
8997.	1577.	-316.	-1258.	1344.	-1582.	3787.	4087.	2104.	-650.	3787.	-8808.	-3487.	2721.	3769.
9498.	1669.	-340.	-1322.	1429.	-1664.	4087.	4387.	2285.	-650.	4087.	-9510.	-3787.	2721.	3572.

LOAD	GAGE 15	GAGE 16	GAGE 17	GAGE 18	GAGE 19	GAGE 20	GAGE 21	GAGE 22	GAGE 23	GAGE 24	GAGE 25	GAGE 26	GAGE 27	GAGE 28
-24.	0.	0.	0.	0.	-7.	0.	-7.	0.	0.	-7.	0.	0.	0.	-7.
468.	-91.	76.	15.	-77.	59.	8.	-84.	61.	0.	-84.	0.	0.	0.	-7.
982.	-175.	160.	23.	-153.	137.	16.	-160.	137.	0.	-160.	-7.	0.	0.	-7.
1476.	-257.	244.	38.	-214.	214.	16.	-237.	206.	8.	-237.	-15.	8.	0.	-7.
1968.	-351.	321.	53.	-283.	290.	16.	-313.	283.	15.	-305.	-23.	15.	0.	-7.
2460.	-442.	405.	78.	-345.	359.	16.	-397.	359.	23.	-374.	-23.	23.	8.	-7.
2953.	-541.	489.	99.	-406.	428.	0.	-481.	428.	30.	-443.	-31.	23.	8.	-15.
3451.	-640.	581.	129.	-467.	497.	-15.	-573.	504.	53.	-504.	-31.	23.	15.	-15.
3959.	-739.	672.	175.	-528.	559.	-51.	-657.	588.	84.	-550.	-38.	23.	15.	-15.
4453.	-838.	764.	223.	-589.	640.	-81.	-741.	672.	109.	-635.	-50.	38.	153.	-77.
4953.	-937.	856.	271.	-650.	722.	-441.	-822.	772.	138.	-718.	-50.	69.	146.	-69.
5470.	-1036.	948.	319.	-711.	803.	-522.	-901.	861.	167.	-799.	-46.	107.	123.	-23.
5978.	-1135.	1040.	367.	-772.	884.	-573.	-982.	940.	196.	-884.	-81.	145.	77.	8.
6486.	-1234.	1132.	415.	-833.	965.	-624.	-1063.	1028.	225.	-965.	-136.	199.	-8.	54.
6986.	-1333.	1224.	463.	-894.	1046.	-675.	-1144.	1119.	254.	-1046.	-176.	268.	-169.	130.
7490.	-1432.	1316.	511.	-955.	1127.	-726.	-1225.	1200.	283.	-1127.	-214.	317.	-199.	157.
7997.	-1531.	1408.	559.	-1016.	1209.	-777.	-1306.	1281.	312.	-1209.	-255.	366.	-276.	257.
8497.	-1630.	1500.	607.	-1077.	1291.	-828.	-1387.	1362.	341.	-1291.	-296.	415.	-376.	344.
8997.	-1729.	1592.	655.	-1138.	1373.	-879.	-1468.	1447.	370.	-1373.	-337.	464.	-499.	429.
9498.	-1828.	1684.	703.	-1199.	1455.	-930.	-1549.	1528.	400.	-1455.	-378.	513.	-572.	513.

COMPOSITE FATIGUE SHEAR PANEL CS3 STRAIN SURVEY

LOAD	GAGE29	GAGE30	GAGE31	GAGE32	GAGE33	GAGE34
-24.	0.	-7.	0.	0.	0.	0.
460.	7.	-7.	0.	0.	-7.	-7.
992.	15.	-15.	-7.	0.	-7.	-7.
1476.	15.	-23.	-7.	8.	-15.	-15.
1809.	15.	-31.	-7.	8.	-15.	-15.
2053.	15.	-31.	-7.	15.	-15.	-23.
3461.	15.	-38.	-7.	23.	-23.	-23.
3669.	15.	-38.	-7.	31.	-23.	-31.
4453.	-130.	-31.	-15.	69.	31.	-77.
4982.	-82.	-69.	-7.	61.	7.	-61.
8470.	-15.	-128.	7.	46.	-15.	-38.
8978.	76.	-183.	23.	23.	-48.	-15.
8463.	199.	-337.	38.	-83.	-77.	23.
8945.	382.	-374.	61.	-84.	-130.	69.
7470.	689.	-527.	99.	-103.	-322.	145.
7957.	1061.	-785.	137.	-313.	-353.	246.
8471.	1421.	-940.	191.	-435.	-488.	337.
8945.	1756.	-1059.	220.	-548.	-607.	481.
9463.	2160.	-1237.	275.	-648.	-735.	505.

COMPOSITE FATIGUE SHEAR PANEL CS4 STRAIN SURVEY

LOAD	GAGE 1	GAGE 2	GAGE 3	GAGE 4	GAGE 5	GAGE 6	GAGE 7	GAGE 8	GAGE 9	GAGE 10	GAGE 11	GAGE 12	GAGE 13	GAGE 14
508.	0.	0.	-7.	0.	0.	-7.	0.	0.	-7.	0.	0.	0.	-7.	0.
1017.	53.	0.	-169.	69.	15.	-76.	61.	-30.	-69.	69.	-15.	-53.	61.	0.
1525.	137.	8.	-169.	152.	15.	-175.	145.	-30.	-160.	165.	-8.	-145.	160.	23.
2033.	221.	-8.	-323.	244.	15.	-202.	236.	-30.	-252.	267.	0.	-220.	260.	38.
2541.	298.	-15.	-323.	328.	23.	-366.	312.	-30.	-335.	343.	-8.	-305.	351.	53.
3049.	357.	-23.	-412.	404.	23.	-459.	389.	-30.	-404.	427.	-15.	-381.	428.	78.
3557.	443.	-38.	-489.	489.	38.	-526.	465.	-30.	-465.	495.	-23.	-457.	512.	91.
4065.	527.	-53.	-588.	564.	61.	-594.	541.	0.	-518.	564.	-61.	-564.	603.	129.
4573.	604.	-676.	-778.	702.	390.	-777.	1404.	2871.	-2408.	305.	-3473.	-3011.	1169.	1520.
5080.	669.	-904.	-1055.	988.	547.	-1052.	1791.	3321.	-2843.	-207.	-4050.	-3399.	1497.	2234.
5588.	1163.	-1064.	-1112.	1112.	782.	-1105.	2043.	3648.	-3186.	-252.	-4629.	-3735.	1795.	2758.
6096.	1252.	-1064.	-1156.	1156.	868.	-1438.	2271.	3884.	-3453.	-193.	-4832.	-4017.	2055.	3169.
6604.	1341.	-1071.	-1207.	1166.	957.	-2006.	2500.	4059.	-3681.	-116.	-5384.	-4276.	2353.	3610.
7112.	1430.	-1071.	-1207.	1166.	103.	-2006.	2500.	4059.	-3681.	-116.	-5384.	-4276.	2353.	3610.
7620.	1519.	-1071.	-1207.	1166.	137.	-2006.	2500.	4059.	-3681.	-116.	-5384.	-4276.	2353.	3610.
8128.	1608.	-1071.	-1207.	1166.	171.	-2006.	2500.	4059.	-3681.	-116.	-5384.	-4276.	2353.	3610.
8636.	1697.	-1071.	-1207.	1166.	205.	-2006.	2500.	4059.	-3681.	-116.	-5384.	-4276.	2353.	3610.
9144.	1786.	-1071.	-1207.	1166.	239.	-2006.	2500.	4059.	-3681.	-116.	-5384.	-4276.	2353.	3610.
9652.	1875.	-1071.	-1207.	1166.	273.	-2006.	2500.	4059.	-3681.	-116.	-5384.	-4276.	2353.	3610.
10160.	1964.	-1071.	-1207.	1166.	307.	-2006.	2500.	4059.	-3681.	-116.	-5384.	-4276.	2353.	3610.
10668.	2053.	-1071.	-1207.	1166.	341.	-2006.	2500.	4059.	-3681.	-116.	-5384.	-4276.	2353.	3610.
11176.	2142.	-1071.	-1207.	1166.	375.	-2006.	2500.	4059.	-3681.	-116.	-5384.	-4276.	2353.	3610.
11684.	2231.	-1071.	-1207.	1166.	409.	-2006.	2500.	4059.	-3681.	-116.	-5384.	-4276.	2353.	3610.
12192.	2320.	-1071.	-1207.	1166.	443.	-2006.	2500.	4059.	-3681.	-116.	-5384.	-4276.	2353.	3610.
12700.	2409.	-1071.	-1207.	1166.	477.	-2006.	2500.	4059.	-3681.	-116.	-5384.	-4276.	2353.	3610.
13208.	2498.	-1071.	-1207.	1166.	511.	-2006.	2500.	4059.	-3681.	-116.	-5384.	-4276.	2353.	3610.
13716.	2587.	-1071.	-1207.	1166.	545.	-2006.	2500.	4059.	-3681.	-116.	-5384.	-4276.	2353.	3610.
14224.	2676.	-1071.	-1207.	1166.	579.	-2006.	2500.	4059.	-3681.	-116.	-5384.	-4276.	2353.	3610.
14732.	2765.	-1071.	-1207.	1166.	613.	-2006.	2500.	4059.	-3681.	-116.	-5384.	-4276.	2353.	3610.
15240.	2854.	-1071.	-1207.	1166.	647.	-2006.	2500.	4059.	-3681.	-116.	-5384.	-4276.	2353.	3610.
15748.	2943.	-1071.	-1207.	1166.	681.	-2006.	2500.	4059.	-3681.	-116.	-5384.	-4276.	2353.	3610.
16256.	3032.	-1071.	-1207.	1166.	715.	-2006.	2500.	4059.	-3681.	-116.	-5384.	-4276.	2353.	3610.
16764.	3121.	-1071.	-1207.	1166.	749.	-2006.	2500.	4059.	-3681.	-116.	-5384.	-4276.	2353.	3610.
17272.	3210.	-1071.	-1207.	1166.	783.	-2006.	2500.	4059.	-3681.	-116.	-5384.	-4276.	2353.	3610.
17780.	3299.	-1071.	-1207.	1166.	817.	-2006.	2500.	4059.	-3681.	-116.	-5384.	-4276.	2353.	3610.
18288.	3388.	-1071.	-1207.	1166.	851.	-2006.	2500.	4059.	-3681.	-116.	-5384.	-4276.	2353.	3610.
18796.	3477.	-1071.	-1207.	1166.	885.	-2006.	2500.	4059.	-3681.	-116.	-5384.	-4276.	2353.	3610.
19304.	3566.	-1071.	-1207.	1166.	919.	-2006.	2500.	4059.	-3681.	-116.	-5384.	-4276.	2353.	3610.
19812.	3655.	-1071.	-1207.	1166.	953.	-2006.	2500.	4059.	-3681.	-116.	-5384.	-4276.	2353.	3610.
20320.	3744.	-1071.	-1207.	1166.	987.	-2006.	2500.	4059.	-3681.	-116.	-5384.	-4276.	2353.	3610.
20828.	3833.	-1071.	-1207.	1166.	1021.	-2006.	2500.	4059.	-3681.	-116.	-5384.	-4276.	2353.	3610.
21336.	3922.	-1071.	-1207.	1166.	1055.	-2006.	2500.	4059.	-3681.	-116.	-5384.	-4276.	2353.	3610.
21844.	4011.	-1071.	-1207.	1166.	1089.	-2006.	2500.	4059.	-3681.	-116.	-5384.	-4276.	2353.	3610.
22352.	4100.	-1071.	-1207.	1166.	1123.	-2006.	2500.	4059.	-3681.	-116.	-5384.	-4276.	2353.	3610.
22860.	4189.	-1071.	-1207.	1166.	1157.	-2006.	2500.	4059.	-3681.	-116.	-5384.	-4276.	2353.	3610.
23368.	4278.	-1071.	-1207.	1166.	1191.	-2006.	2500.	4059.	-3681.	-116.	-5384.	-4276.	2353.	3610.
23876.	4367.	-1071.	-1207.	1166.	1225.	-2006.	2500.	4059.	-3681.	-116.	-5384.	-4276.	2353.	3610.
24384.	4456.	-1071.	-1207.	1166.	1259.	-2006.	2500.	4059.	-3681.	-116.	-5384.	-4276.	2353.	3610.
24892.	4545.	-1071.	-1207.	1166.	1293.	-2006.	2500.	4059.	-3681.	-116.	-5384.	-4276.	2353.	3610.
25400.	4634.	-1071.	-1207.	1166.	1327.	-2006.	2500.	4059.	-3681.	-116.	-5384.	-4276.	2353.	3610.
25908.	4723.	-1071.	-1207.	1166.	1361.	-2006.	2500.	4059.	-3681.	-116.	-5384.	-4276.	2353.	3610.
26416.	4812.	-1071.	-1207.	1166.	1395.	-2006.	2500.	4059.	-3681.	-116.	-5384.	-4276.	2353.	3610.
26924.	4901.	-1071.	-1207.	1166.	1429.	-2006.	2500.	4059.	-3681.	-116.	-5384.	-4276.	2353.	3610.
27432.	4990.	-1071.	-1207.	1166.	1463.	-2006.	2500.	4059.	-3681.	-116.	-5384.	-4276.	2353.	3610.
27940.	5079.	-1071.	-1207.	1166.	1497.	-2006.	2500.	4059.	-3681.	-116.	-5384.	-4276.	2353.	3610.
28448.	5168.	-1071.	-1207.	1166.	1531.	-2006.	2500.	4059.	-3681.	-116.	-5384.	-4276.	2353.	3610.
28956.	5257.	-1071.	-1207.	1166.	1565.	-2006.	2500.	4059.	-3681.	-116.	-5384.	-4276.	2353.	3610.
29464.	5346.	-1071.	-1207.	1166.	1599.	-2006.	2500.	4059.	-3681.	-116.	-5384.	-4276.	2353.	3610.
29972.	5435.	-1071.	-1207.	1166.	1633.	-2006.	2500.	4059.	-3681.	-116.	-5384.	-4276.	2353.	3610.
30480.	5524.	-1071.	-1207.	1166.	1667.	-2006.	2500.	4059.	-3681.	-116.	-5384.	-4276.	2353.	3610.
30988.	5613.	-1071.	-1207.	1166.	1701.	-2006.	2500.	4059.	-3681.	-116.	-5384.	-4276.	2353.	3610.
31496.	5702.	-1071.	-1207.	1166.	1735.	-2006.	2500.	4059.	-3681.	-116.	-5384.	-4276.	2353.	3610.
32004.	5791.	-1071.	-1207.	1166.	1769.	-2006.	2500.	4059.	-3681.	-116.	-5384.	-4276.	2353.	3610.
32512.	5880.	-1071.	-1207.	1166.	1803.	-2006.	2500.	4059.	-3681.	-116.	-5384.	-4276.	2353.	3610.
33020.	5969.	-1071.	-1207.	1166.	1837.	-2006.	2500.	4059.	-3681.	-116.	-5384.	-4276.	2353.	3610.
33528.	6058.	-1071.	-1207.	1166.	1871.	-2006.	2500.	4059.	-3681.	-116.	-5384.	-4276.	2353.	3610.
34036.	6147.	-1071.	-1207.	1166.	1905.	-2006.	2500.	4059.	-3681.	-116.	-5384.	-4276.	2353.	3610.
34544.	6236.	-1071.	-1207.	1166.	1939.	-2006.	2500.	4059.	-3681.	-116.	-5384.	-4276.	2353.	3610.
35052.	6325.	-1071.	-1207.	1166.	1973.	-2006.	2500.	4059.	-3681.	-116.	-5384.	-4276.	2353.	3610.
35560.	6414.	-1071.	-1207.	1166.	2007.	-2006.	2500.	4059.	-3681.	-116.	-5384.	-4276.	2353.	3610.
36068.	6503.	-1071.	-1207.	1166.	2041.	-2006.	2500.	4059.	-3681.	-116.	-5384.	-4276.	2353.	3610.
36576.	6592.	-1071.	-1207.	1166.	2075.	-2006.	2500.	4059.	-3681.	-116.	-5384.	-4276.	2353.	3610.
37084.	6681.	-1071.	-1207.	1166.	2109.	-2006.	2500.	4059.	-3681.	-116.	-5384.	-4276.	2353.	3610.
37592.	6770.	-1071.	-1207.	1166.	2143.	-2006.	2500.	4059.	-3681.	-116.	-5384.	-4276.	2353.	3610.
38100.	6859.	-1071.	-1207.	1166.	2177.	-2006.	2500.	4059.	-3681.	-116.	-5384.	-4276.	2353.	3610.
38608.	6948.	-1071.	-1207.	1166.	2211.	-2006.	2500.	4059.	-3681.	-116.	-5384.	-4276.	2353.	3610.
39116.	7037.	-1071.	-1207.	1166.	2245.	-2006.	2500.	4059.	-3681.	-116.	-5384.	-4276.	2353.	3610.
39624.	7126.	-1071.	-1207.	1166.	2279.	-2006.	2500.	4059.	-3681.	-116.	-5384.	-4276.	2353.	3610.
40132.	7215.	-1071.	-1207.	1166.	2313.	-2006.	2500.	4059.	-3681.	-116.	-5384.	-4276.	2353.	3610.
40640.	7304.	-1071.	-1207.	1166.	2347.	-2006.	2500.	4059.	-3681.	-116.	-5384.	-4276.	2353.	3610.
41148.	7393.	-1071.	-1207.	1166.	2381.	-2006.	2500.	4059.	-3681.	-116.	-5384.	-4276.	2353.	3610.
41656.	7482.	-1071.	-1207.	1166.	2415.	-2006.	2500.	4059.	-3681.	-116.	-5384.	-4276.	2353.	3610.
42164.	7571.	-1071.	-1207.	1166.	2449.	-2006.	2500.	4059.	-3681.	-116.	-5384.	-4276.	2353.	3610.
42672.	7660.	-1071.	-1207.	1166.	2483.	-2006.	2500.	4059.	-3681.	-116.	-5384.	-4276.	2353.	3610.
43180.	7749.	-1071.	-1207.	1166.	2517.	-2006.	2500.	4059.	-3681.	-116.	-5384.	-4276.	2353.	3610.
43688.	7838.	-1071.	-1207.	1166.	2551.	-2006.	2500.	4059.	-3681.	-116.	-5384.	-4276.	2353.	3610.
44196.	7927.	-1071.	-1207.	1166.	2585.	-2006.	2500.	4059.	-3681.	-116.	-5384.	-4276.	2353.	3610.
44704.	8016.	-1071.	-1207.	1166.	2619.	-2006.	2500.	4059.	-3681.	-116.	-5384.	-4276.	2353.	3610.

COMPOSITE FATIGUE SHEAR PANEL C53 STRAIN SURVEY AFTER 100,000 CYCLES

LOAD	GAGE 1	GAGE 2	GAGE 3	GAGE 4	GAGE 5	GAGE 6	GAGE 7	GAGE 8	GAGE 9	GAGE 10	GAGE 11	GAGE 12	GAGE 13
0.	-7.	0.	0.	-7.	-7.	-7.	0.	0.	-7.	0.	-7.	-7.	0.
532.	54.	-60.	-53.	-7.	-7.	-7.	-23.	23.	15.	-7.	7.	-7.	15.
832.	115.	-137.	-114.	-7.	-7.	-15.	31.	31.	31.	-7.	15.	-23.	23.
1525.	181.	-222.	-188.	-15.	0.	-15.	31.	45.	31.	-7.	15.	-31.	31.
2000.	200.	-200.	-200.	-15.	0.	-15.	31.	45.	31.	-15.	23.	-31.	31.
2517.	321.	-300.	-335.	-23.	0.	-15.	46.	61.	38.	-7.	23.	-38.	38.
3041.	375.	-401.	-412.	-23.	7.	-23.	46.	68.	38.	-15.	31.	-46.	38.
3569.	400.	-481.	-555.	-23.	-7.	-15.	84.	82.	31.	0.	7.	-46.	38.
4018.	522.	-756.	-747.	-23.	-7.	-15.	115.	168.	31.	31.	-46.	-61.	31.
4525.	722.	-1031.	-1000.	-54.	61.	7.	100.	206.	-153.	31.	-15.	-77.	84.
5034.	82.	-2351.	-1873.	-54.	122.	-77.	153.	266.	-203.	31.	-77.	-139.	130.
5502.	-532.	-2528.	-61.	-107.	122.	-284.	276.	406.	-543.	84.	-207.	-259.	246.
6008.	-611.	-2722.	-1200.	-230.	230.	-537.	406.	806.	-827.	137.	-350.	-445.	358.
6505.	-827.	-2746.	-1300.	-457.	477.	-821.	543.	1307.	-1087.	150.	-488.	-637.	490.
6931.	-742.	-1894.	-3005.	-685.	574.	-1135.	681.	1909.	-1362.	202.	-635.	-852.	637.
7372.	-674.	-1763.	-3678.	-851.	685.	-1274.	759.	2711.	-1454.	223.	-681.	-951.	723.
7813.	-551.	-1352.	-4005.	-787.	685.	-1408.	834.	3100.	-1646.	321.	-785.	-1105.	829.
8297.	-381.	-512.	-4824.	-880.	894.	-1813.	1023.	3837.	-2013.	405.	-926.	-1373.	906.
8800.	-38.	-23.	-5025.	-887.	934.	-2055.	1141.	4656.	-2411.	481.	-1095.	-1657.	1135.
9307.	207.	-625.	-6113.	-1072.	934.	-2508.	1232.	5315.	-2709.	542.	-1200.	-1854.	1274.
9805.	375.	-1100.	-6410.	-1072.	934.	-2508.	1804.	5773.	-2908.	573.	-1253.	-2010.	1366.

COMPOSITE FATIGUE SHEAR PANEL CS4 STRAIN SURVEY

LOAD	GAGE20	GAGE29	GAGE31	GAGE32	GAGE33	GAGE34
0.	0.	0.	-7.	0.	-7.	0.
148.	15.	15.	-7.	15.	-15.	15.
1617.	15.	8.	3.	15.	-23.	15.
1625.	23.	15.	7.	15.	-23.	15.
2003.	39.	15.	7.	23.	-31.	23.
2517.	39.	23.	15.	23.	-31.	23.
1625.	28.	31.	15.	31.	-38.	31.
2534.	39.	31.	23.	38.	-46.	31.
4018.	-28.	23.	-23.	78.	7.	-23.
4529.	-43.	-33.	-15.	68.	-7.	8.
6204.	84.	-53.	0.	53.	-31.	31.
5243.	152.	-108.	15.	31.	-61.	61.
5252.	269.	-507.	45.	-8.	-167.	89.
2525.	578.	-425.	169.	-84.	-184.	153.
7015.	852.	-523.	158.	-183.	-289.	229.
7531.	1279.	-715.	203.	-395.	-420.	328.
5232.	1213.	-813.	344.	-485.	-550.	488.
8544.	1836.	-1629.	481.	-485.	-685.	498.
8202.	2173.	-1141.	483.	-548.	-758.	565.
9635.	2443.	-1283.	521.	-611.	-859.	626.

COMPOSITE FATIGUE SHEAR PANEL CS4 STRAIN SURVEY AFTER 50,000 CYCLES

LOAD	GAGE 1	GAGE 2	GAGE 3	GAGE 4	GAGE 5	GAGE 6	GAGE 7	GAGE 8	GAGE 9	GAGE 10	GAGE 11	GAGE 12	GAGE 13	GAGE 14
0.	0.	0.	0.	0.	0.	0.	0.	0.	0.	0.	0.	0.	0.	0.
500.	-7.	53.	15.	53.	-15.	-61.	-45.	53.	-53.	84.	-7.	-7.	-7.	0.
1017.	-15.	130.	8.	130.	-23.	-145.	-114.	137.	-130.	229.	-15.	-7.	-7.	8.
1535.	-20.	206.	0.	206.	-23.	-129.	-103.	221.	-206.	359.	-23.	-7.	-7.	0.
2053.	-53.	282.	-8.	282.	-30.	-321.	-259.	306.	-282.	497.	31.	0.	-7.	0.
2571.	-69.	350.	-15.	350.	-45.	-412.	-328.	389.	-350.	581.	-38.	0.	-7.	0.
3089.	-114.	427.	-30.	427.	-38.	-519.	-391.	473.	-419.	766.	-84.	38.	-7.	-8.
3607.	-150.	503.	-150.	503.	1016.	542.	-1250.	511.	-617.	956.	0.	15.	15.	54.
4125.	-308.	579.	-3.	1449.	2350.	1971.	-2515.	861.	-907.	0.	38.	-15.	46.	38.
4643.	-523.	655.	-76.	1646.	2827.	2459.	-2790.	976.	-1021.	0.	84.	-54.	-46.	69.
5161.	-579.	731.	-228.	1006.	2757.	2459.	-2957.	861.	-991.	0.	130.	-92.	-115.	107.
5679.	-327.	807.	-441.	1028.	2813.	2513.	-3056.	1158.	-777.	0.	183.	-138.	-198.	153.
6197.	60.	883.	-669.	1036.	2788.	2544.	-3108.	1418.	-373.	0.	245.	-199.	-314.	276.
6715.	487.	959.	-851.	1036.	2714.	2566.	-3110.	1730.	191.	8.	291.	-253.	-429.	344.
7233.	933.	1034.	-1023.	1036.	2593.	2376.	-3018.	1989.	762.	8174.	337.	-291.	-520.	390.
7751.	1204.	1084.	-1163.	1036.	2476.	2353.	-3005.	2132.	1227.	2949.	337.	-329.	-612.	435.
8269.	1500.	1147.	-1147.	1036.	2358.	2176.	-2905.	2332.	1623.	1841.	337.	-360.	-764.	475.
8787.	1699.	1201.	-1178.	1036.	2222.	2003.	-2808.	2584.	1997.	2208.	337.	-399.	-783.	521.
9305.	1831.	1253.	-1193.	1036.	2100.	2003.	-2828.	2584.	2317.	4583.	429.	-421.	-865.	551.
9823.	1931.	1303.	-1193.	1036.	1971.	2003.	-2751.	2584.	2620.	0.	459.			
10341.	2000.	1353.												
10859.	2103.													

LOAD	GAGE 15	GAGE 16	GAGE 17	GAGE 18	GAGE 19	GAGE 20
0.	0.	0.	0.	0.	0.	0.
500.	15.	8.	7.	-7.	-15.	-7.
1017.	23.	15.	15.	15.	-15.	15.
1535.	30.	8.	8.	15.	-23.	15.
2053.	38.	8.	15.	15.	-31.	23.
2571.	46.	8.	23.	23.	-31.	23.
3089.	54.	15.	31.	31.	-31.	0.
3607.	61.	-23.	53.	-31.	-38.	45.
4125.	84.	-107.	15.	-31.	-77.	76.
4643.	200.	-190.	31.	-60.	-115.	115.
5161.	280.	-298.	61.	-103.	-103.	153.
5679.	360.	-405.	93.	-115.	-120.	206.
6197.	440.	-519.	130.	-115.	-135.	289.
6715.	520.	-649.	151.	-115.	-153.	313.
7233.	600.	-771.	181.	-115.	-170.	359.
7751.	680.	-883.	217.	-115.	-188.	405.
8269.	760.	-997.	253.	-115.	-206.	451.
8787.	840.	-1103.	291.	-115.	-228.	497.
9305.	920.	-1217.	321.	-115.	-250.	543.
9823.	1000.	-1331.	351.	-115.	-272.	589.
10341.	1080.	-1445.	381.	-115.	-294.	635.
10859.	1160.	-1559.	411.	-115.	-316.	681.
11377.	1240.	-1673.	441.	-115.	-338.	727.
11895.	1320.	-1787.	471.	-115.	-360.	773.
12413.	1400.	-1901.	501.	-115.	-382.	819.
12931.	1480.	-2015.	531.	-115.	-404.	865.
13449.	1560.	-2129.	561.	-115.	-426.	911.
13967.	1640.	-2243.	591.	-115.	-448.	957.
14485.	1720.	-2357.	621.	-115.	-470.	1003.
15003.	1800.	-2471.	651.	-115.	-492.	1049.
15521.	1880.	-2585.	681.	-115.	-514.	1095.
16039.	1960.	-2699.	711.	-115.	-536.	1141.
16557.	2040.	-2813.	741.	-115.	-558.	1187.
17075.	2120.	-2927.	771.	-115.	-580.	1233.
17593.	2200.	-3041.	801.	-115.	-602.	1279.
18111.	2280.	-3155.	831.	-115.	-624.	1325.
18629.	2360.	-3269.	861.	-115.	-646.	1371.
19147.	2440.	-3383.	891.	-115.	-668.	1417.
19665.	2520.	-3497.	921.	-115.	-690.	1463.
20183.	2600.	-3611.	951.	-115.	-712.	1509.
20701.	2680.	-3725.	981.	-115.	-734.	1555.
21219.	2760.	-3839.	1011.	-115.	-756.	1601.
21737.	2840.	-3953.	1041.	-115.	-778.	1647.
22255.	2920.	-4067.	1071.	-115.	-800.	1693.
22773.	3000.	-4181.	1101.	-115.	-822.	1739.
23291.	3080.	-4295.	1131.	-115.	-844.	1785.
23809.	3160.	-4409.	1161.	-115.	-866.	1831.
24327.	3240.	-4523.	1191.	-115.	-888.	1877.
24845.	3320.	-4637.	1221.	-115.	-910.	1923.
25363.	3400.	-4751.	1251.	-115.	-932.	1969.
25881.	3480.	-4865.	1281.	-115.	-954.	2015.
26399.	3560.	-4979.	1311.	-115.	-976.	2061.
26917.	3640.	-5093.	1341.	-115.	-998.	2107.
27435.	3720.	-5207.	1371.	-115.	-1020.	2153.
27953.	3800.	-5321.	1401.	-115.	-1042.	2199.
28471.	3880.	-5435.	1431.	-115.	-1064.	2245.
28989.	3960.	-5549.	1461.	-115.	-1086.	2291.
29507.	4040.	-5663.	1491.	-115.	-1108.	2337.
30025.	4120.	-5777.	1521.	-115.	-1130.	2383.
30543.	4200.	-5891.	1551.	-115.	-1152.	2429.
31061.	4280.	-6005.	1581.	-115.	-1174.	2475.
31579.	4360.	-6119.	1611.	-115.	-1196.	2521.
32097.	4440.	-6233.	1641.	-115.	-1218.	2567.
32615.	4520.	-6347.	1671.	-115.	-1240.	2613.
33133.	4600.	-6461.	1701.	-115.	-1262.	2659.
33651.	4680.	-6575.	1731.	-115.	-1284.	2705.
34169.	4760.	-6689.	1761.	-115.	-1306.	2751.
34687.	4840.	-6803.	1791.	-115.	-1328.	2797.
35205.	4920.	-6917.	1821.	-115.	-1350.	2843.
35723.	5000.	-7031.	1851.	-115.	-1372.	2889.
36241.	5080.	-7145.	1881.	-115.	-1394.	2935.
36759.	5160.	-7259.	1911.	-115.	-1416.	2981.
37277.	5240.	-7373.	1941.	-115.	-1438.	3027.
37795.	5320.	-7487.	1971.	-115.	-1460.	3073.
38313.	5400.	-7601.	2001.	-115.	-1482.	3119.
38831.	5480.	-7715.	2031.	-115.	-1504.	3165.
39349.	5560.	-7829.	2061.	-115.	-1526.	3211.
39867.	5640.	-7943.	2091.	-115.	-1548.	3257.
40385.	5720.	-8057.	2121.	-115.	-1570.	3303.
40903.	5800.	-8171.	2151.	-115.	-1592.	3349.
41421.	5880.	-8285.	2181.	-115.	-1614.	3395.
41939.	5960.	-8399.	2211.	-115.	-1636.	3441.
42457.	6040.	-8513.	2241.	-115.	-1658.	3487.
42975.	6120.	-8627.	2271.	-115.	-1680.	3533.
43493.	6200.	-8741.	2301.	-115.	-1702.	3579.
44011.	6280.	-8855.	2331.	-115.	-1724.	3625.
44529.	6360.	-8969.	2361.	-115.	-1746.	3671.
45047.	6440.	-9083.	2391.	-115.	-1768.	3717.
45565.	6520.	-9197.	2421.	-115.	-1790.	3763.
46083.	6600.	-9311.	2451.	-115.	-1812.	3809.
46601.	6680.	-9425.	2481.	-115.	-1834.	3855.
47119.	6760.	-9539.	2511.	-115.	-1856.	3901.
47637.	6840.	-9653.	2541.	-115.	-1878.	3947.
48155.	6920.	-9767.	2571.	-115.	-1900.	3993.
48673.	7000.	-9881.	2601.	-115.	-1922.	4039.
49191.	7080.	-9995.	2631.	-115.	-1944.	4085.
49709.	7160.	-10109.	2661.	-115.	-1966.	4131.
50227.	7240.	-10223.	2691.	-115.	-1988.	4177.
50745.	7320.	-10337.	2721.	-115.	-2010.	4223.
51263.	7400.	-10451.	2751.	-115.	-2032.	4269.
51781.	7480.	-10565.	2781.	-115.	-2054.	4315.
52299.	7560.	-10679.	2811.	-115.	-2076.	4361.
52817.	7640.	-10793.	2841.	-115.	-2098.	4407.
53335.	7720.	-10907.	2871.	-115.	-2120.	4453.
53853.	7800.	-11021.	2901.	-115.	-2142.	4499.
54371.	7880.	-11135.	2931.	-115.	-2164.	4545.
54889.	7960.	-11249.	2961.	-115.	-2186.	4591.
55407.	8040.	-11363.	2991.	-115.	-2208.	4637.
55925.	8120.	-11477.	3021.	-115.	-2230.	4683.
56443.	8200.	-11591.	3051.	-115.	-2252.	4729.
56961.	8280.	-11705.	3081.	-115.	-2274.	4775.
57479.	8360.	-11819.	3111.	-115.	-2296.	4821.
57997.	8440.	-11933.	3141.	-115.	-2318.	4867.
58515.	8520.	-12047.	3171.	-115.	-2340.	4913.
59033.	8600.	-12161.	3201.	-115.	-2362.	4959.
59551.	8680.	-12275.	3231.	-115.	-2384.	5005.
60069.	8760.	-12389.	3261.	-115.	-2406.	5051.
60587.	8840.	-12503.	3291.	-115.	-2428.	5097.
61105.	8920.	-12617.	3321.	-115.	-2450.	5143.
61623.	9000.	-12731.	3351.	-115.	-2472.	5189.
62141.	9080.	-12845.	3381.	-115.	-2494.	5235.
62659.	9160.	-12959.	3411.	-115.	-2516.	5281.
63177.	9240.	-13073.	3441.	-115.	-2538.	5327.
63695.	9320.	-13187.	3471.	-115.	-2560.	5373.
64213.	9400.	-13301.	3501.	-115.	-2582.	5419.
64731.	9480.	-13415.	3531.	-115.	-2604.	5465.
65249.	9560.	-13529.	3561.	-115.	-2626.	5511.
65767.	9640.	-13643.	3591.	-115.	-2648.	5557.
66285.	9720.	-13757.	3621.	-115.	-2670.	5603.
66803.	9800.	-13871.	3651.	-115.	-2692.	5649.
67321.	9880.	-13985.	3681.	-115.	-2714.	5695.
67839.	9960.	-14099.	3711.	-115.	-2736.	5741.
68357.	10040.	-14213.	3741.	-115.	-2758.	5787.
68875.	10120.	-14327.	3771.	-115.	-2780.	5833.
69393.	10200.	-14441.	3801.	-115.	-2802.	5879.
69911.	10280.	-14555.	3831.	-115.	-2824.	5925.
70429.	10360.	-14669.	3861.	-115.	-2846.	5971.
70947.	10440.	-14783.	3891.	-115.	-2868.	6017.
71465.	10520.	-14897.	3921.	-115.	-2890.	6063.
71983.	10600.	-15011.	3951.	-115.	-2912.	6109.
72501.	10680.	-15125.	3981.	-115.	-2934.	6155.
73019.	10760.	-15239.	4011.	-115.	-2956.	6201.
73537.	10840.	-15353.	4041.	-115.	-2978.	6247.
74055.	10920.	-15467.	4071.	-115.	-3000.	6293.
74573.	11000.	-15581.	4101.	-115.	-3022.	6339.
75091.	11080.	-15695.	4131.	-115.	-3044.	6385.
75609.	11160.	-15809.	4161.	-115.	-3066.	6431.
76127.	11240.	-15923.	4191.	-115.	-3088.	6477.
76645.	11320.	-16037.	4221.	-115.	-3110.	6523.
77163.	11400.	-16151.	4251.	-115.	-3132.	6569.
77681.	11480.	-16265.	4281.	-115.	-3154.	6615.
78199.	11560.	-16379.	4311.	-115.	-3176.	6661.
78717.	11640.	-16493.	4341.	-115.	-3198.	6707.
79235.	11720.	-16607.	4371.	-115.	-3220.	6753.
79753.	11800.	-16721.	4401.	-115.	-3242.	6799.
80271.	11880.	-16835.	4431.	-115.	-3264.	6845.
80789.	11960.	-16949.	4461.	-115.	-3286.	6891.
81307.	12040.	-17063.	4491.	-115.	-3308.	6937.
81825.	12120.	-17177.	4521.	-115.	-3330.	6983.
82343.	12200.	-17291.	4551.	-115.	-3352.	7029.
82861.	12280.	-17405.	4581.	-115.	-3374.	7075.
83379.	12360.	-17519.	4611.	-115.	-3396.	7121.
83897.	12440.	-17633.	4641.	-115.	-3418.	7167.
84415.	12520.	-17747.	4671.	-115.	-3440.	7213.
84933.	12600.	-17861.	4701.	-115.	-3462.	7259.
85451.	12680.	-17975.	4731.	-115.	-3484.	7305.
85969.	12760.	-18089.	4761.	-115.	-3506.	7351.
86487.	12840.	-18203.	4791.	-115.	-3528.	7397.
87005.	12920.	-18317.	4821.	-115.	-3550.	7443.
87523.	13000.	-18431.	4851.	-115.	-3572.	7489.
88041.	13080.	-18545.	4881.	-115.	-3594.	7535.
88559.	13160.	-18659.	4911.	-115.	-3616.	7581.
89077.	13240.	-18773.	4941.	-115.	-3638.	7627.
89595.	13320.	-18887.	4971.	-115.	-3660.	7673.
90113.	13400.	-18999.	5001.	-115.	-3682.	7719.
90631.	13480.	-19113.	5031.	-115.	-3704.	7765.
91149.	13560.	-19227.	5061.	-115.	-3726.	7811.
91667.	13640.	-19341.	5091.	-115.	-3748.	7857.
92185.	13720.	-19455.	5121.	-115.	-3770.	7903.
92703.	13800.	-19569.	5151.	-115.	-3792.	7949.
93221.	13880.	-19683.	5181.	-115.	-3814.	7995.
93739.	13960.	-19797.	5211.	-115.	-3836.	8041.
94257.	14040.	-19911.	5241.	-115.	-3858.	8087.
94775.	14120.	-20025.	5271.	-115.	-3880.	8133.
95293.	14200.	-20139.	5301.	-115.	-3902.	8179.
95811.	14280.	-20253.	5			

COMPOSITE FATIGUE SHEAR PANEL CS-1 STRAIN SURVEY AFTER 100,000 CYCLES

LOAD	GAGE 1	GAGE 2	GAGE 3	GAGE 4	GAGE 5	GAGE 6	GAGE 7	GAGE 8	GAGE 9	GAGE 10	GAGE 11	GAGE 12	GAGE 13	GAGE 14
-24.	0.	7.	0.	0.	-7.	-7.	-7.	0.	-7.	0.	-7.	0.	0.	-7.
436.	61.	-73.	-61.	-45.	53.	-61.	-7.	0.	-7.	23.	15.	15.	0.	15.
829.	114.	-38.	-122.	-84.	114.	-107.	-7.	0.	5.	38.	38.	31.	0.	15.
1452.	206.	-45.	-829.	-160.	214.	-206.	-15.	0.	-15.	71.	38.	23.	15.	23.
2003.	299.	-68.	-328.	-836.	306.	-206.	-23.	0.	-15.	53.	53.	31.	23.	31.
2541.	350.	-80.	-410.	-232.	382.	-351.	-31.	0.	-15.	59.	76.	38.	48.	31.
3437.	454.	699.	-150.	-336.	449.	-501.	-69.	36.	0.	84.	84.	31.	-8.	31.
3897.	554.	2275.	1082.	-247.	840.	-938.	-23.	38.	54.	61.	38.	-23.	0.	31.
4429.	1365.	2801.	2241.	-8759.	891.	-1109.	15.	8.	23.	122.	120.	-115.	6.	7.
4852.	1616.	2775.	2424.	-8942.	978.	-1148.	54.	-23.	-15.	122.	280.	-190.	23.	-23.
5005.	1768.	2775.	2424.	-8942.	978.	-1148.	181.	-115.	-169.	121.	780.	-428.	197.	-130.
5046.	2027.	2823.	2553.	-3110.	1578.	-611.	259.	-207.	-368.	344.	1130.	-849.	191.	-277.
5046.	2159.	2861.	2495.	-3454.	2253.	-435.	357.	-314.	-621.	468.	1694.	-901.	395.	-375.
7915.	2279.	2243.	2384.	-8859.	0.	1658.	-47.	-428.	-905.	580.	2131.	-1191.	435.	-501.
8367.	2349.	1896.	1913.	-8883.	0.	3445.	513.	-428.	-1077.	672.	2474.	-1144.	594.	-597.
8923.	2378.	1554.	1645.	-8463.	0.	3995.	569.	-581.	-1394.	771.	2841.	-1512.	573.	-665.
10140.	2415.	1189.	1341.	-8218.	0.	4609.	628.	-643.	-1903.	901.	3360.	-1749.	672.	-738.
11900.	2454.	538.	831.	-1709.	0.	5332.	697.	-727.	-1903.	1031.	360.	-1388.	764.	-850.
10825.	2485.	-82.	252.	-1393.	0.	5332.	750.	-894.	-2210.	1168.	4495.	-2222.	883.	-925.
14914.	2539.	-857.	-442.	-768.	0.	5332.	781.	-894.	-2501.	1306.	4854.	-2474.	962.	-1018.
14930.	2591.	-1615.	-1113.	-114.	0.	5378.	811.	-894.	-2770.	1421.	5720.	-2757.	1039.	-1102.
15071.	2713.	-1854.	-1357.	91.	0.	6044.		-894.						

LOAD	GAGE 15	GAGE 16
-24.	0.	0.
436.	-8.	15.
829.	-15.	31.
1452.	-23.	31.
2003.	-31.	38.
2541.	-38.	46.
3437.	-31.	38.
3897.	-31.	61.
4429.	-61.	61.
4852.	-82.	122.
5005.	-189.	214.
5046.	-307.	321.
7915.	-505.	428.
8367.	-619.	542.
8923.	-811.	634.
10140.	-849.	788.
11900.	-1133.	848.
10825.	-1324.	970.
14914.	-1518.	1160.
14930.	-1715.	1237.
15071.	-1914.	1353.



COMPOSITE SHEAR PANEL CJS STRAIN SURVEY

LOAD	GAGE 1	GAGE 2	GAGE 3	GAGE 4	GAGE 5	GAGE 6	GAGE 7	GAGE 8	GAGE 9	GAGE 10	GAGE 11	GAGE 12	GAGE 13	GAGE 14
0	0	-7	9	0	0	0	0	0	9	-7	0	0	0	-7
400	76	-23	-91	84	-7	-84	-107	0	84	-7	0	-84	-92	-15
800	153	-38	-180	169	-7	-168	-198	0	168	160	0	-168	-176	-15
1200	237	-61	-270	251	-7	-250	-298	0	259	252	8	-252	-268	-15
1600	321	-84	-361	335	-7	-343	-404	15	343	336	8	-336	-344	-23
2000	406	-99	-472	427	-7	-434	-503	38	434	429	0	-427	-435	-23
2400	495	-114	-584	510	0	-518	-593	76	534	457	-15	-568	-527	-46
2800	588	-137	-695	602	15	-617	-701	157	633	573	-53	-649	-629	-61
3200	685	-152	-807	691	312	-716	-803	267	747	619	-137	-733	-726	-91
3600	784	-168	-918	784	562	-840	-937	384	822	655	-230	-840	-844	586
4000	884	-183	-1029	874	813	-916	-1022	501	897	711	-321	-916	-925	1885
4400	984	-198	-1140	964	1066	-1027	-1145	618	974	784	-383	-1027	-1044	2711
4800	1084	-213	-1251	1054	1319	-1127	-1256	735	1054	871	-436	-1127	-1144	3435
5200	1184	-228	-1362	1144	1572	-1209	-1367	852	1134	958	-489	-1209	-1226	4082
5600	1284	-243	-1473	1234	1825	-1290	-1478	969	1214	1045	-542	-1290	-1255	4729
6000	1384	-258	-1584	1324	2078	-1371	-1589	1086	1294	1132	-595	-1371	-1285	5376
6400	1484	-273	-1695	1414	2331	-1452	-1700	1203	1374	1219	-648	-1452	-1341	6023
6800	1584	-288	-1806	1504	2584	-1533	-1811	1320	1454	1299	-701	-1533	-1388	6670
7200	1684	-303	-1917	1594	2837	-1614	-1922	1437	1534	1379	-754	-1614	-1444	7317
7600	1784	-318	-2028	1684	3090	-1695	-2033	1554	1614	1458	-807	-1695	-1509	7964
8000	1884	-333	-2139	1774	3343	-1776	-2144	1671	1694	1538	-860	-1776	-1590	8611
8400	1984	-348	-2250	1864	3596	-1857	-2255	1788	1774	1619	-913	-1857	-1671	9258
8800	2084	-363	-2361	1954	3849	-1938	-2366	1905	1854	1699	-966	-1938	-1754	9905
9200	2184	-378	-2472	2044	4102	-2019	-2477	2022	1934	1779	-1019	-2019	-1838	10552
9600	2284	-393	-2583	2134	4355	-2100	-2588	2139	2014	1859	-1072	-2100	-1921	11199
10000	2384	-408	-2694	2224	4608	-2181	-2699	2256	2094	1939	-1125	-2181	-2004	11846
10400	2484	-423	-2805	2314	4861	-2262	-2810	2373	2174	2019	-1178	-2262	-2087	12493
10800	2584	-438	-2916	2404	5114	-2343	-2921	2490	2254	2099	-1231	-2343	-2170	13140
11200	2684	-453	-3027	2494	5367	-2424	-3032	2607	2334	2179	-1284	-2424	-2253	13787
11600	2784	-468	-3138	2584	5620	-2505	-3143	2724	2414	2259	-1337	-2505	-2336	14434
12000	2884	-483	-3249	2674	5873	-2586	-3254	2841	2494	2339	-1390	-2586	-2419	15081
12400	2984	-498	-3360	2764	6126	-2667	-3365	2958	2574	2419	-1443	-2667	-2502	15728
12800	3084	-513	-3471	2854	6379	-2748	-3476	3075	2654	2499	-1496	-2748	-2585	16375
13200	3184	-528	-3582	2944	6632	-2829	-3587	3192	2734	2579	-1549	-2829	-2668	17022
13600	3284	-543	-3693	3034	6885	-2910	-3698	3309	2814	2659	-1602	-2910	-2751	17669
14000	3384	-558	-3804	3124	7138	-2991	-3809	3426	2894	2739	-1655	-2991	-2834	18316
14400	3484	-573	-3915	3214	7391	-3072	-3920	3543	2974	2819	-1708	-3072	-2917	18963
14800	3584	-588	-4026	3304	7644	-3153	-4031	3660	3054	2899	-1761	-3153	-3000	19610
15200	3684	-603	-4137	3394	7897	-3234	-4142	3777	3134	2979	-1814	-3234	-3083	20257
15600	3784	-618	-4248	3484	8150	-3315	-4253	3894	3214	3059	-1867	-3315	-3166	20904
16000	3884	-633	-4359	3574	8403	-3396	-4364	4011	3294	3139	-1920	-3396	-3249	21551
16400	3984	-648	-4470	3664	8656	-3477	-4475	4128	3374	3219	-1973	-3477	-3332	22198
16800	4084	-663	-4581	3754	8909	-3558	-4586	4245	3454	3299	-2026	-3558	-3415	22845
17200	4184	-678	-4692	3844	9162	-3639	-4697	4362	3534	3379	-2079	-3639	-3498	23492
17600	4284	-693	-4803	3934	9415	-3720	-4808	4479	3614	3459	-2132	-3720	-3581	24139
18000	4384	-708	-4914	4024	9668	-3801	-4919	4596	3694	3539	-2185	-3801	-3664	24786
18400	4484	-723	-5025	4114	9921	-3882	-5030	4713	3774	3619	-2238	-3882	-3747	25433
18800	4584	-738	-5136	4204	10174	-3963	-5141	4830	3854	3699	-2291	-3963	-3830	26080
19200	4684	-753	-5247	4294	10427	-4044	-5252	4947	3934	3779	-2344	-4044	-3913	26727
19600	4784	-768	-5358	4384	10680	-4125	-5363	5064	4014	3859	-2397	-4125	-4000	27374
20000	4884	-783	-5469	4474	10933	-4206	-5474	5181	4094	3939	-2450	-4206	-4083	28021
20400	4984	-798	-5580	4564	11186	-4287	-5585	5298	4174	4019	-2503	-4287	-4166	28668
20800	5084	-813	-5691	4654	11439	-4368	-5696	5415	4254	4099	-2556	-4368	-4249	29315
21200	5184	-828	-5802	4744	11692	-4449	-5807	5532	4334	4179	-2609	-4449	-4332	29962
21600	5284	-843	-5913	4834	11945	-4530	-5918	5649	4414	4259	-2662	-4530	-4415	30609
22000	5384	-858	-6024	4924	12198	-4611	-6029	5766	4494	4339	-2715	-4611	-4498	31256
22400	5484	-873	-6135	5014	12451	-4692	-6140	5883	4574	4419	-2768	-4692	-4581	31903
22800	5584	-888	-6246	5104	12704	-4773	-6251	5999	4654	4499	-2821	-4773	-4664	32550
23200	5684	-903	-6357	5194	12957	-4854	-6362	6116	4734	4579	-2874	-4854	-4747	33197
23600	5784	-918	-6468	5284	13210	-4935	-6473	6233	4814	4659	-2927	-4935	-4830	33844
24000	5884	-933	-6579	5374	13463	-5016	-6584	6350	4894	4739	-2980	-5016	-4913	34491
24400	5984	-948	-6690	5464	13716	-5097	-6695	6467	4974	4819	-3033	-5097	-5000	35138
24800	6084	-963	-6801	5554	13969	-5178	-6806	6584	5054	4899	-3086	-5178	-5083	35785
25200	6184	-978	-6912	5644	14222	-5259	-6917	6701	5134	4979	-3139	-5259	-5166	36432
25600	6284	-993	-7023	5734	14475	-5340	-7028	6818	5214	5059	-3192	-5340	-5249	37079
26000	6384	-1008	-7134	5824	14728	-5421	-7139	6935	5294	5139	-3245	-5421	-5332	37726
26400	6484	-1023	-7245	5914	14981	-5502	-7250	7052	5374	5219	-3298	-5502	-5415	38373
26800	6584	-1038	-7356	6004	15234	-5583	-7361	7169	5454	5299	-3351	-5583	-5498	39020
27200	6684	-1053	-7467	6094	15487	-5664	-7472	7286	5534	5379	-3404	-5664	-5581	39667
27600	6784	-1068	-7578	6184	15740	-5745	-7583	7403	5614	5459	-3457	-5745	-5664	40314
28000	6884	-1083	-7689	6274	15993	-5826	-7694	7520	5694	5539	-3510	-5826	-5747	40961
28400	6984	-1098	-7800	6364	16246	-5907	-7805	7637	5774	5619	-3563	-5907	-5830	41608
28800	7084	-1113	-7911	6454	16499	-5988	-7916	7754	5854	5699	-3616	-5988	-5913	42255
29200	7184	-1128	-8022	6544	16752	-6069	-8027	7871	5934	5779	-3669	-6069	-6000	42902
29600	7284	-1143	-8133	6634	17005	-6150	-8138	7988	6014	5859	-3722	-6150	-6083	43549
30000	7384	-1158	-8244	6724	17258	-6231	-8249	8105	6094	5939	-3775	-6231	-6166	44196
30400	7484	-1173	-8355	6814	17511	-6312	-8360	8222	6174	6019	-3828	-6312	-6249	44843
30800	7584	-1188	-8466	6904	17764	-6393	-8471	8339	6254	6099	-3881	-6393	-6332	45490
31200	7684	-1203	-8577	6994	18017	-6474	-8582	8456	6334	6179	-3934	-6474	-6415	46137
31600	7784	-1218	-8688	7084	18270	-6555	-8693	8573	6414	6259	-3987	-6555	-6498	46784
32000	7884	-1233	-8799	7174	18523	-6636	-8804	8690	6494	6339	-4040	-6636	-6581	47431
32400	7984	-1248	-8910	7264	18776	-6717	-8915	8807	6574	6419	-4093	-6717	-6664	48078
32800	8084	-1263	-9021	7354	19029	-6798	-9026	8924	6654	6499	-4146	-6798	-6747	48725
33200	8184	-1278	-9132	7444	19282	-6879	-9137	9041	6734	6579	-4199	-6879	-6830	49372
33600	8284	-1293	-9243	7534	19535	-6960	-9248	9158	6814	6659	-4252	-6960	-6913	50019
34000	8384	-1308	-9354	7624	19788	-7041	-9359	9275	6894	6739	-4305	-7041	-7000	50666
34400	8484	-1323	-9465	7714	20041	-7122	-9470	9392	6974	6819	-4358	-7122	-7083	51313
34800	8584	-1338	-9576	7804	20294</									

COMPOSITE SHEAR PANEL C95 STRAIN SURVEY

LOAD	GAUGE20	GAUGE30	GAUGE31	GAUGE32	GAUGE34
0.	0.	-8.	-7.	0.	0.
400.	0.	-8.	-7.	-15.	-7.
800.	0.	-8.	-7.	-15.	-7.
1470.	0.	-8.	-15.	-31.	-7.
1800.	0.	-8.	-15.	-31.	-7.
2445.	0.	-8.	-15.	-31.	-7.
2663.	0.	-8.	-15.	-31.	-7.
3451.	0.	-8.	-15.	-31.	-7.
3945.	0.	-8.	-15.	-31.	-7.
4403.	-122.	0.	-31.	-45.	-15.
4700.	-83.	-54.	-61.	-45.	-15.
5494.	78.	-130.	-15.	-31.	-15.
6078.	259.	-220.	83.	-15.	15.
6405.	571.	-275.	91.	-31.	68.
6805.	1050.	-365.	206.	-53.	145.
7603.	1632.	-507.	323.	-438.	290.
8011.	2118.	-1041.	423.	-653.	443.
8305.	2402.	-1104.	510.	-677.	539.
8804.	2804.	-1170.	505.	-677.	634.
9512.	3162.	-1483.	648.	-1110.	718.
10000.	3498.	-1801.	608.	-1832.	787.
10300.	3727.	-1653.	710.	-1313.	848.
11013.	3886.	-1753.	740.	-1416.	901.
				-1518.	938.

COMPOSITE SHEAR PANEL CSS STRAIN SURVEY AFTER 50,000 CYCLES

LOAD	GAGE 1	GAGE 2	GAGE 3	GAGE 4	GAGE 5	GAGE 6	GAGE 7	GAGE 8	GAGE 9	GAGE 10	GAGE 11	GAGE 12	GAGE 13	GAGE 14
0	0	0	0	0	0	0	0	0	0	0	0	0	0	0
500	84	-22114	84	-7	-81	84	-7	91	-8	-8	7	-7	-7	-7
1000	169	-222	169	-7	-168	175	175	175	0	0	7	15	7	-7
1500	253	-430	253	0	-252	257	257	257	-8	0	15	23	7	-7
1900	336	-430	336	-7	-335	351	351	351	-8	8	15	31	15	-15
2300	420	-527	419	-7	-419	450	450	450	-15	15	15	38	23	-15
2700	504	-609	495	-15	-483	534	534	534	-15	15	15	54	33	-15
3100	588	-694	585	61	-473	611	611	611	8	61	0	61	53	-31
3500	672	-778	659	-876	-884	833	909	833	31	-138	-38	122	175	-122
3900	756	-862	741	-1631	-1547	1217	1273	1217	53	-245	-107	191	419	-298
4300	840	-946	825	-2418	-1783	2117	1801	2117	92	-367	-199	268	688	-458
4700	924	-1030	909	-3148	-1844	2804	2631	2804	122	-490	-305	344	988	-611
5100	1008	-1114	993	-3874	-1743	3505	3271	3505	145	-615	-420	421	1285	-784
5500	1092	-1198	1077	-4600	-1623	4200	3934	4200	175	-735	-530	498	1562	-989
5900	1176	-1282	1161	-5326	-1387	4899	4634	4899	205	-859	-680	568	1844	-1039
6300	1260	-1366	1245	-6052	-1060	5598	5333	5598	235	-972	-794	638	2088	-1161
6700	1344	-1450	1329	-6778	-810	6297	6032	6297	265	-1056	-894	707	2316	-1280
7100	1428	-1534	1413	-7504	-480	6996	6731	6996	295	-1140	-1000	777	2537	-1350
7500	1512	-1618	1497	-8230	81	7695	7430	7695	325	-1224	-1082	847	2743	-1459
7900	1596	-1702	1581	-8956	823	8394	8129	8394	355	-1308	-1191	917	2956	-1550
8300	1680	-1786	1665	-9682	1354	9093	8828	9093	385	-1392	-1285	987	3116	-1619
8700	1764	-1870	1749	-10408	1783	9792	9527	9792	415	-1476	-1369	1057	3253	-1680
9100	1848	-1954	1833	-11134	2104	10491	10226	10491	445	-1560	-1453	1127	3383	-1734

LOAD	GAGE 15	GAGE 16	GAGE 17	GAGE 18
0	0	0	0	0
500	0	0	0	-7
1000	0	0	-15	-15
1500	0	0	-15	-15
2000	-8	8	-23	-15
2500	-15	15	-38	-15
3000	-61	46	-38	31
3500	-53	23	-69	77
4000	-15	-23	-69	123
4500	38	-61	-109	169
5000	76	-107	-158	214
5500	107	-153	-207	259
6000	137	-191	-251	304
6500	169	-230	-304	349
7000	183	-259	-351	394
7500	190	-285	-391	439
8000	223	-305	-431	484
8500	237	-334	-472	529
9000	244	-363	-513	574
9500	244	-392	-554	619
10000	244	-421	-595	664

COMPOSITE SHEAR PANEL C56 STRAIN SURVEY

LOAD	GAGE 1	GAGE 2	GAGE 3	GAGE 4	GAGE 5	GAGE 6	GAGE 7	GAGE 8	GAGE 9	GAGE 10	GAGE 11	GAGE 12	GAGE 13	GAGE 14
1000	-84.	-7.	0.	-7.	0.	0.	-7.	-7.	0.	0.	-7.	0.	-7.	0.
1000	436.	-23.	-59.	69.	-15.	-84.	76.	-7.	-84.	91.	0.	-84.	84.	-8.
1000	944.	-38.	-205.	163.	-30.	-160.	160.	-15.	-175.	183.	7.	-175.	160.	9.
1000	1458.	-53.	-305.	237.	-46.	-244.	252.	-15.	-274.	282.	7.	-267.	252.	8.
1000	1969.	-69.	-419.	321.	-53.	-320.	343.	-15.	-356.	373.	15.	-358.	335.	8.
1000	2483.	-84.	-533.	412.	-68.	-407.	487.	-15.	-465.	473.	15.	-450.	419.	15.
1000	2998.	-89.	-649.	486.	-76.	-511.	564.	-23.	-556.	564.	15.	-541.	503.	23.
1000	3512.	-114.	-754.	580.	-76.	-618.	655.	-23.	-640.	655.	15.	-633.	587.	30.
1000	4027.	-122.	-897.	650.	-83.	-756.	694.	-15.	-784.	747.	-7.	-747.	686.	46.
1000	4541.	-145.	-1119.	816.	-103.	-917.	854.	-15.	-974.	890.	-3270.	-3270.	1113.	1104.
1000	5056.	-166.	-1380.	1145.	-128.	-1080.	1074.	-15.	-1153.	90.	-4052.	-3826.	1470.	2040.
1000	5570.	-189.	-1641.	1313.	-151.	-1339.	1284.	-43.	-1407.	-43.	-4631.	-4238.	1837.	2757.
1000	6085.	-212.	-1902.	1481.	-174.	-1514.	1428.	-46.	-1585.	145.	-5089.	-4565.	2165.	3336.
1000	6600.	-235.	-2163.	1649.	-197.	-1689.	1593.	-145.	-1756.	174.	-5415.	-4778.	2485.	3839.
1000	7115.	-258.	-2424.	1817.	-220.	-1860.	1764.	-119.	-1913.	274.	-5837.	-4794.	2799.	4250.
1000	7630.	-281.	-2685.	1985.	-243.	-2016.	1940.	-142.	-2067.	343.	-6259.	-4375.	3011.	4696.
1000	8145.	-304.	-2946.	2153.	-266.	-2177.	2084.	-165.	-2228.	414.	-6681.	-3788.	3260.	5068.
1000	8660.	-327.	-3207.	2321.	-289.	-2348.	2250.	-188.	-2489.	487.	-7103.	-3273.	3517.	5484.
1000	9175.	-350.	-3468.	2489.	-312.	-2519.	2407.	-211.	-2750.	560.	-7525.	-3245.	3773.	5867.
1000	9690.	-373.	-3729.	2657.	-335.	-2680.	2540.	-234.	-2961.	633.	-7947.	-3263.	4030.	6250.
1000	10205.	-396.	-3990.	2825.	-358.	-2841.	2700.	-257.	-3172.	706.	-8369.	-3281.	4287.	6633.
1000	10720.	-419.	-4251.	2993.	-381.	-2992.	2868.	-280.	-3383.	779.	-8791.	-3299.	4544.	7016.
1000	11235.	-442.	-4512.	3161.	-404.	-3160.	3044.	-303.	-3594.	852.	-9213.	-3317.	4801.	7399.
1000	11750.	-465.	-4673.	3329.	-427.	-3328.	3228.	-326.	-3805.	925.	-9635.	-3335.	5058.	7782.
1000	12265.	-488.	-4894.	3497.	-450.	-3496.	3407.	-349.	-4016.	998.	-10057.	-3353.	5315.	8165.
1000	12780.	-511.	-5115.	3665.	-473.	-3664.	3588.	-372.	-4227.	1071.	-10479.	-3371.	5572.	8548.
1000	13295.	-534.	-5326.	3833.	-496.	-3832.	3760.	-395.	-4438.	1144.	-10901.	-3389.	5829.	8931.
1000	13810.	-557.	-5547.	4001.	-519.	-4000.	3952.	-418.	-4649.	1217.	-11323.	-3407.	6086.	9314.
1000	14325.	-580.	-5798.	4169.	-542.	-4168.	4144.	-441.	-4860.	1290.	-11745.	-3425.	6343.	9697.
1000	14840.	-603.	-6019.	4337.	-565.	-4336.	4336.	-464.	-5071.	1363.	-12167.	-3443.	6600.	10080.
1000	15355.	-626.	-6255.	4505.	-588.	-4504.	4504.	-487.	-5282.	1436.	-12589.	-3461.	6857.	10463.
1000	15870.	-649.	-6489.	4673.	-611.	-4672.	4672.	-510.	-5493.	1509.	-13011.	-3479.	7114.	10846.
1000	16385.	-672.	-6721.	4841.	-634.	-4840.	4840.	-533.	-5704.	1582.	-13433.	-3497.	7371.	11229.
1000	16900.	-695.	-6951.	5009.	-657.	-5008.	5008.	-556.	-5915.	1655.	-13855.	-3515.	7628.	11612.
1000	17415.	-718.	-7181.	5177.	-680.	-5176.	5176.	-579.	-6126.	1728.	-14277.	-3533.	7885.	11995.
1000	17930.	-741.	-7411.	5345.	-703.	-5344.	5344.	-602.	-6337.	1801.	-14699.	-3551.	8142.	12378.
1000	18445.	-764.	-7641.	5513.	-726.	-5512.	5512.	-625.	-6548.	1874.	-15121.	-3569.	8399.	12761.
1000	18960.	-787.	-7871.	5681.	-749.	-5680.	5680.	-648.	-6759.	1947.	-15543.	-3587.	8656.	13144.
1000	19475.	-810.	-8101.	5849.	-772.	-5848.	5848.	-671.	-6970.	2020.	-15965.	-3605.	8913.	13527.
1000	20000.	-833.	-8331.	6017.	-795.	-6016.	6016.	-694.	-7181.	2093.	-16387.	-3623.	9170.	13910.
1000	20515.	-856.	-8561.	6185.	-818.	-6184.	6184.	-717.	-7392.	2166.	-16809.	-3641.	9427.	14293.
1000	21030.	-879.	-8791.	6353.	-841.	-6352.	6352.	-740.	-7603.	2239.	-17231.	-3659.	9684.	14676.
1000	21545.	-902.	-9021.	6521.	-864.	-6520.	6520.	-763.	-7814.	2312.	-17653.	-3677.	9941.	15059.
1000	22060.	-925.	-9251.	6689.	-887.	-6688.	6688.	-786.	-8025.	2385.	-18075.	-3695.	10198.	15442.
1000	22575.	-948.	-9481.	6857.	-910.	-6856.	6856.	-809.	-8236.	2458.	-18497.	-3713.	10455.	15825.
1000	23090.	-971.	-9711.	7025.	-933.	-7024.	7024.	-832.	-8447.	2531.	-18919.	-3731.	10712.	16208.
1000	23605.	-994.	-9941.	7193.	-956.	-7192.	7192.	-855.	-8658.	2604.	-19341.	-3749.	10969.	16591.
1000	24120.	-1017.	-10171.	7361.	-979.	-7360.	7360.	-878.	-8869.	2677.	-19763.	-3767.	11226.	16974.
1000	24635.	-1040.	-10401.	7529.	-1002.	-7528.	7528.	-901.	-9080.	2750.	-20185.	-3785.	11483.	17357.

LOAD	GAGE 15	GAGE 16	GAGE 17	GAGE 18	GAGE 19	GAGE 20	GAGE 21	GAGE 22	GAGE 23	GAGE 24	GAGE 25	GAGE 26	GAGE 27	GAGE 28
-84.	0.	0.	-7.	-84.	0.	0.	0.	-7.	-7.	0.	0.	-8.	0.	0.
436.	-81.	84.	7.	-84.	84.	0.	-91.	76.	7.	-82.	0.	-8.	0.	15.
844.	-176.	169.	23.	-169.	169.	8.	-175.	145.	15.	-175.	15.	-8.	15.	8.
1458.	-266.	338.	30.	-338.	338.	8.	-267.	237.	23.	-267.	23.	0.	23.	0.
1969.	-351.	507.	53.	-507.	507.	8.	-351.	321.	23.	-351.	23.	0.	31.	0.
2483.	-442.	676.	53.	-676.	676.	15.	-442.	401.	23.	-442.	23.	0.	31.	0.
2998.	-527.	845.	61.	-845.	845.	15.	-517.	481.	23.	-517.	23.	0.	46.	0.
3512.	-613.	1014.	61.	-1014.	1014.	15.	-535.	560.	23.	-535.	23.	15.	61.	0.
4027.	-697.	1183.	63.	-1183.	1183.	0.	-535.	639.	46.	-535.	23.	15.	61.	-8.
4541.	-777.	1352.	63.	-1352.	1352.	-464.	-617.	718.	441.	-617.	31.	84.	145.	-38.
5056.	-859.	1521.	63.	-1521.	1521.	-714.	-632.	803.	803.	-632.	46.	61.	130.	0.
5570.	-942.	1690.	63.	-1690.	1690.	-981.	-718.	886.	886.	-718.	63.	31.	130.	46.
6085.	-1026.	1859.	63.	-1859.	1859.	-1011.	-751.	969.	1132.	-751.	92.	38.	38.	53.
6600.	-1110.	2028.	63.	-2028.	2028.	-1041.	-793.	1052.	1301.	-793.	107.	-46.	-46.	153.
7115.	-1194.	2197.	63.	-2197.	2197.	-1071.	-835.	1135.	1470.	-835.	130.	-222.	-199.	252.
7630.	-1278.	2366.	63.	-2366.	2366.	-1101.	-877.	1219.	1639.	-877.	151.	-391.	-443.	397.
8145.	-1362.	2535.	63.	-2535.	2535.	-1131.	-919.	1303.	1808.	-919.	176.	-568.	-695.	550.
8660.	-1446.	2704.	63.	-2704.	2704.	-1161.	-961.	1387.	1977.	-961.	191.	-698.	-809.	680.
9175.	-1530.	2873.	63.	-2873.	2873.	-1191.	-1003.	1471.	2146.	-1003.	206.	-783.	-1054.	756.
9690.	-1614.	3042.	63.	-3042.	3042.	-1221.	-1045.	1555.	2315.	-1045.	221.	-836.	-1159.	825.
10205.	-1698.	3211.	63.	-3211.	3211.	-1251.	-1087.	1639.	2484.	-1087.	221.	-889.	-1268.	886.
10720.	-1782.	3380.	63.	-3380.	3380.	-1281.	-1129.	1723.	2653.	-1129.	244.	-941.	-1367.	939.
11235.	-1866.	3549.	63.	-3549.	3549.	-1311.	-1171.	1807.	2822.	-1171.	244.	-994.	-1466.	993.
11750.	-1950.	3718.	63.	-3718.	3718.	-1341.	-1213.	1891.	2991.	-1213.	260.	-1008.	-1565.	1052.
12265.	-2034.	3887.	63.	-3887.	3887.	-1371.	-1255.	1975.	3160.	-1255.	260.	-1061.	-1664.	1105.
12780.	-2118.	4056.	63.	-4056.	4056.	-1401.	-1297.	2059.	3329.	-1297.	260.	-1114.	-1763.	1158.
13295.	-2202.	4225.	63.	-4225.	4225.	-1431.	-1339.	2143.	3498.	-1339.	260.	-1167.	-1862.	1211.
13810.	-2286.	4394.	63.	-4394.	4394.	-1461.	-1381.	2227.	3667.	-1381.	260.	-1220.	-1961.	1264.
14325.	-2370.	4563.	63.	-4563.	4563.	-1491.	-1423.	2311.	3836.	-1423.	260.	-1273.	-2060.	1317.
14840.	-2454.	4732.	63.	-4732.	4732.	-1521.	-1465.	2395.	4005.	-1465.	260.	-1326.	-2159.	1370.
15355.	-2538.	4901.	63.	-4901.	4901.	-1551.	-1507.	2479.	4174.	-1507.	260.	-1379.	-2258.	1423.
15870.	-2622.	5070.	63.	-5070.	5070.	-1581.	-1549.	2563.	4343.	-1549.	260.	-1432.	-2357.	1476.
16385.	-2706.	5239.	63.	-5239.	5239.	-1611.	-1591.	2647.	4512.	-1591.	260.	-1485.	-2456.	1529.
16900.	-2790.	5408.	63.	-5408.	5408.	-1641.	-1633.	2731.	4681.	-1633.	260.	-1538.	-2555.	1582.
17415.	-2874.	5577.	63.	-5577.	5577.	-1671.	-1675.	2815.	4850.	-1675.	260.	-1591.	-2654.	1635.
17930.	-2958.	5746.	63.	-5746.	5746.	-1701.	-1717.	2899.	5019.	-1717.	260.	-1644.	-2753.	1688.
18445.	-3042.	5915.	63.	-5915.	5915.	-1731.	-1761.	2983.	5188.	-1761.	260.	-1697.	-2852.	1741.
18960.	-3126.	6084.	63.	-6084.	6084.	-1761.	-1801.	3067.	5357.	-1801.	260.	-1750.	-2951.	1794.
19475.	-3210.	6253.	63.	-6253.	6253.	-1791.	-1843.	3151.	5526.	-1843.	260.	-1803.	-3050.	1847.
20000.	-3294.	6422.	63.	-6422.	6422.	-1821.	-1885.	3235.	5695.	-1885.	260.	-1856.	-3149.	1900.
20515.	-3378.	6591.	63.	-6591.	6591.	-1851.	-1927.	3319.	5864.	-1927.	260.	-1909.	-3248.	1953.
21030.	-3462.	6760.	63.	-6760.	6760.	-1881.	-1969.	3403.	6033.	-1969.	260.	-1962.	-3347.	2006.
21545.	-3546.	6929.	63.	-6929.	6929.	-1911.	-2011.	3487.	6202.	-2011.	260.	-2015.	-3446.	2059.
22060.	-3630.	7098.	63.	-7098.	7098.	-1941.	-2053.	3571.	6371.	-2053.	260.	-2068.	-3545.	2112.
22575.	-3714.	7267.	63.	-7267.	7267.	-1971.	-2095.	3655.	6540.	-2095.	260.	-2121.	-3644.	2165.
23090.	-3798.	7436.	63.	-7436.	7436.	-2001.	-2137.	3739.	6709.	-2137.	260.	-2174.	-3743.	2218.
23605.	-3882.	7605.	63.	-7605.	7605.	-2031.	-2179.	3823.	6878.	-2179.	260.	-2227.	-3842.	2271.
24120.	-3966.	7774.	63.	-7774.	7774.	-2061.	-2221.	3907.	7047.	-2221.	260.	-2280.	-3941.	2324.
24635.	-4050.	7943.	63.	-7943.	7943.	-2091.	-2263.	3991.	7216.	-2263.	260.	-2333.	-4040.	2377.
25150.	-4134.	8112.	63.	-8112.	8112.	-2121.	-2305.	4075.	7385.	-2305.	260.	-2386.	-4139.	2430.
25665.	-4218.	8281.	63.	-8281.	8281.	-2151.	-2347.	4159.	7554.	-2347.	260.	-2439.	-4238.	2483.
26180.	-4302.	8450.	63.	-8450.	8450.	-2181.	-2389.	4243.	7723.	-2389.	260.	-2492.	-4337.	2536.
26695.	-4386.	8619.	63.	-8619.	8619.	-2211.	-2431.	4327.	7892.	-2431.	260.	-2545.	-4436.	2589.
27210.	-4470.	8788.	63.	-8788.	8788.	-2241.	-2473.	4411.	8061.	-2473.	260.	-2598.	-4535.	2642.
27725.	-4554.	8957.	63.	-8957.	8957.	-2271.	-2515.	4495.	8230.	-2515.	260.	-2651.	-4634.	2695.
28240.	-4638.	9126.	63.	-9126.	9126.	-2301.	-2557.	4579.	8399.	-2557.	260.	-2704.	-4733.	2748.
28755.	-4722.	9295.	63.	-9295.	9295.	-2331.	-2599.	4663.	8568.	-2599.	260.	-2757.	-4832.	2801.
29270.	-4806.	9464.	63.	-9464.	9464.	-2361.	-2641.	4747.	8737.	-2641.	260.	-2810.	-4931.	2854.
29785.	-4890.	9633.	63.	-9633.	9633.	-2391.	-2683.	4831.	8906.	-2683.	260.	-2863.	-5030.	2907.
30300.	-4974.	9802.	63.	-9802.	9802.	-2421.	-2725.	4915.	9075.	-2725.	260.	-2916.	-5129.	2960.
30815.	-5058.	9971.	63.	-9971.	9971.	-2451.	-2767.	4999.	9244.	-2767.	260.	-2969.	-5228.	3013.
31330.	-5142.	10140.	63.	-10140.	10140.	-2481.	-2809.	5083.	9413.	-2809.	260.	-3022.	-5327.	3066.
31845.	-5226.	10309.	63.	-10309.	10309.	-2511.	-2851.	5167.	9582.	-2851.	260.	-3075.	-5426.	3119.
32360.	-5310.	10478.	63.	-10478.	10478.	-2541.	-2893.	5251.	9751.	-2893.	260.	-3128.	-5525.	3172.
32875.	-5394.	10647.	63.	-10647.	10647.	-2571.	-2935.	5335.	9920.	-2935.	260.	-3181.	-5624.	3225.
33390.	-5478.	10816.	63.	-10816.	10816.	-2601.	-2977.	5419.	10089.	-2977.	260.	-3234.	-5723.	3278.
33905.	-5562.	10985.	63.	-10985.	10985.	-2631.	-3019.	5503.	10258.	-3019.	260.	-3287.	-5822.	3331.
34420.	-5646.	11154.	63.	-11154.	11154.	-2661.	-3061.	5587.	10427.	-3061.	260.	-3340.	-5921.	3384.
34935.	-5730.	11323.	63.	-11323.	11323.	-2691.	-3103.	5671.	10596.	-3103.	260.	-3393.	-6020.	3437.
35450.	-5814.	11492.	63.	-11492.	11492.	-2721.	-3145.	5755.	10765.	-3145.	260.	-3446.	-6119.	3490.
35965.	-5898.	11661.	63.	-11661.	11661.	-2751.	-3187.	5839.	10934.	-3187.	260.	-3499.	-6218.	3543.
36480.	-5982.	11830.	63.	-11830.	11830.	-2781.	-3229.	5923.	11103.	-3229.	260.	-3552.	-6317.	3596.
36995.	-6066.	11999.	63.	-11999.	11999.	-2811.	-3271.	6007.	11272.	-3271.	260.	-3605.	-6416.	3649.
37510.	-6150.	12168.	63.	-12168.	12168.	-2841.	-3313.	6091.	11441.	-3313.	260.	-3658.	-6515.	3702.
38025.	-6234.	12337.	63.	-12337.	12337.	-2871.	-3355.	6175.	11610.	-3355.	260.	-3711.	-6614.	3755.
38540.	-6318.	12506.	63.	-12506.	12506.	-2901.	-3397.	6259.	11779.	-3397.	260.	-3764.	-6713.	3808.
39055.	-6402.	12675.	63.	-12675.	12675.	-2931.	-3439.	6343.	11948.	-3439.	260.	-3817.	-6812.	3861.
39570.	-6486.	12844.	63.	-12844.	12844.	-2961.	-3481.	6427.	12117.	-3481.	260.	-3870.	-6911.	3914.
40085.	-6570.	13013.	63.	-13013.	13013.	-2991.	-3523.	6511.	12286.	-3523.	260.	-3923.	-7010.	3967.
40600.	-6654.	13182.	63.	-13182.	13182.	-3021.	-3565.	6595.	12455.	-3565.	260.	-3976.	-7109.	4020.
41115.	-6738.	13351.	63.	-13351.	13351.	-3051.	-3607.	6679.	12624.	-3607.	260.	-4029.	-7208.	4073.
41630.	-6822.	13520.	63.	-13520.	13520.	-3081.	-3649.	6763.	12793.	-3649.	260.	-4082.	-7307.	4126.
42145.	-6906.	13689.	63.	-13689.	13689.	-3111.	-3691.	6847.	12962.	-3691.	260.	-4135.	-7406.	4179.
42660.	-6990.	13858.	63.	-13858.	13858.	-3141.	-3733.	6931.	13131.	-3733.	260.	-4188.	-7505.	4232.
43175.	-7074.	14027.	63.	-14027.	14027.	-3171.	-3775.	7015.	13300.	-3775.	260.	-4241.	-7604.	4285.
43690.	-7158.	14196.	63.	-14196.	14196.	-3201.	-3817.	7099.	13469.	-3817.	260.	-4294.	-7703.	4338.
44205.	-7242.	14365.	63.	-14365.	14365.	-3231.	-3859.	7183.	13638.	-3859.	260.	-4347.	-7802.	4391.
44720.	-7326.	14534.	63.	-14534.	14534.	-3261.	-3901.	7267.	13807.	-3901.	260.	-4400.	-7901.	4444.
45235.	-7410.	14703.	63.	-14703.	14703.	-3291.	-3943.	7351.	13976.	-3943.	260.	-4453.	-8000.	4497.
45750.	-7494.	14872.	63.	-14872.	14872.	-3321.	-3985.	7435.	14145.	-3985.	260.	-4506.	-8099.	4550.
46265.	-7578.	15041.	63.	-15041.	15041.	-3351.	-4027.	7519.	14314.	-4027.	260.	-455		

COMPOSITE SHEAR PANEL CSS STRAIN SURVEY

LONG	GAGE29	GAGE30	GAGE31	GAGE32	GAGE33	GAGE34
-24.	0.	-7.	0.	0.	0.	-7.
438.	0.	-7.	-7.	0.	-8.	0.
944.	0.	-15.	-15.	0.	-15.	0.
1622.	0.	-15.	-23.	0.	-23.	0.
1880.	0.	-15.	-23.	0.	-23.	0.
2409.	15.	-15.	-23.	0.	-23.	7.
2639.	15.	-15.	-31.	0.	-36.	15.
3282.	15.	-15.	-31.	0.	-46.	7.
3537.	0.	-15.	-41.	15.	-53.	0.
4384.	-120.	0.	-41.	15.	-53.	-33.
4859.	-38.	-61.	-46.	31.	-15.	-15.
5442.	38.	-145.	-53.	0.	-53.	73.
5530.	252.	-237.	7.	-38.	-59.	53.
5436.	463.	-344.	46.	-38.	-176.	167.
6046.	764.	-609.	93.	-134.	-223.	183.
7479.	1383.	-712.	162.	-321.	-454.	289.
7867.	1734.	-634.	237.	-444.	-549.	439.
8445.	2184.	-1125.	306.	-568.	-605.	535.
8894.	2487.	-1271.	304.	-636.	-947.	619.
9512.	2764.	-1372.	323.	-683.	-1043.	687.
10329.	3481.	-1485.	412.	-742.	-1160.	743.
10523.	3253.	-1649.	452.	-763.	-1289.	817.
11637.	3418.	-1787.	475.	-842.	-1352.	871.

COMPOSITE SHEAR PANEL C57 STRAIN SURVEY

LOAD	GAGE 1	GAGE 2	GAGE 3	GAGE 4	GAGE 5	GAGE 6	GAGE 7	GAGE 8	GAGE 9	GAGE 10	GAGE 11	GAGE 12	GAGE 13	GAGE 14
0.	-7.	-7.	0.	-7.	-7.	-7.	-7.	-7.	-7.	-7.	-7.	-7.	0.	0.
414.	53.	-23.	-91.	84.	-50.	76.	76.	-15.	-95.	101.	0.	-90.	84.	15.
822.	175.	-30.	-175.	169.	-181.	153.	153.	-15.	-183.	181.	7.	-19.	175.	78.
1291.	267.	-46.	-267.	259.	-259.	237.	237.	-15.	-275.	290.	7.	-290.	257.	53.
1808.	350.	-61.	-350.	351.	-374.	321.	321.	-7.	-359.	380.	0.	-390.	351.	63.
2408.	442.	-69.	-442.	443.	-474.	405.	405.	0.	-435.	470.	0.	-497.	434.	84.
2993.	533.	-84.	-533.	535.	-565.	489.	489.	23.	-512.	564.	-38.	-519.	518.	107.
3681.	625.	-98.	-625.	634.	-657.	588.	588.	59.	-550.	633.	-59.	-772.	617.	120.
3969.	719.	-129.	-719.	719.	-733.	726.	726.	113.	-650.	724.	-69.	-1329.	716.	169.
4463.	810.	-189.	-810.	804.	-842.	1435.	1435.	243.	-819.	840.	-116.	-1315.	1339.	2193.
4957.	902.	-259.	-902.	895.	-964.	1757.	1757.	303.	-875.	900.	-339.	-3058.	1738.	2848.
5478.	1000.	-344.	-1000.	995.	-1071.	2040.	2040.	386.	-953.	1000.	-433.	-4205.	2033.	3385.
5978.	1097.	-421.	-1097.	1093.	-1174.	2307.	2307.	463.	-958.	1097.	-477.	-4559.	2302.	3782.
6499.	1195.	-509.	-1195.	1192.	-1276.	2520.	2520.	540.	-957.	1195.	-502.	-4774.	2576.	3978.
6999.	1292.	-593.	-1292.	1292.	-1378.	2667.	2667.	617.	-957.	1292.	-539.	-4530.	2698.	4086.
7499.	1389.	-678.	-1389.	1389.	-1474.	2837.	2837.	694.	-958.	1389.	-574.	-3605.	2713.	3815.
7999.	1486.	-763.	-1486.	1486.	-1578.	2990.	2990.	771.	-958.	1486.	-610.	-3491.	2713.	3589.
8499.	1583.	-848.	-1583.	1583.	-1678.	3154.	3154.	848.	-958.	1583.	-646.	-3155.	2713.	3484.
8999.	1680.	-933.	-1680.	1680.	-1774.	3328.	3328.	925.	-958.	1680.	-682.	-3034.	2713.	3229.
9499.	1777.	-1018.	-1777.	1777.	-1869.	3502.	3502.	1002.	-958.	1777.	-718.	-2475.	2721.	3931.
9999.	1874.	-1103.	-1874.	1874.	-1964.	3676.	3676.	1079.	-958.	1874.	-754.	-2177.	2736.	2856.
10499.	1971.	-1188.	-1971.	1971.	-2059.	3850.	3850.	1156.	-958.	1971.	-790.	-1834.	2767.	2734.
10999.	2068.	-1273.	-2068.	2068.	-2154.	4024.	4024.	1233.	-958.	2068.	-826.	-1574.	2774.	2557.

LOAD	GAGE 15	GAGE 16	GAGE 17	GAGE 18	GAGE 19	GAGE 20	GAGE 21	GAGE 22	GAGE 23	GAGE 24	GAGE 25	GAGE 26	GAGE 27	GAGE 28
0.	0.	-7.	-7.	-7.	-15.	-7.	0.	-7.	0.	0.	0.	0.	0.	-7.
404.	-83.	76.	-7.	-107.	76.	-7.	-83.	76.	-15.	-51.	-7.	0.	0.	-7.
802.	-175.	162.	-7.	-139.	162.	15.	-183.	160.	-30.	-175.	-7.	0.	0.	-7.
1191.	-267.	233.	-7.	-209.	233.	23.	-275.	232.	-30.	-267.	-7.	0.	0.	-7.
1585.	-350.	325.	-7.	-282.	325.	30.	-351.	322.	-30.	-350.	-7.	0.	0.	-7.
1978.	-437.	403.	-7.	-352.	403.	38.	-431.	410.	-33.	-437.	-7.	0.	0.	-7.
2363.	-524.	494.	-15.	-423.	494.	38.	-503.	489.	-33.	-503.	-7.	0.	0.	-15.
2749.	-612.	585.	-23.	-494.	585.	38.	-577.	563.	-33.	-577.	-15.	0.	0.	-15.
3135.	-700.	676.	-31.	-565.	676.	38.	-642.	628.	-33.	-642.	-15.	0.	0.	-31.
3521.	-788.	767.	-39.	-636.	767.	38.	-717.	703.	-33.	-717.	-15.	0.	0.	-31.
3907.	-875.	858.	-47.	-707.	858.	38.	-792.	778.	-33.	-792.	-15.	0.	0.	-31.
4293.	-963.	949.	-55.	-778.	949.	38.	-867.	853.	-33.	-867.	-15.	0.	0.	-31.
4679.	-1050.	1040.	-63.	-849.	1040.	38.	-942.	928.	-33.	-942.	-15.	0.	0.	-31.
5065.	-1138.	1128.	-71.	-920.	1128.	38.	-1017.	1003.	-33.	-1017.	-15.	0.	0.	-31.
5451.	-1225.	1215.	-79.	-991.	1215.	38.	-1092.	1078.	-33.	-1092.	-15.	0.	0.	-31.
5837.	-1313.	1303.	-87.	-1062.	1303.	38.	-1167.	1153.	-33.	-1167.	-15.	0.	0.	-31.
6223.	-1400.	1390.	-95.	-1133.	1390.	38.	-1242.	1228.	-33.	-1242.	-15.	0.	0.	-31.
6609.	-1488.	1478.	-103.	-1204.	1478.	38.	-1317.	1303.	-33.	-1317.	-15.	0.	0.	-31.
6995.	-1575.	1565.	-111.	-1275.	1565.	38.	-1392.	1378.	-33.	-1392.	-15.	0.	0.	-31.
7381.	-1663.	1653.	-119.	-1346.	1653.	38.	-1467.	1453.	-33.	-1467.	-15.	0.	0.	-31.
7767.	-1750.	1740.	-127.	-1417.	1740.	38.	-1542.	1528.	-33.	-1542.	-15.	0.	0.	-31.
8153.	-1838.	1828.	-135.	-1488.	1828.	38.	-1617.	1603.	-33.	-1617.	-15.	0.	0.	-31.
8539.	-1925.	1915.	-143.	-1559.	1915.	38.	-1692.	1678.	-33.	-1692.	-15.	0.	0.	-31.
8925.	-2013.	2003.	-151.	-1630.	2003.	38.	-1767.	1753.	-33.	-1767.	-15.	0.	0.	-31.
9311.	-2100.	2090.	-159.	-1701.	2090.	38.	-1842.	1828.	-33.	-1842.	-15.	0.	0.	-31.
9697.	-2188.	2178.	-167.	-1772.	2178.	38.	-1917.	1903.	-33.	-1917.	-15.	0.	0.	-31.
10083.	-2275.	2265.	-175.	-1843.	2265.	38.	-1992.	1978.	-33.	-1992.	-15.	0.	0.	-31.
10469.	-2363.	2353.	-183.	-1914.	2353.	38.	-2067.	2053.	-33.	-2067.	-15.	0.	0.	-31.
10855.	-2450.	2440.	-191.	-1985.	2440.	38.	-2142.	2128.	-33.	-2142.	-15.	0.	0.	-31.
11241.	-2538.	2528.	-199.	-2056.	2528.	38.	-2217.	2203.	-33.	-2217.	-15.	0.	0.	-31.
11627.	-2625.	2615.	-207.	-2127.	2615.	38.	-2292.	2278.	-33.	-2292.	-15.	0.	0.	-31.
12013.	-2713.	2703.	-215.	-2198.	2703.	38.	-2367.	2353.	-33.	-2367.	-15.	0.	0.	-31.
12399.	-2800.	2790.	-223.	-2269.	2790.	38.	-2442.	2428.	-33.	-2442.	-15.	0.	0.	-31.
12785.	-2888.	2878.	-231.	-2340.	2878.	38.	-2517.	2503.	-33.	-2517.	-15.	0.	0.	-31.
13171.	-2975.	2965.	-239.	-2411.	2965.	38.	-2592.	2578.	-33.	-2592.	-15.	0.	0.	-31.
13557.	-3063.	3053.	-247.	-2482.	3053.	38.	-2667.	2653.	-33.	-2667.	-15.	0.	0.	-31.
13943.	-3150.	3140.	-255.	-2553.	3140.	38.	-2742.	2728.	-33.	-2742.	-15.	0.	0.	-31.
14329.	-3238.	3228.	-263.	-2624.	3228.	38.	-2817.	2803.	-33.	-2817.	-15.	0.	0.	-31.
14715.	-3325.	3315.	-271.	-2695.	3315.	38.	-2892.	2878.	-33.	-2892.	-15.	0.	0.	-31.
15101.	-3413.	3403.	-279.	-2766.	3403.	38.	-2967.	2953.	-33.	-2967.	-15.	0.	0.	-31.

COMPOSITE SHEET PANEL CST STAIN SURVEY

1000	0/ASE20	6666773	606521	606523	606524
0.	0.	0.	-7.	0.	0.
484.	0.	-8.	-7.	-7.	-7.
3902	0.	-8.	0.	0.	0.
1569	0.	-8.	0.	15.	-15.
1587	0.	0.	0.	23.	-23.
8743	0.	0.	0.	83.	-83.
2753	0.	0.	7.	31.	-31.
451.	0.	8.	7.	31.	-31.
883	-45.	31.	0.	34.	-34.
4552	-115.	7.	0.	60.	-60.
4702	-8.	-7.	-7.	64.	-64.
5478	137.	-75.	23.	15.	15.
6477	361.	-100.	72.	-31.	61.
7893	683.	-477.	65.	-47.	168.
8451	383.	-480.	115.	-30.	314.
8683	1451.	-828.	181.	-37.	337.
8834	1453.	-835.	297.	-430.	435.
8932	1521.	-1245.	290.	-773.	743.
9343	1830.	-1185.	500.	-1063.	1039.
9555	2055.	-1501.	823.	-1423.	1392.
9844	2310.	-1413.	303.	-1843.	1826.
10044	2510.	-1520.	357.	-1843.	1844.
11001	3183.	-1734.	357.	-1843.	1844.
11001	3323.	-1734.	357.	-1843.	1844.

## COMPOSITE SHEAR PANEL C58 STRAIN SURVEY

LOAD	GAGE 1	GAGE 2	GAGE 3	GAGE 4	GAGE 5	GAGE 0	GAGE 7	GAGE 8	GAGE 9	GAGE 19	GAGE 11	GAGE 12	GAGE 15	GAGE 14
0	-7	0	0	-7	0	-7	-7	0	-7	0	0	0	-7	-7
200	84	-8	-82	75	-15	-122	81	8	-98	84	-7	-90	84	-7
400	168	15	-168	153	-30	-241	176	15	-182	168	-7	-198	168	-7
600	252	-30	-252	244	-45	-325	274	30	-275	252	-15	-297	252	-7
800	336	-45	-336	328	-61	-409	366	45	-358	336	-20	-404	336	-7
1000	420	-60	-420	409	-76	-493	472	60	-443	420	-25	-518	420	-23
1200	504	-75	-504	486	-91	-577	571	75	-512	504	-30	-632	504	-38
1400	588	-90	-588	569	-106	-661	678	90	-595	588	-35	-746	588	-45
1600	672	-105	-672	657	-121	-745	785	105	-679	672	-40	-860	672	-52
1800	756	-120	-756	741	-136	-829	882	120	-763	756	-45	-974	756	-59
2000	840	-135	-840	828	-151	-913	989	135	-847	840	-50	-1088	840	-66
2200	924	-150	-924	914	-166	-997	1096	150	-931	924	-55	-1202	924	-73
2400	1008	-165	-1008	999	-181	-1081	1203	165	-1015	1008	-60	-1316	1008	-80
2600	1092	-180	-1092	1084	-196	-1165	1310	180	-1099	1092	-65	-1430	1092	-87
2800	1176	-195	-1176	1169	-211	-1249	1417	195	-1183	1176	-70	-1544	1176	-94
3000	1260	-210	-1260	1260	-226	-1333	1524	210	-1267	1260	-75	-1658	1260	-101
3200	1344	-225	-1344	1344	-241	-1417	1631	225	-1351	1344	-80	-1772	1344	-108
3400	1428	-240	-1428	1428	-256	-1501	1738	240	-1435	1428	-85	-1886	1428	-115
3600	1512	-255	-1512	1512	-271	-1585	1845	255	-1519	1512	-90	-1999	1512	-122
3800	1596	-270	-1596	1596	-286	-1669	1952	270	-1603	1596	-95	-2113	1596	-129
4000	1680	-285	-1680	1680	-301	-1753	2059	285	-1687	1680	-100	-2227	1680	-136

LOAD	GAGE 15	GAGE 16	GAGE 17	GAGE 18	GAGE 19	GAGE 20	GAGE 21	GAGE 22	GAGE 23	GAGE 24	GAGE 25	GAGE 26	GAGE 27	GAGE 28
0	-7	0	0	0	0	-7	0	0	0	0	0	0	0	0
200	-137	52	0	-91	91	-7	-107	59	15	-84	-7	-7	-7	-7
400	-274	103	0	-182	182	-15	-214	117	29	-168	7	-7	-7	-7
600	-411	154	0	-273	273	-23	-325	176	43	-259	13	-15	-15	0
800	-548	205	0	-364	364	-31	-437	234	57	-345	23	-15	0	0
1000	-685	256	0	-455	455	-39	-541	292	71	-434	31	-15	0	0
1200	-822	307	0	-546	546	-47	-647	350	85	-528	31	-7	0	0
1400	-959	358	0	-637	637	-55	-751	408	99	-616	31	0	0	0
1600	-1096	409	0	-728	728	-63	-855	466	113	-704	31	0	0	0
1800	-1233	460	0	-819	819	-71	-959	524	127	-795	31	0	0	0
2000	-1370	511	0	-910	910	-79	-1063	582	141	-886	31	0	0	0
2200	-1507	562	0	-1001	1001	-87	-1167	640	155	-977	31	0	0	0
2400	-1644	613	0	-1092	1092	-95	-1271	698	169	-1068	31	0	0	0
2600	-1781	664	0	-1183	1183	-103	-1375	756	183	-1159	31	0	0	0
2800	-1918	715	0	-1274	1274	-111	-1479	814	197	-1250	31	0	0	0
3000	-2055	766	0	-1365	1365	-119	-1583	872	211	-1341	31	0	0	0
3200	-2192	817	0	-1456	1456	-127	-1687	930	225	-1432	31	0	0	0
3400	-2329	868	0	-1547	1547	-135	-1791	988	239	-1523	31	0	0	0
3600	-2466	919	0	-1638	1638	-143	-1895	1046	253	-1614	31	0	0	0
3800	-2603	970	0	-1729	1729	-151	-1999	1104	267	-1705	31	0	0	0
4000	-2740	1021	0	-1820	1820	-159	-2103	1162	281	-1796	31	0	0	0
4200	-2877	1072	0	-1911	1911	-167	-2207	1220	295	-1887	31	0	0	0
4400	-3014	1123	0	-2002	2002	-175	-2311	1278	309	-1978	31	0	0	0
4600	-3151	1174	0	-2093	2093	-183	-2415	1336	323	-2069	31	0	0	0
4800	-3288	1225	0	-2184	2184	-191	-2519	1394	337	-2160	31	0	0	0
5000	-3425	1276	0	-2275	2275	-199	-2623	1452	351	-2251	31	0	0	0
5200	-3562	1327	0	-2366	2366	-207	-2727	1510	365	-2342	31	0	0	0
5400	-3699	1378	0	-2457	2457	-215	-2831	1568	379	-2433	31	0	0	0
5600	-3836	1429	0	-2548	2548	-223	-2935	1626	393	-2524	31	0	0	0
5800	-3973	1480	0	-2639	2639	-231	-3039	1684	407	-2615	31	0	0	0
6000	-4110	1531	0	-2730	2730	-239	-3143	1742	421	-2706	31	0	0	0
6200	-4247	1582	0	-2821	2821	-247	-3247	1800	435	-2797	31	0	0	0
6400	-4384	1633	0	-2912	2912	-255	-3351	1858	449	-2888	31	0	0	0
6600	-4521	1684	0	-3003	3003	-263	-3455	1916	463	-2979	31	0	0	0
6800	-4658	1735	0	-3094	3094	-271	-3559	1974	477	-3070	31	0	0	0
7000	-4795	1786	0	-3185	3185	-279	-3663	2032	491	-3161	31	0	0	0
7200	-4932	1837	0	-3276	3276	-287	-3767	2090	505	-3252	31	0	0	0
7400	-5069	1888	0	-3367	3367	-295	-3871	2148	519	-3343	31	0	0	0
7600	-5206	1939	0	-3458	3458	-303	-3975	2206	533	-3434	31	0	0	0
7800	-5343	1990	0	-3549	3549	-311	-4079	2264	547	-3525	31	0	0	0
8000	-5480	2041	0	-3640	3640	-319	-4183	2322	561	-3616	31	0	0	0
8200	-5617	2092	0	-3731	3731	-327	-4287	2380	575	-3707	31	0	0	0
8400	-5754	2143	0	-3822	3822	-335	-4391	2438	589	-3798	31	0	0	0
8600	-5891	2194	0	-3913	3913	-343	-4495	2496	603	-3889	31	0	0	0
8800	-6028	2245	0	-4004	4004	-351	-4599	2554	617	-3980	31	0	0	0
9000	-6165	2296	0	-4095	4095	-359	-4703	2612	631	-4071	31	0	0	0
9200	-6302	2347	0	-4186	4186	-367	-4807	2670	645	-4162	31	0	0	0
9400	-6439	2398	0	-4277	4277	-375	-4911	2728	659	-4253	31	0	0	0
9600	-6576	2449	0	-4368	4368	-383	-5015	2786	673	-4344	31	0	0	0
9800	-6713	2500	0	-4459	4459	-391	-5119	2844	687	-4435	31	0	0	0
10000	-6850	2551	0	-4550	4551	-399	-5223	2902	701	-4526	31	0	0	0



COMPOSITE SHEAR PANEL CS8 STRAIN SURVEY

LOAD	GAGE29	GAGE30	GAGE31	GAGE32	GAGE33	GAGE34
0.	0.	-7.	-7.	0.	0.	-7.
506.	0.	-7.	-7.	0.	-15.	-7.
928.	8.	-7.	0.	-8.	-23.	-15.
1476.	8.	-15.	-7.	0.	-23.	-15.
1928.	8.	-15.	-15.	0.	-30.	-15.
2483.	15.	-15.	-15.	0.	-30.	-15.
2977.	15.	-15.	-15.	8.	-46.	-23.
3485.	15.	-15.	-23.	8.	-53.	-23.
3904.	8.	0.	-23.	8.	-53.	-23.
4478.	-114.	-7.	-38.	36.	-8.	-23.
4922.	-38.	-53.	-38.	38.	-20.	-38.
5434.	114.	-137.	-38.	8.	-40.	-7.
5982.	385.	-274.	-7.	-53.	-146.	46.
6487.	207.	-519.	38.	-183.	-305.	144.
7043.	1426.	-753.	80.	-327.	-593.	281.
7521.	1755.	-829.	137.	-411.	-647.	365.
8086.	2621.	-1051.	167.	-480.	-763.	433.
8544.	8257.	-1173.	198.	-533.	-888.	582.
8953.	2523.	-1272.	260.	-586.	-967.	542.
9599.	2751.	-1371.	243.	-632.	-1068.	623.
10044.	2866.	-1478.	266.	-678.	-1173.	684.
10577.	3214.	-1577.	289.	-724.	-1278.	745.
11061.	3412.	-1659.	312.	-754.	-1360.	806.

COMPOSITE SHEAR PANEL CSO STRAIN SURVEY

LOAD	GAGE 1	GAGE 2	GAGE 3	GAGE 4	GAGE 5	GAGE 6	GAGE 7	GAGE 8	GAGE 9	GAGE 10	GAGE 11	GAGE 12	GAGE 13	GAGE 14
0.	0.	0.	0.	0.	0.	0.	0.	0.	0.	0.	0.	0.	0.	0.
485.	-7.	-7.	-7.	-7.	-7.	-7.	84.	15.	-84.	91.	-15.	-91.	63.	-7.
989.	145.	-23.	-84.	160.	-7.	-91.	167.	0.	-168.	175.	-23.	-175.	145.	-7.
1454.	259.	-38.	-168.	251.	-15.	-175.	251.	15.	-244.	287.	-31.	-259.	221.	-7.
1914.	297.	-46.	-251.	326.	-23.	-274.	334.	15.	-321.	358.	-46.	-358.	299.	-15.
2423.	381.	-61.	-326.	418.	-23.	-358.	406.	38.	-405.	450.	-53.	-434.	373.	-23.
2828.	457.	-69.	-411.	503.	-38.	-450.	509.	46.	-489.	541.	-59.	-526.	458.	-38.
3241.	521.	-84.	-503.	587.	-38.	-549.	608.	46.	-573.	632.	-84.	-586.	526.	-61.
3655.	587.	-89.	-587.	671.	-46.	-648.	688.	81.	-684.	724.	-84.	-701.	594.	-84.
4034.	633.	-107.	-671.	747.	-61.	-747.	731.	69.	-794.	823.	-69.	-747.	663.	-167.
4439.	693.	-130.	-747.	821.	-61.	-821.	838.	61.	-874.	893.	-87.	-821.	747.	-167.
4819.	755.	-158.	-821.	909.	-61.	-909.	938.	1239.	-938.	1338.	-3949.	-3794.	1562.	2698.
5248.	819.	-188.	-909.	1029.	-61.	-1029.	1058.	1239.	-1058.	1338.	-3949.	-4457.	1874.	3138.
5681.	881.	-228.	-1029.	1149.	-61.	-1149.	1178.	2735.	-1178.	152.	-5179.	-4626.	2210.	3344.
6046.	949.	-258.	-1149.	1269.	-61.	-1269.	1298.	3330.	-1298.	312.	-4849.	-4297.	2271.	3344.
6478.	1002.	-288.	-1269.	1389.	-61.	-1389.	1418.	3513.	-1418.	312.	-4849.	-3855.	2339.	3824.
6887.	1057.	-328.	-1389.	1509.	-61.	-1509.	1538.	3513.	-1538.	312.	-4849.	-3497.	2339.	3824.
7287.	1102.	-358.	-1509.	1629.	-61.	-1629.	1658.	2674.	-1658.	863.	-4849.	-3497.	2469.	2872.
7686.	1157.	-388.	-1629.	1749.	-61.	-1749.	1778.	2674.	-1778.	863.	-4849.	-3497.	2469.	2872.
8085.	1202.	-418.	-1749.	1869.	-61.	-1869.	1898.	2674.	-1898.	863.	-4849.	-3497.	2469.	2872.
8484.	1257.	-448.	-1869.	1989.	-61.	-1989.	2018.	1898.	-2018.	901.	-3435.	-2789.	2514.	2523.
8883.	1302.	-478.	-1989.	2109.	-61.	-2109.	2138.	1898.	-2138.	901.	-3435.	-2789.	2514.	2523.
9282.	1357.	-508.	-2109.	2229.	-61.	-2229.	2258.	1524.	-2258.	1129.	-3146.	-2459.	2545.	2386.

LOAD	GAGE 15	GAGE 16	GAGE 17	GAGE 18	GAGE 19	GAGE 20	GAGE 21	GAGE 22	GAGE 23	GAGE 24	GAGE 25	GAGE 26	GAGE 27	GAGE 28
0.	0.	0.	0.	0.	0.	0.	0.	0.	0.	0.	0.	0.	0.	0.
485.	-84.	81.	8.	-84.	-7.	-7.	-7.	84.	-23.	-81.	-8.	-7.	0.	-7.
989.	-175.	199.	15.	-175.	-150.	0.	-180.	168.	-38.	-183.	-8.	-7.	0.	0.
1454.	-251.	282.	23.	-251.	-244.	15.	-244.	259.	-53.	-274.	-8.	0.	8.	7.
1914.	-326.	373.	38.	-326.	-329.	23.	-329.	350.	-61.	-356.	-8.	0.	8.	15.
2423.	-406.	458.	46.	-406.	-404.	38.	-404.	442.	-84.	-457.	-8.	-7.	8.	15.
2828.	-489.	529.	53.	-489.	-489.	38.	-489.	541.	-91.	-556.	-15.	0.	15.	23.
3241.	-571.	606.	53.	-571.	-564.	38.	-564.	632.	-99.	-648.	-23.	7.	8.	31.
3655.	-655.	686.	76.	-655.	-632.	0.	-632.	704.	-99.	-738.	-38.	7.	8.	38.
4034.	-731.	782.	114.	-731.	-686.	-61.	-686.	823.	-91.	-846.	-38.	15.	0.	54.
4439.	-809.	839.	188.	-809.	-778.	778.	-778.	875.	-471.	-871.	-38.	31.	46.	54.
4819.	-881.	893.	258.	-881.	-851.	1861.	-851.	938.	-1261.	-938.	-8.	53.	-15.	115.
5248.	-957.	939.	328.	-957.	-881.	1861.	-881.	938.	-1338.	-938.	15.	15.	-115.	199.
5681.	-1032.	979.	398.	-1032.	-957.	2553.	-957.	938.	-1413.	-938.	61.	-46.	-244.	291.
6046.	-1107.	1029.	468.	-1107.	-1032.	3435.	-1032.	938.	-1489.	-938.	123.	-139.	-420.	496.
6478.	-1182.	1079.	538.	-1182.	-1107.	4134.	-1107.	938.	-1565.	-938.	123.	-139.	-536.	565.
6887.	-1257.	1129.	608.	-1257.	-1182.	4838.	-1182.	938.	-1641.	-938.	123.	-139.	-596.	605.
7287.	-1332.	1179.	678.	-1332.	-1257.	5542.	-1257.	938.	-1717.	-938.	123.	-139.	-671.	697.
7686.	-1407.	1229.	748.	-1407.	-1332.	6246.	-1332.	938.	-1793.	-938.	123.	-139.	-747.	765.
8085.	-1482.	1279.	818.	-1482.	-1407.	6950.	-1407.	938.	-1869.	-938.	123.	-139.	-823.	811.
8484.	-1557.	1329.	888.	-1557.	-1482.	7654.	-1482.	938.	-1945.	-938.	123.	-139.	-899.	811.
8883.	-1632.	1379.	958.	-1632.	-1557.	8358.	-1557.	938.	-2021.	-938.	123.	-139.	-975.	811.

COMPOSITE SHEAR PANEL OSD STRAIN SURVEY

LOAD	GAGE 29	GAGE 30	GAGE 31	GAGE 32	GAGE 33	GAGE 34
0.	0.	0.	0.	-7.	0.	0.
425.	0.	0.	-15.	-7.	-8.	15.
859.	15.	8.	-15.	0.	-15.	15.
1294.	15.	8.	-15.	7.	-23.	15.
1674.	20.	8.	-15.	7.	-30.	83.
2053.	30.	8.	-23.	15.	-38.	30.
2431.	40.	15.	-30.	15.	-45.	38.
2805.	51.	15.	-38.	23.	-53.	46.
3178.	78.	23.	-38.	23.	-68.	53.
3555.	99.	38.	-38.	23.	-76.	68.
3934.	99.	38.	-114.	84.	-83.	30.
4310.	0.	38.	-59.	53.	-81.	76.
4688.	159.	-68.	-60.	15.	-153.	129.
5061.	308.	-182.	8.	0.	-209.	198.
5446.	589.	-348.	59.	-91.	-278.	312.
5828.	1138.	-547.	159.	-158.	-335.	418.
6207.	1559.	-745.	297.	-235.	-408.	517.
6583.	1923.	-918.	350.	-304.	-488.	616.
6955.	2310.	-1087.	398.	-378.	-551.	692.
7324.	2693.	-1215.	442.	-418.	-609.	769.
7693.	3081.	-1315.		-448.	-1079.	

COMPOSITE SHEAR PANEL CS10 STRAIN SURVEY

LOAD	GAGE 1	GAGE 2	GAGE 3	GAGE 4	GAGE 5	GAGE 6	GAGE 7	GAGE 8	GAGE 9	GAGE 10	GAGE 11	GAGE 12	GAGE 13	GAGE 14
-24.	0.	-7.	0.	0.	0.	-7.	-7.	23.	-84.	-7.	0.	0.	0.	0.
488.	24.	-15.	-76.	76.	-76.	-99.	76.	38.	-160.	84.	-23.	-92.	76.	-8.
945.	153.	-15.	-153.	153.	-7.	-189.	153.	38.	-160.	176.	-38.	-193.	153.	-15.
1464.	251.	-23.	-205.	237.	-15.	-207.	237.	61.	-229.	267.	-61.	-297.	244.	-23.
1883.	335.	-23.	-205.	321.	-23.	-207.	321.	84.	-229.	351.	-92.	-494.	328.	-38.
2423.	419.	-23.	-374.	405.	-23.	-196.	405.	114.	-374.	443.	-122.	-583.	405.	-48.
2949.	510.	-23.	-435.	489.	-30.	-603.	489.	152.	-443.	527.	-168.	-625.	489.	-68.
3417.	602.	-38.	-504.	573.	-30.	-718.	588.	221.	-489.	597.	-244.	-782.	573.	-106.
3885.	739.	-60.	-550.	657.	-15.	-835.	710.	450.	-367.	557.	-559.	-1059.	649.	-198.
4434.	882.	-255.	-1009.	835.	-355.	-1057.	1459.	2870.	-1741.	15.	-3162.	-1222.	1222.	-1375.
4943.	1227.	-527.	-1474.	1207.	-889.	-1257.	1740.	2786.	-2199.	31.	-3887.	-1833.	1833.	-2834.
5451.	1417.	-1123.	-1694.	1478.	-1026.	-1558.	2322.	3444.	-2740.	160.	-5191.	-2406.	2406.	-3570.
5945.	1591.	-840.	-1854.	1654.	-859.	-1842.	2595.	3457.	-2740.	233.	-5330.	-4534.	2457.	-3564.
6454.	1775.	-537.	-1711.	1711.	-137.	-2451.	2843.	3185.	-2064.	435.	-5178.	-4412.	2459.	-3260.
6977.	2078.	-1777.	-2230.	1711.	-223.	-3440.	2843.	3185.	-2064.	603.	-4987.	-3816.	2497.	-3917.
7487.	2316.	-1657.	-2489.	1711.	-654.	-4040.	2843.	3185.	-2064.	784.	-4758.	-3816.	2520.	-2743.
7995.	2537.	-1857.	-2682.	1711.	-730.	-4737.	2843.	3185.	-2064.	947.	-4452.	-3596.	2520.	-2478.
8505.	2728.	-2435.	-3010.	1711.	-841.	-5431.	2843.	3185.	-2064.	1123.	-4108.	-3223.	2520.	-2204.

LOAD	GAGE 15	GAGE 16	GAGE 17	GAGE 18	GAGE 19	GAGE 20	GAGE 21	GAGE 22	GAGE 23	GAGE 24	GAGE 25	GAGE 26	GAGE 27	GAGE 28
-24.	0.	0.	0.	0.	0.	0.	0.	0.	0.	0.	0.	0.	0.	0.
488.	-21.	82.	8.	-82.	51.	-7.	-91.	84.	-7.	-91.	-7.	-8.	-7.	-7.
945.	-175.	181.	8.	-181.	175.	-15.	-183.	163.	0.	-183.	-15.	0.	-7.	0.
1464.	-257.	258.	23.	-252.	257.	-30.	-282.	259.	0.	-282.	-38.	0.	-15.	0.
1883.	-343.	309.	38.	-328.	358.	-46.	-372.	350.	15.	-373.	-45.	0.	-15.	7.
2423.	-434.	407.	46.	-406.	442.	-76.	-478.	434.	23.	-450.	-23.	0.	-15.	7.
2949.	-513.	503.	60.	-473.	518.	-122.	-579.	528.	46.	-573.	-31.	0.	-15.	7.
3417.	-649.	603.	107.	-535.	602.	-183.	-701.	625.	78.	-602.	-31.	0.	-15.	7.
3885.	-785.	710.	197.	-565.	670.	-213.	-838.	731.	137.	-648.	-15.	0.	-15.	7.
4434.	-921.	840.	289.	-605.	782.	-242.	-1037.	838.	137.	-648.	-15.	0.	-15.	7.
4943.	-1057.	945.	389.	-675.	885.	-282.	-1211.	938.	449.	-648.	-15.	0.	-15.	7.
5451.	-1193.	1037.	489.	-745.	983.	-322.	-1346.	1038.	449.	-648.	-15.	0.	-15.	7.
5945.	-1329.	1137.	591.	-815.	1083.	-361.	-1483.	1038.	449.	-648.	-15.	0.	-15.	7.
6454.	-1465.	1237.	691.	-887.	1183.	-400.	-1621.	1038.	449.	-648.	-15.	0.	-15.	7.
6977.	-1601.	1337.	791.	-959.	1283.	-439.	-1759.	1038.	449.	-648.	-15.	0.	-15.	7.
7487.	-1737.	1437.	891.	-1031.	1383.	-478.	-1897.	1038.	449.	-648.	-15.	0.	-15.	7.
7995.	-1873.	1537.	991.	-1103.	1483.	-517.	-2035.	1038.	449.	-648.	-15.	0.	-15.	7.
8505.	-2009.	1637.	1091.	-1175.	1583.	-556.	-2173.	1038.	449.	-648.	-15.	0.	-15.	7.
9015.	-2145.	1737.	1191.	-1247.	1683.	-595.	-2311.	1038.	449.	-648.	-15.	0.	-15.	7.
9525.	-2281.	1837.	1291.	-1319.	1783.	-634.	-2449.	1038.	449.	-648.	-15.	0.	-15.	7.
10035.	-2417.	1937.	1391.	-1391.	1883.	-673.	-2587.	1038.	449.	-648.	-15.	0.	-15.	7.
10545.	-2553.	2037.	1491.	-1463.	1983.	-712.	-2725.	1038.	449.	-648.	-15.	0.	-15.	7.
11055.	-2689.	2137.	1591.	-1535.	2083.	-751.	-2863.	1038.	449.	-648.	-15.	0.	-15.	7.
11565.	-2825.	2237.	1691.	-1607.	2183.	-790.	-3001.	1038.	449.	-648.	-15.	0.	-15.	7.
12075.	-2961.	2337.	1791.	-1679.	2283.	-829.	-3139.	1038.	449.	-648.	-15.	0.	-15.	7.
12585.	-3097.	2437.	1891.	-1751.	2383.	-868.	-3277.	1038.	449.	-648.	-15.	0.	-15.	7.
13095.	-3233.	2537.	1991.	-1823.	2483.	-907.	-3415.	1038.	449.	-648.	-15.	0.	-15.	7.
13605.	-3369.	2637.	2091.	-1895.	2583.	-946.	-3553.	1038.	449.	-648.	-15.	0.	-15.	7.

COMPOSITE GAGE2 PANEL C810 STRAIN SURVEY

LOAD	GAGE29	GAGE30	GAGE31	GAGE32	GAGE33	GAGE34
-24.	-8.	0.	-8.	0.	0.	0.
459.	0.	0.	0.	0.	0.	0.
945.	-8.	0.	-8.	15.	-8.	0.
1454.	0.	0.	0.	23.	-15.	0.
1863.	8.	0.	0.	70.	-15.	15.
2423.	15.	0.	0.	30.	-23.	15.
2993.	15.	0.	0.	34.	-23.	15.
3417.	15.	0.	-8.	44.	-23.	15.
3875.	15.	0.	0.	53.	-23.	15.
4334.	-167.	0.	0.	64.	-27.	0.
4843.	-15.	-15.	-8.	70.	-27.	0.
5321.	419.	-327.	23.	-83.	-220.	243.
5845.	764.	-543.	48.	-114.	-350.	300.
6354.	1173.	-703.	91.	-222.	-500.	540.
7007.	1861.	-812.	102.	-327.	-631.	634.
7625.	1942.	-1004.	153.	-410.	-813.	821.
8206.	2315.	-1234.	180.	-500.	-973.	857.
8803.	2704.	-1459.	220.	-605.	-1117.	1007.

## APPENDIX B

### COMPRESSION PANEL ANALYSIS

In this appendix, expressions for the functions  $F_{ijkl}^{\alpha\beta}$  in Equation 40 for compression panel total potential energy are given.

The nomenclature used is as follows:

$$\begin{aligned} \phi_n^c &= \cos n\pi \xi, & \psi_m^c &= \cos m\pi \eta \\ \phi_n^s &= \sin n\pi \xi, & \psi_m^s &= \sin m\pi \eta \end{aligned}$$

$$\begin{aligned} \phi_n^c &= C_r e^{\epsilon_r \theta_n \xi} & \psi_m^c &= C_r e^{\epsilon_r \theta_m \eta} \\ \phi_n^s &= S_r e^{\epsilon_r \theta_n \xi} & \psi_m^s &= S_r e^{\epsilon_r \theta_m \eta} \end{aligned}$$

where,

$$\theta_n = i n \pi \quad \text{and} \quad i = \sqrt{-1}$$

$$C_r = \frac{1}{2}, \quad S_r = \frac{\epsilon_r}{2i} \quad \text{and} \quad \epsilon_r = (-1)^r$$

$$n=1, \dots, N, \quad m=1, \dots, M \quad \text{and} \quad h=1, 2$$

Repeated indices imply summation.

$$\int_0^1 \int_0^1 u_{,\xi}^2 d\xi d\eta = A_{nm} A_{pq} F_{1nmpq}'' + 2A_{nm} a_{, \xi} F_{2nm}'' + a_{, \xi}^2 a^2$$

$$F_{1nmpq}'' = \int_0^1 \int_0^1 [\phi_n^c(1-\phi_i^c)]_{,\xi} \psi_m^c [\phi_p^c(1-\phi_s^c)]_{,\xi} \psi_q^c d\xi d\eta$$

$$F_{2nm}'' = \int_0^1 \int_0^1 [\phi_n^c(1-\phi_i^c)]_{,\xi} \psi_m^c d\xi d\eta$$

$$\int_0^1 \int_0^1 w_{,\xi}^2 d\xi d\eta = C_{nm} C_{pq} C_{rs} C_{tu} F_{1nmpqrst}^{12}$$

$$F_{1nmpqrst}^{12} = \int_0^1 \int_0^1 \phi_{n,\xi}^s \psi_m^s \phi_{p,\xi}^s \psi_q^s \phi_{r,\xi}^s \psi_s^s \phi_{t,\xi}^s \psi_u^s d\xi d\eta$$

$$\int_0^1 \int_0^1 u_{,\xi} w_{,\xi}^2 d\xi d\eta = A_{nm} C_{pq} C_{rs} F_{1nmpqrs}^{13} + a_{, \xi} C_{pq} C_{rs} F_{2pqrs}^{13}$$

$$F_{1nmpqrs}^{13} = \int_0^1 \int_0^1 [\phi_n^c(1-\phi_i^c)]_{,\xi} \psi_m^c \phi_{p,\xi}^s \psi_q^s \phi_{r,\xi}^s \psi_s^s d\xi d\eta$$

$$F_{2pqrs}^{13} = \int_0^1 \int_0^1 \phi_{p,\xi}^s \psi_q^s \phi_{r,\xi}^s \psi_s^s d\xi d\eta$$

$$\int_0^1 u_{,\xi} v_{,\eta} d\xi d\eta = A_{nm} b_{pq} F_{1nm}^{21} + A_{nm} b_{pq} F_{2nm}^{21} + a_1 b_{pq} a F_{3pq}^{21} + a_1 a_1$$

$$F_{1nm}^{21} = \int_0^1 [\phi_n^c(1-\phi_1^c)]_{,\xi} \psi_m^c \phi_p^s \psi_{q,\eta}^c d\xi d\eta$$

$$F_{2nm}^{21} = \int_0^1 [\phi_n^c(1-\phi_1^c)]_{,\xi} \psi_m^c d\xi d\eta$$

$$F_{3pq}^{21} = \int_0^1 \phi_p^s \psi_{q,\eta}^c d\xi d\eta.$$

$$\int_0^1 u_{,\xi} w_{,\eta}^2 d\xi d\eta = A_{nm} c_{pq} c_{rs} F_{1nm}^{22} + a_1 c_{pq} c_{rs} a F_{2pqrs}^{22}$$

$$F_{1nm}^{22} = \int_0^1 [\phi_n^c(1-\phi_1^c)]_{,\xi} \psi_m^c \phi_p^s \psi_{q,\eta}^s \phi_r^s \psi_{s,\eta}^s d\xi d\eta$$

$$F_{2pqrs}^{22} = \int_0^1 \phi_p^s \psi_{q,\eta}^s \phi_r^s \psi_{s,\eta}^s d\xi d\eta$$



$$\int_0^1 v_{,\eta} w_{,\xi}^2 d\xi d\eta = \beta_{nm} C_{pq} C_{rs} F_{1nm}^{23} p q r s + b_1 C_{pq} C_{rs} b F_2^{23} p q r s$$

$$F_{1nm}^{23} = \int_0^1 \phi_n^s \psi_{m,\eta}^c \phi_{r,\xi}^s \psi_q^s \phi_{r,\xi}^s \psi_s^s d\xi d\eta$$

$$F_2^{23} = \int_0^1 \phi_{r,\xi}^s \psi_q^s \phi_{r,\xi}^s \psi_s^s d\xi d\eta$$

$$\int_0^1 w_{,\xi}^2 w_{,\eta}^2 d\xi d\eta = C_{nm} C_{pq} C_{rs} C_{tu} F_{1nm}^{24} p q r s t u$$

$$F_{1nm}^{24} = \int_0^1 \phi_n^s \psi_m^s \phi_{r,\xi}^s \psi_q^s \phi_r^s \psi_{s,\eta}^s \phi_t^s \psi_{u,\eta}^s d\xi d\eta$$

$$\int_0^1 w u_{,\xi} d\xi d\eta = C_{nm} A_{pq} F_{1nm}^{25} p q + C_{nm} a_1 a F_2^{25} n m$$

$$F_{1nm}^{25} = \int_0^1 \phi_n^s \psi_m^s [\phi_r^c (1 - \phi_1^c)]_{,\xi} \psi_q^c d\xi d\eta$$

$$F_2^{25} = \int_0^1 \phi_n^s \psi_m^s d\xi d\eta$$

$$\int_0^1 W W_{,\xi}^1 d\xi d\eta = C_{nm} C_{pq} C_{rs} F_{nmpqrs}^{26}$$

$$F_{nmpqrs}^{26} = \int_0^1 \phi_n^s \psi_m^s \phi_p^s \psi_q^s \phi_r^s \psi_s^s d\xi d\eta$$

$$\int_0^1 \psi_{,\eta}^2 d\xi d\eta = B_{nm} b_{pq} F_{nmpq}^{31} + 2B_{nm} b_1 b F_{2nm}^{31} + b_1^2 b^2$$

$$F_{nmpq}^{31} = \int_0^1 \phi_n^s \psi_{m,\eta}^c \phi_p^s \psi_{q,\eta}^c d\xi d\eta$$

$$F_{2nm}^{31} = \int_0^1 \phi_n^s \psi_{m,\eta}^c d\xi d\eta$$

$$\int_0^1 W_{,\eta}^4 d\xi d\eta = C_{nm} C_{pq} C_{rs} C_{tu} F_{nmpqrst}^{32}$$

$$F_{nmpqrst}^{32} = \int_0^1 \phi_n^s \psi_{m,\eta}^s \phi_p^s \psi_{q,\eta}^s \phi_r^s \psi_{s,\eta}^s \phi_t^s \psi_{u,\eta}^s d\xi d\eta$$

$$\int_0^1 W^2 d\xi d\eta = C_{nm} C_{pq} F_{nmpq}^{33}$$

$$F_{nmpq}^{33} = \int_0^1 \phi_n^s \psi_m^s \phi_p^s \psi_q^s d\xi d\eta$$

$$\int_0^1 W W_{,\eta} d\xi d\eta = C_{nm} C_{pq} F_{nmpq}^{34}$$

$$F_{nmpq}^{34} = \int_0^1 \phi_n^s \psi_m^s \phi_p^s \psi_{q,\eta}^s d\xi d\eta$$

$$\int_0^1 \vartheta_{,\eta} W_{,\eta}^2 d\xi d\eta = B_{nm} C_{pq} C_{rs} F_{nmpqrs}^{35} + b_1 C_{pq} C_{rs} F_{2mpqrs}^{35}$$

$$F_{nmpqrs}^{35} = \int_0^1 \phi_n^s \psi_{m,\eta}^s \phi_p^s \psi_{q,\eta}^s \phi_r^s \psi_{s,\eta}^s d\xi d\eta$$

$$F_{2mpqrs}^{35} = \int_0^1 \phi_r^s \psi_{q,\eta}^s \phi_r^s \psi_{s,\eta}^s d\xi d\eta$$

$$\int_0^1 W W_{,\eta}^2 d\xi d\eta = C_{nm} C_{pq} C_{rs} F_{nmpqrs}^{36}$$

$$F_{nmpqrs}^{36} = \int_0^1 \phi_n^s \psi_m^s \phi_p^s \psi_q^s \phi_r^s \psi_s^s d\xi d\eta$$

$$\int_0^1 u_{,\eta}^2 d\xi d\eta = A_{nm} A_{pq} F_{nmpq}^{41}$$

$$F_{nmpq}^{41} = \int_0^1 \phi_n^c \psi_m^c (1-\phi_1^c)^2 \phi_p^c \psi_q^c d\xi d\eta$$

$$\int_0^1 v_{,\xi}^2 d\xi d\eta = B_{nm} B_{pq} F_{nmpq}^{42}$$

$$F_{nmpq}^{42} = \int_0^1 \phi_{n,\xi}^s \psi_m^c \phi_{p,\xi}^s \psi_q^c d\xi d\eta$$

$$\int_0^1 u_{,\eta} v_{,\xi} d\xi d\eta = A_{nm} B_{pq} F_{nmpq}^{44}$$

$$F_{nmpq}^{44} = \int_0^1 \phi_n^c \psi_{m,\eta}^c (1-\phi_1^c) \phi_{p,\xi}^s \psi_q^c d\xi d\eta$$

$$\int_0^1 \int_0^1 u_{,\eta} w_{,\xi} w_{,\eta} d\xi d\eta = A_{nm} C_{pq} C_{rs} F_{nmpqrs}^{35}$$

$$F_{nmpqrs}^{35} = \int_0^1 \int_0^1 \phi_n^c \psi_{m,\eta} (1 - \phi_r^c) \phi_{p,\xi}^s \psi_q^s \phi_r^s \psi_{s,\eta} d\xi d\eta$$

$$\int_0^1 \int_0^1 a_{,\xi}^2 w_{,\xi} w_{,\eta} d\xi d\eta = B_{nm} C_{pq} C_{rs} F_{nmpqrs}^{46}$$

$$F_{nmpqrs}^{46} = \int_0^1 \int_0^1 \phi_{n,\xi}^s \psi_m^c \phi_{p,\xi}^s \psi_q^s \phi_r^s \psi_{s,\eta} d\xi d\eta$$

$$\int_0^1 \int_0^1 w_{,\xi\xi}^2 d\xi d\eta = C_{nm} C_{pq} F_{nmpq}^{51}$$

$$F_{nmpq}^{51} = \int_0^1 \int_0^1 \phi_{n,\xi\xi}^s \psi_m^s \phi_{p,\xi\xi}^s \psi_q^s d\xi d\eta$$

$$\int_0^1 \int_0^1 w_{,\xi\xi} w_{,\eta\eta} d\xi d\eta = C_{nm} C_{pq} F_{nmpq}^{52}$$

$$F_{nmpq}^{52} = \int_0^1 \int_0^1 \phi_{n,\xi\xi}^s \psi_m^s \phi_p^s \psi_{q,\eta\eta} d\xi d\eta$$

$$\int_0^1 \int_0^1 W_{,\xi\xi} W_{,\xi\eta} d\xi d\eta = C_{nm} C_{pq} F_{inmpq}^{53}$$

$$F_{inmpq}^{53} = \int_0^1 \int_0^1 \phi_n^s \psi_m^s \phi_p^s \psi_q^s d\xi d\eta$$

$$\int_0^1 \int_0^1 W_{,\eta\eta}^2 d\xi d\eta = C_{nm} C_{pq} F_{inmpq}^{54}$$

$$F_{inmpq}^{54} = \int_0^1 \int_0^1 \phi_n^s \psi_{m,\eta\eta}^s \phi_p^s \psi_q^s d\xi d\eta$$

$$\int_0^1 \int_0^1 W_{,\eta\eta} W_{,\xi\eta} d\xi d\eta = C_{nm} C_{pq} F_{inmpq}^{55}$$

$$F_{inmpq}^{55} = \int_0^1 \int_0^1 \phi_n^s \psi_{m,\eta\eta}^s \phi_p^s \psi_{q,\eta}^s d\xi d\eta$$

$$\int_0^1 \int_0^1 W_{,\xi\eta}^2 d\xi d\eta = C_{nm} C_{pq} F_{inmpq}^{56}$$

$$F_{inmpq}^{56} = \int_0^1 \int_0^1 \phi_{n,\xi}^s \psi_{m,\eta}^s \phi_{p,\xi}^s \psi_q^s d\xi d\eta$$

$$\int_0^1 u_{,\xi}^2 d\xi = A_{nm} A_{pq} F_{1nmpq}^{s1} + 2A_{nm} a_1 a F_{2nm}^{s1} + a_1^2 a^2$$

$$F_{1nmpq}^{s1} = \int_0^1 \left[ \phi_n^c(1-\phi_1^c) \right]_{,\xi} \psi_m^c \left[ \phi_p^c(1-\phi_1^c) \right]_{,\xi} \psi_q^c \Big|_{\eta=0} d\xi$$

$$F_{2nm}^{s1} = \int_0^1 \left[ \phi_n^c(1-\phi_1^c) \right]_{,\xi} \psi_m^c \Big|_{\eta=0} d\xi.$$

$$\int_0^1 v_{,\xi\xi}^2 d\xi = B_{nm} B_{pq} F_{1nmpq}^{s2}$$

$$F_{1nmpq}^{s2} = \int_0^1 \phi_{n,\xi\xi}^s \psi_m^c \phi_{p,\xi\xi}^s \psi_q^c \Big|_{\eta=0} d\xi.$$

$$\int_0^1 v_{,\eta}^2 d\eta = B_{nm} b_{pq} F_{1nmpq}^{F1} + 2 B_{nm} b_1 b F_{2nm}^{F1} + b_1^2 b^2$$

$$F_{1nmpq}^{F1} = \int_0^1 \left[ \phi_n^s \psi_{m,\eta}^c \phi_p^s \psi_{q,\eta}^c \right]_{\xi=1} d\eta$$

$$F_{2nm}^{F1} = \int_0^1 \left[ \phi_n^s \psi_{m,\eta}^c \right]_{\xi=1} d\eta$$

$$\int_0^1 u_{,\eta\eta}^2 d\eta = A_{nm} A_{pq} F_{1nmpq}^{F2}$$

$$F_{1nmpq}^{F2} = \int_0^1 \left[ \phi_n^c \psi_{m,\eta\eta}^c (1 - \phi_1^c)^2 \phi_p^c \psi_{q,\eta\eta}^c \right]_{\xi=1} d\eta$$

A sample evaluation of the function  $F_{1nmpq}^{F1}$  is shown below.



$$\begin{aligned}
F_{inmpq}'' &= \int_0^1 \int_0^1 [\phi_n^c(1-\phi_1^c)]_{,\xi} [\phi_p^c(1-\phi_1^c)]_{,\xi} \psi_m^c \psi_q^c d\xi d\eta \\
&= \int_0^1 \int_0^1 [\phi_{n,\xi}^c(1-\phi_1^c) - \phi_n^c \phi_{1,\xi}^c] [\phi_{p,\xi}^c(1-\phi_1^c) - \phi_p^c \phi_{1,\xi}^c] \psi_m^c \psi_q^c d\xi d\eta \\
&= \int_0^1 \int_0^1 \underbrace{\phi_{n,\xi}^c \phi_{p,\xi}^c \psi_m^c \psi_q^c d\xi d\eta}_{F_{inmpq}^{11}} - 2 \int_0^1 \int_0^1 \underbrace{\phi_{n,\xi}^c \phi_{p,\xi}^c \psi_m^c \psi_q^c \phi_1^c d\xi d\eta}_{F_{inmpq}^{12}} \\
&\quad + \int_0^1 \int_0^1 \underbrace{\phi_{n,\xi}^c \phi_{p,\xi}^c \psi_m^c \psi_q^c \phi_1^c \phi_1^c d\xi d\eta}_{F_{inmpq}^{15,11}} - \int_0^1 \int_0^1 \underbrace{\phi_{n,\xi}^c \phi_p^c \phi_{1,\xi}^c \psi_m^c \psi_q^c d\xi d\eta}_{F_{inmpq}^{14,13}} \\
&\quad + \int_0^1 \int_0^1 \underbrace{\phi_{n,\xi}^c \phi_p^c \phi_1^c \phi_{1,\xi}^c \psi_m^c \psi_q^c d\xi d\eta}_{F_{inmpq}^{15,11}} - \int_0^1 \int_0^1 \underbrace{\phi_n^c \phi_{p,\xi}^c \phi_{1,\xi}^c \psi_m^c \psi_q^c d\xi d\eta}_{F_{ipqam}^{14,11}} \\
&\quad + \int_0^1 \int_0^1 \underbrace{\phi_n^c \phi_{1,\xi}^c \phi_{p,\xi}^c \phi_1^c \psi_m^c \psi_q^c d\xi d\eta}_{F_{ipqam}^{15,11}} + \int_0^1 \int_0^1 \underbrace{\phi_n^c \phi_p^c \phi_{1,\xi}^c \phi_{1,\xi}^c \psi_m^c \psi_q^c d\xi d\eta}_{F_{inmpq}^{16,18}} \\
&= F_{inmpq}^{11} - 2 F_{inmpq}^{12} - F_{inmpq}^{13} - F_{inmpq}^{14} + F_{inmpq}^{15} + F_{ipqam}^{16} + F_{inmpq}^{17} + F_{inmpq}^{18}
\end{aligned}$$